

**EXPERIMENTAL DESIGN OPTIMIZATION AND
THERMOPHYSICAL PARAMETER ESTIMATION OF COMPOSITE MATERIALS
USING GENETIC ALGORITHMS**

by

Sandrine GARCIA

Dissertation submitted to the Faculty of the
Virginia Polytechnic Institute and State University
in partial fulfillment of the requirements for the degree of

DOCTOR OF PHILOSOPHY

in

MECHANICAL ENGINEERING

Elaine P. Scott, co-Chair
Yvon Jarny, co-Chair
J. Robert Mahan
Zafer Gürdal
Martin Raynaud
Didier Delaunay
Bertrand Garnier

June 04, 1999
Nantes, France

Keywords : Anisotropic Composite Materials - Experimental Design Optimization - Genetic Algorithms - Kinetic Parameters - Parameter Estimation - Thermal Properties - Thermosetting Materials.

Copyright 1999, Sandrine Garcia

UNIVERSITE DE NANTES
ISITEM

ECOLE DOCTORALE
SCIENCES POUR L'INGENIEUR
DE NANTES

Année 1999

N° attribué par la bibliothèque

|||||

Thèse de DOCTORAT

Discipline : Sciences de l'Ingénieur
Spécialité : Transferts Thermiques,
Energétique et Génie des Procédés

Présentée et soutenue publiquement par

Sandrine GARCIA

le 04 juin 1999
à l'ISITEM, Nantes

**EXPERIMENTAL DESIGN OPTIMIZATION AND
THERMOPHYSICAL PARAMETER ESTIMATION OF COMPOSITE MATERIALS
USING GENETIC ALGORITHMS**

<i>President</i>	D. DELAUNAY	Directeur de recherche du CNRS, ISITEM, Nantes
<i>Rapporteur</i>	J. R. MAHAN	Professeur, Virginia Tech, VA, Blacksburg, USA
<i>Rapporteur</i>	M. RAYNAUD	Professeur, INSA de Lyon
	E.P. SCOTT	Professeur, Virginia Tech, VA, Blacksburg, USA
	Y. JARNY	Professeur, ISITEM, Nantes
	Z. GURDAL	Professeur, Virginia Tech, VA, Blacksburg, USA
<i>Invité</i>	B. GARNIER	Chargé de recherche du CNRS, ISITEM, Nantes

Co-Directeurs de thèse : E.P. SCOTT et Y. JARNY

Laboratoire de Thermocinétique de l'ISITEM
La Chantrerie, Rue C. Pauc – BP 90604
44306 Nantes Cedex 03

N° ED 82-371

Experimental Design Optimization and Thermophysical Parameter Estimation of Composite Materials Using Genetic Algorithms

Sandrine Garcia

(ABSTRACT)

Thermophysical characterization of anisotropic composite materials is extremely important in the control of today fabrication processes and in the prediction of structure failure due to thermal stresses. Accuracy in the estimation of the thermal properties can be improved if the experiments are designed carefully. However, on one hand, the typically used parametric study for the design optimization is tedious and time intensive. On the other hand, commonly used gradient-based estimation methods show instabilities resulting in nonconvergence when used with models that contain correlated or nearly correlated parameters.

The objectives of this research were to develop systematic and reliable methodologies for both Experimental Design Optimization (EDO) used for the determination of thermal properties, and Simultaneous Parameter Estimation (SPE). Because of their advantageous features, Genetic Algorithms (GAs) were investigated for use as a strategy for both EDO and SPE. The EDO and SPE approaches used involved the maximization of an optimality criterion associated with the sensitivity matrix of the unknown parameters, and the minimization of the ordinary least squares error, respectively. Two versions of a general-purpose genetic-based program were developed: one is designed for the analysis of any EDO / SPE problems for which a mathematical model can be provided, while the other incorporates a control-volume finite difference scheme allowing for the practical analysis of complex problems. The former version was used to illustrate the genetic performance on the optimization of a difficult mathematical test function.

Two test cases previously solved in the literature were first analyzed to demonstrate and assess the genetic-based {EDO/SPE} methodology. These problems included the optimization of one and two dimensional designs for the estimation at ambient temperature of two and three thermal properties, respectively (effective thermal conductivity parallel and perpendicular to the fibers plane and effective volumetric heat capacity), of anisotropic carbon/epoxy composite materials. The two dimensional case was further investigated to

evaluate the effects of the optimality criterion used for the experimental design on the accuracy of the estimated properties.

The general-purpose genetic-based program was then successively applied to three advanced studies involving the thermal characterization of carbon/epoxy anisotropic composites. These studies included the SPE of successively three, seven and nine thermophysical parameters, with for the latter case, a two dimensional EDO with seven experimental key parameters. In two of the three studies, the parameters were defined to represent the dependence of the thermal properties with temperature. Eventually, the kinetic characterization of the curing of three thermosetting materials (an epoxy, a polyester and a rubber compound) was accomplished resulting in the SPE of six kinetic parameters.

Overall, the genetic method was found to perform extremely well despite the high degree of correlation and low sensitivity of many parameters in all cases studied. This work therefore validates the use of GAs for the thermophysical characterization of anisotropic composite materials. The significance in using such algorithms is not only the solution to ill-conditioned problems but also, a drastically cost savings in both experimental and time expenses as they allow for the EDO and SPE of several parameters at once.

Keywords : Anisotropic Composite Materials - Experimental Design Optimization - Genetic Algorithms - Kinetic Parameters - Parameter Estimation - Thermal Properties - Thermosetting Materials.

Conception Optimale d'Expériences et Estimation de Paramètres Thermophysiques de Matériaux Composites par Algorithmes Génétiques

Sandrine Garcia

(RESUME)

La caractérisation thermophysique de matériaux composites est un enjeu crucial. La précision de l'estimation peut être améliorée si les expériences sont conçues avec pertinence. Cependant, l'étude paramétrique traditionnellement employée pour l'optimisation expérimentale est limitée, et les méthodes d'estimation basées sur le calcul d'un gradient sont instables pour des problèmes mal conditionnés.

L'objectif de ce travail était de développer des méthodologies robustes pour la Conception Optimale d'Expériences (COE) destinées à l'identification de propriétés thermiques, et pour l'Estimation Simultanée de Paramètres (ESP). L'approche utilisée s'appuie sur les spécificités avantageuses des Algorithmes Génétiques (AGs) et consiste en COE à maximiser un critère d'optimisation basé sur la matrice de sensibilité des propriétés recherchées et en ESP, à minimiser l'erreur des moindres carrés. Un programme général basé sur les AGs a été développé sous deux versions, permettant l'analyse soit de modèles analytiques soit de modèles numériques par volumes finis.

Les AGs de COE et d'ESP ont d'abord été testés sur des cas de la littérature, puis appliqués sur des cas nouveaux. Ces études ont été menées selon une approche à la fois numérique et expérimentale. Elles concernent la caractérisation thermique de composites anisotropes carbone/époxy, avec des COE et ESP comportant respectivement jusqu'à sept paramètres expérimentaux, et neuf paramètres thermophysiques. Enfin, la méthodologie d'ESP a été étendue à la caractérisation de cinétiques chimiques de résines thermodurcissables mettant en jeu six paramètres cinétiques.

Malgré de très fortes corrélations et faibles sensibilités de plusieurs paramètres dans toutes les études, les résultats confirment la remarquable robustesse des AGs. L'intérêt de leur utilisation réside non seulement dans la solution de problèmes mal posés, mais aussi dans la réduction de temps et coûts expérimentaux, en permettant des estimations simultanées de plusieurs paramètres.

Mots Clefs : Algorithmes Génétiques - Cinétiques Chimiques - Conception Optimale d'Expériences - Matériaux Composites Anisotropes - Méthodes Inverses - Propriétés Thermophysiques - Résines Thermodurcissables - Sensibilité et Corrélation.

Acknowledgements / Remerciements

I would like to thank the following people for their help and/or support in conducting this research:

Dr. Elaine P. Scott and Dr. Yvon Jarny, my co-advisors, for their assistance and guidance throughout this dual Ph.D. I have particularly appreciated the freedom to manage my own research. It has been an extreme pleasure to work with them and to know them.

NASA Langley Research Center, for funding the first stage of this research performed at Virginia Tech; the CNRS, for providing me with a BDI scholarship during the second stage of this dual program at the Laboratoire de Thermocinétique de l'ISITEM.

Dr. J. R. Mahan and Dr. M. Raynaud for accepting the load of "Rapporteurs"; Dr. Z. Gurdal and Dr. B. Garnier for serving on my committee, and Dr. D. Delaunay for presiding the Jury.

Dr. Mahan and Dr. Scott for all the opportunities they have allowed me to enhance my education since my coming to the States in Aug. 93. Muchas gracias a mi americano padre y mi amiga elena por su apoyo, consejo, y amistad.

Dr. Bertrand Garnier, for responding positively to Dr. Scott's asking regarding the possibility of a dual program. Thanks also for always being ready to answer my many questions.

Le personnel du LTI; plus particulièrement, Arnaud, mon officemate, et Stéphane, pour leur soutien ; merci également à Gwen pour son amitié et son agréable camaraderie.

Liliane et Claude pour me montrer l'importance d'une vie équilibrée entre le travail et le... ti'punch ! Merci pour votre réconfort.

Lionel, pour son généreux soutien au moment des temps durs.

Enfin, ma famille, sans qui la vie perd ses racines (plus particulièrement mes parents, Jacqueline et Josmaël Garcia, mes soeurs, Céline et Sophie, et ma grand-mère, « mamie ! »). Merci pour votre soutien, vos encouragements, et votre amour.

Table of Contents

List of Tables	xi
List of Figures.....	xiv
List of Symbols	xx
List of Abbreviations	xxiii
Chapter 1 Introduction	1
1.1 Motivation	1
1.2 Goals and Objectives.....	5
Chapter 2 Literature Review	10
2.1 Composite Materials.....	10
2.2 Thermophysical Characterization of Composite Materials.....	11
2.2.1 Thermal Characterization	11
2.2.2 Kinetic Characterization	18
2.3 Experimental Design Optimization	22
2.3.1 Sensitivity Study.....	23
2.3.2 Optimality Criterion	24
2.4 Genetic Algorithms (GAs)	28
2.4.1 Description.....	28
2.4.2 Applications in Engineering	30
Chapter 3 Parameter Estimation and Design Optimization: Theoretical Considerations	34
3.1 Parameter Estimation Inverse Methodology	34
3.1.1 Formulation	35
3.1.2 A Gradient-Based Procedure: the Modified Box-Kanemasu Method.....	36
3.1.3 Sensitivity, Correlation and Condition Number Analysis	39
3.1.4 Residuals and Root-Mean-Square (RMS) Analysis	43
3.1.5 Confidence Intervals (CIs).....	45
3.2 Design Optimization Methodology	47
3.2.1 Formulation	47
3.2.2 Optimality Criterion	48
3.2.3 Optimization Technique	52
Chapter 4 Genetic Algorithms (GAs).....	53
4.1 Introduction	53
4.2 Fundamentals.....	54
4.2.1 What Are GAs?	54
4.2.2 How Do GAs Work?	55
4.2.3 What Are the Main Operator Variants Employed in the GA Process?	56
4.2.4 What Differentiates GAs From Conventional Techniques?.....	62

4.2.5	What Are the Strengths and Weaknesses of GAs?	62
4.2.6	For Which Type of Problems Should GAs be Used?	63
4.3	GAs Developed	64
4.3.1	Basic Elitist GA (BEGA)	65
4.3.2	Extended Elitist GA (EEGA)	68
4.3.3	Third GA (GA_3: GAMAIN and GACONDUCT)	70
4.4	Performance Analysis of GAMAIN	75
4.4.1	Description of the Mathematical Test Function	75
4.4.2	Results	76
Chapter 5 Thermal Characterization of Anisotropic Composite Materials		78
5.1	Case Studies of Constant Property Estimation	79
5.1.1	One- and Two-Dimensional Analyses at Ambient Temperature	79
5.1.1.1	Problem Descriptions	80
5.1.1.2	Experimental Data	82
5.1.1.3	Mathematical Model Formulations	82
5.1.1.4	Results and Discussion	88
5.1.1.5	Benefits from Optimizing Experimental Designs	104
5.1.1.6	Effects of the Experimental Design Optimality Criterion	109
5.1.2	Two-Dimensional Analysis Performed at Different Temperature Levels	112
5.1.2.1	Problem Description	112
5.1.2.2	Experimental Methods	113
5.1.2.3	Finite Difference Modeling	118
5.1.2.4	Results and Discussion	121
5.1.2.5	Conclusion	130
5.2	Case Studies of Mixed Temperature Dependent and Constant Property Estimation	131
5.2.1	Two-Dimensional Analysis Over the Range [25-150°C]	131
5.2.1.1	Problem Description	132
5.2.1.2	Finite Difference Modeling	134
5.2.1.3	Results and Discussion	137
5.2.1.4	Conclusion	144
5.2.2	Two-Dimensional Analysis in RTM Mold Over the Range [100-130°C]	145
5.2.2.1	Problem Description	145
5.2.2.2	Experimental Design and Data	147
5.2.2.3	Finite Difference Modeling	150
5.2.2.4	Results and Discussion	151
5.2.2.5	Conclusion	156
Chapter 6 Kinetic Characterization of the Curing of Thermosetting Materials		158
6.1	Kamal and Sourour (K&S) Model	158
6.1.1	Description	158
6.1.2	Motivation for Using the K&S Model	159
6.2	K&S Estimation Problem Formulation	159
6.3	Inhibition Time Estimation Problem Formulation	163
6.4	Materials and Experimental Procedures	164
6.4.1	Description of Materials	164
6.4.2	DSC Experimental Procedures	165

6.5	Results and Discussion.....	168
6.5.1	K&S Estimation.....	168
6.5.1.1	Estimation Procedure.....	168
6.5.1.2	Results and Discussion.....	170
6.5.2	Inhibition Time Estimation.....	195
6.5.3	Conclusion.....	198
Chapter 7	Conclusions and Recommendations.....	199
7.1	Genetic Algorithms	200
7.2	Thermophysical Characterization of Composite Materials.....	200
7.3	Other Thermophysical Characterizations Using GAs	203
7.4	Overall Conclusions	204
7.5	Recommendations	205
Bibliography		207
Appendix A	Mechanisms of a Standard Simple Genetic Algorithm.....	216
Appendix B	GAMAIN.FOR Program and GACOMMON_MAIN.FOR Subroutine.....	219
Appendix C	GACONDUCT.FOR Program and GACOMMON_CONDUCT.FOR Subroutine.....	233
Appendix D	GADAVISF6.FOR Subroutine	254
Appendix E	GA2DOPT.FOR Subroutine	256
Appendix F	GA2DTPPT.FOR Subroutine.....	261
Appendix G	GA2DRTM.FOR Subroutine	267
Appendix H	GAKINETIC.FOR Subroutine and its dependencies.....	272
Vita		280

List of Tables

Table 4.1	Genetic parameter optimal setting ($n_p=2$).....	76
Table 5.1	Effect of the population size, n_s , and the number of generations, n_g , in the one dimensional experiment.....	90
Table 5.2	Determination of the optimal design for the one dimensional experiment ($n_s=n_g=200, f_{eval}=40200$).....	91
Table 5.3	Investigation of the significance of each design variable in Configuration 1 of the two dimensional experiment (Phase 1, $n_s=n_g=25, f_{eval}=650$).....	92
Table 5.4	Investigation of the significance of each design variable in Configuration 2 of the two dimensional experiment (Phase 1, $n_s=n_g=25, f_{eval}=650$).....	92
Table 5.5	Effect of the population size n_s and the number of generations n_g in Configuration 1 of the two dimensional experiment (Phase 2).....	93
Table 5.6	Determination of the optimal designs for Configuration 1 of the two dimensional experiment (Phase 2, $n_s=125, n_g=50, f_{eval}=6375$).....	93
Table 5.7	Determination of the optimal design for Configuration 2 of the two dimensional experiment (Phase 2, $n_s=125, n_g=50, f_{eval}=6375$).....	94
Table 5.8	Values for population size n_s , number of generations n_g , and EEGA elitist parameters, n_{best1} , n_{pop} , n_{best2} , and n_{best3} used in the one dimensional and two dimensional Configuration 1 optimization problems with the BEGA and EEGA.....	96
Table 5.9	Optimal designs for the one dimensional and two dimensional Configuration 1 optimization problems.....	97
Table 5.10	Correlation matrices for the simultaneous estimation of three thermal properties (k_x , k_y and C) with the two dimensional Configuration 1 design using the modified Box-Kanemasu method.....	99
Table 5.11	Genetic parameters, n_s , n_g , and n_{pop} , elitist parameters, n_{best1} , n_{best2} , and n_{best3} , and number of function evaluations, f_{eval} , used in the estimation problems with the EEGA.....	100
Table 5.12	Estimated mean thermal properties for the one dimensional estimation problem using both EAL and EEGA.....	100
Table 5.13	Estimated thermal properties, k_x , k_y and C , the least squares error, S , and the Root Mean Squares, RMS_i and RMS_M , for the two dimensional Configuration 1 estimation problem using EEGA.....	103

Table 5.14	Experimental conditions, determinant D^+ , eigenvalues λ_{1-3}^+ , condition number λ_1^+/λ_3^+ and magnitude of the non-dimensional sensitivity coefficients corresponding to an optimal and non-optimal design of the Configuration 1 of the two dimensional problem.....	105
Table 5.15	Estimated thermal properties k_x , k_y and C , least square error S and correlation terms $r_{kx/ky}$, $r_{kx/C}$ and $r_{ky/C}$ for an optimal and non-optimal simulated two dimensional Configuration 1 experiment.....	106
Table 5.16	Predicted optimal experimental designs using EEGA for the one- and Configuration 1 of the two-dimensional experiments according to D -, E - and A -optimality	110
Table 5.17	Estimated thermal properties, k_x , k_y , and C , the least squares error, S , and correlation terms $r_{kx/ky}$, $r_{kx/C}$ and $r_{ky/C}$ for the one- and Configuration 1 of the two-dimensional experiments designed according to D -, E - and A -optimality	111
Table 5.18	Genetic convergence parameters setting	122
Table 5.19	Estimated thermal properties k_x , k_y and C , least square error S , and Root Mean Square error RMS at six different temperature levels in the range [30-150°C].....	124
Table 5.20	Correlation matrices for the simultaneous estimation of k_x , k_y and C from experiment #3 at 50°C and 150°C	128
Table 5.21	Comparison of slopes with temperature associated with linear regressions for the properties k_x , k_y and C with previously published results (carbon/epoxy composite type).....	129
Table 5.22	Initial guesses for the parameters to be estimated used in the optimization stage	134
Table 5.23	Optimal experimental parameters for the two dimensional experiment designed for the simultaneous estimation of the thermal properties as temperature dependent over the range [25-150°C].....	137
Table 5.24	Non optimal experimental designs investigated	138
Table 5.25	Predicted thermophysical parameters, least squares and root mean squares errors, obtained from simulated data using the two dimensional optimal experiment designed in the temperature range [25-150°C].....	142
Table 5.26	Results of the preliminary numerical analysis.....	149
Table 5.27	Predicted thermophysical parameters obtained from experimental data from a non reticulated carbon/epoxy sample in RTM mold.....	152
Table 6.1	Conditions of experiments performed using DSC.....	168

Table 6.2	Genetic convergence parameters setting	170
Table 6.3	K&S detailed estimation results - Epoxy resin.....	171
Table 6.4	K&S detailed estimation results - Polyester resin	172
Table 6.5	K&S detailed estimation results - Rubber compound	173
Table 6.6	Correlation matrices for the experiment at 15°C/min using the final estimates for A_2 , E_2 , m and n obtained with Strategy I and for A_2 , E_2 , m , n , A_1 and E_1 obtained with Strategy III and II	177
Table 6.7	K&S estimation results – Summary	185
Table 6.8	Inhibition time estimation results	198
Table A.1	Summary of evaluation and ranking processes over the initial population.....	216
Table A.2	Summary of crossover process over the parent population, and mutation, evaluation and ranking processes over the children population	217
Table A.3	New ranked population at generation 1	218

List of Figures

Figure 2.1	Typical reaction rate evolution versus time during curing of thermosetting polymers	18
Figure 3.1	Schematic of parameter estimation inverse methodology	35
Figure 4.1	Typical Genetic Algorithm flowchart.....	55
Figure 4.2	General structure of a standard simple Genetic Algorithm	57
Figure 4.3	Flowcharts of BEGA and EEGA.....	65
Figure 4.4	Simplified flowchart of GA_3	70
Figure 4.5	Function f_6 vs. x with y set to 0.....	76
Figure 4.6	Fitness evolution vs. n_g	76
Figure 4.7	Population evolution (initial to final generation).....	77
Figure 5.1	One-dimensional boundary conditions	81
Figure 5.2	Two-dimensional boundary conditions (a) Configuration 1 and (b) Configuration 2	81
Figure 5.3	Schematic of the optimized one dimensional experiments	89
Figure 5.4	Schematic of the optimized two dimensional experiments (a) Configuration 1 and (b) Configuration 2	89
Figure 5.5	Temperature and residual distribution from the one dimensional model for the first experiment.....	101
Figure 5.6	Dimensionless sensitivity coefficients from the two dimensional (Configuration 1) model	102
Figure 5.7	Linear dependence between the dimensionless sensitivity coefficients of k_x and k_y from the two dimensional (Configuration 1) model	102
Figure 5.8	Temperature and residual distribution from the two dimensional (Configuration 1) model for the first experiment	103
Figure 5.9	Dimensionless sensitivity coefficients from the two dimensional (Configuration 1) non optimal experimental design.....	106

Figure 5.10 Linear dependence between the dimensionless sensitivity coefficients of k_x and k_y from the two dimensional (Configuration 1) non optimal experimental design	106
Figure 5.11 Curves iso- S vs. k_y and C with k_x fixed (from the two dimensional Configuration 1 estimation problem)	108
Figure 5.12 Curves iso- S vs. k_x and k_y with C fixed (from the two dimensional Configuration 1 estimation problem)	108
Figure 5.13 Simplified schematic of the experimental set up and apparatus ALIS	115
Figure 5.14 Detailed view of the sandwich structure inside the aluminum mold.....	116
Figure 5.15 Thermocouple position and numbering	117
Figure 5.16 Boundary conditions analyzed in the numerical model.....	119
Figure 5.17 Control-volume discretization (grid 10×33 elements) from half sandwich structure	119
Figure 5.18 Experimental temperature and heat flux histories from experiment #3 at 50°C	121
Figure 5.19 Estimated thermal properties and linear regressions	123
Figure 5.20 Calculated and measured temperature and residual distributions from experiment #3 at 50°C	125
Figure 5.21 Calculated and measured temperature and residual distributions from experiment #3 at 150°C	125
Figure 5.22 Dimensionless sensitivity coefficients from experiment #3 at 50°C.....	126
Figure 5.23 Dimensionless sensitivity coefficients from experiment #3 at 150°C.....	126
Figure 5.24 Typical two dimensional temperature distribution obtained when the heater is turned off (at $t = t_h = 35$ s).....	127
Figure 5.25 Simplified schematic of the experimental set up to be optimized.....	133
Figure 5.26 Heating law considered in optimization process (heat flux q imposed from the electrical heater).....	133
Figure 5.27 Control-volume discretization (grid 15×45 elements) from the complete experimental design	135
Figure 5.28 Control-volume discretization (grid 15×38 elements) from half experimental design	136

Figure 5.29	Dimensionless sensitivity coefficients and temperature evolution vs. time from the two dimensional optimal design for the estimation of temperature dependent thermal properties.....	139
Figure 5.30	Dimensionless determinant and temperature evolution for the optimal and two non optimal designs	139
Figure 5.31	Dimensionless sensitivity coefficients from the non optimal design #1	140
Figure 5.32	Dimensionless sensitivity coefficients from the non optimal design #2	140
Figure 5.33	Modified dimensionless determinant for the optimal design	141
Figure 5.34	Calculated and simulated temperature and residual distributions from run #2.....	143
Figure 5.35	Calculated and simulated temperature and residual distributions from run #3	143
Figure 5.36	Minimization of the least squares error S from run #2.....	144
Figure 5.37	Experimental RTM mold.....	148
Figure 5.38	Detailed view of the x -symmetrical RTM mold placed between both plates of the experimental press ALIS	149
Figure 5.39	Two dimensional boundary conditions associated with the RTM mold analysis	150
Figure 5.40	Control-volume discretization (grid 27×71 elements) from half RTM mold...	151
Figure 5.41	Predicted linear regression for the volumetric heat capacity, C , over the range $[100-130^\circ\text{C}]$	152
Figure 5.42	Temperature distributions from the five thermocouples embedded in the composite in RTM mold.....	154
Figure 5.43	Dimensionless sensitivity coefficients from thermocouple TC_1	154
Figure 5.44	Dimensionless sensitivity coefficients from thermocouple TC_2	155
Figure 5.45	Dimensionless sensitivity coefficients from thermocouple TC_3	155
Figure 5.46	Dimensionless sensitivity coefficients from thermocouple TC_4	156
Figure 6.1	Schematic of estimation Strategy I.....	161
Figure 6.2	Schematic of estimation Strategy II.....	161
Figure 6.3	Schematic of estimation Strategy III	161

Figure 6.4	Simplified schematic of DSC-7 apparatus.....	165
Figure 6.5	Numerical integration of the exothermal peak measured with DSC	166
Figure 6.6	Dimensionless sensitivity coefficients with respect to the cure rate for the epoxy experiment at 15°C/min and using estimates obtained with Strategy I.....	174
Figure 6.7	Dimensionless sensitivity coefficients with respect to the degree of cure for the epoxy experiment at 15°C/min and using estimates obtained with Strategy III.....	174
Figure 6.8	Dimensionless sensitivity coefficients with respect to the cure rate for the epoxy experiment at 15°C/min and using estimates obtained with Strategy II	174
Figure 6.9	Linear dependence between dimensionless sensitivity coefficients with respect to the cure rate for the epoxy experiment at 15°C/min and using estimates obtained with Strategy I.....	174
Figure 6.10	Linear dependence between dimensionless sensitivity coefficients with respect to the degree of cure for the epoxy experiment at 15°C/min and using estimates obtained with Strategy III.....	175
Figure 6.11	Linear dependence between dimensionless sensitivity coefficients with respect to the cure rate for the epoxy experiment at 15°C/min and using estimates obtained with Strategy II.....	175
Figure 6.12	Dimensionless sensitivity coefficients with respect to the cure rate for the polyester experiment at 15°C/min and using estimates obtained with Strategy I.....	175
Figure 6.13	Dimensionless sensitivity coefficients with respect to the degree of cure for the polyester experiment at 15°C/min and using estimates obtained with Strategy III.....	175
Figure 6.14	Dimensionless sensitivity coefficients with respect to the cure rate for the polyester experiment at 15°C/min and using estimates obtained with Strategy II	176
Figure 6.15	Dimensionless sensitivity coefficients with respect to the cure rate for the rubber experiment at 15°C/min and using estimates obtained with Strategy I.....	176
Figure 6.16	Dimensionless sensitivity coefficients with respect to the degree of cure for the rubber experiment at 15°C/min and using estimates obtained with Strategy III.....	176

Figure 6.17	Dimensionless sensitivity coefficients with respect to the cure rate for the rubber experiment at 15°C/min and using estimates obtained with Strategy II	176
Figure 6.18	Simulation of isothermal cure rates using estimates obtained with Strategy I – Epoxy compound.....	178
Figure 6.19	Simulation of isothermal cure rates using estimates obtained with Strategy III – Epoxy compound.....	178
Figure 6.20	Simulation of isothermal cure rates using estimates obtained with Strategy II – Epoxy compound	178
Figure 6.21	Simulation of isothermal cure rates using estimates obtained with Strategy I – Polyester compound	179
Figure 6.22	Simulation of isothermal cure rates using estimates obtained with Strategy III – Polyester compound	179
Figure 6.23	Simulation of isothermal cure rates using estimates obtained with Strategy II – Polyester compound.....	179
Figure 6.24	Simulation of isothermal cure rates using estimates obtained with Strategy I – Rubber compound	180
Figure 6.25	Simulation of isothermal cure rates using estimates obtained with Strategy III – Rubber compound.....	180
Figure 6.26	Simulation of isothermal cure rates using estimates obtained with Strategy II – Rubber compound	180
Figure 6.27	Simulation of the cure rate using estimates obtained with Strategy II - Epoxy compound	186
Figure 6.28	Simulation of the degree of cure using estimates obtained with Strategy II - Epoxy compound.....	187
Figure 6.29	Simulation of the cure rate using estimates obtained with Strategy II - Polyester compound	188 & 189
Figure 6.30	Simulation of the degree of cure using estimates obtained with Strategy II - Polyester compound	190 & 191
Figure 6.31	Simulation of the cure rate using estimates obtained with Strategy II and III - Rubber compound	192
Figure 6.32	Simulation of the degree of cure using estimates obtained with Strategy II and III - Rubber compound.....	193

Figure 6.33 Linear regression between the inhibition time model parameters - Epoxy compound196

Figure 6.34 Linear regression between the inhibition time model parameters - Polyester compound196

Figure 6.35 Linear regression between the inhibition time model parameters - Rubber compound196

Figure 6.36 Simulation of inhibition time vs. temperature – Epoxy compound.....197

Figure 6.37 Simulation of inhibition time vs. temperature – Polyester compound197

Figure 6.38 Simulation of inhibition time vs. temperature – Rubber compound197

Figure A.1 Function g vs. x216

Figure A.2 Weighted roulette wheel with slots sized according to the chromosomes' fitness of the initial population217

List of Symbols

A_1, A_2	Arrhenius constants (min^{-1})
\mathbf{b}	Estimated parameter vector using the Gauss linearization method
B	Parameter of the inhibition time model
C_p	Specific heat (J/kgK)
C	Volumetric heat capacity, ($\rho C_p, \text{J/m}^3\text{K}$)
$CRITERION$	Variation Size to be checked in the convergence criterion (used in the GA_3)
d	Element of the $\mathbf{X}^T\mathbf{X}$ matrix
D	Determinant of the $\mathbf{X}^T\mathbf{X}$ matrix
E_1, E_2	Arrhenius constants or activation energy constants (kJ/mole)
f	Fitness of a chromosome
f_{eval}	Number of function evaluation
$f6$	Mathematical test function
h	Scalar interpolation factor in the modified Box-Kanemasu method
h_1, h_2, h_f	Convection coefficients used in Section 5.2.2 ($\text{W/m}^2\text{K}$)
$h(t, T)$	Integral function used in the inhibition time model (s)
$h(t)$	Enthalpy function (J/s)
ΔH	Total heat of reaction (J)
i, j	Node position along the x - and y -axis, respectively (numerical model)
k	Thermal conductivity (W/mK)
k_x	Thermal conductivity perpendicular to the fiber plane (W/mK)
k_y	Thermal conductivity parallel to the fiber plane (W/mK)
K_1, K_2	Kinetic rate constants (min^{-1})
L	Length (m)
L_p	Heating length (m)
$LASTG$	Maximum allowable number of generations
$LASTCRITERG$	Number of generations during which the convergence criterion must be satisfied for the run to stop (used in the GA_3)
$MING$	Number of generations without checking the convergence criterion (used in the GA_3)
m, n	Kinetic exponents
$n_{best1}, n_{best2}, n_{best3}$	Elitist genetic parameters used in the EEGA
n_{pop}	Number of initial population investigated with the EEGA
n_g	Number of generations
n_p	Number of parameters
n_s	Population size
N_i	Number of observations (per experiment / sensor)
N_j	Number of experiments
N_k	Number of sensors
N_{tot}	Total number of observations
p	Probability
p_c	Probability used in the crossover (genetic operator)
p_{mj}	Probability used in the jump mutation (genetic operator)
p_{mc}	Probability used in the creep mutation (genetic operator)
p_r	Probability used in the generational replacement (genetic operator)

p_t	Probability used in the tournament selection (genetic operator)
P	$[\mathbf{X}^T\mathbf{X}]^{-1}$ with OLS estimator
q	Heat flux (W/m^2)
r	Correlation term
R	Random number uniformly distributed between 0 and 1 [Chapter 4]
	Gas constant ($\text{kJ}/\text{mole}\cdot\text{K}$) [Chapter 6]
R_c	Contact resistance ($\text{m}^2\text{K}/\text{W}$)
s	Sample standard deviation around the mean
s_i	Sample standard deviation of an individual experiment
S	Least squares function
S_1, S_2, S_3	Least squares function associated with Strategies I, II and III, respectively
t	Time (s)
t_n	Total overall experimental time (s)
t_h	Heating time (s)
t_{12}	Cooling time optimized in Section 5.2.1 (s)
t_{ref}	Parameter of the inhibition time model (s)
T	Temperature ($^{\circ}\text{C}$ or K)
T_{ref}	Reference temperature selected in the inhibition time model (s)
U	Matrix used with MAP estimator
v	Rate of cure ($d\alpha/dt$, min^{-1})
V_f	Fiber volume fraction
V_T	Temperature rate imposed in DSC experiments ($^{\circ}\text{C}/\text{min}$)
W	Weighted matrix used with ML and MAP estimators
x	Location on x -axis
X	Sensitivity coefficient
X	Sensitivity matrix
$\mathbf{X}^T\mathbf{X}$	Fisher information matrix
y	Location on y -axis

Greek

α	Thermal diffusivity (m^2/s) [Chapter 5]; Degree of cure [Chapter 6]
β	True parameter vector
δ	Perturbation size
Δ	Step/Variation
η	Dependent variable (measured quantity in estimation procedure)
η	Observation vector
κ_{xy}	Ratio of thermal conductivities k_y/k_x
λ	Eigenvalue of the $\mathbf{X}^T\mathbf{X}$ matrix
μ	Prior information parameter vector
ρ	Density (kg/m^3)
σ	Standard deviation

Superscripts

+	dimensionless
~	experimental
-	mean

<i>k</i>	iteration
<i>f</i>	fiber or fluid
<i>m</i>	matrix

Subscripts

<i>a</i>	ambient
<i>av</i>	average
<i>eff</i>	effective
<i>i</i>	initial
<i>ind</i>	induction
<i>max</i>	maximum
<i>min</i>	minimum
<i>p</i>	plate
<i>ref</i>	reference
<i>s</i>	sensor

List of Abbreviations

ALIS	Laboratory Apparatus from ISitem
CI s	Confidence Intervals
EDO	Experimental Design Optimization
BEGA	Basic Elitist Genetic Algorithm
DSC	Differential Scanning Calorimetry
EEGA	Extended Elitist Genetic Algorithm
GA_3	Third Genetic Algorithm (2 versions: GAMAIN and GACONDUCT)
GAs	Genetic Algorithms
K&S	Kamal and Sourour (kinetic model)
LTI	Laboratoire de Thermocinétique de l'ISITEM
MAP	Maximum A Posteriori (estimator)
ML	Maximum Likelihood (estimator)
OLS	Ordinary Least Squares (estimator)
RMS	Root-Mean-Square error
RTM	Resin Transfer Molding
SPE	Simultaneous Parameter Estimation
TC	Thermocouple
VT	Virginia Tech (Virginia Polytechnic Institute and State University)

CHAPTER 1

Introduction

1.1 Motivation

Composite materials can offer superior performance over standard metals, including higher strength-to-weight ratios and better corrosion and wear resistance. Because of these improved characteristics the use of these materials has been growing rapidly in this past quarter century. Composite technology prevails in a wide variety of fields, including the aerospace, aeronautics, automotive, tooling and sporting goods industries, to name but a few. In these high technology applications it is important that the properties of these advanced materials be known for design purposes. Knowledge of the thermal properties is particularly important in modeling composite fabrication processes and in predicting thermal stresses developed when the materials are subjected to non-isothermal environments. On the one hand, composite fabrication processes involve high coupling between heat transfer within the material and exothermic chemical reactions. The control of these thermal phenomena is a crucial aspect for improvement in productivity and quality of components. Such control requires the ability to simultaneously predict both the temperature distribution within the material and the rate of cure. This necessitates the knowledge of both the thermal properties and the parameters of the kinetic model governing the curing process. On the other hand, thermal stress analysis is essential in the design of aerospace structures and vehicles, as these structures undergo extreme and dynamic thermal conditions. The thermal loads applied on the materials induce large temperature gradients within the structure, which in turn result in the development of thermal stresses and thus possible structural failure. To prevent this, the temperature response of the structure to an applied heat flux must be investigated, which necessitates knowledge of the thermal properties.

The thermal properties necessitated in both fields of study described above include the effective conductivity and volumetric heat capacity. These properties are thermally dependent and due to the anisotropic characteristic of composite materials the conductivity is also directionally dependent. Composites with polymeric matrix and unidirectional fibers are considered in this work. Two conductivity components, parallel and perpendicular to the fiber plane, thus govern conduction within the material. Many experimental and analytical methods have been proposed for determining these thermal properties. An alternative is to use a parameter estimation procedure that consists of the minimization of an objective function, and that allows for the simultaneous estimation of the thermal properties. The objective function usually contains the sum of squared error between measured and calculated temperatures from a mathematical model. Experiments are therefore required with this approach.

The accuracy of the estimated properties is directly related to the sensitivity of the temperature distribution with respect to the thermal properties and can be increased if the experiments are carefully designed (Beck and Arnold, 1977). Experimental parameters such as sensor location, heating time, and heating area are important factors to be considered in the design. Optimization of experimental designs used in the prediction of thermal properties is therefore crucial in maximizing the amount of information that can be obtained from the experiments. The optimal input conditions are typically found by maximizing a single criterion associated with the sensitivity matrix of the unknown properties to be estimated. Among the different design criteria, the *D*-optimality criterion is the most commonly used and is often recommended because it allows thermal property estimates to be obtained with minimum variances. Due to the complexity of an analytical scheme in most cases, the optimization technique typically applied is a stepwise parametric study. However, because it is an iterative process, this technique is tedious and time intensive and therefore restricts the researchers from expanding their work to the optimization of a large number of design variables (e.g. more than three) and to complex designs. In addition to its lack of efficiency, the parametric study does not guarantee the determination of global optima.

The optimal designs are then used in a parameter estimation procedure. Commonly used procedures involve the computation of the gradient. One recommended procedure (Beck and Arnold, 1977) is the modified Box-Kanemasu method that has proven to be effective provided there is sufficient information from the sensitivity coefficients of the unknown thermal properties, and no correlation between the properties. Generally speaking, two parameters are considered correlated when their sensitivity coefficients are nearly (more than 90% as a rule of thumb) linearly dependent. The modified Box-Kanemasu method is a modification of the

Gauss method, which is a first-order unconstrained descent method. However, when used with models that contain correlated or nearly correlated properties, the modified Box-Kanemasu method can show instabilities resulting in non-convergence. Indeed, correlation or near-correlation among parameters is known to be a limiting factor for the converged application of gradient-based estimation procedures. One difficulty in the simultaneous estimation of both directional thermal conductivities of composite materials is that these parameters are correlated. Typically, the approach is, therefore, to first determine the component orthogonal to the fibers using measurements from a specific experimental design and then to assume this property known to estimate the component in the transverse direction using another design.

Correlation is also encountered among the parameters of the kinetic model governing the curing during composite material processing. These parameters usually involve one or two rate constant(s) which follow an Arrhenius law, and one or two exponent(s). Application of gradient-based procedures for the simultaneous estimation of the kinetic parameters is therefore restricted to the identification of the uncorrelated parameters assuming the others to be known.

The need for systematic and reliable methodologies for both (1) Experimental Design Optimization (EDO) used in the determination of thermal properties, and (2) Simultaneous Parameter Estimation (SPE), provided the motivation for this research. The driving force was on developing EDO and SPE procedures that overcome the limits of commonly used ones, parametric studies and gradient-based methods, respectively. Primary efforts were focused on selecting an optimization/estimation method that could efficiently search a multimodal parametric space for a global optimum. The three main types of search methods include calculus-based methods, enumerative techniques and random/probabilistic search algorithms. The first and second type were eliminated as they involve methods that present the same attributes (and therefore same limits) as gradient-based methods and parametric studies, respectively. Methods from the third type, and more particularly those presenting the attribute of probabilistic evolutionary search, have actually achieved increasing popularity as researchers have recognized the shortcomings of the two previous types. Besides their non-gradient nature, their main advantages encompass the ability to avoid local optima and to handle complex non-linear objective functions while being straightforward to apply. Genetic Algorithms (GAs), which belong to the field of evolutionary computation, are based on

genetic and selection mechanisms of nature, and provide for the minimization of an objective function using a probabilistic directed search without the use of derivatives. These algorithms have been theoretically and empirically proven to provide robust searches in complex spaces (Goldberg, 1981), and in this last decade, have shown their effectiveness and efficiency in the engineering field. Because of their advantageous features, GAs were investigated for use in this study as a strategy for both EDO and SPE. The motivation in using GAs was their potential to overcome both the lack of efficiency of parametric studies, and the restriction to the estimation of non-correlated parameters of gradient-based methods, as introduced earlier. Note the originality of this research as there is no knowledge of previous work done with GAs in the field of the thermophysical characterization of anisotropic composite materials.

This work is associated with a dual US-French PhD program between the Department of Mechanical Engineering at Virginia Tech (VT), USA, and the Laboratoire de Thermocinétique de l'ISITEM (LTI) of the University of Nantes, France. The project was initiated at VT as part of a multi-year research cooperation with the Thermal Structures Branch of NASA Langley Research Center, Hampton, VA, USA. The goal of this cooperation, which started in 1993 and ended in 1998, was to develop methodologies for the Thermal Characterization of Aerospace Structures. The strategy used in this multi-year research effort was to first develop methodologies for relatively simple systems and then to systematically modify these methodologies to analyze complex structures. This can be thought of as a building block approach. This work was built upon the previous analysis performed by Moncman (1994) and Hanak (1995). (Also note Moncman et al., 1995). Moncman developed experimental designs for the estimation of thermal properties of composites subjected to one-dimensional heat transfer. Hanak focused on two-dimensional designs and on the experimental verification of these designs. This latter work emphasized the limits of the traditionally used techniques in both design optimization and thermal property estimation. By overcoming these limits, the contribution of this investigation will enable instrumentation of a complex structure and simultaneous acquisition of meaningful property data.

The second stage of this dual program was performed at the LTI in Nantes. The project was incorporated into the applications of the research Group “Thermique des Matériaux et des Procédés de Mise en Forme” (*Thermal Analysis of Materials and of Fabrication Processes*), the goal of which is to analyze inverse problems associated with thermal effects in composite material fabrication processes. The development of genetic-based EDO and SPE

methodologies were thought here to contribute to both the thermal characterization of composite materials and the kinetic characterization of curing processes for the control of composite fabrication processes.

1.2 Goals and Objectives

The overall goals of this research were divided into two major areas:

- I. the development of an Experimental Design Optimization methodology for thermal property estimation,
- and,
- II. the development of a Simultaneous Parameter Estimation methodology for general use.

The emphasis was on formulating sufficiently general and robust approaches allowing for practical applications of the methodologies. In order to achieve these goals, a generalized genetic-based methodology was developed for both areas of interest.

Specific short-term objectives were formulated and are:

1. develop an optimization code based on GAs and validate the optimization methodology on test problems;
2. expand the GA code to include an estimation procedure and validate the estimation methodology on test problems, in particular problems involving correlations among the properties to be estimated;
3. analyze the effects of the optimality criterion in terms of the consequent accuracy of the thermal property estimates;
4. formulate the GA code as a general-purpose computer program for the analysis of any mathematical model; demonstrate its performance on a mathematical test function given in the literature and investigate the effects of genetic operators in terms of convergence of the algorithm;
- and,
5. extend the optimization/estimation methodology to a variety of optimal design and simultaneous parameter estimation problems.

The first two objectives were directed towards the appraisal of using GAs as both EDO and SPE methodologies. First, a standard GA with real-number coding and featuring a Basic Elitist strategy (BEGA) was developed for the optimization of experiments. The optimization methodology was demonstrated and verified using two test cases previously solved in the literature using a parametric study. The experiments investigated included one- and two-dimensional optimal designs performed by Moncman (1994) and Hanak (1995), respectively, for the estimation of thermal properties of composite materials. In the first case, sensor location and heating time were optimized for the simultaneous estimation of the effective thermal conductivity through the fiber plane and the volumetric heat capacity. In the second case, four parameters involving sensor location, heating time and heating area, were optimized in experiments used to simultaneously estimate both effective thermal conductivities perpendicular and parallel to the fibers and the volumetric heat capacity. In both cases, the experimental design was optimized by maximizing the objective function based on the *D*-criterion. To improve the computational efficiency of the BEGA, particularly for expensive objective functions, the algorithm was modified to form an Extended Elitist GA (EEGA). The EEGA was applied to the two test cases discussed above, and the performance of the EEGA was compared with the results from both the BEGA and parametric studies.

The EEGA was then applied towards the estimation of thermal properties. Here, the algorithm was used to minimize an objective function based on the least squares error. Two case studies involving nonlinear parameter estimation were used to demonstrate the effectiveness of the EEGA. The first concerned the simultaneous estimation of two and three thermal properties of an anisotropic composite material using the experimental designs optimized in the optimization test problems described above. These estimation problems were investigated previously by Hanak (1995). The second test case involved a one-dimensional transient analysis of combined conduction and radiation heat transfer in an insulative foam material (polystyrene) for the simultaneous estimation of four thermal and radiative properties. These included the effective thermal conductivity, volumetric heat capacity and extinction coefficient of the material, and the volumetric heat capacity of the heater. This study was realized in cooperation with J. Guynn (1996) as part of his master's thesis in Mechanical Engineering at VT. The results are not reported in this dissertation however, but can be found in the literature (Garcia et al., 1998). In both case studies, the properties were estimated as constants at ambient temperature.

Once the GA-based optimization/estimation methodologies were assessed, a study was conducted to evaluate the effects of the optimality criterion used for the experimental design on the accuracy of the estimated thermal properties. The one- and two-dimensional transient heat transfer analyses associated with the simultaneous estimation of two and three thermal properties of an anisotropic material (Hanak, 1995) and discussed previously, were also used here. The experimental designs in both analyses were optimized using the *A*-, *D*-, and *E*-optimality criteria, which are the three main criteria proposed for the design of experiments. Based on these optimal designs, simulated data were generated using an analytical mathematical model of the design. The thermal properties were then estimated from the simulated data from each experimental design, and the confidence intervals of the resulting estimates were compared. EEGA was used as both the optimization and estimation methodologies.

The completion of the first three specific objectives concluded the first stage of this dual Ph.D. program initiated at VT. The genetic-based optimization and estimation methodologies developed at VT were used by Hanuska (1998; also in Hanuska et al., 1999) for the thermal characterization of a complex aerospace structure (composite/honeycomb panel). This work was performed as part of his master's thesis in Mechanical Engineering at VT and concluded the multi-year research cooperation sponsored by the Thermal Structure Branch of NASA Langley Research Center.

The second stage of this dual program was performed at the LTI in Nantes. Efforts focused on accomplishing the last two specific objectives. Prior to formulating a general-purpose computer program, a third GA, GA_3, was developed built upon both the previous work and the experience gained in the GA field. The algorithm was then constructed in two parts, an invariant and an adaptation part, following the structure of the program CONDUCT developed by Patankar (1991). The invariant part contains the general calculation scheme that is common to all possible EDO/SPE problems within the overall restrictions of the program. It is written without any knowledge or assumption about the particular details of the problem to be solved. The user provides the problem specification in the adaptation part. Based on the GA_3 structure, two versions were developed. The GAMAIN version was designed for the analysis of any optimization/estimation problems for which a mathematical model can be provided in the adapt part. In heat transfer analyses for which an analytical solution cannot be obtained, the GA CONDUCT version was used. The latter combines the feature of GA_3 with

a finite difference program based on an extension of the program CONDUCT. Therefore, the use of GACONDUCT allows for any EDO/SPE applications that deal with the computation of conduction and duct flow heat transfer in two-dimensional rectangular or cylindrical geometry.

To illustrate the performance of the GA_3, a mathematical function called f_6 (Davis, 1991) was optimized using GAMAIN. This test case was also used as a basis for the investigation of the effects of some genetic operator variants in terms of convergence of the algorithm.

The general-purpose optimization/estimation GA_3 program was then applied to a variety of EDO and SPE problems. The applications performed were in agreement with the research environment at the LTI. As part of an industrial contract, the GACONDUCT was used in the simultaneous estimation of the thermal properties of composite materials (effective thermal conductivities perpendicular and parallel to the fibers and volumetric heat capacity) over the temperature range [30-150°C]. To take into account the temperature dependence in the properties, these latter were sought to be estimated as constant at six different temperature levels that covered the required range. Taking advantage of the estimation problem similarities with the two-dimensional transient heat transfer analysis performed by Hanak (1995), experiments were based on the same basic experimental design, and the same nondimensional optimal experimental parameters were used. Additionally, this study required the use of an apparatus to control the initial temperature inside the samples. An interesting personal aspect of this application was the opportunity to gain experience in conducting experimental work. This study was then used as a basis to investigate the optimization of the experimental design for the simultaneous estimation of parameters describing the temperature dependence in the thermal properties. This dependence was approximated by a piece-wise linear function with temperature. Nine parameters were used to represent the thermal properties over the range [25-150°C]. The D -optimality criterion was used to optimize seven experimental parameters. These latter included sensor location, heating parameters, and heating area. The estimation methodology was then demonstrated on simulated data generated from the optimal design.

The GACONDUCT was also applied to the simultaneous estimation of seven thermophysical parameters associated with the processing of composite materials in a two-dimensional RTM (Resin Transfer Molding) mold. This work was performed in cooperation with D. Lecoite (1999) as part of his PhD project at the LTI. The parameters estimated

included the temperature dependence of the material thermal properties over the range [100-130°C]. The results obtained were compared with those from Lecoite who used a parametric study to estimate the conductivity parallel to the fibers assuming both the orthogonal component and the volumetric capacity to be known.

Finally, a study was conducted for the kinetic characterization of the curing of composite matrix materials, namely thermosetting materials. Such characterization is an important aspect in the control of the thermal phenomena during composite material fabrication. This control involves modeling the coupling between heat transfer and exothermic chemical reaction inside the matrix material and thus requires knowledge of the dependence with temperature of not only the thermal properties but also the rate of cure. This latter is described by a kinetic model governing the curing process. Because of its popularity in the composite industrial world, the model from Kamal and Sourour (1973) was selected for the prediction of the curing process of an epoxy, a polyester and a rubber. Furthermore, the use of this model provided the investigation of a complex simultaneous estimation problem as strong correlations are present among the kinetic parameters involved. The general-purpose program GAMAIN was applied for the determination of these parameters. The experimental data required in the estimation methodology were obtained from Differential Scanning Calorimetry (DSC).

CHAPTER 2

Literature Review

This chapter summarizes the present state of knowledge pertaining to the areas of interest of this research. These are thermophysical characterization of composite materials, experimental design optimization, and Genetic Algorithms (GAs). After a brief description of composite materials in the first section, the second deals with both thermal characterization of composite materials and kinetic characterization of the curing of composite matrix resins. Particular attention is given to optimal experiments designed for the estimation of thermal properties in the third section, while the review of previous uses of GAs in the last section focuses on their application in engineering.

2.1 Composite Materials

A composite material is composed of two or more materials joined together to form a new medium with properties superior to those of its individual components. Often, the term composite is used for fiber-reinforced composites, although different reinforcement forms exist. Fiber-reinforced composites (laminates) consist of several unidirectional layers arranged at the same or different angles and, therefore, present heterogeneous, anisotropic properties. These materials can be classified as continuous or discontinuous. The most commonly used reinforced fibers are carbon/graphite and glass, while the major types of matrix resins consist of thermosetting, elastomer and thermoplastic materials with the addition of a curing agent. The composite materials and matrix resins focused on in this study consist of continuous carbon fiber/epoxy matrix combinations (with unidirectional fibers), and epoxy, polyester and rubber mixtures, respectively.

The use of composite materials is constantly increasing in modern industry. The main

reasons are low weight, high performance in terms of both mechanical and thermal properties, and relatively low cost. The study of the different aspects of physical and chemical phenomena taking place during material production is therefore of intensifying interest. In order to predict and control the fabrication/molding processes, thermophysical characterization of these materials is required. Due to the high coupling between heat transfer from conduction within the composite being cured and heat release from exothermal effects of the reticulation reaction, such characterization is comprised of both thermal and kinetic components. This necessitates that the thermal properties and the parameters of the kinetic model governing the curing process are known.

On one hand, because a composite is made of at least two different materials each with different thermal properties, effective thermal properties are usually needed and were considered in this research, assuming the materials to be homogeneous in each direction. Therefore, in the work presented here, the subscript “eff” was omitted. The thermal properties estimated were the thermal conductivity and volumetric heat capacity. These properties depend on temperature and as a result of fiber orientation, the thermal conductivity is also directionally dependent. Both temperature and directional dependence make the determination of the thermal properties a challenging task.

On the other hand, the kinetic parameters to be determined are associated with the model selected to govern the curing of the matrix resin. Therefore, one difficulty in adequate kinetic characterization is the selection of an appropriate model.

2.2 Thermophysical Characterization of Composite Materials

2.2.1 Thermal Characterization

Much work has been done for the accurate determination of the thermal properties of isotropic and anisotropic materials. Parameter estimation techniques can be typically classified as experimental and inverse. Experimental techniques are associated with a particular experiment (the technique is actually referred to by the name of the experiment), while inverse techniques include a wide variety of methods, all of which involve the use of experimental data in conjunction with a mathematical model describing the thermal phenomena. In the field of composite materials, a third class of techniques exists, which is

commonly referred to as analytical (also called “micromechanical”). The following provides a synopsis of the three classes.

- **Analytical methods**

Analytical methods are based on the mathematical analysis of the components of the composite. Their use involves the assumption that the thermal properties of the individual composite elements, namely the matrix and the fiber, are known, along with the volume fraction of the fibers. Several such models for the effective thermal properties of composites have been proposed. One very well known model is the Rule-of-Mixtures for which one can write

$$k = k_f V_f + (1 - V_f) k_m \quad \text{and} \quad \frac{k}{\rho C_p} = \frac{V_f k_f + V_m k_m}{V_f (\rho C_p)_f + V_m (\rho C_p)_m} \quad (2.1)$$

where k is the thermal conductivity with heat flow parallel to the fibers, (ρC_p) is the volumetric heat capacity, k_f and $(\rho C_p)_f$ and k_m and $(\rho C_p)_m$ are the properties of the fiber and the matrix, respectively, and V_f and V_m are the fiber and matrix volume fraction, respectively. Progehoff et al. (1976) indicated that none of the correlations developed accurately predicts the thermal properties of all types of composites. Their work also provides a review of additional models to predict the thermal conductivity of composite systems.

- **Experimental Methods**

Experimental methods can be further classified into steady-state and transient methods (Degiovanni, 1994). Steady-state techniques are limited to the sole estimation of thermal conductivity. The guarded hotplate method is a frequently used steady-state technique in which the specimen is heated by a hot metal plate attached to it and the resulting temperature is measured at the interface. The (effective) thermal conductivity is directly determined from Fourier’s law. One disadvantage with this technique is that it is expensive and time consuming due to the necessity for the experiment to be repeated at different temperature levels, and for the material to reach steady state.

Transient techniques allow for the estimation of several properties, such as the thermal diffusivity, thermal conductivity and/or other groups incorporating the conductivity and volumetric heat capacity. The most common transient method is the flash method in which the front surface of a small cylindrical specimen is exposed to an energy pulse and the temperature history is recorded on the back surface. The thermal diffusivity is identified from adjusting the theoretical temperature history obtained from a mathematical model to the measured temperature history. This can be achieved from the use of two different estimation methodologies (André and Maillet, 1999):

- 1/ the solution from analytical expressions associated with the knowledge of the Fourier number from either two partial times or two periods.
- 2/ the minimization of the least-squares error between calculated and measured data over several observations. The definition of this error as well as the inverse estimation procedure needed to minimize it are discussed later. Researchers at the Laboratoire d'Energétique et de Mécanique Théorique et Appliquée (LEMETA, Nancy, France), for instance, use successively both estimation methods (André and Maillet, 1999).

The heat capacity is typically determined using Differential Scanning Calorimetry (DSC). This experimental method is based on the principal of differential enthalpic analysis and involves providing heat both to a very small sample and to an inert reference sample at a varying rate so as to maintain their temperatures equal. The calorimeter is employed in scanning mode to determine the heat capacity as function of temperature. The product of the heat capacity with density results in the volumetric heat capacity.

The guarded hotplate, the flash, and the DSC methods are the major experimental techniques currently used to determine the thermal properties of composite materials. One however realizes that these methods do not allow for either the simultaneous estimation of the thermal properties, or the investigation of complex structures involving several materials which cannot be disassembled. In addition, besides the DSC method, the other methods are limited to the estimation of constant properties at a particular temperature level.

- **Inverse Methods**

Definition

The limitations of the experimental methods have led to the increased use of inverse parameter estimation techniques. Note that in the heat transfer area, one commonly refers to parameter estimation problems as the problems of determining unknown thermal properties based on known boundary and initial conditions, while inverse heat conduction problems are associated with the finding of boundary and initial conditions (function estimation) given known thermal properties. Parameter estimation methods are non-invasive techniques that allow for the simultaneous estimation of the thermal properties of individual materials as well as complex structures for any kind of appropriate experiments, provided these are feasible and a mathematical model can be formulated. “Appropriate experiments” implies that information is provided about the unknown properties. For instance, it is necessary for the experiments to be transient to estimate the volumetric heat capacity and for one of the boundary conditions to be a heat flux condition in order to estimate thermal conductivity and volumetric heat capacity simultaneously.

Inverse parameter estimation methods are based on the minimization of an objective function containing both calculated and measured temperatures (Beck and Arnold, 1977). Depending on the amount of information available about the experimental data and the parameters to be estimated, three main estimators are available to define the objective function. These include:

- 1/ Ordinary Least Squares (OLS) estimator, in which no prior knowledge about either the parameters estimated or the variances of the measurement errors is required.
- 2/ Maximum Likelihood (ML) estimator, in which prior knowledge about the variance of the measurement errors can be implemented.
- 3/ Maximum A Posteriori (MAP) estimator, in which prior knowledge about the variance of both the measurement errors and the estimated parameters is used.

All three estimators are described in detail by Beck and Arnold (1977). The OLS estimator is by far the most frequently used for the estimation of thermal properties as no prior knowledge is needed. This estimator was considered in this research. The associated objective function, the least squares error S , is expressed by:

$$S(\boldsymbol{\beta}) = \sum_{k=1}^{N_k} \sum_{i=1}^{N_i} [T_{ki}(\boldsymbol{\beta}, \tilde{x}, \tilde{t}) - \tilde{T}_{ki}]^2 \quad (2.2)$$

where $\boldsymbol{\beta}$ is the true parameter vector containing the unknown thermal properties, \tilde{x} and \tilde{t} are position and time for the i^{th} observation from the k^{th} sensor, N_k and N_i are the numbers of sensors and observations, respectively, T is the calculated temperature from the mathematical model governing the heat transfer phenomena and \tilde{T} is the measured temperature. In using Eq. (2.2), the thermal properties are found by minimizing the sum of squared differences between the measured and calculated data. It should be mentioned that if the parameters are to be estimated from measurements of two dependent variables, say T and q , then the least squares errors associated with each dependent variable should be nondimensionalized by dividing by the respective measurement variance, allowing thus the addition of both errors to form a global error. This was investigated by Robinson (1998). Note also that although parameter and function estimation problems are both inverse problems, the ill-posedness of the latter may require the addition of regularization terms in the objective function (Beck et al., 1985).

Techniques

The minimization of Eq. (2.2) could conceivably be performed by any optimization technique. However, parameter estimation has generally been performed with only a few methods, none of them being a standard. Actually, the use of one method over another is often specific to a certain field of study. The simplest parameter estimation method is the parametric study, which is a numerical iterative method. This study is usually performed in two phases: the first includes determining the general range of the properties optimal values, while the second narrows this range to determine the values more precisely. If needed, the process is repeated to converge to the final estimates. As one can easily guess, this technique is tedious and time intensive and, in addition, the process does not guarantee that the global minimum of S will be found. But, because it is so easy to implement, the parametric study is often used to estimate one or two properties.

One commonly used gradient-based technique is the Gauss linearization method which is a first unconstrained descent method. The minimization of S is realized by differentiating S with respect to $\boldsymbol{\beta}$, setting the resulting equation equal to zero, and then solving iteratively for \mathbf{b} , the estimated parameter vector for $\boldsymbol{\beta}$ using the Taylor series approach to linearize the

equation. This method is described (Beck and Arnold, 1977) as one of the simplest and most effective methods for seeking minima provided the initial estimates are in the neighborhood of the minima, and this latter is reasonably well defined. In this last condition it is meant that, on one hand, the dependent variable (usually T) is sufficiently sensitive to changes in the properties, and on the other hand, the properties are far from being nearly correlated. Box and Kanemasu (1972) modified the Gauss method by changing the step size used in seeking minima with an aim to compensate for poor initial estimates or severe nonlinearity in the model which could cause large oscillations to occur from one iteration to another, leading then to non-convergence of the estimates. A further improvement involving the check that the function S decreased from one iteration to another was realized by Bard (1974). This consisted in reducing the step size by one-half if the function was not decreasing. The modified Box-Kanemasu method, however, still required the minima to be reasonably well-defined as explained above. Theoretical details on this method are given in Chapter 3.

Beck was the first to use the Gauss method to estimate the thermal diffusivity in 1963. He then expanded the Gauss application to the estimation of the thermal conductivity simultaneously with the volumetric heat capacity of nickel from one-dimensional transient temperature measurements (1966). The simultaneous estimation of the thermal conductivity perpendicular to the fiber plane and the volumetric heat capacity of composite materials has been widely performed using both the Gauss and modified Box-Kanemasu methods. Scott and Beck (1992a) estimated these thermal properties for carbon/epoxy composites as function of temperature and fiber orientation. Their results show that the thermal properties increase with temperature and that different stacking orientations result in significantly different thermal conductivity values. These authors also developed a methodology for the estimation of these two properties in the same composite materials during curing (1992b). Garnier et al. (1992) were able to estimate these two properties using temperature measurements made with thin resistance thermometers and surface thermocouples instead of internal temperature measurements. The work from Moncman (1994) and Hanak (1995) show that the simultaneous estimation of the thermal conductivity perpendicular to the fiber plane and the volumetric heat capacity of composite materials has become successfully routine. The Gauss method was also used by Jurkowski et al. (1992) for the simultaneous estimation of the thermal conductivity of thermoplastic materials and thermal contact resistance, assuming the volumetric heat capacity to be known. As in the work from Garnier et al. (1992), no embedded sensors were used. One interesting conclusion from this study is that small

sensitivity coefficients or the unbalance of the sensitivity matrix resulted in the instability of the estimation procedure. This particular remark goes along with the fact that both the Gauss and modified Box-Kanemasu methods have been found to show instabilities resulting in non-convergence when used with models that contain correlated or nearly correlated thermal properties. For instance, Hanak (1995) used the modified Box-Kanemasu method in association with two-dimensional transient experimental data and was unable to simultaneously estimate the thermal conductivities along two perpendicular planes and the volumetric heat capacity of anisotropic composite materials because of correlation between both thermal conductivities. Copenhaver (1996; also in Copenhaver et al., 1998) was also faced with non-convergence of the modified Box-Kanemasu method when trying to simultaneously estimate correlated radiative and conductive properties of a honeycomb sandwich structure. A quantification of correlation is given in the next chapter (Section 3.1.3).

Several different approaches have been used to address this correlation-based non-convergence problem. One approach is to modify the experimental design. For example, Loh and Beck (1991) were able to simultaneously estimate both thermal conductivities and the volumetric heat capacity of an anisotropic carbon/epoxy composite through the use of nine thermocouples embedded at various locations within the sample. It is interesting to note that the number and location of the sensors were fixed a priori by the authors and the potential correlation problem was never detected. Correlation may have still been present but the use of multiple sensors allowed it to be bypassed. Box has actually shown that high correlations among the parameters can be due to a large extent to the nature of the model itself and thus no experimental design could be expected to yield uncorrelated parameter estimates (Beck and Arnold, 1977). Loh and Beck used the Gauss method and found the conductivity parallel to the fiber plane to be about seven times larger and to increase more with temperature than transverse to the fiber plane. A similar approach was accomplished by Dowding et al. (1996) for the simultaneous estimation of the thermal properties of anisotropic carbon/carbon composites. Nevertheless, modifications of the experimental design, such as the use of internal sensors, are not always feasible, especially when nondestructive testing is required. In addition, the use of embedded thermocouples can be a source of important bias. In characterizing this bias, Taktak (1991) reported that experiments showed higher dependence of the temperature disturbance on errors in the embedded thermocouple locations than errors in the thermal properties. Another approach used to address the correlation problem is to modify the minimization method. For example, Copenhaver (1996) (note also Copenhaver et

al., 1998) used a constrained parameter estimation procedure based on a penalty function method, with limited success, to simultaneously estimate three nearly correlated thermal properties of a honeycomb sandwich structure.

The approach investigated in the present work involves the use of a robust non-gradient method, namely the Genetic Algorithm (GA) method, in the minimization procedure. The motivation for using GAs was to circumvent difficulties of non-convergence in cases when the parameters are correlated or nearly so. An overview of these algorithms is provided in the last section of this chapter.

2.2.2 Kinetic Characterization

The curing of thermosetting materials is a complicated process, the main parts of which are chemical transformation coupled with heat transfer. For the chemical transformation and more particularly, the exothermic source term, to be characterized, a kinetic model is required. Kinetic models can be divided into two general types: on one hand, the models based on the knowledge of each elementary chemical reaction, and on the other hand, the empirical ones that try to represent the kinetics of reactions when the reaction path is not well known. These latter have the advantage of allowing for the analysis of complex transformations, which is the case for the curing of elastomer or thermosetting compounds used in molding processes. They provide relationships between reaction rate ($d\alpha/dt$), degree of reaction (α) and temperature (T). In the field of thermosetting polymers, several different empirical models have been developed to characterize curing. They are often referred to as describing autocatalyzed reaction rate mechanisms as the material contain substances (curing agents) that accelerate the reaction rate. Figure 2.1 illustrates a typical reaction rate evolution versus time during curing of a thermosetting material. For the complete representation, the kinetic model is preceded

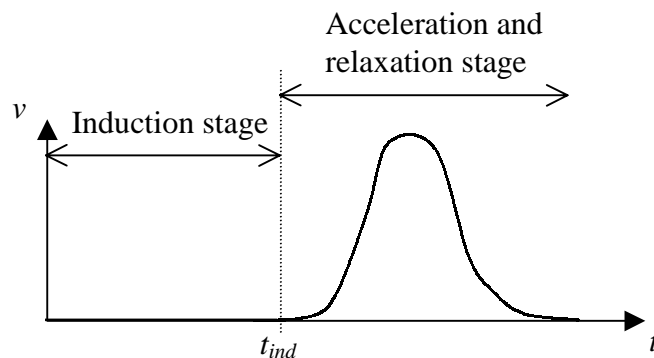


Figure 2.1 Typical reaction rate evolution versus time during curing of thermosetting polymers.

with a model describing the induction stage, t_{ind} . This represents the time during which the reaction is inhibited as a result of inhibition substances contained within the material.

The model from Kamal and Sourour (1973) is a very well known empirical kinetic model, which has been found to provide a reasonable degree of accuracy for a variety of thermosetting systems. It contains two rate constants K_1 and K_2 that are assumed to have an Arrhenius temperature dependence and two kinetic exponents m and n to describe the order of the curing mechanism as shown below.

$$\frac{d\alpha}{dt} = (K_1 + K_2 \times \alpha^m)(1 - \alpha)^n, \quad K_i = A_i \exp\left[-\frac{E_i}{RT}\right], \quad i = 1,2 \quad (2.3)$$

The parameters K_1 and K_2 represent the catalytic and the autocatalytic nature of the reaction, respectively. When the parameter K_1 is negligible, the terms containing the dependent variables T and α can be mathematically separated. The model becomes then similar to that suggested by Piloyan et al. (1966). Jarny et al. (1993) developed for that case a new model expressed by the product of a rate constant K that follows the Arrhenius law and a polynomial function of α expressed below:

$$\frac{d\alpha}{dt} = K(T) \times F(\alpha) \quad (2.4)$$

The model from Jarny et al. has been successfully applied to the kinetic characterization of the curing of a rubber (Amiaud, 1993), an epoxy (Bailleul, 1993; 1997; Bailleul et al., 1996), and a polyester resin (Mouchnino, 1997).

Using the kinetic model from Kamal and Sourour (1973), one typically assumes a known combined order mechanism ($m+n$), which is generally second order (Kamal et al., 1973), and therefore the parameters estimated are the two rate constants K_1 and K_2 . The most commonly used method of determining them involves the use of linear regression and isothermal Differential Scanning Calorimetry (DSC) which provides heat flux measurements. The rate constants are identified at different temperatures from which the Arrhenius constants can be deduced. One of the disadvantages with this approach is that the Arrhenius constants cannot be estimated directly.

An alternate approach is to use an inverse parameter estimation method that can be used for nonlinear models. As mentioned in the previous section, this involves the minimization of an objective function, for instance the least squares error. Scott and Saad (1993a,b) studied the model from Kamal and Sourour assuming a combined second-order, autocatalyzed reaction

rate mechanism during the first portion of the cure to describe the curing of an amine epoxy resin. Using the Box-Kanemasu method, they were able to perform the direct estimation of the four Arrhenius constants from both isothermal DSC and dielectric data. They conducted sensitivity analyses that showed that the degree of cure was most sensible to changes in the parameters K_1 and K_2 than the rate of cure. Furthermore, Scott and Saad pointed out that the use of the degree of cure as the dependent variable associated with isothermal data allowed minimization of the correlation between the sensitivity coefficients of the parameters and maximization of their magnitudes. On the contrary, strong linear dependence between the coefficients of the parameters A_1 and E_1 and A_2 and E_2 was stressed when using dynamic data. In comparison with the commonly used linear regression method, the work by Scott and Saad is a great improvement in the curing characterization of epoxy systems. However, their study assumed a known combined order mechanism, restricting thus the estimation procedure to the four Arrhenius parameters. In addition, by limiting the estimation procedure proposed by Scott and Saad to isothermal experiments, one cannot investigate materials that react very fast and for which only dynamic data can be obtained.

For the cure modeling of a polyester resin, Guyonvarch (1995; also in Guyonvarch et al., 1995) also used the model from Kamal and Sourour in association with isothermal DSC data. To limit both the number of parameters to be estimated and the presence of correlation among the sensitivity coefficients, he assumed the parameter m to be known, and set its value arbitrarily to unity. His work involved the application of the Gauss-Newton method in two steps: first, he tried to identify simultaneously the rate constants K_1 and K_2 along with the parameter n ; next, he fixed n to the average estimated value obtained previously (with an error of $\pm 18\%$), and determined the values of K_1 and K_2 . Eventually, knowing K_1 and K_2 at each different temperature investigated, the four Arrhenius constants could be found from a graphical procedure. It is interesting to note that simulations using the completed kinetic model fit isothermal DSC runs well, but were relatively far off when dynamic DSC data were considered.

One can note the work of Bournez et al. (1999) who investigated the estimation of five kinetic parameters associated with an equation derived from the Kamal and Sourour model, simultaneously with the thermal properties (conductivity, heat capacity and density) of a rubber modified epoxy resin. Their work presents a methodology to determine these thermophysical parameters from a single dynamic experiment carried out in an experimental mold. The Gauss method and the MAP estimator were used as the estimation procedure.

However, because of significant magnitude differences between the sensitivity coefficients of the parameters, the simultaneous estimation was restricted to a sequential estimation by groups of parameters of similar influence (sensitivity) on the temperature response. The most influential parameter was found to be the Arrhenius constant E of the kinetic model used, and was identified alone first.

The limitations of the work of Scott and Saad (1993a,b), Guyonvarch (1995) and Bournez et al. (1999) show that the investigation of nonlinear kinetic models, and in particular the model from Kamal and Sourour, in association with the use of dynamic experimental data remains a very difficult estimation problem. The difficulties come mainly because of strong correlations and difference of influence (sensitivity) on the model among the parameters. The ability to solve such estimation problems would be particularly significant in the field of composite matrix resins as kinetic models are used to characterize curing during fabrication processes which involve dynamic experiments. This was one of the objectives of the work presented here.

It is relevant to note that with the use of the two kinetic models described in Eqs. 2.3 and 2.4, an induction period should be defined to represent the time during which the reaction is inhibited, e.g., corresponding to null thermal effects, as illustrated in Fig. 2.1 (Garnier, 1990). This period is governed by its own kinetic model that depends both on temperature and on the “thermal history” of the material being analyzed. Bailleul (1997; also in Bailleul et al., 1996) used an integral function $h(t,T)$ that is a function of time and which represents (in absolute value) the time left before curing starts. The induction period, t_{ind} , is over when the function $h(t,T)$ becomes null.

$$h(t,T) = t_{ref} - \int_0^t \exp\left[-B \times \left(\frac{T_{ref}}{T} - 1\right)\right] dt \quad (2.5)$$

The inhibition model described by the function $h(t,T)$ involves the selection of an arbitrary reference temperature, T_{ref} , within the range investigated and the determination of two parameters, t_{ref} and B . This estimation is very difficult because of the correlation between the sensitivity coefficients of the two parameters, and typically the values for t_{ref} and B are obtained using a parametric study. The inhibition time model used in the current research for the kinetic characterization of the curing of thermosetting materials (Chapter 6) is based on a modification of Bailleuil’s integral function.

Eventually, to obtain the experimental data required in the estimation procedure, calorimeters such as Differential Scanning Calorimetry (DSC) apparatuses are usually used because heat flux released by the chemical reaction is proportional to the rate of reaction (Scott and Saad, 1993a,b, Garnier et al., 1993). As far as the evaluation of DSC apparatus is concerned, three precision indicators have been proposed by Garnier and Danès (1994). These indicators are based on isothermal operation of the DSC while empty, and include a time constant from a constant slope increase to a constant level, a time drift and background noise. Note however, that some recent work (Sommier, 1998) has shown for some thermosetting materials the feasibility of using microdielectrometry for the online study of degree of cure evolution during curing.

2.3 Experimental Design Optimization

This section deals with optimization in the service of design-of-experiments, that is optimization employed to provide the maximum amount of insight and information on the phenomena being analyzed. A review of optimization in relationship to experiments in four aspects has been reported by Haftka et al. (1997). These aspects include the use of optimization for designing efficient experiments (called “analytical optimization”, the subject of this section), the use of experiments to perform optimization (called “experimental optimization”), the use of techniques developed for experimental optimization in numerical optimization and eventually, the importance of experimental validation of optimization. In their review, Haftka et al. provide applications from a variety of fields.

Design-of-experiments for the estimation of parameters has been subject to numerous studies. Most of the early publications deal with the field of statistical inference and data analysis (Brown et al., 1985), while an increasing number of publications can be found over the past two decades in the field of engineering design. When the purpose of the experiments is to estimate properties, the objective of experimental design optimization is to improve the accuracy of the predicted properties. The selected design variables are “sized” to minimize the uncertainty in the resulting property estimates, thus providing the most accurate estimates (Beck and Arnold, 1977; Walter and Pronzato, 1994). Design-of-experiments can be performed simply by carefully examining the sensitivity coefficients of the parameters to be estimated or, in a more rigorous methodology associated with optimal experimental design theory, by applying an optimality criterion. In both cases, this procedure is an imperative step prior to the implementation of the inverse parameter estimation procedure. Based on the book

of Beck and Arnold (1977), the work of Raynaud (1999) illustrates with simple examples the various steps that must be accomplished in the strategy for optimization of experimental design and estimation of parameters.

2.3.1 Sensitivity Study

First of all, a careful sensitivity study can enable the distinction of which properties can be correctly estimated (known as identifiability study). The sensitivity coefficients are the derivatives of the experimental process variables, such as temperature, with respect to the unknown parameters, for example, the thermal conductivity. Obviously, uncorrelated parameters with the highest sensitivity coefficients should be chosen to be identified. In the analysis of sublimation-dehydration within a porous medium, Scott (1994) conducted a sensitivity study which examined the importance of the material properties on the solution. Scott was able to conclude for which parameter temperature provided the most accurate information. A similar study was performed by the current author (1994) in investigating the simultaneous estimation of the thermal conductivities of individual components constituting high temperature superconductive thermal bridges. She found that only the effective thermal conductivity of the composite superconductive thermal bridges could be estimated.

Sensitivity studies also allow improvement of an experimental design to be used in the determination of properties by selecting experimental conditions that minimize sensitivity to parameters assumed known (set to nominal values) in the mathematical model. This ensures that uncertainty from these supposedly known parameters does not greatly affect the accuracy of the estimation of the unknown desired parameters. One example in which such a sensitivity study is particularly adequate is in the investigation of the effect of convection heat transfer coefficients used at boundary conditions. Usually, the sensitivity to these parameters is low at the beginning of the experiments and then increases. The choice of the optimal total overall experimental time should take into account that the sensitivity to the known convection heat transfer coefficients must remain low.

Sensitivity studies can also be used to find the experimental conditions that maximize the magnitude of the sensitivity coefficients of the unknown parameters. However, one can easily guess that when two or more parameters are sought, the use of the magnitude of the individual sensitivity coefficients as a reference becomes messy and, therefore, the design activity needs to be posed in terms of an optimality criterion (objective function) to maximize. The work of Totorelli and Michaleris (1994) that reviews the state of design sensitivity

analysis is noted. This review shows that sensitivity applications in optimization are numerous and gives many references, including those for thermal systems.

2.3.2 Optimality Criterion

- **Definition**

An optimality criterion can be interpreted as a measure of the goodness of the design. Although its establishment should not be codified in terms of a single recipe, the optimality criterion is usually associated with the Fisher information matrix of the design (named after R. A. Fisher's pioneering contributions to statistical inference, Kiefer, 1975a; Walter and Pronzato, 1994). The Fisher information matrix is defined by $\mathbf{X}^T\mathbf{X}$, where \mathbf{X} is the sensitivity matrix. The most often encountered optimality criteria include the maximization of the determinant of $\mathbf{X}^T\mathbf{X}$ (*D*-optimality), maximization of the minimum eigenvalue of $\mathbf{X}^T\mathbf{X}$ (*E*-optimality) and maximization of the trace of $\mathbf{X}^T\mathbf{X}$ (*A*-optimality). Theoretical details on these criteria are given in Chapter 3. The first criterion is the most common. Note that Alifanov et al. (1995) have shown that an optimality criterion based on the maximization of the inverse of the condition number of the Fisher information matrix is the most appropriate for the study of heat conduction, but that the use of *D*-optimality is nearly equivalent. The effect of *D*-optimality is, in the normal case, to minimize the volume of the usual confidence ellipsoids of the estimated values, providing the minimum variance estimators. *D*-optimality proponents have also pointed out that this criterion is invariant under linear transformation of the estimated vector. That is, the same design is *D*-optimum for estimating $Z\boldsymbol{\beta}$ as for estimating $\boldsymbol{\beta}$ if Z is a nonsingular matrix. However, this criterion has been found to weigh heavily on the parameters with the highest sensitivity while sacrificing much in the accuracy of the parameters with the least sensitivity in order to make the confidence volume small (Kiefer, 1975b; 1981). For instance, in the design of experiments for the thermal characterization of honeycomb core structures (conductive and radiative properties), Copenhaver (1996) pointed out that the use of the *D*-optimality criterion would increase the accuracy of the parameters with high sensitivity at the expense of creating a large error in those with low sensitivity. Other known criteria associated with the Fisher information matrix exist, for instance the *C*-, *L*-, *V*- and *G*-optimality, with the latter two being more appropriate for response estimation than parameter estimation. This family of criteria has been discussed in more details by Kiefer (1974; 1975a) and Walter and Pronzato (1990).

Another strategy in the selection of the objective function is to develop a compromise or compound criterion (Kiefer, 1974; 1975b). This heading describes criteria “built-up” from simpler criteria. Such a strategy has the effect of combining the features and/or of eliminating some of the objections of the single criteria used to build up the compound criterion. Pronzato and Walter (1989) defined the *V*-criterion, which is similar to the *D*-optimality criterion, but which assumes that prior lower and upper bounds are available for the noise associated with the measurements. Because of the shortcomings displayed by the *D*-optimality criterion, Copenhaver (1996) used a combination of *D*-optimality with the minimization of the maximum scaled length of the confidence intervals. This latter criterion was actually proposed earlier by Lohman et al. (1992). The work from Nenarokomov et al. (1998) is a recent example of the use of a compound criterion, in which not only measurement noise but also uncertainties in the known model parameters have been incorporated in the *D*-criterion. Some previous developments have also emphasized the use of multicriteria optimization as a strategy in the design process (Eschenauer et al., 1990). This results from the fact that nowadays, in many engineering applications, often several conflicting criteria have to be considered by the designer. Such optimization problems for multiple criteria are called either *Vector* or *Multicriteria* Optimization Problems and the output from the optimization process is called a set of Pareto optimum. The utilization of multicriteria in the optimization of experimental designs used to estimate thermal properties has not been thoroughly investigated yet.

- **Optimization Techniques for the Design-of-Experiments**

Following the selection of the optimality criterion, a mathematical optimization procedure is needed to determine the optimal experimental parameters which satisfy the selected criterion. In the general field of design-of-experiments for the estimation of parameters, three classes of procedures have been distinguished. The first class contains exhaustive search algorithms which generate and evaluate all possible designs. This is very time consuming. Welch (1982) developed a variant called “branch and bound” in which a binary tree of minimization problems is generated. Not all designs are generated and evaluated. By exploiting bounds on the minimization, only the branches which might contain the optimal design are created. Although such algorithms guarantee that the global optimal design will be found, the computing costs are still extremely high. The second class includes analytical procedures which consist of maximizing the objective function by differentiating it with respect to each of the design variables and then solving the resulting set of equations

simultaneously for the optimal values of the design variables. Due to the complexity of the equations involved, this method is rarely chosen. Finally, the third class has usually been concerned with the exchange algorithms, which are iterative combinatorial random optimization procedures. Mitchell (1974) developed an efficient such algorithm called DETMAX which has been extensively used for determining D -optimum designs in a variety of engineering applications (Eschenauer et al., 1990). DETMAX is based on the notion of sequence of excursions from an initial design, in which several points are added in one single step and subsequently the same number of points that result in the smallest increase in the determinant (D -optimality) are removed. This algorithm was found to generate high quality D -optimal designs at relatively low computing costs but did not ensure that the global optimum will be found. Note that the “simulated annealing” approach, introduced by Kirkpatrick et al. (1983), was thought by Mitchell to be a potential optimization procedure to be applied to exchange algorithms for deriving experimental designs. What is interesting with this last remark is that simulated annealing and genetic algorithms, which were used in this work, share some of their stochastic steps.

- **Design-of-Experiment Applications for the Estimation of Thermal Properties**

In the design-of-experiments for the estimation of thermal properties, a simple iterative numerical approach, the parametric study, which belongs to the class of “exhaustive” procedures, has typically been used for its simplicity (Beck and Arnold, 1977). As described in Section 2.2.1, this methodology can get very confusing and time consuming for even a very few design variables. In addition, if the increment size is too large, the maximum determinant can be missed. Nevertheless, the parametric study has been extensively used with the D -optimality criterion. This technique was applied by Beck (1966) to determine the optimal conditions for the simultaneous estimation of the thermal conductivity and specific heat, and to determine the optimum transient experiment for estimating the thermal contact conductance (Beck, 1969). Taktak et al. (1991) used this procedure to estimate the thermal properties of isotropic composite materials by optimizing the number of sensors, sensor placement, and the duration of an imposed heat flux. A similar approach was performed by Garnier (1996) but for an insulating material in a cylindrical geometrical form. Based on the work from Taktak et al., one-and two-dimensional D -optimal experimental designs have also been developed by Moncman (1994; also in Moncman et al., 1995) and Hanak (1995) using a parametric study for the simultaneous estimation of thermal properties of anisotropic composite materials.

These included both the in-plane and through-the-thickness thermal properties. The Moncman and Hanak studies were used as test cases in the current work. Note that Hanak emphasized that one of the disadvantages of performing a parametric study is the possibility of overlooking the global optimum. Indeed, in studying the same two-dimensional design optimization analysis that Moncman had performed previously, using smaller increments to segment the design space, he found a design that produced a larger determinant than the optimal design developed by Moncman.

Recently, Rigollet et al. (1998) used D -optimality to investigate the optimal temporal domain for the most accurate estimation of the thermal diffusivity and effusivity of chromium coatings on steel. They use a pulsed photothermal method to obtain the required experimental data for the property estimation. From the estimates obtained, they could deduce the conductivity and volumetric heat capacity of the chromium coatings. Confidence intervals for these latter properties were calculated from classical logarithmic derivatives and comprised of both confidence intervals associated with the diffusivity and effusivity estimates considering measurement errors only, and those of supposedly known parameters (chromium effusivity and thickness of the coatings). Rigollet et al. showed that the uncertainties in the supposedly known parameters had by far the greatest effect on the accuracy of the calculated thermal conductivity and volumetric heat capacity. This work points out that not only should one focus on optimizing some critical design variables for the most accurate estimation of the unknown properties, but also, when preparing and conducting the optimal experiments, one should take care to minimize the uncertainties in other experimental parameters that are supposed to be known, such as material thickness. Note that a review of the most important sources of errors that can introduce bias in the final estimates can be found in Jarny and Maillet (1999).

Discussion of the present state of knowledge should be concluded with the importance for the optimal designs to be verified. This ensures that the best possible estimates have been obtained and allows for the validation of not only the optimization procedure but also the mathematical model used to describe the process. Hanak (1995) demonstrated that the optimal design provided the most accurate combined thermal property estimates by testing the optimal design along with two non-optimal designs. The non-optimal experimental parameters were chosen so that they did not satisfy the D -optimal criterion used in the optimization technique. Hanak's results showed that an individual property might be estimated with greater accuracy at a non-optimal setting but the combination of properties reached a higher accuracy at the

optimal setting. Validation of optimization through experiments is particularly relevant when the system is based on an analytical model which is not valid in the entire design space (Haftka et al., 1997).

2.4 Genetic Algorithms (GAs)

2.4.1 Description

Genetic Algorithms were developed by Holland (1975). Although these algorithms emerged simultaneously with two other streams known as Evolution Strategies (ES) and Evolutionary Programming (EP), GAs are today the most widely known type of evolutionary algorithms (Back, 1994). Differing from conventional search techniques, the common feature of these algorithms is to simulate the search process of natural evolution and take advantage of the Darwinian survival-of-the fittest principle. In short, Evolutionary algorithms start with an arbitrarily initialized population of coded individuals, each of which represents a search point in the space of potential solution. The goodness of each individual is evaluated by a fitness function which is defined from the objective function of the optimization problem. Then, the population evolves toward increasingly better regions of the search space by means of both random and probabilistic (or deterministic in some algorithms) biological operations. The three main evolutionary algorithms (GAs, ES and EP) were developed independently from each other as each emphasized different biological operators as being most important to a successful evolution process. The basic operators used in GAs consist of selection (the selection of parents for breeding), crossover (the exchange of parental information to create children) and mutation (the changing of an individual). In addition, following the Darwinian theory, an elitism operator (the protection of best individuals) is found in more elaborated GAs. The fundamentals behind GAs are detailed in Chapter 4, along with the relevant characteristics that differentiate these algorithms from conventional optimization methods. Note however here that the ergodicity of the biological operators used in GAs makes them potentially effective at performing global search (in probability) (Gen and Cheng, 1997). Also, GAs have the attribute of a probabilistic evolutionary search (although it is most commonly referred to as a randomized search), and are neither bound to assumptions regarding continuity nor limited by required prerequisites. Citing Goldberg (1989), GAs are blind.

Note that some efforts have been directed towards building an analogy between the representational mechanisms of GAs and their biological counterparts, thus producing a *lingo* (Goldberg, 1989 and Mitchell, 1996). In this correspondence terminology, an individual is thought of as a *chromosome* (*chromosomal string*) and the *genotype* is composed of the collection of possible chromosomes. Each chromosome consists of *genes* which may take on some number of values called *alleles*. Each gene has a particular *locus*, its position in the chromosome. Eventually, the solution point encoded by the chromosome represents the phenotype. This terminology, generally used within the GA field (artificial intelligence), was not used in this dissertation.

The GA technique has been theoretically and empirically proven to provide robust searches in complex spaces. Much of the early work of GAs used a universal internal representation involving fixed-length binary chromosomes with binary genetic operators. Consequently, most of the theory developed (which could fill several volumes!) is based on binary coding. In developing the Fundamental Theorem of GAs, Holland (1975) focused on modeling ideal Simple GAs (SGAs) to better understand and predict GA behavior [this theorem, also called the *Schema Theorem*, states that short, low-order schemata (particular genes sequences) with above-average fitness receive exponentially increasing trials in subsequent generations]. Many properties in terms of the binary genetic operators effectiveness were concluded from this theorem. However, Mitchell (1996) pointed out that these properties give some limited insight into the GA behavior. Mitchell believes that a more useful approach to understanding and predicting GA behavior would be analogous to that of statistical mechanics in physics whose traditional goal is to describe the laws of physical systems in terms of macroscopic quantities, such as pressure and temperature, rather than in terms of the microscopic particles (molecules) making up the system. Such an approach will aim at laws of GA behavior described by more macroscopic statistics such as “mean fitness in the population” or “mean degree of symmetry in the chromosomes” rather than keeping track of the huge number of individual components in the system (e.g., the exact genetic composition of each population).

Regarding theoretical guidelines about which GA to apply, the real problems encountered by GAs usually compel tailoring the GA at hand as the use of different encoding and operator variants could provide different solutions (Davis, 1991; Michalewicz, 1996). One realizes that there are therefore no rigorous guidelines for predicting which variants and more particularly, which encoding, works the best. By addressing the binary/floating point

debate, the work by Field (1996) confirms that there is no best approach and that the best representation depends on the problem at hand. Davis (1991) also recommends a problem-oriented approach, in which domain knowledge should be incorporated into the GA as much as possible, and the GA should be hybridized with other local optimization methods that work well. The current author believes hybrid GAs to be the most effective solution to complex optimization.

As one can understand, there are many controversies in the GA community over the approaches used, revealing that GA theory is by no means a closed book (indeed, there are more open questions than solved ones). One final point worth mentioning about the GA theory is that many of today's algorithms show enormous differences to the original SGA.

2.4.2 Applications in Engineering

Although the evolution simulation implemented in GAs appears to be a crude simplification of biological reality, over three decades of applications have clearly demonstrated the robustness of the resulting non-gradient algorithms. GAs have been applied to all (and more) of the areas Holland (1975) had indicated: optimization in engineering and computer science, combinatorial optimization such as job-shop scheduling, automatic programming and machine learning, biotechnology, economics and social sciences, financial forecasting, art and music, game-playing, to name the most relevant. Because of the complexity and the abstraction associated with the traditional binary coding generally used to encode design variables, research on GAs has been slow to spread from computer science to engineering. Over the past few years, however, application to real-world problems has increased greatly as many researchers started to adapt the algorithm encoding to the most natural representation of the search space. The *Handbook of Genetic Algorithms* (Davis, 1991) is a striking evidence of the possible real world GA applications in industry. Some recent interesting demonstrations of the effectiveness of GAs with both integer and real-number coding in the fields of structural optimization, and more particularly composite structure optimization, parameter estimation and thermal sciences are outlined below. Note that GAs have not been utilized very much in heat transfer.

In structural optimization, Furuya and Haftka (1993) determined optimal actuator locations on large space structures using GAs with integer coding. They showed that the performance of the algorithms with integer coding was at least as good as or better than the performance with binary coding. Doyle (1995) illustrated GAs with real-number coding to

efficiently locate the size and location of a crack in a frame structure. The inverse problem of identifying the number, location and shape of holes to make in structural components with an aim to optimizing their weight has been investigated by Nakamura and Taomoto (1996) using successively a GA and the conjugate gradient method. The design was performed in two steps: first, the total number of holes and their initial location and shape were estimated using the GA; then, the optimal shape and location were identified by the gradient-based optimization method.

For composite laminate design and optimization, Soremekum (1997) modified a basic GA to include a second chromosome string so that composite laminates comprised of multiple materials could be studied with greater efficiency. Using this modified GA, Soremekum performed the minimization of both the cost and weight of a simply supported composite plate under different combinations of axial loading, and obtained a Pareto-optimal set of designs. Multi-objective optimization of laminated ceramic composites was also previously performed by Belegundu et al. (1994) using GAs. Exploiting the GA property of implicit parallelism for the design of composite laminate structures, McMahon (1998) developed a distributed GA with migration which was aimed to operate on a parallel processor. The migration algorithm was found to diminish the normalized cost and improve the reliability of a GA optimization run.

Using GAs as a parameter estimation technique, Carroll (1996a and b) could simultaneously estimate a set of unknown parameters that best matched a chemical laser model prediction with experimental data. Jones et al. (1996) used GAs to determine the optical properties and the particle size distribution function of propellant smoke from angular light-scattering measurements. A combination of the gradient-based Gauss method and a GA was applied by Wright (1996) to determine the specific acoustic admittance of the inlet and outlet ports of a combustion chamber. By exploiting the advantages of both techniques, Wright was able to arrive at accurate estimates of the acoustic boundary conditions for nearly any candidate system. A similar procedure was conducted by Autrique and Souza de Cursi (1997) who implemented a stochastic modification based on GAs into classical gradient-based methods for the control of the vulcanization process. They showed that such an implementation was efficient for global optimization. Raudensky et al. (1995) applied GAs in solution of inverse heat conduction problems, while a GA for an inverse radiation problem was used by Li and Yang (1997). Lorion et al. (1999) have just reported the use of GAs for the successful estimation of thermal diffusivity in a multi-layer material. Their work also involves a comparison of results obtained on a homogeneous material using both GAs and the

Levenberg-Marquard method. In this comparison, GAs were found to provide more accurate and stable results than the gradient-based method.

The feasibility of GAs to solving heat transfer problems was illustrated by Davalos and Rubinsky (1996). In this work, two simple cases of conduction heat transfer were considered. These included 1) conduction in a one-dimensional slab, with one side kept constant at the temperature of zero which was also the initial temperature, while the other side temperature changed with a constant rate; and 2) conduction in a two-dimensional square in which the temperature of three sides was zero (also the initial temperature), while the temperature on the fourth side changed with a constant rate. The temperature distribution was encoded as a string of normalized temperatures (the parameters to determine) at discrete spatial and temporal locations. The fitness function to evaluate the chromosomes was based on the conservation of energy incorporating both local and global conservation. For both test cases, the accuracy of the results obtained with the GA was remarkable.

In the field of thermosciences, the optimized cooling of electronic components is one intractable optimization problem type that requires the use of GAs. Queipo et al.(1994) used these algorithms to find optimal or nearly optimal arrangements of convectively cooled components placed in-line on the bottom wall of a ventilated two-dimensional channel. They concluded that GAs allow a cost effective approach for investigating highly complex numerical and experimental thermoscience problems where it is desirable to obtain a family of acceptable problem solutions, as opposed to a single optimum solution. This work showed the adaptability of GAs. In the optimization of a chip design layout on a circuit board, Sakait and Chang (1996) were also able to easily take heat source constraints into consideration using GAs. These algorithms were used as well for the thermal design of finned surfaces (Fabbri, 1997).

One industrial thermal area in which GAs are extensively used involves power systems, e.g. power plant operation cycle management and cogeneration systems planning. The thermoeconomic models used are typically highly nonlinear. Applications of GAs are sought for the simultaneous optimization of the configuration, design and operation of the installation over its entire economic lifetime by minimizing the time integral of total cost (Olsommer and al., 1997). The GA that allows achievement of such a task combines binary, integer and real encoding and is used on a parallel processor. This large scale optimization shows the incredible possibilities and robustness of GAs.

On the basis of the applications reported above, GAs have been found to be very

powerful optimization procedures. Therefore, in this research these algorithms were investigated for use in designing optimal experiments to determine thermal properties, and in the subsequent simultaneous estimation of the properties. The use of GAs in these areas was particularly sought for the optimization of several experimental parameters and the simultaneous estimation of multiple thermal properties regardless of the presence of correlation among the properties. It is of interest to note that there is no knowledge of previous attempts to use GAs in these areas. The GAs developed in this work were based on real encoding. It should be mentioned here that for the task of optimizing functions of real variables, Evolutionary Strategy approaches have shown some appreciable robustness. However, although they have been around for about 30 years (Schwefel, 1995), these algorithms are still unknown to many investigators and much less theory than for GAs has been developed. Consequently, the ES approach was not investigated in this work.

CHAPTER 3

Parameter Estimation and Design Optimization: Theoretical Considerations

This chapter provides the theoretical tools needed in developing a genetic-based methodology for both experimental design optimization and simultaneous parameter estimation, and in performing the studies reported in Chapters 5 and 6. The inverse methodology for parameter estimation is first introduced, including problem formulation, and presentation and discussion of a popular gradient-based procedure, the modified Box-Kanemasu method. Some important factors to examine are described, namely sensitivity coefficients, correlation matrix, condition number, residuals, root-mean-square error and confidence intervals of the parameter estimates. The second section deals with the methodology for designing optimal experiments to be used for property estimation. The optimization problem is formulated and the main optimality criteria are discussed.

3.1 Parameter Estimation Inverse Methodology

Parameter estimation typically involves the determination of one or more parameters contained in a vector β . The parameters are inherent in a mathematical model of a measurable (dependent/state) variable, η , of some physical process. In the following, general considerations are provided based on such a variable η which is assumed to be a function of known independent variables such as position and/or time, contained in the vector \tilde{x} . Note that in the thermal characterization problems treated in Chapter 5, the dependent variable is temperature, and the vector β contains for instance thermal conductivity and specific heat, while in the kinetic characterization problems treated in Chapter 6, the dependent variable is either the cure rate or the degree of cure of the reaction, and β contains kinetic parameters.

3.1.1 Formulation

Parameter estimation can be seen as an optimization in which the objective is to select the values of some unknown parameters in such a way that an objective function is minimized. This latter is specified by the estimator scheme chosen to be applied. The three main estimators, Ordinary Least Squares (OLS), Maximum Likelihood (ML) and Maximum a posteriori (MAP) were introduced in Chapter 2. The objective functions associated with these estimators are expressed by different sum-of-squares functions which contain calculated and measured values of the state variables considered. It is however possible to give a sum-of-squares that is suitable for OLS, ML and MAP estimation when appropriately specialized. In matrix form, this function is (Beck and Arnold, 1977):

$$S(\boldsymbol{\beta}) = [\boldsymbol{\eta}(\boldsymbol{\beta}, \tilde{\mathbf{x}}) - \tilde{\boldsymbol{\eta}}]^T \mathbf{W} [\boldsymbol{\eta}(\boldsymbol{\beta}, \tilde{\mathbf{x}}) - \tilde{\boldsymbol{\eta}}] + [\boldsymbol{\beta} - \boldsymbol{\mu}]^T \mathbf{U} [\boldsymbol{\beta} - \boldsymbol{\mu}] \quad (3.1)$$

where $\boldsymbol{\beta}$ is the true parameter vector and $\boldsymbol{\eta}(\boldsymbol{\beta}, \tilde{\mathbf{x}})$ and $\tilde{\boldsymbol{\eta}}$ are the modeled and observation vector, which comprise of calculated and measured values of η at specific values of the independent variables contained in $\tilde{\mathbf{x}}$, respectively. Both \mathbf{W} and \mathbf{U} are symmetric and square $n_p \times n_p$ matrices, where n_p is the number of unknown parameters. In MAP estimation, \mathbf{W} is set equal to the inverse of the covariance matrix of the measurement errors, \mathbf{U} is the inverse of the covariance matrix of the prior information parameters and $\boldsymbol{\mu}$ is the prior information parameter vector. In ML estimation, \mathbf{W} is the same as in MAP but \mathbf{U} is set to zero. Eventually, in OLS estimation, no information is assumed and \mathbf{W} is set to the matrix identity while \mathbf{U} is set to zero.

Independently of the inverse technique used to minimize S , the inverse methodology can be schematized as shown in Fig. 3.1.

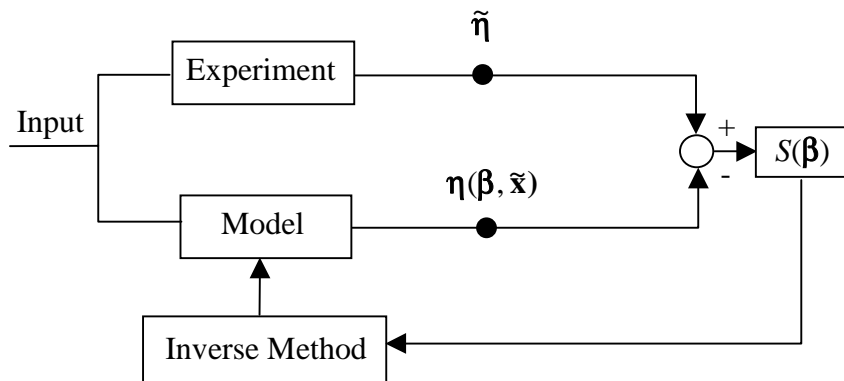


Figure 3.1 Schematic of parameter estimation inverse methodology.

3.1.2 A Gradient-Based Procedure: the Modified Box-Kanemasu Method

- **Description**

Application of a gradient-based procedure as an inverse technique involves setting the derivative of the function S with respect to the parameter vector equal to zero:

$$\nabla_{\boldsymbol{\beta}} S = 2 \left[-\nabla_{\boldsymbol{\beta}} \boldsymbol{\eta}^T(\boldsymbol{\beta}, \tilde{\mathbf{x}}) \right] \mathbf{W} \left[\boldsymbol{\eta}(\boldsymbol{\beta}, \tilde{\mathbf{x}}) - \tilde{\boldsymbol{\eta}} \right] - 2\mathbf{U}[\boldsymbol{\beta} - \boldsymbol{\mu}] = 0 \quad (3.2)$$

The derivative of $\boldsymbol{\eta}$ with respect to $\boldsymbol{\beta}$ is called the sensitivity matrix and is denoted by $\mathbf{X}(\boldsymbol{\beta})$. Each component of this matrix is a sensitivity coefficient which is associated with a parameter and relates how the dependent variable changes with respect to that particular parameter. Sensitivity coefficients will be discussed in the next section. For nonlinear-in-parameter models (this is the case for all problems investigated in this work) the sensitivity matrix is a function of the parameters, and Eq. (3.2) cannot be explicitly solved for the parameter vector $\boldsymbol{\beta}$. Note that linear estimation implies that the model investigated is of the form $\boldsymbol{\eta}(\boldsymbol{\beta}, \tilde{\mathbf{x}}) = \mathbf{X}\boldsymbol{\beta}$, where \mathbf{X} is independent of $\boldsymbol{\beta}$. Therefore, two approximations are used to linearize Eq. (3.2). The first involves replacing $\mathbf{X}(\boldsymbol{\beta})$ with $\mathbf{X}(\mathbf{b})$, where \mathbf{b} is an estimate of $\boldsymbol{\beta}$. The second uses the first two terms of the Taylor series of $\boldsymbol{\eta}(\boldsymbol{\beta}, \tilde{\mathbf{x}})$ about \mathbf{b} to approximate $\boldsymbol{\eta}(\boldsymbol{\beta}, \tilde{\mathbf{x}})$. These simplifications, along with the use of an iterative scheme (in which the first estimate of $\boldsymbol{\beta}$ could be $\boldsymbol{\mu}$) lead to the following solution for \mathbf{b} :

$$\mathbf{b}^{(k+1)} = \mathbf{b}^{(k)} + \underbrace{\mathbf{P}^{(k)} \left[\mathbf{X}^T(\mathbf{b}^{(k)}) \mathbf{W} \left[\boldsymbol{\eta}(\boldsymbol{\beta}, \tilde{\mathbf{x}}) - \tilde{\boldsymbol{\eta}} \right] + \mathbf{U} \left[\mathbf{b}^{(k)} - \boldsymbol{\mu} \right] \right]}_{\Delta_g \mathbf{b}^{(k)}} \quad (3.3)$$

where $\mathbf{P} = \left[\mathbf{X}^T(\mathbf{b}^{(k)}) \mathbf{W} \mathbf{X}(\mathbf{b}^{(k)}) + \mathbf{U} \right]^{-1}$ (3.4)

Eq. (3.3) is known as the Gauss linearization equation. This method specifies a direction and step size that the parameter vector should be changed in order for S to be a minimum. To improve convergence, the Box-Kanemasu modification reduces the step size $\Delta_g \mathbf{b}^{(k)}$ by implementing a scalar interpolation factor h which is a quadratic approximation of S . Eq. (3.3) then becomes:

$$\mathbf{b}^{(k+1)} = \mathbf{b}^{(k)} + h^{(k+1)} \Delta_g \mathbf{b}^{(k)} \quad (3.5)$$

A further correction modifies h to ensure that S continuously decreases. The solution for the estimates is obtained when the parameter values do not change significantly from iteration to iteration. For a more in-depth description, refer to Beck and Arnold (1977).

- **Discussion**

Important points about the use of this gradient-based procedure can be made in reference to Eqs. (3.3) and (3.5), and more particularly, regarding the direction of the step size $\Delta_g \mathbf{b}^{(k)}$. First, one can understand that the use of information (matrices \mathbf{W} and \mathbf{U} , and vector $\boldsymbol{\mu}$) may help finding a better $\Delta_g \mathbf{b}^{(k)}$ provided this information is appropriate. If the prior information is not in the neighborhood of the final estimates, its use may actually have the opposite effect than its purpose and prevent the method from converging. For that reason, the MAP estimator is usually not used ($\mathbf{U}=0$). Using ML and OLS estimators, one can see that the values of the initial estimates should be given great care as they are used to calculate $\Delta_g \mathbf{b}^{(k)}$. Due to the implementation of the scalar factor $h^{(k+1)}$, the modified Box-Kanemasu method offers a little more flexibility in the choice of the initial estimates than the Gauss-Newton method which has been shown to require “good” initial values to be stable. Nevertheless, experience has proven that even the use of the modified Box-Kanemasu method still requires “correct” initial values, e.g. not too far from the neighborhood of the final values.

Two final points worth mentioning are related to the sensitivity matrix and the \mathbf{P} matrix [Eq. (3.4)]. Obviously, if the sensitivity coefficient of one parameter is negligible, it has some effect on the associated direction and step size for that parameter and thus on the final estimate. In addition, the \mathbf{P} matrix may also be disrupted from a negligible sensitivity coefficient, thus affecting the estimation of all other parameters. Eventually, unique estimation of the parameters as independent variables is possible only if the \mathbf{P} matrix exists, e.g. in ML or OLS estimation ($\mathbf{U}=0$), the Fisher information matrix defined by $\mathbf{X}^T \mathbf{X}$ is non-singular ($|\mathbf{X}^T \mathbf{X}| \neq 0$, known as the identifiability condition). This implies that the sensitivity coefficients are linearly independent, in other words, not correlated. Note that the condition $|\mathbf{X}^T \mathbf{X}| \neq 0$ also requires that the number of measurements in $\tilde{\boldsymbol{\eta}}$ be equal to or greater than the

number of parameters. This requirement is usually always satisfied in the heat transfer field and in order to minimize the measurement error, it is actually recommended to use a number of measurements at least equal to 20 times the number of parameters (Raynaud, 1999).

In the light of this analysis, considering the use of OLS estimation, application of the modified Box-Kanemasu method requires the following conditions:

- 1) “correct” initial estimates,
- 2) sufficient sensitivity information, and
- 3) uncorrelated parameters.

Note that quantification about conditions 2) and 3) are provided by two respective rules of thumb detailed in the following section. When the three conditions above are fulfilled, then the modified Box-Kanemasu method has been proven to be very effective. But in case these conditions are not met, which characterizes ill-conditioning, the method has been shown to oscillate with increasing amplitude and not converge (Garcia, 1994; Hanak, 1995; Guynn, 1996; and Copenhaver, 1996).

One area in which efforts must be focused prior to the actual implementation of the estimation procedure is the optimization of the experimental design that is used to generate the observation vector $\tilde{\mathbf{r}}$. Based on an adequate optimality criterion related to conditions 2) and 3), such optimization should facilitate the estimation of the parameters. Optimization of experimental designs is the subject of Section 3.2. However, in the case of very ill-posed estimation problems, it is possible that even after experimental optimization, not only is the sensitivity information still insufficient, but also some parameters are still correlated (Hanak, 1995; Guynn, 1996; and Copenhaver, 1996). Note that Box has actually shown that high correlations among the parameters can be due to a large extent to the nature of the model itself and thus no experimental design could be expected to yield uncorrelated parameter estimates (reported by Beck and Arnold, 1977). In that case, the modified Box-Kanemasu method (and most probably any other gradient-based procedures) is simply ineffective. One solution commonly applied is to follow the principle of parsimony (Beck and Arnold, 1977) that states that the smallest possible number of parameters should be estimated. However, this considerably restricts researchers to estimation of a few parameters by experimental design. In

addition, if the same mathematical model is used, the unknown parameters that cannot be estimated are usually set to nominal values that then introduce a bias in the final estimates. The magnitude of this bias will be a direct consequence of the uncertainty contained in the nominal values, the sensitivity to these values, and the degree of correlation between the parameters to be estimated and the supposedly known one. Therefore, there is a need to develop a methodology capable of solving such ill-defined simultaneous parameter estimation problems. Genetic Algorithms were investigated in this research because they were thought to have this potential. These algorithms are described in the next chapter.

3.1.3 Sensitivity, Correlation and Condition Number Analysis

Of particular interest before starting any estimation procedure is the careful analysis of both sensitivity of the mathematical model to the unknown parameters, and degree of correlation of the parameters. These concepts are important since small magnitudes of the sensitivity coefficients and near-linear dependence among the coefficients are limiting factors to the stability, and thus convergence, of gradient-based estimation procedures, as outlined earlier. In addition, computation of the condition number of the Fisher information matrix $\mathbf{X}^T\mathbf{X}$ can allow assessment of any ill-conditioning characteristic of the estimation problem. In the following, expressions for the sensitivity coefficients and the correlation matrix are detailed and then two rules of thumb that are useful to quantify sensitivity and correlation, respectively, are provided. This section concludes with the mathematical definition of the $\mathbf{X}^T\mathbf{X}$ matrix condition number and its physical signification.

- **Sensitivity**

A sensitivity coefficient, X_β , is defined as the effect that a change in a particular parameter β has on the state variable and is expressed by (Beck and Arnold, 1977):

$$X_\beta = \left. \frac{\partial \eta}{\partial \beta} \right|_{\gamma_i \neq \beta} \quad (3.6)$$

where γ_i are all parameters other than β that remain constant. The larger X_β , the more sensible η is to β and the easier the estimation of this parameter (provided the inverse method converges). In addition, viewing the sensitivity coefficients can allow insight to be obtained

into the adequacy of the mathematical model and that of the experimental design. When performing a sensitivity study, it is meaningful to examine the dimensionless sensitivity X_{β}^+ given by:

$$X_{\beta}^+ = \beta \left. \frac{\partial \eta^+}{\partial \beta} \right|_{\gamma_i \neq \beta} \quad (3.7)$$

where η^+ is the dimensionless dependent variable. One convenient and generally appropriate expression for η^+ is:

$$\eta^+ = \frac{\Delta \eta}{(\Delta \eta)_{\max}} \quad (3.8)$$

where $\Delta \eta = \eta - \eta_{\min}$ and $(\Delta \eta)_{\max} = \eta_{\max} - \eta_{\min}$. The term η_{\min} is the minimum value of η (which is also the initial value in all problems investigated in this work), while $(\Delta \eta)_{\max}$ is the maximum increase of η between the beginning and end of the experiment. Eq. (3.7) can then be rewritten as:

$$X_{\beta}^+ = \frac{\beta}{(\Delta \eta)_{\max}} X_{\beta} \quad (3.9)$$

Whenever the sensitivity coefficients can be solved for analytically, this solution must obviously be selected. However, when no analytical expressions are available, such as when using a numerical model, a numerical alternative must be applied. In this work, the convenient finite difference method was implemented. Note that this method is the numerical alternative recommended by Beck and Arnold. This choice was supported by the fact that on one hand, the inverse estimation methodology developed in this work is based on genetic algorithms which do not use sensitivity coefficients. On the other hand, the finite difference accuracy obtained in computing these coefficients is generally acknowledged to be sufficient for the experimental optimization.

A Taylor series expansion was used to approximate the derivative. To minimize the computational cost, a forward difference approximation (first-order accurate) was chosen which gave for X_{β} :

$$X_{\beta} = \frac{\eta(\beta + \Delta \beta) - \eta(\beta)}{\Delta \beta} + o(\Delta \beta), \quad \Delta \beta = \delta \times \beta \quad (3.10)$$

where one can see that the truncation error of the approximation is of order $o(\Delta\beta)$. Thus a smaller δ (and thus a smaller $\Delta\beta$) would yield a more accurate approximation. However, care has to be taken so as not to make δ too small in order to avoid numerical round-off errors. The work from Tortorelli and Michaleris (1994) indicates that when using single precision, δ values of 10^{-3} and 10^{-4} would provide reasonable accuracy, while when using double precision, accurate results were obtained for δ values of 10^{-4} to 10^{-10} . In addition, the double-precision computations were more reliable, as expected. Although these conclusions are based on the study of a linear elliptic system (which for instance governs linear steady-state conduction), they are nevertheless pertinent here since pertaining to numerical computation. In this work, whenever the finite difference method was used to compute sensitivity coefficients, several perturbation sizes, δ , were tested to verify that reliable results were obtained. Generally, the perturbation sizes used were between 10^{-4} and 10^{-6} using double precision.

- **Correlation**

As mentioned earlier, correlation between the parameters, e.g. linear dependence, plays a critical role in gradient-based inverse methods. One way to investigate correlation is to simply plot the sensitivity coefficients against each other. If they appear to be nearly linear dependent the corresponding parameters are correlated and cannot be estimated simultaneously (Beck and Arnold, 1977). Another way is to plot the sum-of-squares function S . Contours that are long, narrow and curving are frequently associated with near-linear dependence. Because plots can often be inconclusive, it is recommended to compute the correlation coefficients, r_{ij} , defined by Walpole and Myers (1993):

$$r_{ij} = \frac{\text{cov}(\beta_i, \beta_j)}{\sigma_i \sigma_j} \quad (3.11)$$

where σ_i and σ_j are the standard deviations of parameters i and j , respectively. Assuming the standard statistical assumptions apply, which involve uncorrelated, additive, normally distributed errors with zero mean and constant variance σ^2 , errorless independent variables and no prior information regarding the parameters, then the approximate (from linear OLS estimation) covariance matrix of the estimation vector β is $[\mathbf{X}^T \mathbf{X}]^{-1} \sigma^2$. Therefore, the

correlation terms, r_{ij} , can be approximated using:

$$r_{ij} = \frac{P_{ij}}{\sqrt{P_{ii} P_{jj}}}, \quad i, j = 1, \dots, n_p \quad (3.12)$$

where the P_{ij} terms can be found from Eq. (3.4). The r matrix is symmetric with the diagonal terms being unity (obviously, each parameter is completely correlated with itself) and the off-diagonal terms being between -1 and 1 . As the magnitude of these terms approaches unity, the properties approach linear dependence. Beck and Arnold (1977) stated that this condition of linear dependence is almost satisfied in the region of the minimum S in many more cases than would be expected. However, because parameters are never completely correlated (provided one uses an appropriate experimental design as defined in Section 2.2.1), the sum of squares error S has a unique minimum point and thus a unique set of parameters. That minimum point may not be very pronounced, however.

It is important to note that unlike linear estimation, Eq. (3.12) is an approximation for nonlinear models, with the approximation being better for cases which are less nonlinear than others. This comment, along with the standard statistical assumptions made above, also applies for all subsequent expressions. Regarding the validity of these assumptions, the residuals analysis (described in Section 3.1.4) is one convenient means to verifying it.

- **Sensitivity and Correlation Quantification**

Two rules of thumb can be used to quantify sensitivity and correlation. One would like:

- the magnitude of the dimensionless sensitivity coefficients to be greater than 0.1, and
- the magnitude of the off-diagonal correlation terms to be lower than 0.9.

Although those values are by no means “exact”, experience has proven that they were pertinent. Indeed, when using traditional gradient-based estimation procedures, lower X^+ than 0.1 and greater r_{ij} than 0.9 usually lead to problems with convergence and resolution of accurate parameter estimates.

- **Condition Number**

The condition number of the Fisher information matrix $\mathbf{X}^T\mathbf{X}$ can be defined as:

$$cond = \frac{|\lambda_1|}{|\lambda_{n_p}|} \quad (3.13)$$

where λ_1 and λ_{n_p} are the largest and smallest eigenvalues of the $\mathbf{X}^T\mathbf{X}$ matrix (which has a rank n_p), respectively. From this definition, one can understand that a large condition number could come from:

- a large difference between the largest and smallest eigenvalues, which is directly related to a large difference between the highest and lowest sensitivity coefficient magnitudes,
- a very small value for the smallest eigenvalue, which is directly related to a very small value for the lowest sensitivity coefficient magnitude, and
- the presence of linear dependence(s) between the parameter sensitivity coefficients.

The condition number of the $\mathbf{X}^T\mathbf{X}$ matrix can therefore be thought of as a quantification of the illness of the estimation problem. It indicates that, in addition to sufficient sensitivity information and uncorrelated parameters, one wishes to have sensitivity magnitudes on the same order for all parameters. There is unfortunately no rule of thumb for this number. However, the comparison between two condition numbers associated with two different $\mathbf{X}^T\mathbf{X}$ matrices can allow assessment of which matrix, and therefore, which estimation conditions, are the most stable. Notice here, that the condition number is independent of the measurement error.

3.1.4 Residuals and Root-Mean-Square (RMS) Analysis

Two other very important factors in the parameter estimation are the examination of both the residuals and Root-Mean-Square error after the final estimates have been obtained.

- **Residuals**

The residuals are the differences between calculated and observed values of the state variable, that is:

$$e_i = \eta_i(\boldsymbol{\beta}) - \tilde{\eta}_i, \quad i = 1, \dots, N_i \quad (3.14)$$

where N_i is the number of observations taken at a specific sensor. Through the visual inspection of the residuals, one can learn much about the validity of the estimation procedure and of the model. In addition, this examination allows the testing of which assumptions made in the computation of the correlation matrix, RMS, confidence intervals of the final estimates, and in the determination of the optimal design (these concepts which have not yet been discussed will be in the following) seem to be valid regarding the measurement errors. Draper et al. (1981) present a thorough investigation into this subject, emphasizing that plots of the residuals are very illustrative. One would like to have small, centered around zero, and uncorrelated measurement errors. However, often the shape of the residuals contains a “signature”, which means that the shape is the same for different experiments and presents few sign changes. This indicates some bias or inconsistency in the mathematical model. Note that the inconsistency may result from inaccurate values used for presumably known parameters (thermocouple position, dimensions, material properties other than those estimated, temperature and heat flux measurements, to name the most relevant). Uncertainties in these latter can indeed have strong effects on the accuracy of the final estimates. Because tests based on data that were used to derive the model can be deceptive and dangerous, of interest is the model testing using a new set of data. That is, the examination of the residuals from an additional sensor whose measurements were not used to compute the sum of squares error S . However, this is not always possible, for instance in the case where a numerical mathematical model is used and where measurements from all other sensors are implemented to specify the boundary conditions.

Note that for transient models, the concept of sequential estimation (Beck and Arnold, 1977) in which the parameters are estimated at each time step is also a very convenient means of evaluating the adequacy of the model and that of the design (in addition to the advantage of observing the effects of additional data on the sequential estimates). However, this concept was not utilized in the current work as its implementation into the genetic algorithm

procedure developed was thought to increase the computation cost considerably.

- **Root-Mean-Square (RMS) Error**

The Root-Mean-Square error is defined by

$$\text{RMS} = \sqrt{\frac{S(\boldsymbol{\beta})}{(N_{tot} - n_p)}}, \quad (3.15)$$

where N_{tot} is the total number of observations used to compute S ; that is for instance, if there are N_i observations from m thermocouples, $N_{tot}=m \times N_i$, while if N_j experiments of N_i observations from only one thermocouple are considered, then, $N_{tot}=N_j \times N_i$. Ideally, the RMS should be small, and usually, the larger N_{tot} , the smaller the RMS (and consequently, the smaller the confidence intervals around the estimates which are discussed next).

When mean thermal property values are computed from a number of different experiments investigated individually, it is common to look at both the RMS_i , which is found for each experiment using the thermal properties estimated for that experiment i , and the RMS_M , which is found using the mean values applied to a particular experiment.

3.1.5 Confidence Intervals (CIs)

Confidence Intervals (CIs) of estimated parameters are used to determine the accuracy of the estimates. For a given nonlinear OLS estimation, assuming the only source of error is the measurement error, the CIs of the individual estimates can be approximated using the formula:

$$\hat{\beta}_k = b_k \pm t_{1-\alpha/2}(N_{tot} - n_p) \sqrt{P_{kk} \frac{S(\boldsymbol{\beta})}{N_{tot} - n_p}} \quad (3.16)$$

where $\hat{\beta}_k$ is the predicted property, b_k is an estimate for β_k , P_{kk} represents the k^{th} diagonal term of the \mathbf{P} matrix, S is the least squares error and t is the student t -distribution for $N_{tot}-n_p$ degrees of freedom and $\alpha/2$ is the confidence range (Walpole and Meyers, 1993). For a large value of $N_{tot}-n_p$ and 95 % probability, $t_{1-0.05/2}(\infty)$ is 1.96 and Eq. (3.16) can be rewritten as:

$$\beta_k = b_k \pm 1.96\text{RMS}\sqrt{P_{kk}} \quad (3.17)$$

The CIs indicated here basically describe the possible amount of variation in the estimates due to, on one hand, the sensitivity of the model to the parameter and the condition number of the Fisher information matrix (through the \mathbf{P} matrix) and, on the other hand, the resulting RMS. Therefore, inaccurate estimates may come from very small sensitivity of the model to the parameters as well as an ill-defined Fisher information matrix (for instance due to correlation between parameters; see the paragraph about the definition of the condition number and its physical signification) or inadequacy to reproduce the experimental data (possible sources of high residuals have been discussed in the previous section). Recall that this expression is derived for linear-in-parameter models. It is, however, pertinent here to mention the work of Grimstadt and Mannseth (1998) who reported a Monte Carlo analysis that aimed to check the validity of using these approximate CIs for nonlinear estimation. These authors indicate that use of such approximation was almost always justified even for the highly nonlinear model they analyzed

It is advised to check that the CI magnitude agrees with the sensitivity analysis, that is the parameter which has the largest sensitivity coefficient should have the smallest CI. Because of the consideration of the measurement errors only, if the Fisher information matrix is well-defined, the CIs may result in very small value. However, recall that uncertainties in the presumably known parameters have also some effects on the accuracy of the final estimates that may often be much larger than the effect of the measurement errors. For a true measure of confidence in the estimates, uncertainties in the variables set as known should be included (Jarny and Maillet, 1999). Because several different estimation problems were investigated in this research, uncertainties besides the measurement errors were, however, not analyzed and the parameter CIs were simply calculated from Eq. (3.17)

In the case of multiple estimates, the CIs of the mean values of n estimates, \bar{b}_k , can be computed from two expressions which are (Walpole and Myers, 1993):

$$\bar{b}_k \pm t_{1-\alpha/2}(n-1) \frac{s}{\sqrt{n}} \quad (3.18)$$

$$\bar{b}_k \pm t_{1-\alpha/2}(n-1) \frac{\sqrt{\sum_{i=1}^n \frac{s_i^2}{n^2}}}{\sqrt{n}} \quad (3.19)$$

In both equations, t is the value of the t -distribution for $n-1$ degrees of freedom and $\alpha/2$ is the confidence range. Equation (3.19) is expected to be more appropriate than Eq. (3.18) because it includes the sample standard deviation s_i of each individual experiment [$s_i = \text{RMS}\sqrt{P_{kk}}$ from Eq. (3.17)], whereas Eq. (3.18) assumes the same standard deviation around the mean, s , for the n experiments.

3.2 Design Optimization Methodology

Because all estimators (OLS, ML and MAP) require experimental measurements, the acquisition of data with the most sensitivity for the unknown parameters entails experimental design optimization. In the following, the optimization problem is first formulated. Then, three optimality criteria are described and discussed with an emphasis on the well known D -criterion. This section concludes with the need for a robust and reliable optimization technique.

3.2.1 Formulation

In the specific case of optimizing experimental designs used for parameter estimation, the objective is to obtain the greatest possible accuracy; that is, to minimize the variance of the n_p estimated parameters. Consider for an exact (e.g. unbiased) experiment that some observations $\tilde{\eta}_i$ are taken and the seven standard statistical assumptions given in Section 3.1.3 (and denoted 11111-11 in Beck and Arnold, 1977) apply. The $n_p \times n_p$ Fisher information matrix is $\mathbf{X}^T \mathbf{X}$ and the approximate (from linear OLS estimation) covariance matrix of the estimation vector $\boldsymbol{\beta}$ is $[\mathbf{X}^T \mathbf{X}]^{-1} \sigma^2$ (where σ^2 is the assumed equal variance of the measurement error). From this, one understands that the objective function, called the optimality criterion here, should be based on inferential properties of the $\mathbf{X}^T \mathbf{X}$ matrix and, therefore, depends on the sensitivity matrix \mathbf{X} . Before describing the main optimality criteria proposed for the design of experiments, one important factor to mention is the intelligent selection of the experimental parameters that are anticipated to have a substantial effect on the model response, and more

particularly on the magnitude of the sensitivity coefficients. The experimental parameters can be associated with the experimental setup as well as with the experimental procedure. Usually boundary conditions, time, and sensor location are the most critical experimental parameters. In addition, one should keep in mind that the optimal experiment should be designed to be experimentally reproduced. Therefore, feasibility of the experimental design (for instance, in implementing particular boundary conditions) should be one priority. Clearly, the closer experiments are to the optimal design, the more accurate the estimated properties will be. This also implies that the standard statistical assumptions are respected as much as possible.

An additional relevant point pertains to the fact that the optimal values determined for the experimental parameters with respect to an optimality criterion should also be appropriate regarding the minimization of the model response sensitivity to the “supposedly” known parameters. As outlined by Raynaud (1999), design-of-experiment should be formulated in terms of two objectives: the maximization of an optimality criterion for the estimation of unknown parameters as well as the minimization of the sensitivity to all other parameters.

3.2.2 Optimality Criterion

- **Description**

The three most often encountered optimality criteria proposed for the design of experiments are the *D*-, *A*- and *E*-optimality criteria. These criteria provide various measures of the size of the confidence region of the estimates. With the assumption that the observations are normally distributed, the confidence region is described by ellipsoids in the parameter space. In addition to the seven standard statistical assumptions, these criteria are subject to some constraints such as maximum duration of the experiments, maximum range of the dependent variable, and large number of observations with uniform spacing in time. Following is a brief outline of their definition and simple geometrical meaning (Kiefer, 1981):

- the *D*-criterion, which is the most commonly used, involves the maximization of the determinant of the Fisher information matrix $\mathbf{X}^T\mathbf{X}$ (or minimization of the determinant of $[\mathbf{X}^T\mathbf{X}]^{-1}$). The determinant of $[\mathbf{X}^T\mathbf{X}]^{-1}$ being proportional to the square of the confidence region hypervolume, *D*-optimality has the effect of minimizing this hypervolume. This criterion therefore minimizes the generalized variance of the estimates.

- the A -criterion involves the maximization of the trace of the $\mathbf{X}^T\mathbf{X}$ matrix (or minimization of the trace of $[\mathbf{X}^T\mathbf{X}]^{-1}$). Because the trace of $[\mathbf{X}^T\mathbf{X}]^{-1}$ is proportional to the sum of squares of lengths of the principal axis of the confidence region, A -optimality has the effect of minimizing the quadratic average of principal axis lengths. This criterion therefore minimizes the average variance of the estimates.
- the E -criterion involves the maximization of the minimum eigenvalue of the $\mathbf{X}^T\mathbf{X}$ matrix (or minimization of the maximum eigenvalue of $[\mathbf{X}^T\mathbf{X}]^{-1}$). The maximum eigenvalue of $[\mathbf{X}^T\mathbf{X}]^{-1}$ being proportional to the square of the maximum diameter of the confidence region, E -optimality has therefore the effect of minimizing this maximum diameter.

Obviously, the geometrical and theoretical meaning given here for these optimality criteria is not exact for real estimation problems (nonlinear estimation problems in which the standard statistical assumptions are not satisfied and neither is the “equal spacing” constraint). However, by solving the simpler analogue formulation, one can get an idea on how good (if not optimum) the design can be in more complex form.

The analysis of the effect of these three criteria on the accuracy of the parameter estimates was one of the specific objectives of this research (see Section 5.1.1.6). In dimensionless terms, the maximization of these criteria can be defined as the maximization of:

$$D^+ = \left[\left[d_{ij}^+ \right] \right] \quad (3.20)$$

$$E^+ = \min |\lambda_i^+| \quad (3.21)$$

$$A^+ = \sum_{i=1}^{n_p} d_{ii}^+ \quad (3.22)$$

where d_{ij}^+ and λ_i^+ are the ij^{th} element and the i^{th} eigenvalue of the dimensionless $\mathbf{X}^T\mathbf{X}$ matrix. The d_{ij}^+ elements can be calculated from:

$$d_{ij}^+ = \frac{1}{t_N (T_{\max}^+)^2} \frac{1}{N_k} \sum_{k=1}^{N_k} \int_0^{t_N} X_{ik}^+(t) X_{jk}^+(t) dt, \quad i, j = 1, \dots, n_p \quad (3.23)$$

where T_{\max}^+ is the maximum dimensionless temperature being reached at steady state. Note that time could also be dimensionless. The use of both dimensionless terms and the averaging

over the squared maximum temperature allows, on one hand, comparison of competing designs which, for instance, involve different boundary conditions and, on the other hand, results to be obtained for a specific design that can be applicable to any material. When performing the integration over time numerically, one should obviously use the same computational time step to compare competing designs.

- **Discussion**

Now that these optimality criteria have been defined, it is important to stress that the objective behind designing experiments with respect to either D -, A - or E -optimality is related to the size of the confidence region of the estimates only. On no account is possible correlation(s) between the estimated parameters to be minimized. While one wishes to design experiments in which there is minimum correlation as well as maximum sensitivity of the measured variable to changes in the parameters being estimated (which recall correspond to conditions 2 and 3 in Section 3.1.2), this is not possible using one of the three optimality criterion described here. D -optimality is recommended because, by minimizing the generalized variance of the estimation vector, it allows the most accurate global estimation. However, it is possible that a D -set of final estimates might be more correlated (while globally more accurate) than a set of estimates obtained from a different design than the D -optimal. This will actually be the result of the analysis performed in Section 5.1.1.5. Accuracy and correlation are two different concepts which have been long associated because of the use of gradient-based methods that cannot operate properly in the presence of correlation. However, correlation is simply a characteristic between parameters and it is inherent to the mathematical model investigated, as stressed by Box and reported by Beck and Arnold (1977).

One criterion that one could think of as both maximizing the accuracy of the estimated parameters (by maximizing their sensitivity coefficients) and minimizing the correlation between them is the condition number of the Fisher information matrix $\mathbf{X}^T\mathbf{X}$. However, there is no mathematical proof that minimizing this number would guarantee such output. Besides, Alifanov et al. (1995) have reported that D -optimality was nearly equivalent as an optimality criterion based on the $\mathbf{X}^T\mathbf{X}$ condition number. Finally, results of Section 5.1.1.5, for instance, will show that it is possible to obtain for a specific D -optimal design a globally more accurate

set of estimated parameters which indicates higher correlation terms between the parameters but, more important, a lower condition number than for a non-optimal design.

One important point to realize in design optimization is that as models are usually nonlinear, the sensitivity coefficients depend on the unknown parameters. Therefore, an iterative design optimization must be implemented. Such iterative scheme consists in 1) performing the optimization using initial estimates for all unknown parameters, 2) conducting the experiments as prescribed from the optimal design, and 3) generating estimates from the parameter estimation inverse method. If the new estimates from the experiments are found to be completely different than the previous values used, the optimal parameter settings have to be redetermined. As one can easily guess, for time-consuming direct models, this iterative procedure cannot be rigorously followed. One useful output that has been typically found is that the optimal values for the design variables often lie within an optimal range. This means that the use of initial estimates of the unknown properties different than their actual values may allow for nearly the same optimal design variable values [provided the initial guesses used are not much different than, say, 100 % of the actual final estimates (Moncman, 1994; present study)]. Therefore, the initial estimate values do not have to be exactly the true estimates.

One final point deals with the optimization of a particular parameter, the overall total experimental time. A usual and convenient means to find the optimal setting for this parameter is to calculate a modified value of the optimality criterion chosen once the other experimental parameters have been optimized by maximizing the actual optimality criterion (using an optimization technique). The modification considered consists of computing the criterion without averaging the integral contained in Eq. (3.23) over time. When the modified value of the criterion does not change any more in time, it indicates that little additional information is being provided for the estimation of the parameters and thus the experiments can be concluded. The corresponding time is the value for the overall total experimental time. Note that usually a conservative value is selected.

3.2.3 Optimization Technique

The determination of the optimal experimental variables which satisfy the optimality criterion chosen for the objective function is performed through the application of an optimization technique. As reported in Chapter 2, the typically used parametric study presents drastic drawbacks. On this basis, the use of a robust and reliable method is necessary. The development of an experimental design optimization methodology based on Genetic Algorithms was one of the overall objectives of this work. These algorithms are described in the next chapter.

CHAPTER 4

Genetic Algorithms

This chapter focuses on an emerging evolutionary method called Genetic Algorithms (GAs). After a brief introduction, as GAs were already introduced in Chapter 2, the following section is devoted to presenting the fundamentals behind these algorithms. Next, the three algorithms developed throughout this work are described and discussed. Eventually, this chapter concludes with the demonstration of the robustness of the third GA developed on the optimization of a mathematical test function.

4.1 Introduction

Traditionally, there are two major classes of optimization algorithms which are classified into calculus-based and enumerative techniques (Goldberg, 1989). Calculus-based optimization techniques employ the gradient-directed searching mechanism, starting from an initial guessed solution, and therefore are local in scope. Although these techniques are well developed, they maintain significant drawbacks. Indeed, for ill-defined or multimodal objective functions, instability and/or local optima are usually obtained. In addition, because the objective function is often problem-oriented, implementation of these techniques can be very complex. Many enumerative schemes have been suggested to handle the local optima problem but at the expense of computational inefficiency. A third class that has achieved increasing popularity is the random/probabilistic search algorithm. More particularly, the 1970's has seen the emergence of evolutionary algorithms which employ mechanisms of natural selection to solve optimization problems (Michalewicz, 1996). These algorithms were thought of as the answer to the question of how the search should be organized so that there is

a high likelihood of locating a near-optimal solution. Genetic Algorithms are today the most widely used evolutionary algorithms.

4.2 Fundamentals

The purpose here is not to give a thorough theoretical analysis of the GAs mechanism, as there are excellent introductory tutorials in the literature (Goldberg, 1989; Davis, 1991; Michalewics, 1996; and Mitchell, 1996). There is also *The Hitch-Hicker's Guide to Evolutionary Computation* available on the internet (Heitkoetter and Beasley, 1994). Instead, the objective of this section is to provide some answers to explicit questions one may have about GAs. In the following, the structure of a simple GA will be presented along with a general overview of the main techniques/variants that are employed in the GA process. Then, the most important features which differentiate GAs from conventional optimization techniques are described. Eventually, the strengths and weaknesses of GAs are outlined and the type of problems for which the use of these algorithms is pertinent is indicated.

4.2.1 What Are GAs?

Like all evolutionary algorithms, a GA is a search procedure modeled on the mechanics of natural selection rather than a simulated reasoning process. Developed by Holland (1975), these algorithms were originally used for the study of artificial systems. Since their inception GAs have been subject to a growing interest as an optimization technique in nearly all kinds of engineering applications. Today, there are so many different GAs that it turns out, as Mitchell states (1996), that there is no rigorous definition of GAs accepted by all in the evolutionary computation community that differentiate GAs from other evolutionary computation methods. Indeed, some currently used GAs can be very far from Holland's original conception. However, it can be said that most methods called "GAs" have at least the following elements in common: populations of individuals, selection according to the individuals' fitness, crossover to produce new individuals, random mutation of new individuals, and replacement of the populations. These elements are illustrated next, in the description of how a simple GA works. A typical GA flowchart appears in Fig. 4.1.

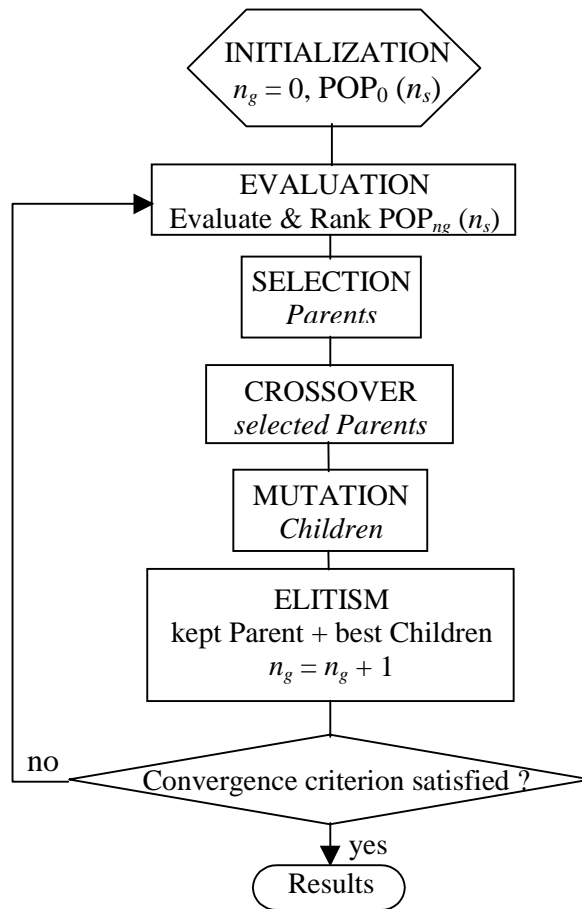


Figure 4.1 Typical Genetic Algorithm flowchart.

4.2.2 How Do GAs Work?

GAs are based on the collective learning process within a population of individuals (trial solutions called chromosomes), each of which represents a search point in the space of potential solutions to a given problem. The chromosomes code a set of parameters (called genes). The population (of size n_s) is generally randomly initialized (at the generation $n_g=0$) in the parametric search space (see POP_0 in Fig.4.1). The individuals are evaluated and ranked in terms of a fitness function. Then, the population evolves towards fitter regions of the search space by means of the sequential application of genetic operators. The basic operators of a simple GA consist of selection (selection of parents for breeding), crossover (mating of parents to create children) and mutation (random changing of a gene). Following the Darwinian theory of survival of the fittest, an elitism operator is usually found in the generational replacement. A generation is accomplished when the sequence defined by the application of all operators to the individual parents is performed, as illustrated in Fig. 4.1.

The GA produces as many generations as necessary until the convergence criterion is reached. The goal, throughout this process of simulated evolution, is to obtain the best chromosome in the final population to be a highly evolved solution to the problem.

The main techniques/variants that are employed in the GA process for encoding, fitness evaluation, parent selection, crossover, mutation, replacement and convergence are reviewed next.

4.2.3 What Are the Main Operator Variants Employed in the GA Process?

The genetic operators have all several variants which can be applied in a randomly and/or probabilistic (sometimes deterministic for some algorithms) process. These variants may be quite specific in single applications but a number of standard variants are used by most GAs. The following paragraphs briefly review the main standard genetic operator variants. Again, note that it is not intended to give descriptions of all variants mentioned, as the literature cited earlier provides excellent details about all. However, when describing the GAs developed (Section 4.3) the variants used will be explained. Figure 4.2 introduces the general structure of a standard simple GA (based on Fig. 4.1). In addition, as an introductory tutorial, the mechanisms behind the genetic operator variants of such a simple GA are developed in Appendix A using a simple function optimization example.

- **Description**

Encoding Scheme

To enhance the performance of a GA, a chromosome representation that stores problem-specific information is desired. Although GAs were developed to work on chromosomes encoded as binary strings (Fig. 4.2), it is today common knowledge that for numerical optimization problems, one should use a GA with floating point representation. One important point that may, however, not be obvious when one starts to use GAs (which was my case) is that the crossover variants used should be appropriate to the encoding used. There indeed exist both conventional (binary) and arithmetical crossover techniques to fit the two different representations. Note that when using the real representation, a chromosome is a vector of n_p genes for the n_p parameters. It should be emphasized here that because much of the early work of GAs used a universal coding involving abstract binary chromosomes (that needed to be

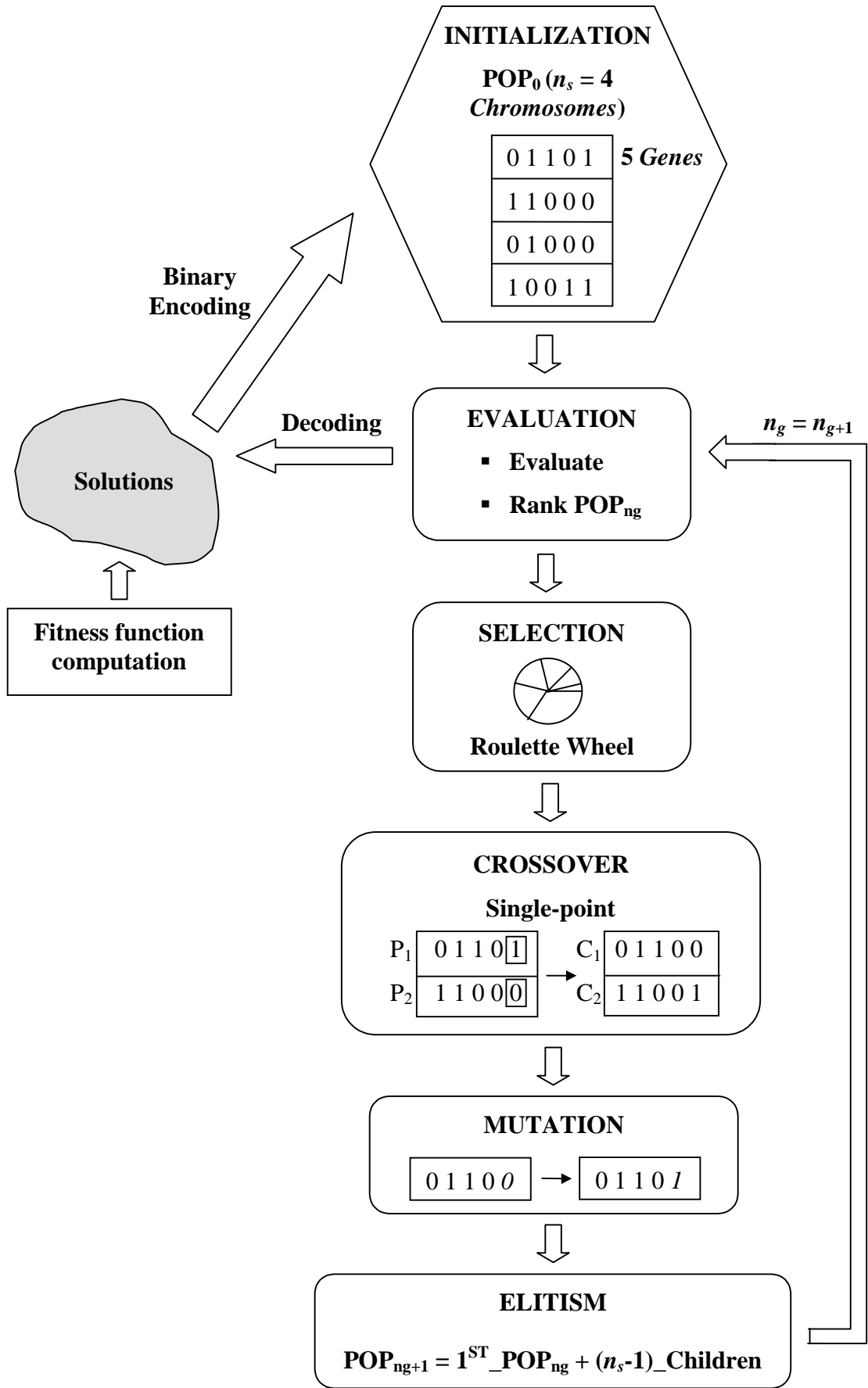


Figure 4.2 General structure of a standard simple Genetic Algorithm.

decoded), research on GAs has been slow to spread from computer science to engineering, and very little theory exist in the literature on real-valued encoding.

Fitness Function

The fitness plays the role of the environment in which the chromosomes are to be evaluated (Fig. 4.2). This is thus a crucial link between the GA and the system. This function can be simply taken as the objective function to optimize or as a transformation (scaling) of it. It is assumed that the fitness function to be optimized is positive. In cases where the objective function happens to be negative, the fitness function will be a transformation of the objective function.

Parent Selection

Basically, the selection operator determines which of the individuals in the current population (of size n_s) will be allowed to pass their genetic material to the next generation. Using the GA language, one says that it builds up the mating pool by selecting n_s individuals from the current population. There are many ways to achieve effective selection, including proportionate, ranking and tournament schemes. The key assumption is to give preference to fitter individuals. Using fitness proportionate selection, the number of times an individual is expected to reproduce is equal to its fitness divided by the average of fitnesses in the population. The most popular and easiest mechanism is the roulette wheel selection (Fig. 4.2) where each chromosome in the current population has a roulette wheel slot sized in proportion to its fitness. However, depending on the environment (fitness), proportionate and ranking selection schemes may lead to premature convergence or on the contrary, to a slow finishing. Those are well-known severe technical problems of GAs. However, both problems can be avoided if scaled fitness values are used instead of the original values. Another way to circumvent these problems is to use a more adequate selection operator. In many applications, tournament selection has proved to yield superior results to fitness rank selection. In the simplest form, the so-called binary selection, two chromosomes are selected randomly from the current population but only the one with the higher fitness value is inserted into the mating pool with a probability p_t . One interesting feature about this selection scheme is that one can adjust the selection pressure directly from the tournament probability p_t (typically larger than 0.5). Regardless of which selection technique is used, the selection operator produces an intermediate population, the mating pool, which consists only of individuals that are members

of the current population. The following two operators, crossover and mutation, are then applied to this mating pool in order to generate children.

Crossover

The crossover operator is the key operator to generate new individuals in the population. Note that the fact that the use of crossover increases the performance of a GA has been proved by two theories, namely the Holland's Schema Theorem (1975) and the Goldberg's Building Block Hypothesis (1989). In addition, it has been shown that so-called "deceptive" problems (Goldberg, 1989) can be made "easy" by the use of an appropriate definition of the crossover function. This operator is applied to each pair of the mating pool with a crossover probability p_c , usually taken from $[0.6,1]$, to produce one or two children. With probability $1-p_c$, no changes are made to the parents (they are simply cloned), but with probability p_c , genetic material is exchanged between the two parents. In the simplest crossover, the single point crossover (Fig. 4.2), a crossover point is randomly selected and the portions of the two chromosomes beyond this point are exchanged. Multipoint crossover is similar except that multiple cross points are chosen at random with no duplication. Uniform crossover generalizes the scheme by making every gene a potential crossover point. Single, multipoint and uniform crossovers are generally considered conventional binary techniques, and when real encoding is used, arithmetic crossovers are the most suited.

Mutation

This operator should allow a GA the finding of solutions which contain genes that are non-existent in the initial population. It can also prevent the GA from losing some genetic material without any chance of adopting it again. Often viewed as a background operator, mutation modifies gene values according to a mutation probability. Using binary encoding, this simply means changing a 1 to a 0 and vice versa with a small probability (Fig. 4.2). Using real encoding, when a global modification called jump mutation is applied, each gene in any chromosome is replaced with a random value (from the entire parametric search space) with probability p_{mj} . A "mutation-based" operator can also be applied locally with the creep variant (not a pure mutation operator in the sense of GAs) which consists in the addition or subtraction with probability p_{mc} of a small value to the gene (1% of the actual gene value). Whereas the crossover operator reduces the diversity in the population, the mutation operator increases it again. The higher the mutation probability, the smaller is the danger of premature convergence. A high mutation probability will however transform a GA into some kind of

random search algorithm, which is of course not the intention of the algorithm! Mutation probabilities are usually small (so as not to interfere with the combination of the best features of parents made by the crossover operation), and range from 0.001 to 0.10, the higher values being typically applied with real encoding.

Replacement Strategies

In the simplest form of GAs, when the operation of selection, crossover and mutation are completed on the n_s individuals of the current population, this entire population is replaced with the children created. This is the traditional generational replacement. Variations where not all individuals are replaced in each generation exist. The simplest case of such a strategy is the elitist strategy where the individual with the highest fitness (according to the Darwinian theory of survival of the fittest) is directly transferred from the old to the new generation and only the other n_s-1 children are generated by the application of genetic operators (Fig. 4.2). Generational replacement with probability p_r is often used in which $n_s \times p_r$ parents are replaced with children while the $n_s \times (1-p_r)$ best parents are kept. An alternative to replacing an entire population at once is to replace one organism in the population whenever a new organism is created. This variant is known as a steady-state GA.

Convergence Criterion

The most widely used stopping conditions are either that a given number of generations have been done already, or that the population has become uniform. When the first condition is chosen, GAs are typically iterated for anywhere from 10 to 500 or more iterations. User-defined convergence criterion that are better suited to the problem being solved should be preferred (although most of the studies do not address this problem). It is however not easy to define such a criterion, as it will be shown in this work.

Performance Criteria

What does it mean for a GA to perform well or poorly? Some performance criteria can provide answers to this question. The best fitness reached (best-so-far) is a typical one. One criterion for computational cost is the number of function evaluations. Indeed, in almost all GA applications, the time to perform a function evaluation vastly exceeds the time required to execute other parts of the algorithm (which are thus considered to take negligible time). Note that because randomness plays a large role in each run (two runs with different random number seeds will generally produce different output), often GA researchers report statistics

(about the best fitness for instance) averaged over many different runs of the GA on the same problem.

Besides the genetic operators presented here, there exist a number of different operators (inversion, reordering), in addition to advanced features (diploid, dominant and recessive genes, sharing fitness function) which are used in different applications but not yet widely. GAs are still far from maturity.

- **Discussion**

Undoubtedly, GAs possess the attributes of a probabilistic search technique for the global optimum, while it is unfortunately often referred to as a randomized search. It is important to realize that the global optimum solution will not be found in one GA run. GAs are however robust in producing near-optimal solutions, with a high degree of probability to obtain the global optimum (Kroittmaier, 1993).

One may realize at this point that the main challenge in constructing a general-purpose GA programming environment is the selection of the genetic operator variants from the diversity of adaptive techniques that exist, as well as the settings of the genetic parameter values (population size, selection, crossover and mutation probabilities, which could be called “fine tune” parameters as they play a decisive role in the GA success). Indeed, GAs using binary representation and single-point crossover and binary mutation are robust algorithms but are never the best algorithms to use for any problem. There are unfortunately few heuristics to guide a user in the selection of appropriate operators and genetic parameter settings for a particular problem. What can be grasped from the literature is that good GA performance requires the choice of a moderate population size, a high crossover probability and a low mutation probability (for instance, inversely proportional to the population size in using real encoding). This lack of heuristics is a well known problem in GAs. With some experience, one may have an idea about which variants and “right” values to use. Note that such a procedure could be compared with the choice of a numerical scheme and then the grid discretization and number of iterations to apply when using a numerical formulation to solve, for instance, a heat transfer problem.

There are, however, two important issues in GAs that one should use as a guide (this is what I realized before developing the third GA): exploiting the best solutions and exploring the search space. On one hand, the selection operator associated with the fitness function

gives the tendency between exploitation and exploration and is therefore very important. It is usually considered the evolution operator. On the other hand, crossover and mutation are classified as search operators. The first allows both exploitation and exploration, while the second concentrates on exploration. The elitism operator can be viewed as a preservation operator which exploits the best solution(s). As one may guess, a GA efficiency consists of an adequate balance between exploitation and exploration.

4.2.4 What Differentiates GAs From Conventional Techniques?

GAs differ from conventional optimization and search procedures in several fundamental ways. Goldberg (1989) has summarized these as follows:

1. GAs work with a coding of solution set, not the solutions themselves; note that this remark applies particularly more to binary encoding.
2. GAs search from a population of solutions, not a single solution.
3. GAs use payoff information (fitness function), not derivatives or other auxiliary knowledge.
4. GAs use probabilistic transition rules, not deterministic rules.

4.2.5 What Are the Strengths and Weaknesses of GAs?

- **Strengths**

There are major advantages of applying GAs to optimization (or estimation) problems. Easily programmed, GAs are derivative-free calculations and therefore, are neither bound to assumptions regarding continuity, nor limited by required prerequisites. As Goldberg stated, GAs are blind. They can handle any kind of objective function and any kind of constraints (e.g., linear or nonlinear) defined on discrete, continuous or mixed search spaces. In addition, as stated earlier, they are robust in producing near-optimal solutions, with a high degree of probability to obtain the global optimum. Another strength of GAs is their flexibility to be parallelizable and hybridized with other techniques. A parallel GA operates on multiple population pools; whenever computer facilities offer the use of several processors, such a GA can allow for powerful runs. A hybrid search combines local search with a GA. It is an interesting alternative wherein a number of promising initial solutions generated during the GA search are used as the starting point for a locally convergent optimization algorithm.

Davis (1991) advocates hybridization of GAs with domain-specific techniques, usually the ones that were typically used for the problem being investigated. Hybrid GAs are believed to have potential for ill-conditioned inverse problems, and the development of such procedure is actually one of the recommendations of this work (see Chapter 7). Note that hybrid GAs however lose some of their general robustness as they become more specific to the problem at hand.

- **Weaknesses**

Although the GA is a powerful optimization tool, it does have certain weaknesses in comparison to other optimization techniques. A poorly designed GA can perform nearly as badly as a random search. In short, because a GA's performance is highly application-specific, it must be adapted to the task on hand (Davis, 1991). Furthermore, a GA application is sometimes more an art than a science. Besides, due to the randomness part of the GA operations, it is difficult to predict its performance. The success of a GA and its effectiveness in any application can only be determined by experimentation. Another significant drawback is the high CPU cost involved.

4.2.6 For Which Type of Problems Should GAs be Used?

In the light of their strengths and weaknesses, one can guess that for unimodal functions that are smooth, there is no sense in using GAs. Rather, the use of these algorithms seeks to “solve” problems that are intractable with classical procedures. The mathematical function **f6** described in Section 4.4.1 shows the kind of complicated problems a GA can be called upon to solve. Typically for a GA to be used, the design space is large (for instance in the optimization of complex experimental designs), multi-modal, noisy, and fraught with discontinuities. Their use over traditional gradient-based optimization techniques also finds its rationale for problems where the gradient information leads to instabilities (for instance in ill-posed parameter estimation problems). Indeed, because GAs do not require gradient information, but only the computation of values of the objective function to optimize, when applied to parameter estimation problems these algorithms are therefore not limited by correlations that may exist between the parameters. Consequently, GAs provide a general powerful approach to inverse problem solving, in which a good numerical model of the direct problem and a representation for potential solution are the only prerequisite. In addition, it is

relevant to recall here that the use of gradient-based methods for nonlinear estimation necessitates the linearization of the model (see Section 3.1.2). This is not the case when applying GAs.

Note that because there are so many different GAs, many open questions exist about the type of problems for which GAs are best suited and, in particular, the type of problems on which they outperform other search algorithms.

To conclude this section, it should be mentioned that GAs and gradient-based methods should not be considered competing approaches but instead, whenever possible, should work together as these two types of techniques are believed to be complementary. This comment goes along with the advocacy of Davis (1991) to hybridize them (refer to the previous section for an explanation of hybrid GAs). Davis has shown that hybridization of these techniques can lead to better performance than using any of them in isolation.

4.3 GAs Developed

With an aim toward overcoming the limitations of traditional techniques used in experimental design optimization and simultaneous parameter estimation (described in Chapter 3), the main features of Genetic Algorithms (with real encoding) were thought to be exploited and applied to both fields. With very little theory on real encoding existing in the literature, three “GAs” have been developed in this work, each time improving the last version over the previous one. This research has started with a standard GA featuring a Basic Elitist strategy (BEGA) and then it was improved by implementing an Extended Elitist strategy (EEGA) following as much as possible the Darwinian principle of survival of the fittest. Eventually, from the knowledge gained in the GA field, a third GA was developed in which genetic operators more appropriate for real encoding were used, and a convergence criterion was implemented. These three algorithms are successively described next.

4.3.1 Basic Elitist GA (BEGA)

- **Description**

The first GA developed, which was modeled according to the algorithm described by Furuya and Haftka (1993), was called Basic Elitist GA (BEGA) because it used a basic elitist strategy. A detailed description of the BEGA is given here for the particular case of the optimization test problems treated in Section 5.1.1. Note that a single chromosome thus designates a vector of design variables. A simplified flowchart of the BEGA is shown in Fig. 4.3.

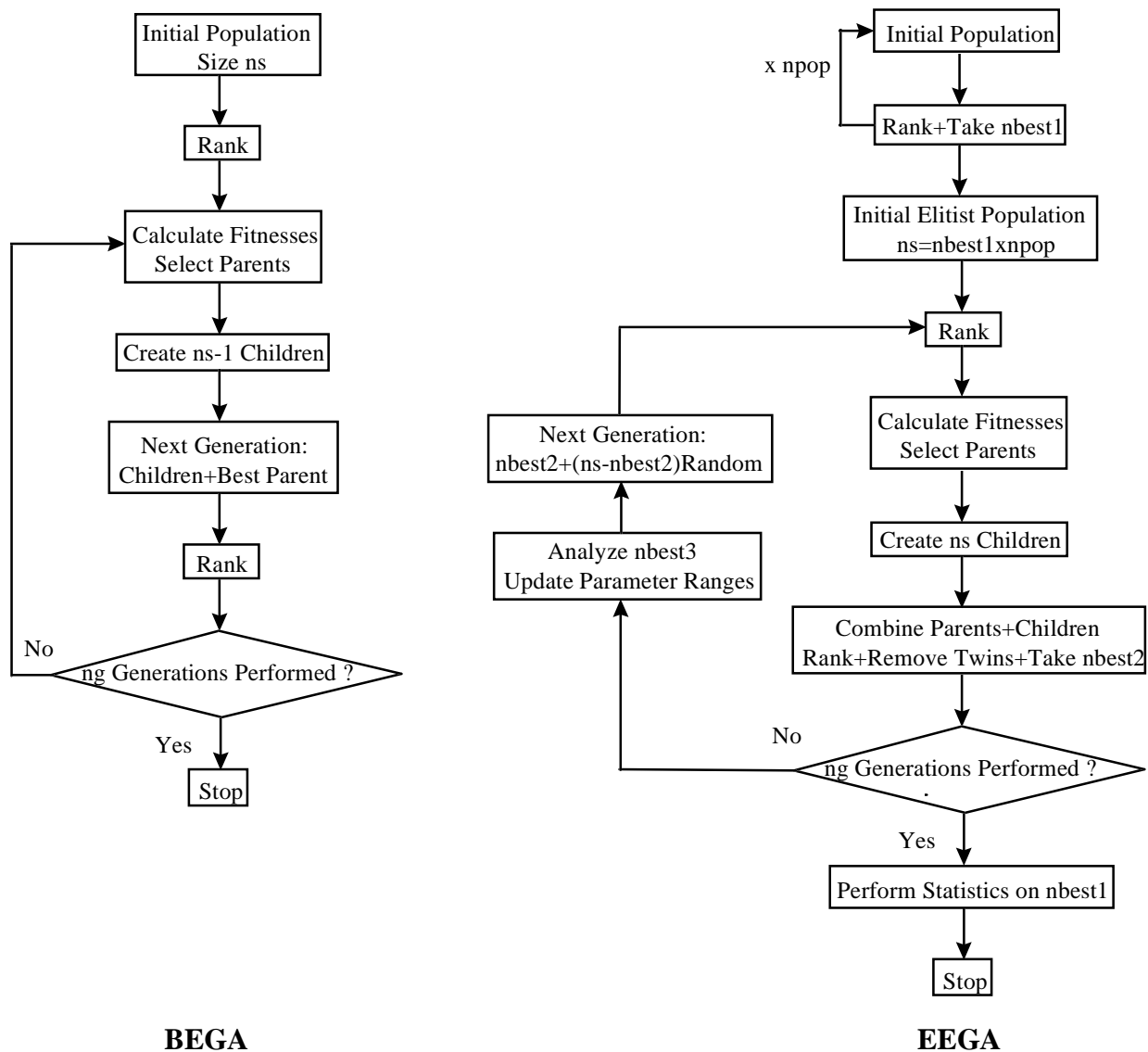


Figure 4.3 Flowcharts of BEGA and EEGA.

Design Coding

In the optimization of the one-dimensional experiment (Fig. 5.1), a chromosome describing a particular design contained two genes for the sensor location x_s^+ and the heating time t_h^+ . Along the same lines, in the optimization of the two-dimensional experiments (Fig. 5.2), each chromosome contained four genes for the design variables x_s^+ , y_s^+ , L_p^+ and t_h^+ . The ranges of the real genes depended on the lower and upper bounds of the design variables which were specified by the experiments. For instance, the chromosome x_s^+ (dimensionless sensor location perpendicular to the fibers) ranged from zero to one.

Initial Population

The optimization algorithm started by generating the initial parent population of n_s candidate chromosomes (designs). Each individual was created by randomly selecting n_p gene values (design variable) from the design space. The chromosomes were then ranked in terms of the value of the dimensionless determinant D^+ using the D -criterion. Obviously, the best string had the highest D^+ .

Selection

Parents were selected by pairs for breeding using a proportionate rank-based fitness technique. The fitness of the i^{th} ranked chromosome was defined as $f_i = n_s + 1 - i$ allowing for the highest ranked chromosome to have the highest fitness parameter and thus to be most likely to contribute to the determination of the next generation strings. The probability of the i^{th} ranked chromosome to be selected as a parent was given by $p_i = \frac{2f_i}{n_s(n_s + 1)}$. The selection process was then accomplished at random, according to the roulette wheel mechanism: the i^{th} ranked chromosome was selected if $P_{i-1} \leq R \leq P_i$, where $P_i = \sum_{j=1}^{i-1} p_j$ and R was a uniformly distributed random number between zero and one.

Crossover

The children were made by the mating of the $(2n_s)$ pairs of parents selected for breeding according to the single-point crossover (with a crossover probability p_c of 1.). Note that the simplest crossover operation was chosen to be used because the primary goal using the BEGA was to test the effectiveness of GAs comparatively to the parametric study in the optimization

of experimental designs. This process began by generating a random integer k , the cut-off point, between 1 and n_p-1 , where n_p was the number of genes. A child was designed by using the first k genes of parent 1 and the remaining ones came from parent 2 (see App. A). For instance, consider in the one-dimensional analysis the chromosomes with $x_s^+=0.5$, $t_h^+=1.0$ and $x_s^+=0.7$, $t_h^+=1.5$ as parents 1 and 2, respectively. As $n_p=2$ (recall that there are two design variables in the one-dimensional analysis), the only possible child chromosome (one child per pairs of parents) could be $x_s^+=0.5$, $t_h^+=1.5$.

Mutation

Jump mutation was implemented by changing at random the value of a gene. This process ensured that new genes were generated, thus preventing the solution from locking on a non-optimum value. The mutation probability p_m was taken arbitrarily as 0.05. If the gene was mutated, it was replaced by another one randomly chosen from the allowable range of values for that gene.

When the operations of selection, crossover and mutation were completed on the n_s parent population, a new generation was created from the n_s-1 child chromosomes in addition to the best parent chromosome. This addition denotes the basic elitist strategy of the BEGA. Over the course of several generations, the algorithm tended to converge on the chromosome giving the maximum determinant, which was hence considered as the predicted optimal design. Note that the stopping criterion was simply to perform n_g generations. The number of function evaluations f_{eval} was calculated from $f_{eval} = n_s \times (n_g + 1)$.

- **Discussion**

The results obtained using the BEGA (see Section 5.1.1.4) showed that this algorithm was limited when the objective function was highly expensive to calculate (two-dimensional design optimization case). More precisely, the optimization method using the BEGA tended to be as time intensive as the parametric study, although it resulted in improved efficiency and was less tedious to apply.

4.3.2 Extended Elitist GA (EEGA)

- **Description**

The second algorithm was developed to improve the efficiency of the BEGA. It used the same genetic operators as the BEGA but with an extended elitist strategy and was thus called Extended Elitist GA (EEGA). Following is an outline of the five main differences between the EEGA and the BEGA. These differences can also be viewed in the simplified flowcharts shown in Fig. 4.3. The EEGA was applied to both the optimization and estimation test problems treated in Section 5.1.1, in addition to the estimation of the thermal and radiative properties of an insulative material (not reported in this dissertation but which can be found in Garcia et al., 1998).

1. A pure random search was initially performed to obtain appropriate starting conditions for the lower and upper bounds of each gene (parameter to be optimized/estimated). The purpose of this seeding was, therefore, to help direct the GA search. Note that this initial search was run separately from the EEGA run.
2. The EEGA started by a successive random search for a number of n_{pop} initial subpopulations in which only the n_{best1} first ranked chromosomes were kept within each subpopulation. This produced an initial elitist population of size $n_s = n_{pop} \times n_{best1}$. (Note that by carefully selecting the parameter space, steps 1 and 2 are comparable to the use of *a priori* information).
3. n_s children were created according to the BEGA and then combined with the parent population. After ranking this combined population of size $2n_s$, the “twins” were removed (usually a small number much lower than n_s) and only the n_{best2} first ranked chromosomes were kept, where $n_{best2} < n_s$.
4. The parameter ranges were updated from the analysis of the n_{best3} first ranked chromosomes, where $n_{best3} \leq n_{best2}$. Additional random chromosomes numbering $(n_s - n_{best2})$ were then generated from the just updated parameter ranges and were added to the n_{best2} first ranked chromosomes to form the next generation. By allowing some “new blood” to be brought into the population, population diversity is preserved, therefore preventing, it is thought, the EEGA from premature convergence on a non-optimal chromosome. This feature was also thought to compensate for the use of only the simple

single point crossover which did not produce new gene values.

- Steps 3 and 4 were repeated until n_g generations had been achieved, and then the means and the 95% confidence intervals [Eq. (3.18)] for each gene were determined for each of these n_{best1} chromosomes. These confidence intervals were a good means of evaluating the convergence of the EEGA. Note that the number of function evaluations was now given by $f_{eval} = (n_{pop} \times n_s) + [n_s + (n_s - n_{best2})] \times n_g$.

It is important to note that when EEGA was used as an estimation procedure, the output for a particular experimental data set included the means of each gene (thermal property) and the approximate 95% confidence intervals representing the ranges of values which the actual properties lay within for that particular experiment. The calculation of this confidence interval was described in Section 3.1.5 [Eq. (3.17)].

- **Discussion**

The results obtained using the EEGA on the test problems (see Section 5.1.1.4) showed that this algorithm outperformed both the BEGA and the parametric study. However, when applied to the estimation of the thermal properties of an insulative material (Garcia et al., 1998) in which the objective function (least-squares error) presented a “local minimum plain” and a “global minimum valley” on the same order of magnitude, the EEGA tended to direct the search to the local plain at the expense of global perspective. This was the output from the use of the extended elitism strategy which resulted in a strong forced evolution feature preventing the GA from performing a good balance between exploitation and exploration. The removing of twins and the addition of random “blood” were not sufficient to keep a diverse population and prevent a *super chromosome* from dominating the population which then caused premature convergence. In addition, the use of the simple single-point crossover (originally designed for binary encoding) was simply too poor with real encoding as it could not allow new genes to be created.

Based on both the BEGA and EEGA behavior analysis, a third GA was developed. Two main prescriptions were taken into account which were:

1. Elitism should be used cautiously in adequacy with the objective function landscape.

2. One cannot use a naïve simple GA and modify it by implementing all kinds of (elitism) features to make it work properly. Rather, one should use from the beginning an adapted GA to the problem being solved. In my case, this implied to use genetic operators adapted to a real-number encoding.

4.3.3 Third GA (GA_3: GAMAIN and GACONDUCT)

- **Description**

Figure 4.4 illustrates a simplified flowchart of the GA_3. Some of the genetic operator variants were defined in Section 4.2.3. Note that in the problems treated using the GA_3 in

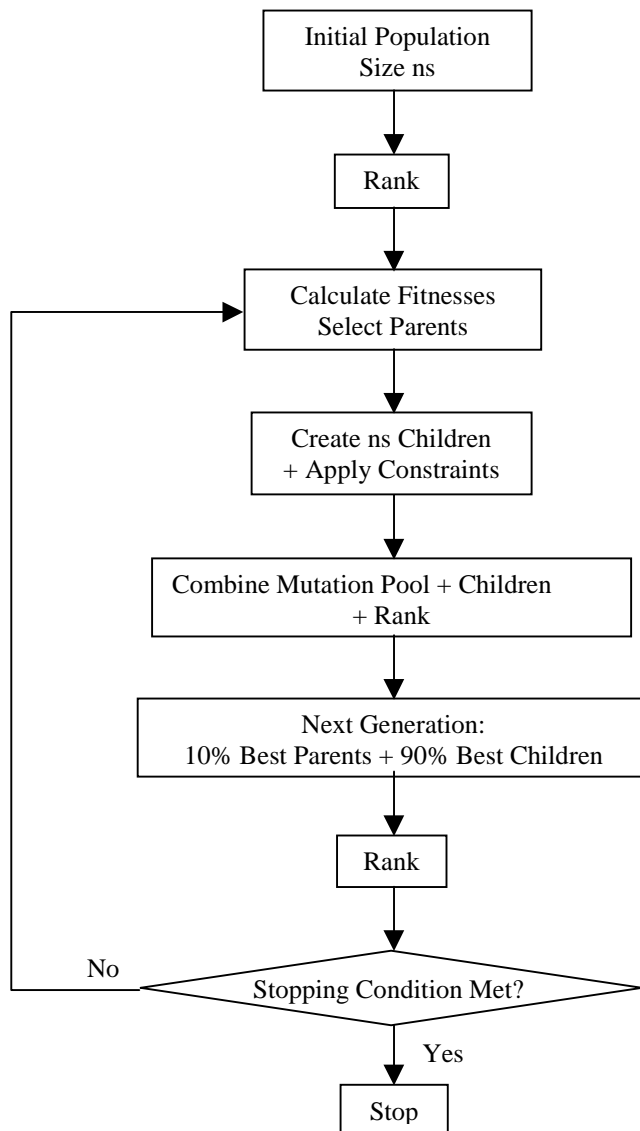


Figure 4.4 Simplified flowchart of GA_3.

the current research (Sections 5.1.2, 5.2.1, 5.2.2 and Chapter 6), the values used for the setting of the genetic parameters (p_t , p_c , p_{mj} , p_{mc} and p_r) were determined from a performance analysis described in Section 4.4. The major enhancements with the EEGA came from the use of:

1. binary tournament selection (see Paragraph *selection* in Section 4.2.4) which helps prevent premature convergence (Goldberg, 1989). An elitist scheme was actually implemented in which each chromosome of the top half of the current ranked population competes with a second chromosome randomly chosen from the entire population (and which cannot be a duplicate of the first chromosome). The chromosome with the higher fitness value is inserted into the mating pool with a probability p_t set to 0.9 (in 10% of the cases, the parent selected is the less fit).
2. an arithmetic crossover (Doyle, 1994) well suited for real encoding and which allows for the creation of new genes even outside the initial parameter ranges. Two children C_1 and C_2 are created per pair of parents P_1 and P_2 with a probability p_c taken as 0.9 (10% of the parents are cloned) using: $C_1 = \left(\frac{P_1 + P_2}{2}\right) + |P_1 - P_2| \times R$, $C_2 = \left(\frac{P_1 + P_2}{2}\right) - |P_1 - P_2| \times R$, where R is a random number uniformly distributed between 0 and 1.
3. both the jump mutation and the creep variant with probabilities $p_{mj}=1/n_s$ and $p_{mc}= p_{mj}/2$, respectively, where n_s is the population size. The chromosome before mutation is copied onto a “mutation pool” and when the elitist replacement is applied (see below), the mutation pool is mixed with the resulting children pool. This means that good gene information is not lost by applying mutation.
4. an elitist generational replacement with a probability $p_r=0.9$, in which 10% of the top ranked parent population was kept into the next generation while 90% were replaced with the 90% best created chromosomes from the combined pool as described above.
5. a convergence criterion based on a small percentage change (1%) in both all gene values and the objective function value of the best (so far) chromosome (recall that the objective function is the optimality criterion, to be maximized, when performing experimental design optimization, and the least-squares error, to be minimized, when performing parameter estimation). The stopping condition is to first, execute *MING* generations without checking the convergence criterion. Next, this latter is checked at the end of each generation. If it is met during *LASTCRITERG* generations, then the run is stopped; if not, then at most *LASTG* generations are executed. Note that if the convergence criterion is

met for a number of generations less than *LASTCRITERG* and then the best-so-far chromosome changes, then the generation counter for the convergence criterion is reset.

In addition to these five points that are related to genetic operations, some improvements were made by using two types of nondimensionalization for the chromosomes. When the parameter range to investigate [parmin-parmax] (in which the initial population is defined) was less or equal than 2 orders of magnitude, e.g. $\frac{parmax}{parmin} \leq 100$, then a linear nondimensionalization was used; otherwise, a logarithmic nondimensionalization was applied, allowing then for large ranges to be scanned. Regardless of which type was used, the chromosomes were defined between zero and unity. In terms of the population size, a formula for binary encoding (Carroll, 1996a,b) was thought to be applied for real representation. The ideal population size was taken to be the product between the number of parameters to be determined and the average number that the parameters could take. Therefore, with a nondimensionalization between zero and unity, considering the case where the parameters could take 100 values in that range, the ideal population size was defined as $n_s = 100 \times n_p$.

A last improvement in developing the GA_3 is related to an important aspect of the optimization (or estimation) process. This aspect deals with applying knowledge-based control mechanisms to improve the solution. Constraints are a convenient means of incorporating domain knowledge as much as possible. In the GA_3, such incorporation was realized in two ways. First, into the fitness function (which is simply the objective function) by assigning penalties for chromosomes whose raw fitnesses were known to be infeasible. Those penalties made the chromosome be rejected when the elitism operator was applied. Second, constraints were also applied directly on the genes so that the search focused on the prescribed parameter ranges (note that these ranges were usually quite large for the first run). In this second way, any created gene that was lower than zero or higher than unity (which could happen with the use of the arithmetic crossover) were redefined as zero and unity, respectively. Analyses of the final population would indicate whether the prescribed ranges were adequate or not (for instance, if the genes were concentrated around zero or unity, then the prescribed ranges were inadequate).

Finally, note that in the GA_3 scheme, several EEGA features were removed, namely:

- the initial random search which resulted in an initial elitist population but was too computationally costly;
- the dangerous (because concentrated the search on local optima) procedure that updated the parameter ranges, and
- the procedure that eliminated the twins as no twins could be generated with the new crossover (this also had the effect of removing the procedure that inserted random chromosomes to replace the twins eliminated).

Also, note that, like with the EEGA, when the GA_3 was used as an estimation procedure, the output for a particular experimental data set included the means of each gene (thermophysical parameter) and the approximate 95% confidence intervals [Eq. (3.17)] representing the ranges of values in which the actual properties lay for that particular experiment.

• Discussion

With these attributes, the GA_3 algorithm was expected to show a better balance between exploitation (of the current population) and exploration (of new good solutions) than the EEGA. One very important point is that the number of evaluations performed with the GA_3, which can be approximated by $f_{eval} = n_s \times (n_g + 1)$, is, for the same population size n_s and number of generations n_g , much lower than with the EEGA. Therefore, in terms of computation cost, the GA_3 was a definitive improvement over the EEGA.

The results obtained using the GA_3 (Sections 5.1.2, 5.2.1, 5.2.2 and Chapter 6) showed that this algorithm performed very well, especially as far as not directing the solution to local optima. However, the weakness of the convergence criterion was highlighted in estimation applications in which the sensitivity of the measured quantity to some parameters was very small. Therefore, one of the recommendations of this work (Chapter 7) concerns the definition of a more suitable convergence criterion, in direct relation with the sensitivity of the measured quantity to the genes (parameters).

An issue when developing the GA_3 was the need for flexibility and adaptability so that the algorithm could handle both the Experimental Design Optimization (EDO) and

Simultaneous Parameter Estimation (SPE) of a problem since the direct solution is unchanged. Therefore, some key constants (flags) were defined so that by changing their default values and defining the appropriate genes (parameters), the GA_3 would perform either EDO (according to *D*-, *E*- or *A*-optimality by setting the appropriate flag) or SPE. The idea behind using such judicious default values (that are all specified in a default subroutine) was taken from the structure of the excellent program CONDUCT developed by Patankar (1991). Based on the GA_3 genetic features, and the flexibility for both EDO and SPE, two algorithm versions, GAMAIN and GACONDUCT were developed. Both versions follow the general structure of CONDUCT, e.g. they consist of an adaptation and an invariant part. The invariant part contains the general calculation scheme that is common to all possible EDO/SPE applications within the overall restrictions of the respective version used. The adaptation part provides the problem specification. The GAMAIN version was written for the analysis of problems for which a mathematical direct solution is to be provided by the user. For heat transfer problems for which an analytical solution does not exist, the GACONDUCT version was then developed by combining the general features of the GA_3 with those of an extension of the program CONDUCT, which is based on a control-volume-based finite difference numerical method. This extension involves modifications made by Dr. D. J. Nelson¹, which allow for the study of orthotropic properties in rectangular geometry (for instance k_x and k_y). Note that by benefiting from the possibilities of the program CONDUCT, the use of GACONDUCT allows for any EDO/SPE applications that deal with the computation of conduction and duct flow heat transfer in two-dimensional rectangular or cylindrical geometry.

Multiple comments are implemented throughout both versions and explain the meaning and the possible setting (depending on the problem to be solved) of the different key flags. Appendices B and C provide the listings (Fortran files) of GAMAIN.FOR and GACOMMON_MAIN.FOR, and GACONDUCT.FOR and GACOMMON_CONDUCT.FOR, respectively.

¹ Professor of Mechanical Engineering at Virginia Tech.

4.4 Performance Analysis of GAMAIN

To illustrate the performance of the GA_3 and to determine the “optimal” setting of the genetic parameters (p_t , p_c , p_{mj} , p_{mc} , and p_r), a mathematical test function was optimized using GAMAIN. The following provides a brief description of this function along with the results for the optimal setting.

4.4.1 Description of the Mathematical Test Function

The expression of the mathematical function **f6** optimized is shown in Eq. (4.1). This function was used by Schaffer et al. (1989) and Davis (1991) for the evaluation of different GAs.

$$f_6(x, y) = 0.5 - \frac{\left[\sin \sqrt{x^2 + y^2} \right]^2 - 0.5}{\left[1.0 + 0.001 \times (x^2 + y^2) \right]^2}, \quad x, y \in [-100, 100] \quad (4.1)$$

This function is symmetric in x and y . Note that the expression for **f6** could have been simplified using the norm $r = \sqrt{x^2 + y^2}$, but then, the complexity of this function would have disappeared. Figure 4.5 illustrates the distribution of this function with y being held constant at its optimal point while x ranges from -100 to 100 (the same graph would be obtained if x and y were switched). The goal is to optimize **f6**, e.g. to find values of x and y which produce the greatest possible value for **f6**. This function has several features that make it an interesting test case:

1. **f6** has a single global optimum (which is **f6(x=0,y=0) = 1**);
2. **f6** shows strong oscillations with increased magnitudes until the global optimum is reached; this is often called multimodality;
3. the global region occupies a tiny fraction of the total area

From this, one anticipates the output from the application of a gradient-based method to become “stuck” on a local hill.

4.4.2 Results

The listing of the adapt subroutine GDAVISF6.FOR (that works with the program GAMAIN given in Appendix A) is provided in Appendix D. Only the results of the analysis of the effects of the genetic parameter settings are reported here. The optimal setting for the genetic parameters investigated is shown in Table 4.1. This setting was found to be superior to any others as it allowed the global optimum of the function **f6** to be found with a 100% probability (on the basis of 20 runs).

Table 4.1 Genetic parameter optimal setting ($n_p=2$).

n_s	p_t	p_c	p_{mi}	p_{mc}	p_r	$MING^{(1)}$	$LASTCRITERG^{(2)}$
200 =100 n_p	0.9	0.9	0.005 =1/ n_s	0.0025 = $p_{mc}/2$	0.9	20	20

⁽¹⁾ initial number of generations that must be performed without checking the convergence criterion.

⁽²⁾ number of generations during which the convergence criterion must be satisfied.

Figure 4.6 shows a typical increase of both the fitness (function **f6**) of the best individual and the average fitness of the population, while Fig. 4.7 illustrates the population evolution from the initial to the final state.

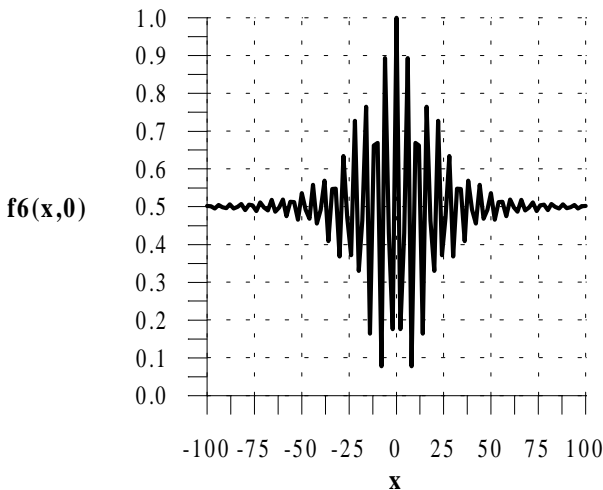


Figure 4.5 Function f6 vs. x with y set to 0.

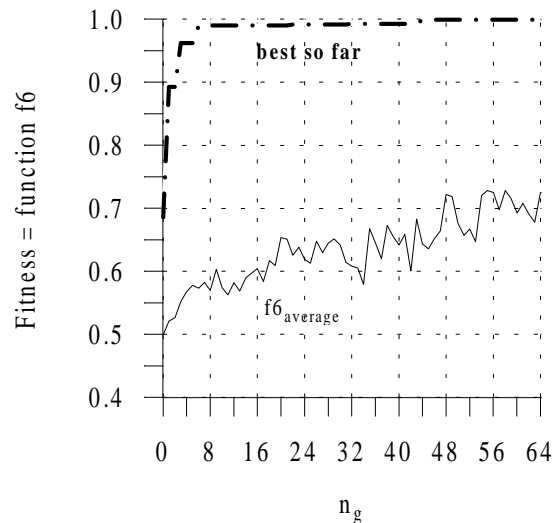


Figure 4.6 Fitness evolution vs. n_g .

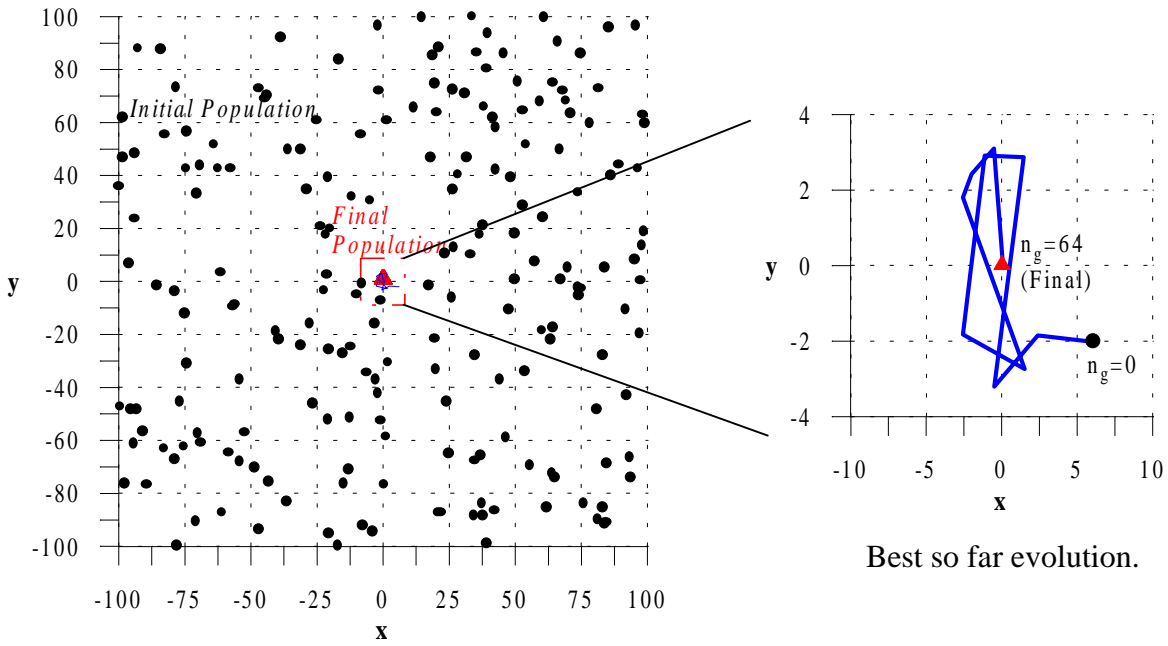


Figure 4.7 Population evolution (initial to final generation).

Because settings of genetic parameters can be a very difficult and time intensive task, the optimal setting found for the optimization of the function **f6** was used subsequently (except for n_s , $MING$, and $LASTCRITERG$ that were problem dependent). Note that this setting was probably not the best in all problems treated subsequently; however Davis has reported that robust settings work well across a variety of problems.

CHAPTER 5

Thermal Characterization of Anisotropic Composite Materials

This chapter is devoted to presenting the different analyses performed for the thermal characterization of anisotropic composite materials. Two of the studies involved two stages. First, the optimization of an experimental design to be used in the prediction of unknown thermal properties; and then, the simultaneous estimation of the unknown properties from the optimal experiments. The studies included the optimization of three, five and seven key experimental parameters, and the simultaneous estimation of two, three, seven and up to nine thermophysical parameters to represent the dependence of the thermal properties on temperature. Recall that by thermal properties is meant *effective* thermal properties, as introduced in Chapter 2. In addition, the effects of the choice of the criterion used to optimize the experimental designs on the accuracy of the property estimates was analyzed for one of the case studies. In all cases, genetic-based optimization/estimation methodologies were applied.

The first section focuses on case studies involving constant property estimation, whereas case studies of mixed temperature dependent and constant property estimation form the subject of the second section. The first subsection provides the analyses performed on two test cases (Moncman, 1994; and Hanak, 1995) towards the assessment of using genetic algorithms as a strategy for both experimental design optimization and simultaneous parameter estimation methodologies. The first two algorithms developed, the BEGA and the EEGA, were successively applied. The test cases involved one- and two-dimensional transient heat transfer for the simultaneous estimation at ambient temperature of two (the conductivity perpendicular to the fiber plane, k_x , and the volumetric heat capacity, C) and three thermal properties (the conductivity parallel to the fiber plane, k_y , in addition to the two previous) of a composite material, respectively. In both the optimization and estimation stages, the GAs

performance was compared with the results from Moncman and Hanak. The two-dimensional case was further investigated with an aim to demonstrating the benefit from optimizing experimental designs. Finally, both one- and two-dimensional test cases were used as a basis for the investigation of the effects of the choice of the optimality criterion on the accuracy of the property estimates.

Applications treated in the following subsections were solved using the general-purpose GACONDUCT version of the third algorithm developed (GA_3). Here, the appraisal of the GA strategy was not the primary issue, and the analyses concentrated on the physical problems. The second and third subsections are both associated with two-dimensional transient heat transfer for the simultaneous estimation of the thermal properties k_x , k_y and C of composite materials over the temperature range [30-150°C]. The difference between the studies was that in one the properties were constant at specific temperature levels (Section 5.1.2), and in the other were temperature-dependent using a piece-wise linear function in temperature (Section 5.2.1). This latter case included the consideration of a contact resistance between the sample and aluminum components used in the experimental mold. Finally, the simultaneous estimation of the thermal properties k_x , k_y and C of a composite material from two-dimensional transient experiments in RTM (Resin Transfer Molding) mold is described in Section 5.2.2. The experimental temperatures ranged from 100 to 130°C. Both k_y and C were identified as temperature dependent while k_x was determined as a constant over the prescribed range. Here again, a contact resistance between the sample and a mold component was considered. This study was based on the work of Lecointe (1999), who used a parametric study to identify k_y and R_c as constants assuming k_x and C to be known.

5.1 Case Studies of Constant Property Estimation

5.1.1 One- and Two-Dimensional Analyses at Ambient Temperature

This subsection reports the initial steps performed in the development of genetic-based optimization/estimation methodologies. The objectives were to test the proposed methodologies on two problems previously analyzed in the literature (Moncman, 1994; and Hanak, 1995), and consequently, the primary analyses focused on the performance of the GAs. The problems investigated involved experimental design optimization and simultaneous thermal property estimation. The BEGA and then the EEGA were demonstrated on the optimization stage, while only the EEGA was applied in the estimation stage. Both algorithms

are described in Chapter 4. A description of the test problems is first provided, followed by the brief specification of the experimental data used in the estimation methodology. Then, the mathematical models that allowed for the temperature distribution and the optimality criterion to be calculated in the estimation and optimization stage, respectively, are formulated. The fourth subsection shows and discusses the results obtained. Next, the benefit from optimizing experimental designs is outlined and, eventually, the effects of three optimality design criteria described in Chapter 3 are investigated.

5.1.1.1 Problem Descriptions

The test problems analyzed include one- and two-dimensional experimental designs used to simultaneously estimate thermal properties of a composite material AS4 carbon fiber/3502 epoxy matrix at ambient temperature.

In the one-dimensional experimental design shown in Fig. 5.1, the sides of a planar sample were insulated while an imposed heat flux was applied across the entire top surface and the bottom surface was held at constant temperature. Moncman (1994) sought to optimize three design variables which were the (unique) sensor location x_s^+ , the duration of the heat flux t_h^+ and the overall experimental time t_n^+ , for the simultaneous estimation of the thermal conductivity through the fiber plane, k_x , and the volumetric heat capacity, C .

The two-dimensional analysis was an extension of Moncman's work for the estimation of the thermal conductivity in the fiber plane, k_y , simultaneously with the two properties k_x and C . Hanak (1995) investigated two different experimental configurations on planar rectangular samples (Fig. 5.2). The purpose of using two different sets of boundary conditions was to demonstrate the influence of these latter on the estimated properties. Both configurations had a uniform heat flux applied over a portion of one boundary, with the remainder of the boundary insulated. In addition, Configuration 1 had constant temperatures at the remaining three boundaries, while Configuration 2 had a constant temperature boundary opposite to the heat flux boundary, with the remaining two boundaries insulated. The (unique) sensor location perpendicular and parallel to the fibers, x_s^+ and y_s^+ respectively, the duration of the heat flux t_h^+ , the heating length L_p^+ and the overall experimental time t_n^+ were the five design variables to be optimized.

Both Moncman and Hanak's optimization analyses were performed using dimensionless terms ($^+$) so that their results could be applicable to any material. They used a parametric

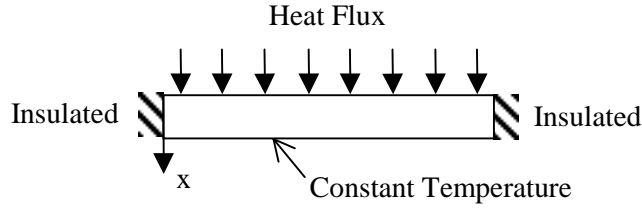


Figure 5.1 One-dimensional boundary conditions.

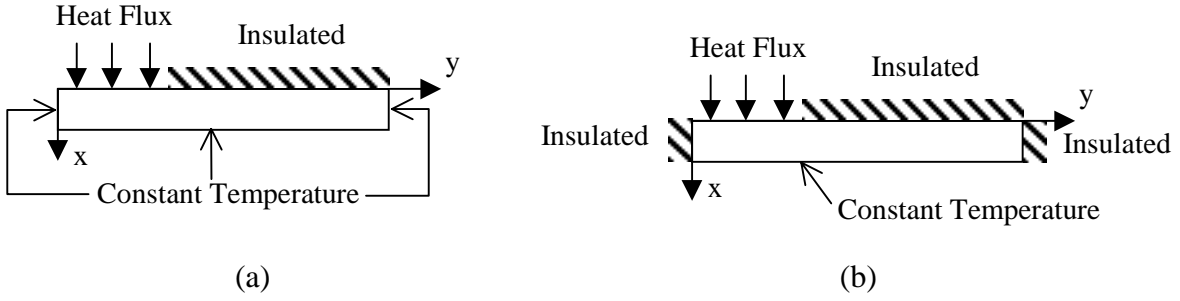


Figure 5.2 Two-dimensional boundary conditions
(a) Configuration 1 and (b) Configuration 2.

study to optimize the design variables according to D -optimality. Recall from Chapter 3 that, in using the D -criterion, the time-averaged determinant of the dimensionless $\mathbf{X}^T \mathbf{X}$ matrix, D^+ , is maximized. \mathbf{X} stands for the sensitivity matrix. In the one- and two-dimensional test problems, $\mathbf{X}^T \mathbf{X}$ was a 2-by-2 and a 3-by-3 matrix, respectively. The criterion D^+ is expressed as $||[d_{ij}^+]$, where the coefficients d_{ij}^+ given by Eq. (3.23) are reported here for convenience (using a unique sensor):

$$d_{ij}^+ = \frac{1}{t_n^+ (T_{\max}^+)^2} \int_0^{t_n^+} X_i^+(t) X_j^+(t) dt^+, \quad i, j = 1, \dots, n_p \quad (5.1)$$

In Eq. (5.1), t is time, t_n is the duration of the experiment, n_p is the number of parameters (β), i.e. thermal properties to be estimated, X_i^+ are the dimensionless sensitivity coefficients calculated from $X_i^+(t^+) = \beta_i \frac{\partial T^+(t^+)}{\partial \beta_i}$, and T_{\max}^+ is defined as the maximum dimensionless temperature reached at steady state (Moncman, 1994). The integration contained in the d_{ij}^+ coefficients is determined numerically.

Note that, as explained in Chapter 3 (Section 3.2.2), the optimal overall experimental time, t_n^+ , of each specific design was determined by evaluating the modified determinant D_m^+ without time-averaging, using the optimal values of the other design variables. The optimal overall experimental time corresponded to the time when no significant information about

D_m^+ was provided. Consequently, in the one-dimensional analysis, the actual number of design variables was two (x_s^+ and t_h^+), and in the two-dimensional analysis, there were four design variables (x_s^+ , y_s^+ , L_p^+ and t_h^+).

The one- and two-dimensional simultaneous estimation test problems considered in this work were investigated by Hanak (1995). He used the modified Box-Kanemasu method with an Ordinary Least Squares (OLS) approach in an attempt to estimate the properties for both problems. The objective function to be minimized over N_i measurements was therefore the simple sum-of-squares error expressed by:

$$S(\boldsymbol{\beta}) = \sum_{i=1}^{N_i} [T_i(\boldsymbol{\beta}, \tilde{t}) - \tilde{T}_i]^2 \quad (5.2)$$

where $T_i(\boldsymbol{\beta}, \tilde{t})$ and \tilde{T}_i are the calculated and measured temperatures obtained at the unique optimal sensor location, respectively, and $\boldsymbol{\beta}$ is the parameter vector to be estimated. Although the modified Box-Kanemasu method proved to be effective in the one-dimensional case, the two-dimensional estimation resulted in non-convergence due to correlation between the thermal properties. Hanak then restricted his two-dimensional analysis to the simultaneous estimation of the thermal conductivity in the fiber plane, k_y , and the volumetric heat capacity, C , assuming the thermal conductivity through the fibers plane, k_x , to be known from the one-dimensional estimation.

5.1.1.2 Experimental Data

The measured temperature histories used in the estimation methodology were obtained from the one- and two-dimensional (Configuration 1) optimal experiments conducted by Hanak (1995). In-depth descriptions of both experimental set-ups can be found in his thesis. The geometrical ratio of the composite sample (AS4 carbon fiber / 3502 epoxy matrix) was $L_{xy}=0.06$. Note that the one- and two-dimensional experiments were repeated ten and nine times, respectively, from three separate experimental set-ups.

5.1.1.3 Mathematical Model Formulations

In performing the optimization and estimation stages, mathematical models were required. The term T_{max}^+ and the dimensionless sensitivity coefficients were needed in the

optimization procedure, while the temperature distribution at the optimal sensor location was needed in the estimation procedure. Considering ideal conditions (which, recall from Chapter 3, is the regular procedure in designing optimal experiments), Moncman developed exact models for all cases previously described. These models were thus used in the optimization process. In conducting the experiments, Hanak however found that the “constant temperature” boundary conditions were not exactly constant. Therefore, in the estimation process, he used a finite element program in which the measurements from thermocouples placed at the location of the “constant temperature” boundary conditions were incorporated. In applying the GAs to the estimation problems, analytical models that were proved to be appropriate were developed as they were much easier to implement in the estimation methodology. The following provides brief descriptions of the ideal analytical models used in the optimization process in both the parametric study and the GAs, and of the modified analytical models used in the genetic-based estimation methodology.

- **One-Dimensional Formulation**

From the conservation of energy, the temperature distribution within the material in the one-dimensional analysis is governed by the one-dimensional diffusion equation.

$$\frac{\partial}{\partial x} \left(k_x \frac{\partial T}{\partial x} \right) = C \frac{\partial T}{\partial t}, \quad 0 \leq x \leq L_x, \quad t \geq 0; \quad (5.3)$$

where L_x is the thickness of the sample in the x -direction. The initial and boundary conditions are described by:

$$-k_x \left. \frac{\partial T}{\partial x} \right|_{x=0} = q_x(t) \quad x = 0 \quad 0 < t \leq t_h \quad (5.4a)$$

$$\left. \frac{\partial T}{\partial x} \right|_{x=0} = 0 \quad x = 0 \quad t > t_h \quad (5.4b)$$

$$T(x, t) = T_{0,x} \quad x = L_x \quad t > 0 \quad (5.4c)$$

$$T(x, t) = T_i \quad 0 < x < L_x \quad t = 0 \quad (5.4d)$$

where T_i and $T_{0,x}$ are the initial and known temperature boundary condition, respectively. The ideal conditions considered in the optimization process are explained as follows. Since the experiments were conducted at room temperature, the temperature at the boundary $x = L_x$ was assumed to be equal to the initial temperature, i.e. $T_{0,x} = T_i$. In addition, the boundary conditions were assumed to be constant. Since the composites had a simple geometry, exact

temperature solutions could be developed for these ideal conditions. Using the Green's function method, the following distribution was derived (Moncman, 1994):

$$T(x,t) = T_{0,x} + \frac{2L_x}{k_x} q_x \sum_{m=1}^{\infty} \frac{1}{\beta_m^2} \left[1 - e^{\left(-\beta_m^2 \frac{\alpha_x t}{L_x^2}\right)} \right] \cos\left(\beta_m \frac{x}{L_x}\right), \quad t \leq t_h \quad (5.5a)$$

$$T(x,t) = T_{0,x} + \frac{2L_x}{k_x} q_x \sum_{m=1}^{\infty} \frac{1}{\beta_m^2} \left[e^{\left(-\beta_m^2 \frac{\alpha_x (t-t_h)}{L_x^2}\right)} - e^{\left(-\beta_m^2 \frac{\alpha_x t}{L_x^2}\right)} \right] \cos\left(\beta_m \frac{x}{L_x}\right), \quad t > t_h \quad (5.5b)$$

where β_m is an eigenvalue represented by $\beta_m = \pi\left(m - \frac{1}{2}\right)$.

In dimensionless terms, this becomes:

$$T^+(x^+, t^+) = 1 - x^+ - 2 \sum_{m=1}^{\infty} \frac{1}{\beta_m^2} e^{\left(-\beta_m^2 t^+\right)} \cos(\beta_m x^+), \quad t^+ \leq t_h^+ \quad (5.6a)$$

$$T^+(x^+, t^+) = 2 \sum_{m=1}^{\infty} \frac{1}{\beta_m^2} \left[e^{\left(-\beta_m^2 (t^+ - t_h^+)\right)} - e^{\left(-\beta_m^2 t^+\right)} \right] \cos(\beta_m x^+), \quad t^+ > t_h^+ \quad (5.6b)$$

where $T^+ = \frac{T - T_{0,x}}{q_x L_x / k_x}$, $t^+ = \frac{\alpha_x t}{L_x^2} = \frac{k_x t}{CL_x^2}$ and $x^+ = \frac{x}{L_x}$.

The dimensionless temperature, T^+ , represents the ratio of the increase in temperature to the maximum increase reached at steady state which is calculated using Fourier's law. From this, T_{max}^+ was given by $T^+(x^+=0, t^+=t_h^+=\infty)$ and the dimensionless sensitivity coefficients were obtained by differentiating Eqs. (5.6a and b) with respect to k_x and C and multiplying by the respective properties. These equations can be found in Moncman (1994). This information was then used in the optimization methodology (in both the parametric study and the GAs) to determine the maximum value for D^+ as given by Eq. (5.1), and the corresponding optimal experimental parameters.

Ideal conditions were, however, not possible to achieve experimentally and the experimental temperatures and heat fluxes at the ideally constant temperature and heat flux boundaries, respectively, were found to vary slightly (Hanak, 1995). In the estimation stage, Hanak therefore used a finite element program called Engineering Analysis Language (Whetstone, 1983) because it could easily accommodate experimental variations in temperature and heat flux at the ideal boundaries. Nevertheless, it was found through a careful investigation that constant temperature and heat flux values calculated from averaged

experimental values over the duration of the experiment could be used for the respective boundary conditions in the model without significant bias. As the use of an analytical model was much simpler and faster to implement into the genetic-based estimation methodology than implementing this latter into the program EAL, the exact solutions given in Eqs. (5.5a and b) were modified to take into account the new boundary conditions. The temperature distribution became:

$$T(x, t) = T_i + 2 \sum_{m=1}^{\infty} \left[\frac{q_x L_x}{k_x} + \beta_m \sin(\beta_m)(T_{0,x} - T_i) \right] \frac{1}{\beta_m^2} \left[1 - e^{\left(-\beta_m^2 \frac{\alpha_x t}{L_x^2} \right)} \right] \cos\left(\beta_m \frac{x}{L_x} \right), \quad t \leq t_h \quad (5.7a)$$

$$T(x, t) = T_i + 2 \sum_{m=1}^{\infty} \left\{ \frac{q_x L_x}{k_x} \left[e^{\left(-\beta_m^2 \frac{\alpha_x (t-t_h)}{L_x^2} \right)} - e^{\left(-\beta_m^2 \frac{\alpha_x t}{L_x^2} \right)} \right] + \beta_m \sin(\beta_m)(T_{0,x} - T_i) \left[1 - e^{\left(-\beta_m^2 \frac{\alpha_x t}{L_x^2} \right)} \right] \right\} \frac{1}{\beta_m^2} \cos\left(\beta_m \frac{x}{L_x} \right) \quad t > t_h \quad (5.7b)$$

where q_x and $T_{0,x}$ stood then for the averaged experimental values over the duration of the experiment. This solution was used in the GAs. One important point is that the determination of both the experimental heating and total time, t_h and t_n , from their respective dimensionless optimized values required the knowledge of the thermal diffusivity in the x -direction, e.g. $\alpha_x = k_x / C$. Therefore an initial estimate of 4×10^{-7} m²/s based on previous known composites was applied. Note that if the actual property was found to be completely different, the experiments would have been repeated with a better estimate.

- **Two-Dimensional Formulation**

In the two-dimensional analysis, the temperature distribution within the material is governed by the two dimensional diffusion equation obtained from the conservation of energy and expressed as:

$$\frac{\partial}{\partial x} \left(k_x \frac{\partial T}{\partial x} \right) + \frac{\partial}{\partial y} \left(k_y \frac{\partial T}{\partial y} \right) = C \frac{\partial T}{\partial t}, \quad 0 \leq x \leq L_x, \quad 0 \leq y \leq L_y, \quad t \geq 0; \quad (5.8)$$

where L_y and L_p are the thickness of the sample in the y -direction and the portion of the sample where the heat flux is imposed, respectively. The initial and boundary conditions are

described by:

$$-k_x \left. \frac{\partial T}{\partial x} \right|_{x=0} = q_x(t) \quad x = 0 \quad 0 < y < L_p \quad 0 < t \leq t_h \quad (5.9a)$$

$$\left. \frac{\partial T}{\partial x} \right|_{x=0} = 0 \quad x = 0 \quad 0 < y < L_p \quad t > t_h \quad (5.9b)$$

$$\left. \frac{\partial T}{\partial x} \right|_{x=0} = 0 \quad x = 0 \quad L_p < y < L_y \quad t > 0 \quad (5.9c)$$

$$T(x, y, t) = T_i \quad 0 < x < L_x \quad 0 < y < L_y \quad t = 0 \quad (5.9d)$$

$$T(x, y, t) = T_{0,x} \quad x = L_x \quad 0 < y < L_y \quad t > 0 \quad (5.9e)$$

The boundary conditions along the y-axis for Configuration 1 are:

$$T(x, y, t) = T_{0,y1} \quad 0 < x < L_x \quad y = 0 \quad t > 0 \quad (5.9f)$$

$$T(x, y, t) = T_{0,y2} \quad 0 < x < L_x \quad y = L_y \quad t > 0 \quad (5.9g)$$

while the boundary conditions at the same locations for Configuration 2 are:

$$\left. \frac{\partial T}{\partial y} \right|_{y=0} = 0 \quad 0 < x < L_x \quad y = 0 \quad t > 0 \quad (5.9h)$$

$$\left. \frac{\partial T}{\partial y} \right|_{y=L_y} = 0 \quad 0 < x < L_x \quad y = L_y \quad t > 0 \quad (5.9i)$$

The terms $T_{0,x}$, $T_{0,y1}$ and $T_{0,y2}$ are the known temperature boundary conditions. Again, considering ideal conditions (e.g., constant boundary conditions where $T_{0,x} = T_{0,y1} = T_{0,y2} = T_i$ as experiments were conducted at room temperature), an exact solution could be derived using the Green's function method (Moncman; 1994).

For Configuration 1, the ideal model is:

$$T(x, t) = T_{0,x} + \frac{4q_x L_x}{k_x \pi} \sum_{n=1}^{\infty} \sum_{m=1}^{\infty} \frac{1}{nB_{m,n}} \cos\left(\frac{\beta_m x}{L_x}\right) \sin\left(\frac{n\pi y}{L_y}\right) \left[1 - \cos\left(\frac{n\pi L_p}{L_y}\right) \right] \left[1 - e^{(-Z_{m,n}t)} \right] \quad t \leq t_h \quad (5.10a)$$

$$T(x, t) = T_{0,x} + \frac{4q_x L_x}{k_x \pi} \sum_{n=1}^{\infty} \sum_{m=1}^{\infty} \frac{1}{nB_{m,n}} \cos\left(\frac{\beta_m x}{L_x}\right) \sin\left(\frac{n\pi y}{L_y}\right) \left[1 - \cos\left(\frac{n\pi L_p}{L_y}\right) \right] \left[e^{(-Z_{m,n}(t-t_h))} - e^{(-Z_{m,n}t)} \right] \quad t > t_h \quad (5.10b)$$

where $Z_{m,n} = \frac{n^2 \pi^2 k_y}{L_y^2 C} + \frac{\beta_m^2 k_x}{L_x^2 C}$.

The dimensionless form is expressed by:

$$T^+(x^+, y^+, t^+) = \frac{4}{\pi} \sum_{m=1}^{\infty} \sum_{n=1}^{\infty} A_{m,n}^+(x^+, y^+) \left[1 - e^{(-B_{m,n}t^+)} \right], \quad t \leq t_h^+ \quad (5.11a)$$

$$T^+(x^+, y^+, t^+) = \frac{4}{\pi} \sum_{m=1}^{\infty} \sum_{n=1}^{\infty} A_{m,n}^+(x^+, y^+) \left[e^{(-B_{m,n}(t^+ - t_h^+))} - e^{(-B_{m,n}t^+)} \right], \quad t^+ > t_h^+ \quad (5.11b)$$

where $A_{m,n}^+(x^+, y^+) = \frac{1}{nB_{m,n}} \sin(n\pi y^+) \cos(\beta_m x^+) \left[1 - \cos(n\pi L_p^+) \right]$,

$$B_{m,n} = n^2 \pi^2 L_{xy}^2 \kappa_{xy} + \beta_m^2, \quad L_{xy} = \frac{L_x}{L_y}, \quad \kappa_{xy} = \frac{k_y}{k_x}, \quad L_p^+ = \frac{L_p}{L_y}, \quad \text{and } y^+ = \frac{y}{L_y}.$$

For Configuration 2, the ideal dimensionless form is:

$$T^+(x^+, y^+, t^+) = \frac{4}{\pi} \sum_{m=1}^{\infty} \sum_{n=1}^{\infty} \frac{1}{nB_{m,n}} \cos(\beta_m x^+) \cos(n\pi y^+) \sin(n\pi L_p^+) \left[1 - e^{(-B_{m,n}t^+)} \right] + 2L_p^+ \sum_{m=1}^{\infty} \frac{1}{\beta_m^2} \cos(\beta_m x^+) \left[1 - e^{(-\beta_m^2 t^+)} \right], \quad t \leq t_h^+ \quad (5.12a)$$

$$T^+(x^+, y^+, t^+) = \frac{4}{\pi} \sum_{m=1}^{\infty} \sum_{n=1}^{\infty} \frac{1}{nB_{m,n}} \cos(\beta_m x^+) \cos(n\pi y^+) \sin(n\pi L_p^+) \left[e^{(-B_{m,n}(t^+ - t_h^+))} - e^{(-B_{m,n}t^+)} \right] + 2L_p^+ \sum_{m=1}^{\infty} \frac{1}{\beta_m^2} \cos(\beta_m x^+) \left[e^{(-\beta_m^2(t^+ - t_h^+))} - e^{(-\beta_m^2 t^+)} \right], \quad t > t_h^+ \quad (5.12b)$$

As one can see, the two-dimensional temperature distribution resulted in a double series containing both transient and steady-state terms. To increase computational efficiency, the steady-state terms, which only needed to be determined once for each temperature distribution computation, were determined separately. From this, T_{max}^+ was given by $T^+(x^+=0, y^+=0.5, t^+=t_h^+=\infty)$ with $L_p^+=1$ (heat flux over the entire sample top surface). Equations for the dimensionless sensitivity coefficients associated with Configuration 1 were obtained by differentiating Eqs. (5.10a and b) with respect to k_x , k_y and C and multiplying by the respective properties. These equations, along with those for the dimensionless sensitivity coefficients associated with Configuration 2, can be found in Moncman (1994). This information was then used in the optimization methodology (in both the parametric study and the GAs) to determine the maximum value for D^+ as given by Eq. (5.1), and the corresponding optimal experimental parameters. Note that unlike the optimization of the one-

dimensional experiment, two-dimensional optimal designs do not completely present dimensionless equations. Indeed, the ratio of both the sample dimensions (L_{xy}) and the thermal conductivities (κ_{xy}) are required. Based on previously reported data for similar composites, Hanak used an initial estimate of 5.0 for κ_{xy} . However, if this guess proved to be inaccurate, the {optimization+estimation} procedure would have been repeated with a better estimate.

Again, for the estimation stage, the exact solutions were modified to take into account constant average values for the temperature boundary conditions. This gave for the temperature distribution of Configuration 1:

$$T(x, t) = T_i + 4 \sum_{n=1}^{\infty} \sum_{m=1}^{\infty} \left\{ \frac{1}{n\pi} \left[\frac{q_x L_x}{k_x} \left[1 - \cos\left(\frac{n\pi L_p}{L_y}\right) \right] + (T_{0,x} - T_i) [1 - \cos(n\pi)] \beta_m \sin(\beta_m) \right] \right. \\ \left. + n\pi L_{xy}^2 \frac{\sin(\beta_m)}{\beta_m} \left[(T_{0,y1} - T_i) + (T_{0,y2} - T_i) \cos(n\pi) \right] \right\} \frac{1}{B_{m,n}} \left[1 - e^{(-Z_{m,n}t)} \right] \cos\left(\frac{\beta_m x}{L_x}\right) \sin\left(\frac{n\pi y}{L_y}\right) \\ t \leq t_h \quad (5.13a)$$

$$T(x, t) = T_i + 4 \sum_{n=1}^{\infty} \sum_{m=1}^{\infty} \left\{ \frac{1}{n\pi} \frac{q_x L_x}{k_x} \left[1 - \cos\left(\frac{n\pi L_p}{L_y}\right) \right] \left[e^{(-Z_{m,n}(t-t_h))} - e^{(-Z_{m,n}t)} \right] \right. \\ \left. + \left[\frac{1}{n\pi} (T_{0,x} - T_i) [1 - \cos(n\pi)] \beta_m \sin(\beta_m) + \right. \right. \\ \left. \left. n\pi L_{xy}^2 \frac{\sin(\beta_m)}{\beta_m} \left[(T_{0,y1} - T_i) + (T_{0,y2} - T_i) \cos(n\pi) \right] \right] \left[1 - e^{(-Z_{m,n}t)} \right] \right\} \frac{1}{B_{m,n}} \cos\left(\frac{\beta_m x}{L_x}\right) \sin\left(\frac{n\pi y}{L_y}\right) \\ t > t_h \quad (5.13b)$$

where q_x , $T_{0,x}$, $T_{0,y1}$ and $T_{0,y2}$ stood then for the averaged experimental values over the duration of the experiment. This solution was used in the genetic-based estimation methodology. Note that the two-dimensional estimation problem based on the Configuration 2 design was not investigated in the present research.

5.1.1.4 Results and Discussion

In this work, the D -optimization of the one-dimensional design and of both configurations of the two-dimensional experiments was first analyzed using the BEGA. Then, the EEGA was applied to the optimization of the one-dimensional design and Configuration 1 only of the two-dimensional design, and next, to the estimation problems associated with these designs. In each application, the performance of the GAs was evaluated and compared

with the previous results obtained. In testing the algorithms, emphasis was placed on the computing time (or number of function evaluations) used. One should refer to Chapter 4 to better understand the result differences between applying the BEGA and the EEGA, which is related to their different functioning characteristics. One important common feature was the use of a prescribed number of generations, n_g , as the convergence criterion. Optimization jobs were run on the Virginia Tech College of Engineering's Silicon Graphics Power Challenge XL server, while estimation jobs were run on the Virginia Tech Mechanical Engineering Department's IBM RS6000 Model 560, because estimation was less costly in computing time.

- **Optimization of Experimental Parameters**

For ease and clearness in understanding the results, Figures 5.3 and 5.4 below provide schematics of the one- and two-dimensional optimized experimental designs.

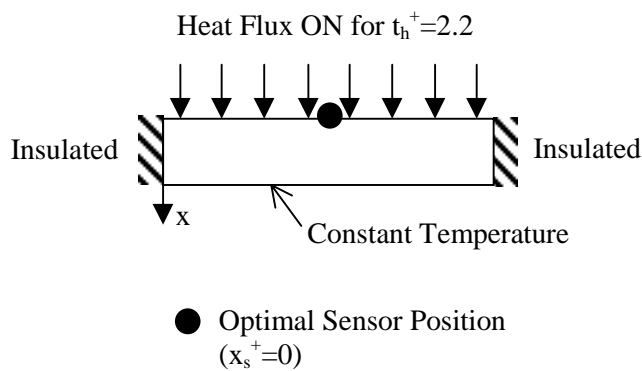


Figure 5.3 Schematic of the optimized one-dimensional experiments.

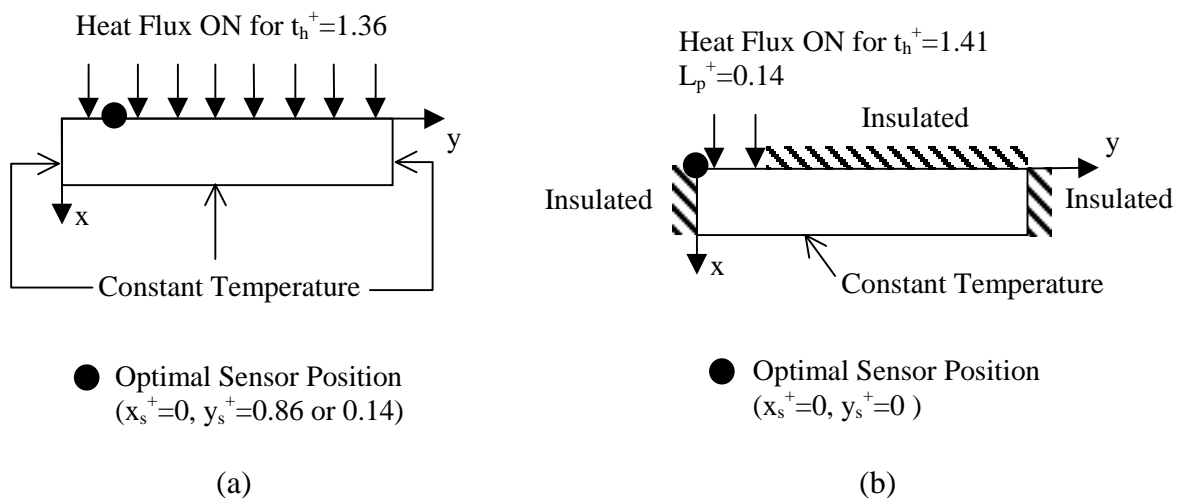


Figure 5.4 Schematic of the optimized two-dimensional experiments
(a) Configuration 1 and (b) Configuration 2.

Application of the BEGA

With the use of the simplest crossover operation and a basic elitism feature in the BEGA (see Chapter 4), a large population of designs was *a priori* anticipated to ensure the generation of any good sets of design variables. Therefore, for each problem, an initial investigation of the effect of the genetic parameters was carried out. The performance of the algorithm was evaluated by averaging ten runs, with the means and their 95 % confidence intervals calculated for the maximum determinant and each design variable. The means were then compared to the optimal determinants and experimental parameters found by Moncman (1994) and Hanak (1995).

One-Dimensional Optimal Experimental Design

Recall that the design variables to be optimized were the sensor location x_s^+ and the heating time t_h^+ . The ranges used for each design variable were identical to those used by Moncman. The effect of population size, n_s , and number of generations, n_g , were first analyzed to decide which combination of these parameters should be utilized in determining the optimal design. In this analysis, the impact of the computing time (or the number of function evaluations f_{eval}) was not investigated because the dimensionless determinant D^+ was found to be very inexpensive to calculate. From Table 5.1, one can see that the maximum D^+ was obtained for the combination with both the largest n_s and n_g (case d), as logically expected. Because the computing time was inexpensive, the combination chosen was the one with the largest n_s and n_g that gave the maximum determinant.

Table 5.1 Effect of the population size, n_s , and the number of generations, n_g , in the one dimensional experiment.

Case	f_{eval}	n_s	n_g	x_s^+	t_h^+	$D^+_{max}(10^{+2})$
a	2550	50	50	0.0054	2.13	1.9643
b	10200	200	50	0.0019	2.32	1.9856
c	10050	50	200	0.0017	2.44	1.9810
d	40200	200	200	0.0002	2.24	1.9899
Best	40200	200	200			

Table 5.2 shows the results of the ten optimization runs performed using the combination of n_s and n_g discussed above. One result is particularly important: the mean of the maximum D^+ is higher than the maximum D^+ found by Moncman using the parametric study. This result ensures that optimal experimental parameters have been obtained and allows for the validation of the optimization procedure based on GAs. The final optimal experimental parameters should be taken as their respective mean values rounded to the most physically possible values. This would give $x_s^+=0.0$ and $t_h^+=2.29$ for the optimal experimental design. These values are actually very close to the optimal parameters given by Moncman ($x_s^+=0.0$ and $t_h^+=2.20$). Table 5.2 also outlines a general feature of GAs, which is that in the analysis, significant parameters cannot be distinguished from non-significant ones (Kroittmaier, 1993). Consider experiments 4 and 5: even though the sensor locations are almost equal, experiment 4 has still a comparatively much higher t_h^+ . This indicates the importance of the sensor location in the optimal design.

Table 5.2 Determination of the optimal design for the one-dimensional experiment ($n_s=n_g=200, f_{eval}=40200$).

Exp.	x_s^+	t_h^+	$D^+_{max}(10^{+2})$
1	0.0007	2.21	1.9877
2	0.0006	2.33	1.9896
3	0.0015	2.25	1.9838
4	0.0001	2.33	1.9919
5	0.0002	2.24	1.9899
6	0.0005	2.32	1.9911
7	0.0012	2.24	1.9853
8	0.0007	2.31	1.9899
9	0.0002	2.33	1.9914
10	0.0005	2.32	1.9909
Mean	0.0006 \forall 0.0003	2.29 \forall 0.04	1.9892 \forall 0.0019
Moncman's	0.0000	2.20	1.9878

The demonstration of the BEGA on the one-dimensional problem provided a good basis to gain confidence in the algorithm. It also showed that when the objective function is inexpensive to calculate, the BEGA does not have any computation time restriction (relative to the number of design variables to optimize). The parametric study, however, requires the analysis of every point in the search space, and thus is generally time consuming even for inexpensive objective functions.

Two-Dimensional Optimal Experimental Design

In the two-dimensional analysis, recall that two configurations were investigated in which four design variables needed to be optimized. These latter were the sensor location parallel and perpendicular to the fibers, x_s^+ and y_s^+ respectively, the heating length L_p^+ and the heating time t_h^+ . The design variables were expected not to all have the same effect on D^+ . Since x_s^+ was anticipated to have the largest influence on D^+ , the two-dimensional analysis was conducted in two phases. Phase one was performed with a coarse combination of population size and number of generations ($n_s=25$ and $n_g=25$) which required a low CPU time (~25 min) using the design variable ranges employed by Hanak. The objective was to obtain some insight on the relative importance of each design variable. The first phase allowed for both configurations to fix the optimal value of x_s^+ to zero so that only three design variables needed to be optimized in Phase two, and it also allowed to narrow the bounds of the variables to $L_p^+ \geq 0.5$ and $0.9 \leq t_h^+ \leq 3.1$ for Configuration 1 (Table 5.3), and $1.0 \leq t_h^+ \leq 3.0$ for Configuration 2 (Table 5.4).

Table 5.3 Investigation of the significance of each design variable in Configuration 1 of the two-dimensional experiment (Phase 1, $n_s=n_g=25$, $f_{eval}=650$).

Exp.	x_s^+	y_s^+	L_p^+	t_h^+	$D^+_{max}(10^{+7})$
1	0.003	0.11	0.62	2.84	2.80
2	0.061	0.14	0.61	1.18	2.81
3	0.072	0.14	0.98	2.59	2.52
4	0.041	0.15	0.66	2.80	2.54
5	0.054	0.82	0.93	1.52	1.95
Conclusions	0.000	-	≥ 0.5	$0.9 \leq t_h^+ \leq 3.1$	

Table 5.4 Investigation of the significance of each design variable in Configuration 2 of the two-dimensional experiment (Phase 1, $n_s=n_g=25$, $f_{eval}=650$).

Exp.	x_s^+	y_s^+	L_p^+	t_h^+	$D^+_{max}(10^{+7})$
1	0.052	0.01	0.15	2.06	3.12
2	0.007	0.61	0.76	1.21	2.86
3	0.035	0.41	0.57	2.51	1.60
4	0.072	0.79	0.88	2.04	1.99
5	0.054	0.82	0.93	1.52	2.23
Conclusions	0.000	-	-	$1.0 \leq t_h^+ \leq 3.0$	

For Configuration 1, the second phase was managed in a similar manner as the analysis carried out for the one-dimensional problem: first, the effect of n_s and n_g were studied (Table 5.5); then the combination chosen for these genetic parameters was used to perform ten optimization runs (Table 5.6). For Configuration 2, Phase two corresponded directly to the computation of ten optimization runs using the same combination of n_s and n_g chosen for Configuration 1 (Table 5.7).

Table 5.5 Effect of the population size n_s and the number of generations n_g in Configuration 1 of the two-dimensional experiment (Phase 2).

Case	CPU (min)	f_{eval}	n_s	n_g	y_s^+	L_p^+	t_h^+	$D^+_{max}(10^{+7})$
a	80	2550	50	50	0.124	0.902	1.17	5.1121
b	250	6375	125	50	0.860	0.995	1.40	5.3817
c	250	6300	50	125	0.141	0.988	1.41	5.3798
d	590	15750	125	125	0.138	0.991	1.41	5.3977
Best	250	6375	125	50				

Table 5.6 Determination of the optimal designs for Configuration 1 of the two-dimensional experiment (Phase 2, $n_s=125$, $n_g=50$, $f_{eval}=6375$).

Exp.	$y_s^+ *$	L_p^+	t_h^+	$D^+_{max}(10^{+7})$
1	0.860 (0.140)	0.995	1.40	5.3817
2	0.141 (0.859)	0.994	1.40	5.3621
3	0.139 (0.861)	0.999	1.38	5.4076
4	0.857 (0.143)	0.992	1.39	5.3302
5	0.138 (0.862)	0.990	1.41	5.3888
6	0.143 (0.857)	0.989	1.40	5.3763
7	0.861 (0.139)	0.996	1.36	5.3983
8	0.138 (0.862)	0.999	1.38	5.4158
9	0.139 (0.861)	0.998	1.42	5.3663
10	0.861 (0.139)	0.997	1.40	5.4025
Mean	0.860 (0.140) $\forall 0.001$	0.995 $\forall 0.003$	1.39 $\forall 0.01$	5.3830 $\forall 0.0183$
Hanak's	0.860	1.000	1.36	5.3782

* for $L_p^+=1.0$, the problem is symmetric (flux applied across the entire boundary)

Table 5.7 Determination of the optimal design for Configuration 2 of the two-dimensional experiment (Phase 2, $n_s=125$, $n_g=50$, $f_{eval}=6375$).

Exp.	y_s^+	L_p^+	t_h^+	$D_{max}^+(10^{+7})$
1	0.0009	0.142	1.39	5.2604
2	0.0011	0.139	1.40	5.2753
3	0.0019	0.137	1.39	5.2825
4	0.0005	0.141	1.41	5.2471
5	0.0002	0.138	1.40	5.2792
6	0.0012	0.140	1.40	5.2699
7	0.0007	0.137	1.43	5.2230
8	0.0015	0.139	1.38	5.2707
9	0.0004	0.140	1.39	5.2782
10	0.0001	0.141	1.40	5.2651
Mean	0.0008 ∇ 0.0004	0.139 ∇ 0.001	1.40 ∇ 0.01	5.2651 ∇ 0.0130
Hanak's	0.000	0.140	1.41	5.2570

In the investigation of the effects of the genetic parameters n_s and n_g for Configuration 1, two conflicting factors were taken into consideration: the genetic parameters and the CPU time. Initially, as it is a fact that both the population size and number of generations should increase proportionally with the number of parameters to optimize, the use of a population size and number of generations at least as large as in the one-dimensional case was *a priori* presumed. However, because the computation of D^+ was found to be highly expensive, some compromises needed be settled between the two conflicting factors mentioned above. From Table 5.5, one can see that the increase in D^+ from case b ($n_s=125$ and $n_g=50$) to case d ($n_s=125$ and $n_g=125$) was only about 0.3% while the required CPU time (and consequently f_{eval}) almost tripled. Therefore, the combination given by case b was chosen to determine the optimal design for both Configuration 1 and 2.

The results of the ten optimization runs for Configuration 1 and 2, are provided in Tables 5.6 and 5.7, respectively. Again, the means of the maximum D^+ from this study are higher than the maximum D^+ found by Hanak using the parametric study. These results definitely confirmed the assessment of the optimization procedure based GAs. Selecting the optimal experimental parameters as their respective means rounded to the closest physically possible values, the optimal design for Configuration 1 gave $x_s^+=0.0$, $y_s^+=0.86$, $L_p^+=1.0$ and $t_h^+=1.39$; for Configuration 2, it gave $x_s^+=0.0$, $y_s^+=0.0$, $L_p^+=0.14$, and $t_h^+=1.40$. These values

are very close to the optimal experimental parameters determined by Hanak ($x_s^+=0.0$, $y_s^+=0.86$, $L_p^+=1.0$ and $t_h^+=1.36$ for Configuration 1; $x_s^+=0.0$, $y_s^+=0.0$, $L_p^+=0.14$ and $t_h^+=1.41$ for Configuration 2).

Note, that even though care was taken to settle compromises between the population size and number of generations, and the CPU time, and to conduct the analysis in two phases, each optimization run still required about 200 min. This occurred because the objective function was highly expensive to calculate. The large computing time was due to the computation of the steady-state solution of the two thermal conductivity sensitivity coefficients. Efforts were thus focused on ways to calculate those steady-state solutions faster. It was found that the number of eigenvalues and eigenfunctions used in the double series could not be much minimized as it affected the accuracy of the sensitivity coefficient distribution. A study was then conducted to approximate the shape of these terms which were found to be somewhat similar. Unfortunately, no approximate function was shown to be effective.

Conclusion

For both test problems, the BEGA improved the maximization of the objective function specified by the D -criterion. However, it was shown that when the objective function was highly expensive to calculate, as in the two-dimensional analysis, the optimization methodology using the BEGA posed two problems: first, two phases were required to reduce the initial design space, and second, because of the need to average the results over several runs, the procedure tended to be as time intensive as the parametric study although less tedious to apply. From these conclusions, efforts were focused on improving the efficiency of the genetic-based optimization methodology through the development of the EEGA.

Application of the EEGA

The performance of the EEGA was evaluated for the one-dimensional design problem and for Configuration 1 of the two-dimensional design problem, and compared with the results from both the BEGA and parametric studies. In the following, results for both problems are jointly given.

Table 5.8 summarizes the GA parameter values used for the EEGA. With an aim to comparing the EEGA with the BEGA, the values used for this latter are also reported. The selection of the population size, n_s , and number of generations, n_g , used in the EEGA was based on the values used in the BEGA and on growing experience in the GA field. The elitist parameters n_{pop} , n_{best1} , n_{best2} and n_{best3} (refer to the description of the EEGA in Chapter 4, Section 4.3.2) were chosen arbitrarily based on a population size of 50. Note that the logic applied to select n_s and n_g was simply that since the EEGA was expected to perform much better than the BEGA, it was anticipated that smaller population sizes and a smaller number of iterations could be used with the EEGA, and thus, one does not intend to claim the “right” values for n_s and n_g have been applied. Furthermore, the basis for the comparison between both GAs was to show that the EEGA could find the global optimum more efficiently than the BEGA, e.g. in only one phase run and in less CPU time. There was no priority in attempting to improve the BEGA’s results as these were already found to improve those from the parametric study. Therefore, no comparison was done between the BEGA and the EEGA for similar population sizes and number of generations.

Table 5.8 Values for population size n_s , number of generations n_g , and EEGA elitist parameters, n_{best1} , n_{pop} , n_{best2} , and n_{best3} used in the one-dimensional and two-dimensional Configuration 1 optimization problems with the BEGA and EEGA.

		n_s	n_g	n_{best1}	n_{pop}	n_{best2}	n_{best3}
1D	BEGA	200	200	N/A	N/A	N/A	N/A
	EEGA	50	10	20% $n_s = 10$	$n_{best1}/n_s = 5$	$n_s - n_{best1} = 40$	30
2D	BEGA	125	50	N/A	N/A	N/A	N/A
	EEGA	50	20	20% $n_s = 10$	$n_{best1}/n_s = 5$	$n_s - n_{best1} = 40$	30

The predicted optimal experimental designs for the two test problems obtained from the EEGA are shown in Table 5.9. The results [means and 95 % confidence intervals, Eq.(3.18)] from the BEGA and the parametric study are reported for convenience in comparison. One can see that the objective to improve the efficiency of the BEGA was reached. Indeed, not only was the two-dimensional optimization performed directly in one phase, but the CPU time was also minimized. This is evident in the reduction of the number of function evaluations, f_{eval} , by a factor of 4.4 due to the use of a smaller population size and fewer generations. Note that looking at this reduction factor is actually the best way to compare the CPU time involved. The smaller population size was a result of the selective procedure used by the EEGA to generate the initial population; here, only two runs were performed to examine the effects of different random seeds.

Furthermore, due to the benefit of the additional features implemented in the EEGA, particularly updating the parameter ranges, it was observed that the most significant chromosome x_s did not predominate the effects of the other chromosomes; thus, the optimization did not present a slow finishing, which allowed it to be performed in just one phase. Thus, the two problems which limited the efficiency of the BEGA were circumvented with the EEGA.

Table 5.9 Optimal designs for the one-dimensional and two-dimensional Configuration 1 optimization problems.

		x_s^+	y_s^+	L_p^+	t_h^+	$D_{max}^+(\mathbf{10}^{+7})$	f_{eval}
1-D	Moncman	0.	N/A	N/A	2.20	1.9878	N/A
	BEGA Mean	$(6.0 \nabla 3.0) \times 10^{-4}$	N/A	N/A	2.29 $\nabla 0.04$	1.9892 $\nabla 0.0019$	40200
	EEGA Run 1	$(3.0 \nabla 1.0) \times 10^{-5}$	N/A	N/A	2.32 $\nabla 0.00$	1.9926 $\nabla 0.0000$	850
	EEGA Run 2	$(6.0 \nabla 1.0) \times 10^{-5}$	N/A	N/A	2.33 $\nabla 0.00$	1.9914 $\nabla 0.0000$	850
2-D	Hanak	0.	0.860	1.0	1.36	5.3782	N/A
	BEGA Mean	0.	0.860 $\nabla 0.001$	0.995 $\nabla 0.003$	1.39 $\nabla 0.01$	5.3830 $\nabla 0.0183$	6375
	EEGA Run 1	$(3.0 \nabla 0.3) \times 10^{-5}$	0.863 $\nabla 0.000$	0.993 $\nabla 0.001$	1.40 $\nabla 0.00$	5.3890 $\nabla 0.0000$	1450
	EEGA Run 2	$(7.0 \nabla 4.0) \times 10^{-6}$	0.862 $\nabla 0.000$	0.996 $\nabla 0.002$	1.40 $\nabla 0.00$	5.3913 $\nabla 0.0000$	1450

In addition, the use of EEGA resulted in an increase of the value of D^+ for both test problems. As mentioned earlier, this result was not a priority in developing the EEGA as the BEGA had already been shown to improve the maximization of D^+ over the parametric study. This is, however, the logical output from an enhanced optimization algorithm such as the EEGA. The fact that the number of function evaluations was considerably reduced for the one-dimensional experiment does not have any significance because the objective function in this case was very inexpensive to compute.

Another significant point is that, as one may recall from the description of the EEGA in Chapter 4, the output from this algorithm comprised of statistics performed on the n_{best1} first designs of the final population. The very small confidence intervals found around the means therefore verified the convergence of the final population to the optimal design. This result

also showed that there was no need to average the performance of the EEGA over ten runs as was done for the BEGA. Thus, there was a considerable reduction in the CPU time required for obtaining reliable results. It is nevertheless recommended that optimization be performed at least twice to show reproduction in the results using different seeds. Table 5.9 indicates that the two different random number seeds used with the EEGA had a negligible effect on the optimal mean values obtained for the objective function and the design variables. They could, however, have generated a difference in how quickly the EEGA found the optimal design (e.g., in the value of f_{eval}), but this behavior was not investigated. Note, however, that the number of function evaluations using the EEGA seemed still a little high and it was believed that the EEGA could benefit from the use of different genetic operators more suitable to real-valued encoding (this later led to the development of the GA_3 algorithm).

Conclusion

By keeping the best information generated throughout the search process, the EEGA performed much more efficiently than the BEGA, and thus also outperformed the parametric study both qualitatively and quantitatively. The elitist features implemented in the EEGA helped direct the search for the optimal design, thus leading to more rapid convergence. In addition, the use of the EEGA resulted in a richer final population (in terms of the value of the D -criterion) which allowed for an assessment of convergence.

Before giving the results for the estimation of properties, it should be recalled that the values found for the optimal dimensionless design variables of the two-dimensional optimization problems depend on the ratio of both the sample dimensions (L_{xy}) and the thermal conductivities (κ_{xy}). The former is fixed by geometrical consideration and was 0.06 here. The latter, however, is set as an initial guess. Based on previously reported data for similar composites, an initial estimate of 5.0 was used for κ_{xy} .

- **Estimation of Properties**

As mentioned previously Hanak used the modified Box-Kanemasu method in an attempt to estimate the properties for both the one- and two-dimensional problems. The method proved to be effective in the one-dimensional case, but the two-dimensional estimation resulted in non-convergence due to correlation between the thermal properties (see

Table 5.10). From this, a preliminary analysis was performed in this work on applying the modified Box-Kanemasu method to the two-dimensional Configuration 1 estimation problem using multiple sensors adequately chosen, and “very good” initial guesses for the estimates (nearly the same as the true estimates). The aim was to investigate if such additional information would help the gradient-based procedure to properly converge. Note that this analysis was conducted prior to investigating the use of GAs for the estimation of the thermal properties. The following provides a summary of the study.

Table 5.10 Correlation matrices for the simultaneous estimation of three thermal properties (k_x , k_y and C) with the two-dimensional Configuration 1 design using the modified Box-Kanemasu method.

	Hanak (1995) One sensor Experimental data			Present study Three sensors, good initial guess Simulated data with noise ($\sigma = 0.1^\circ\text{C}$)		
	k_x	k_y	C	k_x	k_y	C
k_x	1			1		
k_y	-0.998	1		-0.982	1	
C	-0.986	0.985	1	-0.537	0.492	1

The use of three sensors was considered: the first satisfied D -optimality and the second and third were chosen to maximize the sensitivity to the thermal conductivity in the fiber plane, k_y , and the sensitivity to the volumetric heat capacity, C , respectively. Simulated temperature histories were generated from these sensors using specified estimates for the three thermal properties (k_x , k_y and C) and the exact analytical model given by Eqs. (5.10a and b). Note that with an aim to comparing with the results from Hanak, shown in Table 5.10, the number of observations simulated was the same as the number of experimental observations used. The simulated data were then used as the observation vector in the modified Box-Kanemasu method. When exact data were used, all three original properties were recovered, as expected, since it was also possible with only one sensor (Hanak, 1995). When uniform random errors of deviation 0.1°C were added to the exact data, non-converged solutions were obtained, again as with only one sensor. The use of initial values close to the specified property values did not allow convergence either. The correlation matrix indicated in Table 5.10 showed, however, much lower correlation terms than when trying to estimate the properties from one sensor only and without good knowledge for the initial guess, thus indicating the benefit from the additional information. Nevertheless, the correlation term between both thermal conductivities was still higher than 0.9, making it very difficult for the

gradient-based method to converge with data containing noise. It became apparent from this study that a more complex design with, for instance, additional embedded sensors was probably necessary for the modified Box-Kanemasu method to become effective, compared to the work performed by Loh and Beck (1991) discussed in Chapter 2. As nondestructive testing was a requirement in the two-dimensional estimation problem presented here, this design modification was not possible. The investigation of GAs as the estimation procedure was then the logical following step.

The EEGA was first applied to the simple one-dimensional problem of estimating k_x and C of a composite material (AS4 carbon fiber / 3502 epoxy matrix) to gain confidence in using the algorithm to perform simultaneous estimation in a case where correlation was insignificant. These properties were estimated for each of the ten experiments performed, using the values for the genetic and elitist parameters for the EEGA given in Table 5.11. The analytical solution given in Eqs. (5.7a, b) was applied to obtain temperature histories at the optimal sensor location. The means of the ten estimates, the associated 95% confidence intervals (CIs) obtained from Eq. (3.18), and the mean value of the objective function, S , are compared to the corresponding results from Hanak in Table 5.12. Note that the use of the EEGA resulted in a smaller mean value of S and equal or smaller CIs than the use of the modified Box-Kanemasu method by Hanak [6]. Table 5.12 also indicates the 95% CIs obtained from Eq. (3.19) and which take into account the CIs of the estimates for each of the ten experiments, as explained in Chapter 3. The small magnitude of these 95% CIs reflects the reliability of the estimated parameters.

Table 5.11 Genetic parameters, n_s , n_g , and n_{pop} , elitist parameters, n_{best1} , n_{best2} , and n_{best3} , and number of function evaluations, f_{eval} , used in the estimation problems with the EEGA.

	n_s	n_g	n_{pop}	n_{best1}	n_{best2}	n_{best3}	f_{eval}
1-D	50	10	5	10	40	30	850
2-D	50	15	5	10	40	30	1150

Table 5.12 Estimated mean thermal properties for the one-dimensional estimation problem using both EAL and EEGA.

	k_x (W/mK)	C (MJ/m ³ K)	S (EC) ²
Hanak (EAL)	0.62 \forall 0.01	1.65 \forall 0.01	1.28 \forall 0.21
EEGA	0.63 \forall 0.01 ^a \forall 0.01 ^b	1.61 \forall 0.01 ^a \forall 0.03 ^b	0.71 \forall 0.22

^a and ^b obtained using Eq. (3.18) and (3.19), respectively.

The residuals were also investigated; these are shown in Fig. 5.5 for the first experiment. Note there is a slight bias in the model, particularly when the heater is turned on at $t = 0$ s and when it is turned off at $t = 130$ s. The bias can be estimated from the difference between the total RMS and the experimental variance which can be estimated from data before the heat flux is applied (not shown). In this case, the total RMS_i for this experiment is only 1.17% of the maximum temperature rise; thus, both the bias and experimental variance are quite small, with the variance being smaller than the bias error. Also from Fig. 5.5, the small difference between the RMS_i and the RMS_M indicates the experiments were highly repeatable.

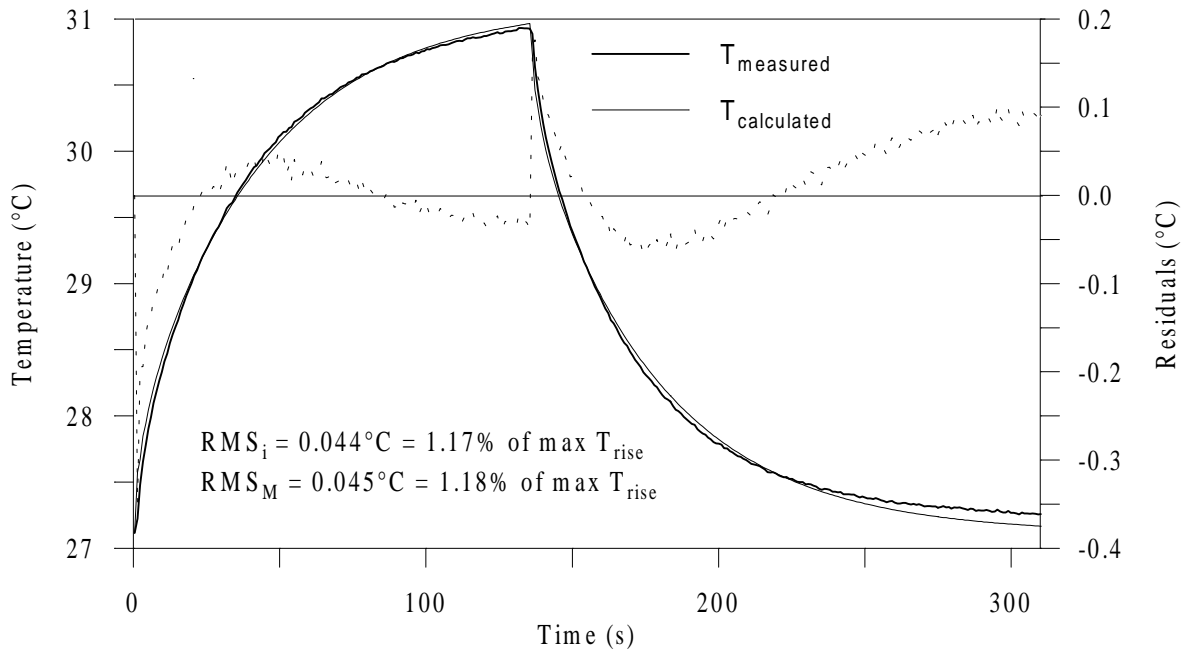


Figure 5.5 Temperature and residual distribution from the one-dimensional model for the first experiment.

The one-dimensional solution provided the basis for the two-dimensional case (Configuration 1). Once again, the analytical solution with constant heat flux and temperature boundary conditions calculated from averaged experimental values was used [Eqs. (5.13a and b)]. A sensitivity analysis was first conducted to gain insight into the problem. The dimensionless sensitivity coefficients for k_x , k_y and C are shown in Fig. 5.6. Note that the superscript ⁽⁺⁾ that denotes “dimensionless” is henceforth omitted for convenience. The coefficient X_{k_y} is very small compared to X_{k_x} , and these coefficients are linearly dependent, as indicated by Fig. 5.7. This suggested that k_y and C would be more difficult to estimate than k_x , with k_y being the most difficult, and that k_x and k_y are correlated. These thermal properties were

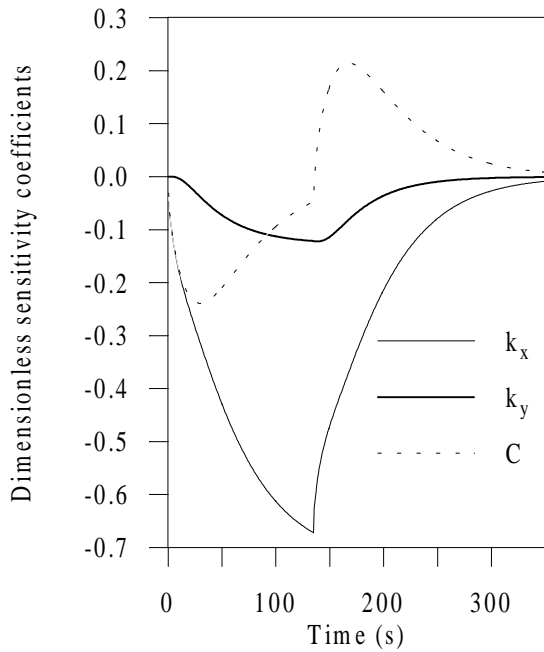


Figure 5.6 Dimensionless sensitivity coefficients from the two-dimensional (Configuration 1) model.

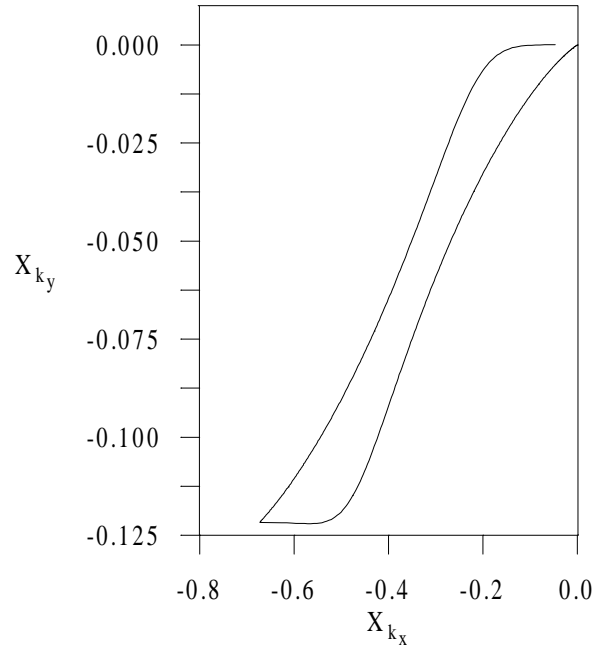


Figure 5.7 Linear dependence between the dimensionless sensitivity coefficients of k_x and k_y from the two-dimensional (Configuration 1) model.

then estimated for the nine experiments performed using the same experimental procedures. These results, along with the associated 95% CIs of the estimates, the least squares error S , and the Root-Mean-Square values for each of the experiments are given in Table 5.13 along with the associated mean values over all of the experiments. The 95 % CIs for each experiment were approximated from linear estimation [Eq. (3.17)] and are related to the sensitivity coefficients for each property value shown in Fig. 5.6. Thus, the CIs for k_x were the smallest, while those associated with k_y were the largest. The high correlation between the thermal conductivities indicated in Fig. 5.7 is also shown in the off-diagonal term associated with k_x and k_y of the correlation matrix calculated for the first experiment and equal to 0.995 (see Table 5.14 in Section 5.1.1.5).

The residuals were also investigated; these are shown in Fig. 5.8 for the first experiment. One can see that the residuals are small and centered around zero. Note again a slight bias in the two-dimensional model, particularly when the heater is turned on and off. This bias seems to be about the same order of magnitude as the bias shown in the one-dimensional model.

Table 5.13 Estimated thermal properties, k_x , k_y and C , the least squares error, S , and the Root-Mean-Square, RMS_i and RMS_M , for the two-dimensional Configuration 1 estimation problem using EEGA.

Exp.	k_x (W/mK)	k_y (W/mK)	C (MJ/m ³ K)	S (EC) ²	RMS _i		RMS _M	
					(EC)	ΔT_{max} ^a (%)	(EC)	ΔT_{max} ^a (%)
1	0.63 ∇ 0.01	1.51 ∇ 0.28	1.64 ∇ 0.02	0.35	0.033	0.96	0.054	1.63
2	0.63 ∇ 0.01	1.48 ∇ 0.25	1.60 ∇ 0.02	0.38	0.032	0.90	0.054	1.52
3	0.64 ∇ 0.01	1.44 ∇ 0.30	1.58 ∇ 0.02	0.45	0.036	1.03	0.062	1.78
4	0.66 ∇ 0.02	1.30 ∇ 0.50	1.69 ∇ 0.04	1.08	0.054	1.58	0.058	1.71
5	0.65 ∇ 0.02	1.44 ∇ 0.48	1.68 ∇ 0.03	0.72	0.044	1.29	0.046	1.32
6	0.66 ∇ 0.03	1.30 ∇ 0.53	1.69 ∇ 0.05	1.25	0.058	1.72	0.060	1.79
7	0.66 ∇ 0.02	1.45 ∇ 0.50	1.68 ∇ 0.04	0.99	0.054	1.58	0.061	1.78
8	0.66 ∇ 0.03	1.63 ∇ 0.61	1.66 ∇ 0.04	1.61	0.068	2.05	0.083	2.47
9	0.66 ∇ 0.02	1.51 ∇ 0.43	1.67 ∇ 0.03	0.79	0.048	1.41	0.056	1.66
Mean	0.65 ∇ 0.01 ^b	1.45 ∇ 0.15 ^b	1.66 ∇ 0.02 ^b	0.76 ∇ 0.33 ^c	1.39 %		1.74 %	

^a % ΔT_{max} is the RMS as a percent of the maximum temperature rise, ΔT_{max} .

^b CIs calculated with Eq. (3.19).

^c CIs calculated with Eq. (3.18).

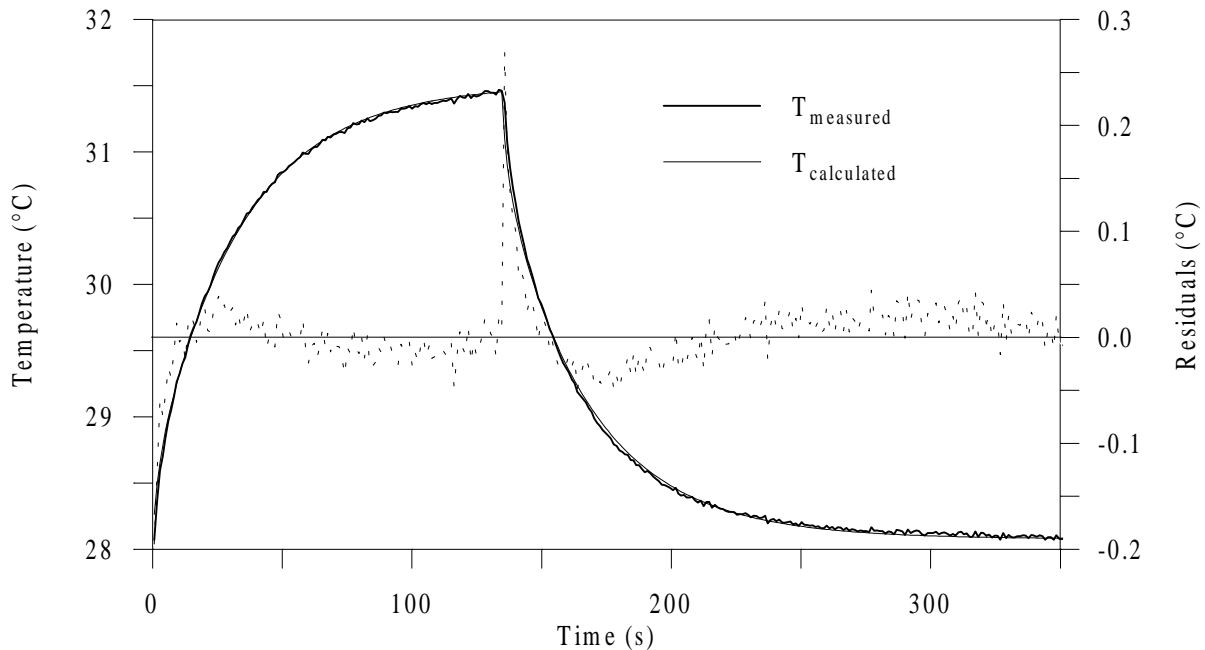


Figure 5.8 Temperature and residual distribution from the two-dimensional (Configuration 1) model for the first experiment.

The small magnitude of the mean value of S highlights the excellent behavior of the estimation procedure although the thermal conductivities were highly correlated. In addition, both the small 95 % CIs of the estimates and those placed around the means, and the RMS values

demonstrated that experiments were very repeatable. Furthermore, the mean estimates for k_x and C are very close to those provided by the one-dimensional estimation, and their 95 % CIs overlap. Thus, these results demonstrated that EEGA is an effective strategy for the simultaneous estimation of correlated thermal properties.

- **Conclusion**

It should be mentioned that the elitist features implemented in the EEGA were suitable here because the objective function presented one unique global optimum. However, as explained in Chapter 4, a later application of the EEGA to a multimodal estimation problem [*The simultaneous estimation of the thermal properties of an insulated material*, a study conducted in cooperation with J. Guynn as part of his master-of-science thesis at Virginia Tech, which is not reported in this dissertation but can be found in Garcia et al. (1998)] pointed out that these features tended to direct the search to a local optimum.

Also, one important point to underline is the verification that the ratio of the two-dimensional estimated thermal conductivities and the thermal diffusivity in the x -direction are both in agreement with the initial guesses used in the optimization process and in the determination of the experimental times, respectively. Recall that initial estimates of 5.0 for κ_{xy} and of 4×10^{-7} m²/s for α_x , were used. On one hand, the ratio of the estimated mean thermal conductivities presents a value of 2.23 which is about half the value of the initial guess. However, it was found through a careful investigation using the EEGA, that the use of geometrical ratio values between 0.04 and 0.08 (0.06 was used here), and conductivity ratio values between 2 and 7 provided nearly the same optimal design variable values as those obtained here. On the other hand, the thermal diffusivity $\alpha_x (= k_{x,\text{mean}}/C_{\text{mean}})$ presents a value of 3.91×10^{-7} m²/s, which is very close to the initial estimate. Therefore, a good agreement between the optimization process and the estimation results was found.

5.1.1.5 Benefit From Optimizing Experimental Designs

The earlier analysis of the two-dimensional Configuration 1 problem was further developed with an aim to illustrating the need for experimental optimization. It was intended to show that observations taken with optimal (more particularly D -optimal) operating conditions *globally* provide better information than others taken with non-optimal operating

conditions, allowing then for *globally* more accurate estimates. Note that verification of optimal designs has previously been experimentally investigated by Taktak (1992) and Hanak (1995).

The non-optimal conditions were selected as follows. On one hand, the heating area was chosen to completely cover the top surface and the thermocouple position was placed at half sample length where the temperature is maximum. On the other hand, considering $T^+ \propto [1 - \exp(-t^+ / \tau^+)]$ during the heating time [refer to Eq. (5.11a)], the non-optimal heating time value chosen represents the double of the time constant τ^+ defined by $(B_{1,1})^{-1}$. Table 5.14 summarizes the optimal and non-optimal experimental conditions used, the resulting determinant, eigenvalues and condition number of the dimensionless matrix $\mathbf{X}^T\mathbf{X}$, and the sensitivity magnitudes to the parameters.

Table 5.14 Experimental conditions, determinant D^+ , eigenvalues λ_{1-3}^+ , condition number λ_1^+/λ_3^+ and magnitude of the non-dimensional sensitivity coefficients corresponding to an optimal and non-optimal design of the Configuration 1 of the two-dimensional problem.

	x_s^+	y_s^+	L_p^+	t_h^+	D_{max}^+	λ_1^+	λ_2^+	λ_3^+	λ_1^+/λ_3^+	$ X_{kx} $	$ X_{ky} $	$ X_C $
Opt.	0.	0.86	1.	1.36	5.38×10^{-7}	0.219	2.5×10^{-2}	$1. \times 10^{-4}$	2194	< 0.67	< 0.13	< 0.24
Non-opt.	0.	0.5	1.	0.8	2.63×10^{-7}	0.177	3.9×10^{-2}	3.9×10^{-6}	45978	< 0.67	< 0.0081	< 0.30

First of all, notice how poor the information is with optimal conditions. Indeed, the magnitude of the non-dimensional sensitivity coefficients X_{ky} stays lower than 0.13 and the matrix $\mathbf{X}^T\mathbf{X}$ indicates an important condition number of 2194. These features characterized an ill-posed estimation problem that does not allow for an accurate estimation of the property k_y and also entails correlations between the sensitivity coefficients, as shown earlier. Now, the results obtained for the non-optimal experiment display not only a negligible coefficient X_{ky} but also a condition number 21 times larger than in the optimal case, which implies a more unfavorable *global* situation to consider the simultaneous estimation of the three properties. The dimensionless sensitivity coefficients for the non-optimal experiment, which are to be compared with the optimal coefficients illustrated in Fig. 5.6, are shown in Fig. 5.9. On one hand, the magnitudes of the coefficients X_{kx} and X_C are not disturbed by the non-optimal conditions (X_C has even slightly increased). This indicates that while the non-optimal conditions used are inadequate for the simultaneous estimation of the three properties, they

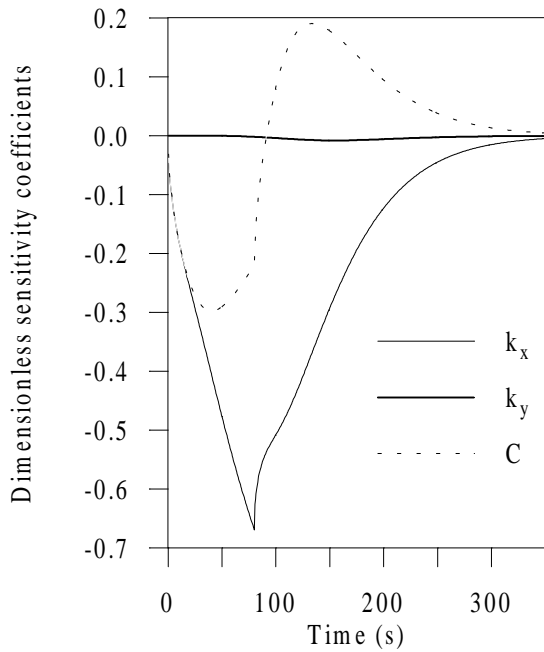


Figure 5.9 Dimensionless sensitivity coefficients from the two-dimensional (Config. 1) non-optimal experimental design.

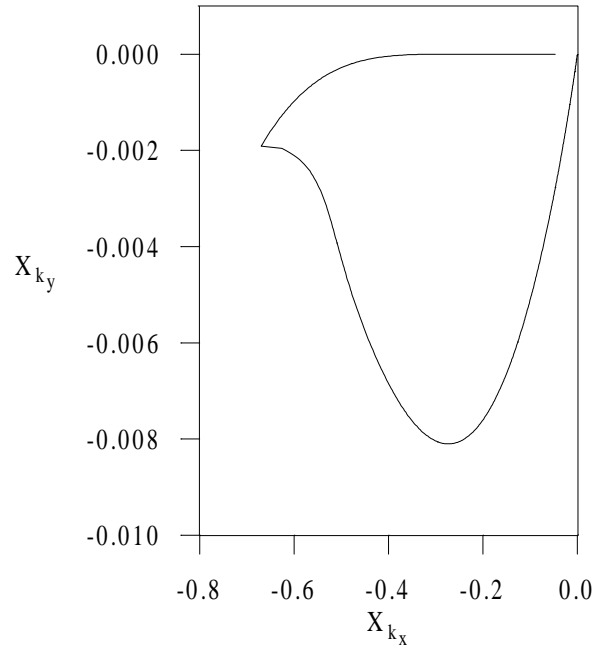


Figure 5.10 Linear dependence between the dimensionless sensitivity coefficients of k_x and k_y from the two-dimensional (Config. 1) non-optimal experimental design.

would be appropriate if one considers the estimation of k_x and C only. On the other hand, X_{k_x} and X_{k_y} do not seem to be linearly dependent as shown in Fig. 5.10. This feature is discussed below.

With an aim to demonstrating the relevance of D -experimental optimization, the estimation results obtained using the EEGA and simulated experimental data with the optimized and non-optimized design are reported in Table 5.15. The simulated data were generated by adding uniform random errors (with a deviation of 0.1°C) to exact data obtained from exact analytical models [Eq. (5.10a and b)] of the optimized and non-optimized design, using $k_x=0.63 \text{ W/mK}$, $k_y=1.51 \text{ W/mK}$ and $C=1.64 \text{ MJ/m}^3\text{K}$.

Table 5.15 Estimated thermal properties k_x , k_y and C , least-square error S and correlation terms r_{k_x/k_y} , $r_{k_x/C}$ and $r_{k_y/C}$ for an optimal and non-optimal simulated two-dimensional Configuration 1 experiment.

	k_x (W/mK)	k_y (W/mK)	C (MJ/m ³ K)	S ($^\circ\text{C}$) ²	r_{k_x/k_y}	$r_{k_x/C}$	$r_{k_y/C}$
Opt.	0.66 ± 0.03	1.38 ± 0.55	1.62 ± 0.05	4.95	0.995	0.916	0.913
Non-opt.	0.69 ± 0.02	1.91 ± 33.61	1.79 ± 0.04	39.94	0.68	0.58	0.66

The estimation performed with the optimal conditions resulted in a least square error S one-eighth as large as with non-optimal conditions. Furthermore, note that the 95% CIs [Eq. (3.16)] of properties estimated using the optimized design are *globally* smaller (more homogenous) than those of properties estimated using the non-optimized design. The individual properties k_x and C may be estimated with slightly greater accuracy at the non-optimal experimental setting, but the combination of the three properties maintain a higher accuracy at the optimal setting. The value of the CI associated to k_y is actually so large that obviously, the non-optimal conditions do not allow for the simultaneous estimation of this property with the two others. These results therefore illustrate a well-known property of the D -optimality criterion which is to allow for the best possible simultaneous estimation of all unknown properties using the experimental configuration investigated.

Table 5.15 indicates that using optimal conditions the thermal properties are all correlated, with a strong correlation term of 0.995 between the two conductivity components. Using non-optimal conditions however, no correlation is shown. These behaviors act along the fact that the non-optimal conditions simply do not take into consideration the property k_y as anticipated from the nearly null sensitivity to that property. Therefore, the correlation degrees obtained with the non-optimized experimental design have no value for the problem of simultaneously estimating the three properties. Figures 5.11 and 5.12 represent iso- S curves on which the disproportion between the sensibility to k_x and C on one side, and to k_y on the other side, is outlined. Note the long and narrow contours which are synonymous of strong near-linear dependence. These curves were constructed from exact data generated using the property values as indicated above.

Conclusion

This study has illustrated some theoretical considerations about relationships between sensitivity, correlation, condition number and optimality criteria, that were discussed in Chapter 3. On one hand, the results confirm that D -optimization globally maximizes the sensitivities to the parameters. In addition, the equivalence between the D -optimality criterion and the condition number has been outlined. On the other hand, it has been shown that minimum correlation does not imply maximum accuracy. Therefore, the use of an optimality criterion based on minimizing parameter correlation(s) would not be adequate. One important feature that has also been stressed is that one wishes uniform magnitude (about the same order) for the parameter sensitivity coefficients. Large differences in sensitivity magnitude to

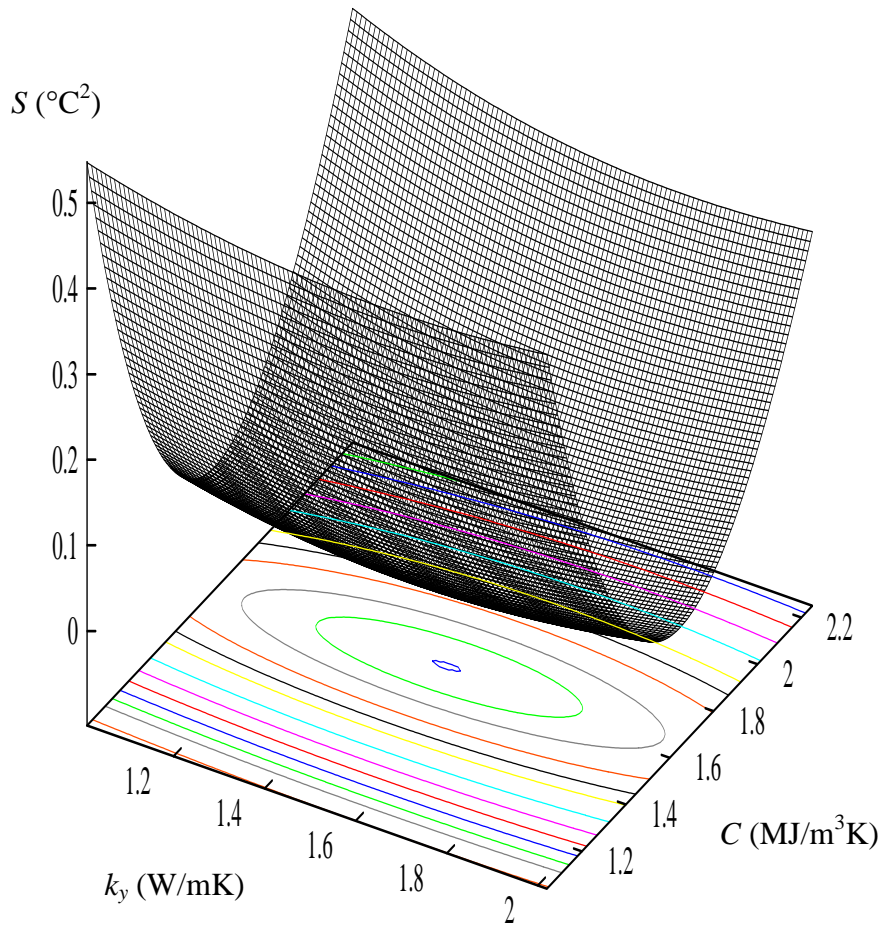


Figure 5.11 Curves iso- S vs. k_y and C with k_x fixed.

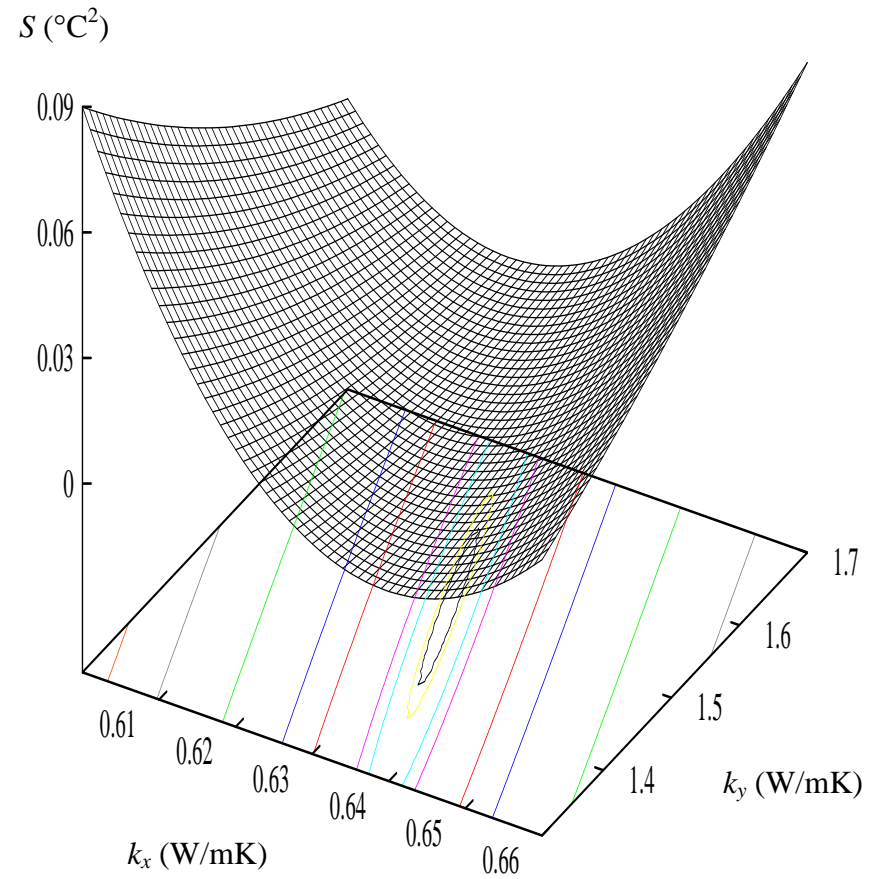


Figure 5.12 Curves iso- S vs. k_x and k_y with C fixed.

(from the two-dimensional Configuration 1 estimation problem)

one (or more) parameter has indeed more effect on the condition number than correlation between two (or more) parameters.

5.1.1.6 Effects of the Experimental Design Optimality Criterion

If the optimization of experimental designs according to D -optimality *globally* provides better estimates as illustrated above, a pertinent question is then “what are the other optimality criteria such as the E - and A - useful for?” (assuming one makes abstraction of their statistical characteristics described in Chapter 3). The purpose of this analysis was to answer this question, e.g. to evaluate the effects of the D -, E - and A -optimality criterion for the experimental design on the accuracy of the estimated thermal properties. Recall from Chapter 3 that in using the E - and A - criterion, the time-averaged minimum eigenvalue and trace of the dimensionless matrix $\mathbf{X}^T\mathbf{X}$, respectively, is maximized. This is defined in dimensionless terms as the maximization of $E^+ = \min|\lambda_i^+|$ and $A^+ = \sum_{i=1}^{n_p} d_{ii}^+$, where λ_i and d_{ii} are the i^{th} eigenvalue and the i^{th} diagonal element [defined in Eq. (5.1)] respectively, of the dimensionless matrix $\mathbf{X}^T\mathbf{X}$. These optimality criteria are subjected to the same experimental constraints as the D -criterion. In this analysis, the experimental designs for the one- and two-dimensional (Configuration 1) problems were first optimized using the three optimality criteria and using the exact dimensionless sensitivity models developed by Moncman (1995) and explained previously. Then, once again, uniform random errors were added to exact data generated from exact analytical models [Eqs. (5.10a and b)] of the optimized designs to simulate actual experimental data. In order to generate these data, k_x and C were set equal to 0.6 W/mK and 1.5 MJ/m³K, respectively, for both problems, and in addition, k_y was set equal to 1.9 W/mK in the two-dimensional problem. These simulated data were subsequently used to estimate the thermal properties and associated confidence intervals [Eq. (3.16)]. The effect of the optimality criteria on the accuracy of the estimated properties was then evaluated by comparing both the CIs associated with these properties and the objective function, S . The EEGA was used for both the optimization and estimation processes.

Recall that the experimental design variables optimized in the one-dimensional problem were the sensor location perpendicular to the fibers, x_s^+ , and the duration of the heat flux, t_h^+ . The two-dimensional problem included these variables in addition to the sensor location parallel to the fibers, y_s^+ , and the heating area, L_p^+ . The same total dimensionless experimental time was

used in each problem for all criteria. Here, values of 4.90 and 3.90 were used for the one- and two-dimensional problems, respectively. These values were determined using the D -optimality without time averaging and corresponded to the times when no significant additional information was gained through the use of additional data, as explained previously. The results for the optimized experimental designs using the A -, D -, and E -optimality criterion are shown in Table 5.16.

Table 5.16 Predicted optimal experimental designs using EEGA for the one-dimensional and Configuration 1 of the two-dimensional experiments according to D -, E - and A -optimality.

	Opt. Crit.	t_h^+	x_s^+	y_s^+	L_p^+
1-D	A-	4.90	0.	N/A	N/A
	D -	2.32	0.	N/A	N/A
	E -	1.22	0.07	N/A	N/A
2-D	E -	1.34	0.	0.91	1.
	D -	1.40	0.	0.86	1.
	A-	3.90	0.	0.50	1.

Several key points should be noted here. First, the optimal sensor location, x_s^+ , was approximately at the heated surface for all cases. This is where the sensitivity of k_x is maximized, suggesting that this property is dominant. Second, the A -optimality criterion resulted in the heating times, t_h^+ , equal to the values for the total experimental time, suggesting that less information will be available for the transient related property C . Also, in the two-dimensional design, the optimal sensor location, y_s^+ , for this criterion is at half the length of the composite, which is the location where the temperature gradient perpendicular to the fiber plane is the greatest for a heating area, L_p^+ , of 1.0, and constant temperature boundary conditions at the edges. The E -optimality, on the other hand, resulted in the shortest t_h^+ , suggesting that more information is available on C due to its transient nature, while less is available for k_x due to its dominance at steady-state conditions. The last criterion, the D -optimality, provided values for both t_h^+ and y_s^+ which fell between those found for the A - and E -optimality criteria, implying the D -optimality balances the effects of these other criteria.

These optimal designs were then utilized in the estimation procedure using the simulated data. The thermal property estimates and the associated 95 % CIs are shown in Table 5.17. Here, the effects of the D -, E - and A -criteria on the accuracy of the estimates follow from the discussion of the optimal designs given in Table 5.16.

Table 5.17 Estimated thermal properties, k_x , k_y , and C , the least squares error, S , and correlation terms r_{k_x/k_y} , $r_{k_x/C}$ and $r_{k_y/C}$ for the one-dimensional and Configuration 1 of the two-dimensional experiments designed according to D -, E - and A - optimality.

	Opt. Crit.	k_x (W/mK)	k_y (W/mK)	C (MJ/m ³ K)	S (EC ²)	r_{k_x/k_y}	$r_{k_x/C}$	$r_{k_y/C}$
1-D	A-	0.600 \forall 0.002	N/A	1.49 \forall 0.03	9.09	N/A	0.38	N/A
	D-	0.599 \forall 0.003	N/A	1.50 \forall 0.02	9.09	N/A	0.12	N/A
	E-	0.598 \forall 0.004	N/A	1.50 \forall 0.02	9.10	N/A	0.12	N/A
2-D	A-	0.599 \forall 0.008	1.74 \forall 8.59	1.49 \forall 0.05	7.50	0.97	0.84	0.80
	D*	0.573 \forall 0.025	2.44 \forall 0.64	1.52 \forall 0.03	7.44	0.99	0.65	0.63
	E-	0.585 \forall 0.033	2.08 \forall 0.41	1.50 \forall 0.04	7.51	0.99	0.30	0.26

* more data points were simulated here than for the study shown in Table 5.15; therefore, when comparing the estimation results associated with D -optimality, both the CIs and the correlation terms are lower, while the least square error, S , is larger.

First, the A -optimality resulted in the highest accuracy for the property with the highest sensitivity, i.e. k_x , but did so at the expense of the other properties, particularly k_y in the two-dimensional problem. Looking at the off-diagonal terms in the correlation matrix (refer to Section 3.1.3), the correlation between k_x and k_y was nearly the same for all criteria, while the correlations between each of the thermal conductivities and C were the highest with the A -optimality. The E -optimality had the opposite effects. Here, the accuracy of k_x was the lowest, while the accuracy of the property with the lowest sensitivity, i.e. k_y , was the highest. Also, the correlations between each of the thermal conductivities and C were the lowest with this criterion. Finally, the D -optimality offered a slightly lower least-squares function, S , than the other two criteria, and sought to compromise their opposite effects. Hence, the accuracy of k_x was higher than that found using the E -criterion, while lower than that from the A -criterion, and the opposite trend was found for k_y . Also, the correlations between the thermal conductivities and C were lower than those for the A -criterion, while higher than those for the E -. From these features, the D -criterion appears to minimize the variances of the estimates in the best global manner.

Note that the non-optimal conditions investigated in the previous section could correspond to a combination between A -optimality (sensor located at half the length of the sample which maximizes the accuracy on k_x) and available transient information for the accurate estimation of the property C (short heating time).

Conclusion

The results from this study can be concluded as follows:

- *D*-optimality provides the highest accuracy overall.
- *A*-optimality provides the highest accuracy for the property with the highest sensitivity, but does so at the expense of the accuracies of all other properties.
- *E*-optimality provides the highest accuracy for the property with the least sensitivity.

In terms of the comparative performance of the competing designs obtained applying these three criteria, the results point out that *A*-optimality should not be used.

5.1.2 Two-Dimensional Analysis Performed at Different Temperature Levels

This section and the next one (Section 5.2.1) deal with two-dimensional heat transfer for the simultaneous estimation of the thermal properties (k_x , k_y and C) of anisotropic composite materials over the temperature range [30-150°C]. While here the properties are estimated as constants at specific temperature levels using a design optimized previously, the optimal experiment to identify the properties as temperature dependent is investigated in the next Section. In the following, a description of the estimation problem is first provided. Then, the experimental methods used to procure the measured temperature histories required in the estimation process are presented, followed by the formulation of the mathematical model used to generate the calculated temperature histories. Eventually, the estimation results obtained applying the general-purpose GACONDUCT program are given and discussed.

5.1.2.1 Problem Description

The problem considered involved the simultaneous estimation over the temperature range [30-150°C] of the thermal conductivities parallel and perpendicular to the fiber plane and the volumetric heat capacity of anisotropic carbon/epoxy composites. This work was conducted in the context of an industrial research contract with the LTI/Nantes, and was sought to be a good application to confirm the robustness of the estimation methodology implemented in the genetic method. Two different carbon/epoxy composites were considered. The difference between the materials included the aspect ratio ($L_x/L_y = L_{xy}$), the fiber orientation and the addition of an aluminum coating for one of the materials. Because the analysis performed was the same for both materials, only one study is reported here. Note that both studies were the subject of industrial reports.

The materials were in a thin planar rectangular form with an aspect ratio of 0.047. Because of the similarities found with the two-dimensional analysis performed in Section 5.1.1, the properties were sought to be estimated as constants at different temperature levels using the basic D -optimal design of the Configuration 1. Recall that this optimal experimental design, sketched in Fig. 5.4a, included a uniform heat flux over the top boundary and constant temperature at the other three boundaries perpendicular to the xy plane, while those parallel to the xy plane were insulated. This configuration with constant-temperature boundary conditions on the sample sides was preferred over the insulated boundary conditions of Configuration 2 as Hanak (1995) showed that it provides more information for the estimation of the thermal conductivity in the fiber plane. Note that the use here of the same values for the dimensionless optimal experimental parameters as for the carbon/epoxy composites investigated by Hanak involved the assumption of a thermal conductivity ratio κ_{xy} of 7 (for an aspect ratio of 0.047).

The required temperature range was split into six levels, thereby defining the temperature levels to investigate as 30, 50, 75, 100, 125 and 150°C. An apparatus called ALIS (Laboratory Apparatus from ISITEM) was used to control and monitor the initial temperature inside the sample. The details of the experimental set-up are given in the next subsection.

As in the experiments performed at Virginia Tech by Hanak, a temperature rise occurred at the “constant temperature” boundaries. Due to the physical limitations of the experimental set up, the rise in this application was too significant to allow for the use of an analytical solution with average experimental values for the boundary conditions. Therefore, a numerical solution involving a control-volume-based finite difference method was applied which could accommodate any experimental variations. The numerical code used consists of an extension of the program CONDUCT developed by Patankar (1991). Its combination with the third GA developed in this research formed the general-purpose program GACONDUCT described in Chapter 4 and which was used for the estimation procedure.

5.1.2.2 Experimental Methods

- **Experimental Set Up**

The experimental set up was designed after the D -optimal Configuration 1 of the two-dimensional experiments sketched in Fig. 5.4a. Recall that the critical experimental design variables were the location of the sensor used in the estimation procedure ($x_s^+ = 0$ and $y_s^+ = 0.14$

or 0.86), the heating length ($L_p^+=1$), the heating time ($t_h^+=1.4$) and the total experimental time ($t_n^+=3.9$). The carbon/epoxy composite planar samples had an average thickness of 3 mm and an Area of 64×64 mm². Note that the term “average” is employed because when the samples were received, they were found to be non-homogeneous in thickness presenting discrepancies of up to 10% with respect to the average value. The optimal sensor location was then $x_s=0$ and $y_s=8.96$ or 55.04 mm, and the heating length was $L_p=64$ mm (heater covering the entire top surface). Assuming a diffusivity in the x -direction of 4×10^{-7} m²/s, the heating and total time were taken as 35 s and 100 s, respectively, from $t=t^+(L_x^2/\alpha_x)$ (see Section 5.1.1.2). The following summarizes the experimental apparatus used and then gives details about the major components.

The apparatus consisted of two square composite plates, an electric resistance heater, an aluminum mold made of four individual blocks, two aluminum plates and foils, thermal grease, 16 thermocouples, and eventually the apparatus ALIS. Figure 5.13 illustrates ALIS, which consists of an experimental press including two instrumented parallel plates. The plate temperatures are controlled either electrically or using circulation of fluids which are thermally regulated using “Lauda” type apparatuses. Note that in-depth description of ALIS can be found in Bailleul (1993). The use of ALIS enabled the samples (two samples were used for symmetry) to be placed under pressure ($P=8$ bars) and regulated their temperature via their boundaries. In this study, electrical heating was used for the plates. The set up was symmetric with respect to the heater, as shown in Fig. 5.13. The thermocouples placed on the samples were attached to the thermocouple junction box of the apparatus ALIS using thermocouple plug connectors. The junction box of ALIS was hardwired to an ice-bath to provide the necessary reference temperature for the thermocouples. The ice bath was in turn hardwired to the data acquisition system used. The heater was placed in series with a DC power supply and a high resolution Keithley digital multimeter (model # 2000) which allowed measurement of the current and voltage drop across the heater. Information from the thermocouples and the multimeter readings was sent to the data acquisition system through serial ports on a personal computer using RS-232. The system converted the thermocouple voltages into temperatures.

The electric resistance heater (part # HK-913, Minco Products Inc.) of dimensions 64×64 mm was selected not to include internally attached leads, which would have required

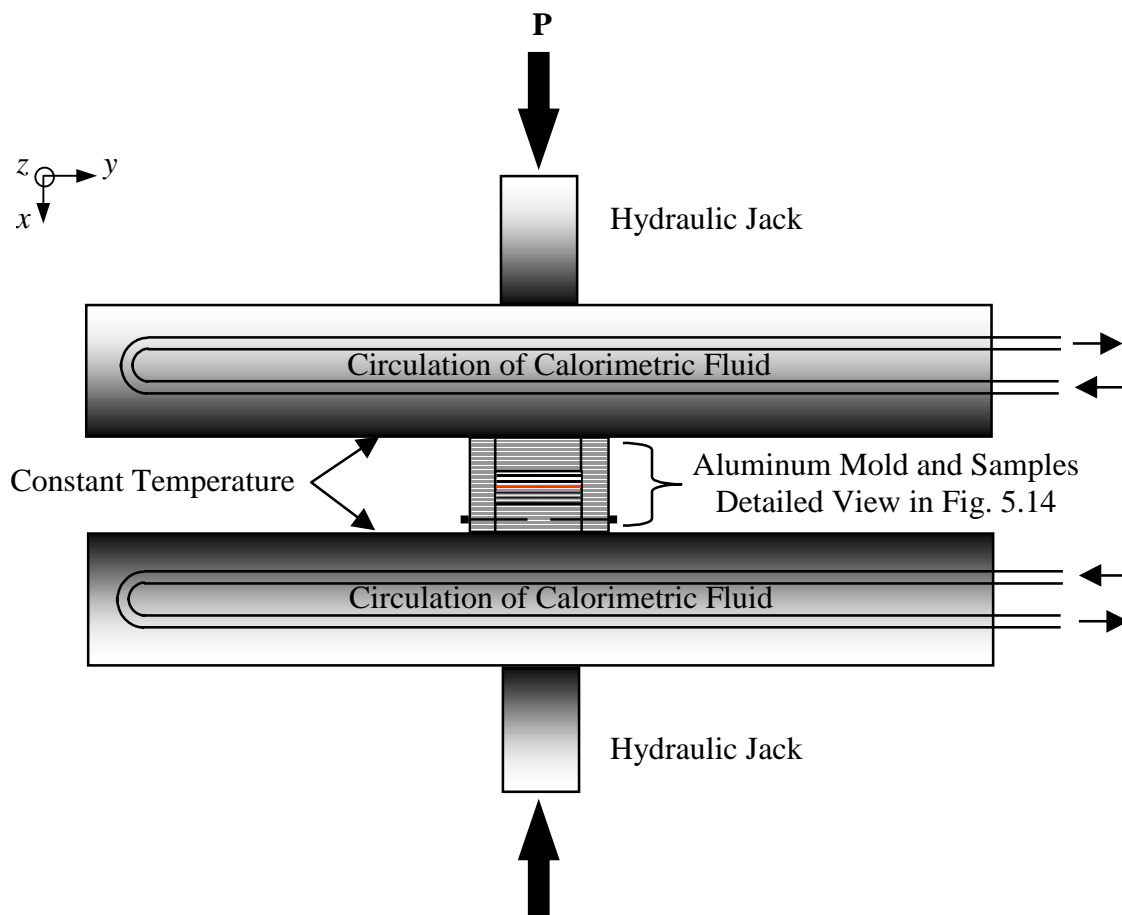


Figure 5.13 Simplified schematic of the experimental set up and apparatus ALIS (not to scale).

modification of the samples by adding a notch to allow space for the leads. The heater however presented the disadvantage of having a high electric resistance ($R=360 \Omega \pm 15\%$, and was measured as 359.6Ω). Variations of the resistance with temperature were neglected. In order to negate the effects of non-uniform heat flux developed because the heater consisted of a foil heating element covered by a thin layer of Kapton, aluminum plates of thickness equal to the distance between the centers of two adjacent heating elements (1 mm) were placed between the heater and each sample.

The sandwich composite-aluminum plate-heater-aluminum plate-composite was placed in an aluminum mold made of four individual pieces. Two metal round-headed screws located at the bottom of the mold (Fig. 5.13) were tightened a little to maintain the composite sides in good contact with the mold. The resulting assembly was in turn placed between the two heating plates of the press ALIS. An aluminum foil was actually put between the bottom and

top surfaces of the mold and the heating plates and thermal grease (based on alumina, $k=7$ W/mK) was applied to ensure good contact. The purpose of the mold was to provide the temperature conditions imposed to the heating plates and to act as a thermal guard. Because of the much larger dimensions of the heating plates than the mold (see Fig. 5.13 although not to scale), and the fact that both the plates and mold were at the same temperature, convection and radiation heat transfer were neglected around the mold and outside of the composite samples and therefore no particular insulation was applied. Note that the aluminum plates used to homogenize the heat flux were sized slightly smaller than the composite samples and small pieces (spurs) of insulating material were affixed to their sides both to prevent them from being in contact with the mold and to be sure they were adequately centered, as illustrated in Fig. 5.14. It was important that the entire heat flux generated by the heater entered the composite.

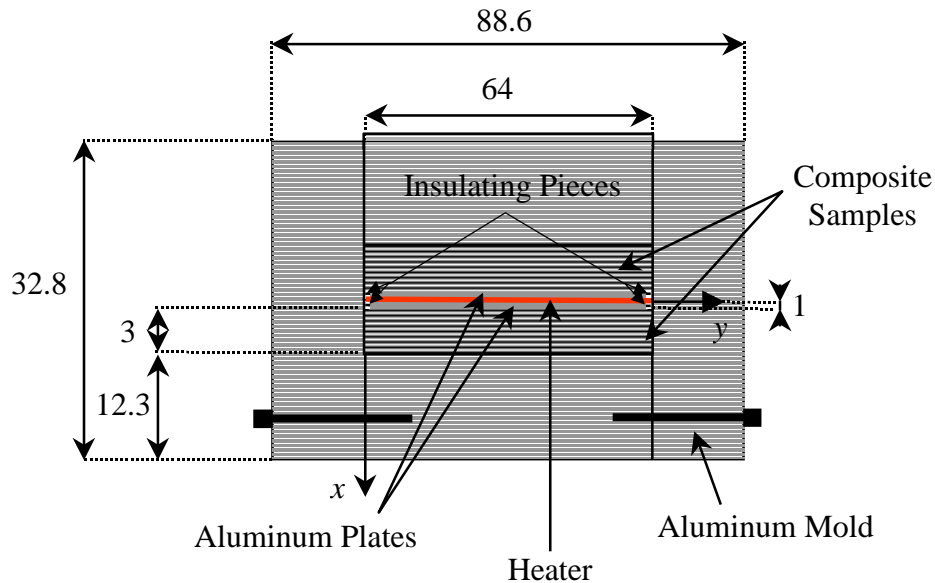
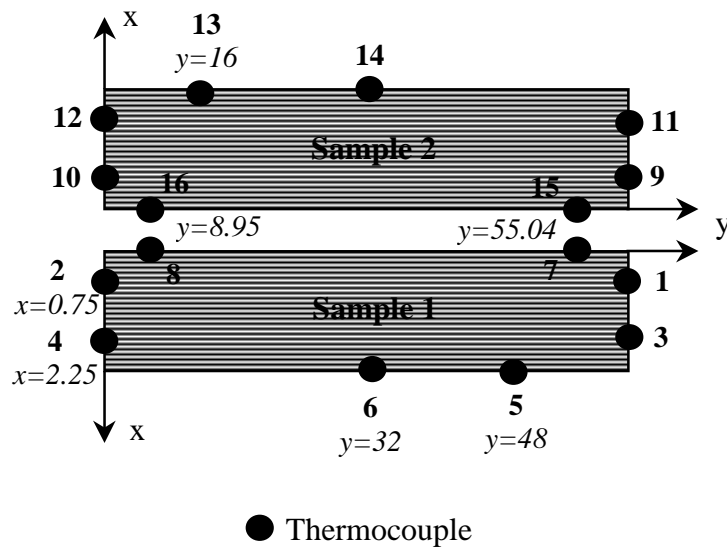


Figure 5.14 Detailed view of the sandwich structure inside the aluminum mold (dimensions in mm - not to scale).

Figure 5.15 shows the location of the thermocouples used. Note that the number of thermocouples was limited to sixteen because of the number of channels available in the data acquisition system. Each sample was instrumented with eight type K (Chromel-Alumel) thermocouples of diameter $80 \mu\text{m}$ (gage). The use of this thermocouple type and size allowed for a good compromise between accuracy and time consumption in preparing the experiments. Temperature rises occurred on all surfaces where a constant-temperature boundary condition was implemented. Therefore, the purpose of the two thermocouples on each side of the



● Thermocouple
 Sample dimensions: $L_x=3$, $L_y=64$

Figure 5.15 Thermocouple position and numbering (dimensions in mm - not to scale).

samples (# 1,2,3,4 and 9,10,11,12) and the two on the bottom surface (#5,6 and 13,14) was to record the temperature histories of the boundary conditions which were then implemented in the numerical model. The implementation procedure is discussed later. The thermocouples placed on the heated surfaces (# 7,8,15,16) corresponded to the optimal sensor position and were used in the estimation methodology. The advantage of the symmetrical set-up was that it allowed thermocouple readings of the same temperature history to be averaged. This not only reduced the amount of measurement noise that existed in any thermocouple measurement, but also enabled the bias due to the non-uniform thickness of the “planar” samples to be folded into measurement noise.

- **Experimental Procedure and Data**

The assembly procedure which involved producing and installing the thermocouples into the composite samples, and producing the aluminum mold and plates, was performed by D. Letourneur¹ (I participated in fabricating some thermocouples with the aim of learning and monitoring the process of making them). Note that the development of high performance experimental tools for accurate metrology has always been one of the priorities of the LTI. The data acquisition program was written by N. Lefevre¹ in Quick Basic following an IEEE

¹ Technician at the LTI/Nantes.

communication protocol. The program allowed a set of experimental data to be recorded approximately every 3 s. Experiments proceeded as follows:

- The power was adjusted once (at room temperature) to supply the selected heat flux value (discussed later). The current I was adjusted to satisfy $q=RI^2/2A$.
- The heating plates were set to a specified temperature level through the monitoring system of the press ALIS; time was allowed for the apparatus to reach this temperature level.
- Data were taken for approximately 20 s, measuring the apparatus at steady-state at the specified temperature level.
- The power supply of the electrical heater was turned ON manually (simultaneously with a time watch).
- After completing the required heating time of 35 s, the power supply was turned OFF.
- After completing the required total experimental time of 100 s, the experiment was terminated.

For each temperature level, experiments were repeated three times using the same experimental set up. Experimental data consisted of the measured times, temperature histories from the heated and constant temperature-boundary conditions and the specified heat flux. Note that the thickness variations of the composite samples as the temperature level increased were found to be negligible (viewing the records of the ALIS upper plate's displacement). Both the measured heat flux and temperature history from the constant-temperature boundaries were used as the boundary conditions in the numerical model.

5.1.2.3 Finite Difference Modeling

- **Geometrical Modeling**

Due to the symmetry in the y -direction, only half of a composite sample was modeled. The two-dimensional boundary conditions are sketched in Fig. 5.16. One can see that the geometric modeling included the thin aluminum plate placed between the heater and the sample. The little "hole" containing air and the piece of insulating material afixed to the plate edge was however neglected. A contact resistance between the sample and the aluminum plate was taken into consideration and given a value of 10^{-4} m²·K/W [based on reported data

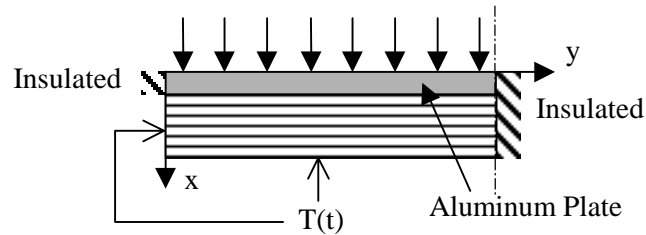


Figure 5.16 Boundary conditions analyzed in the numerical model.

approximating the aluminum/composite interface [Incropera and DeWitt, 1996]. The resistance was then modeled as a layer with thickness 0.1 mm, thermal conductivity 1 W/m²·K (in the direction perpendicular to the layer only) and null thermal capacitance. The thermal capacitance of the heater was neglected due to its very small thickness (0.15 mm).

Figure 5.17 shows the control-volume discretization performed using the scheme called practice *B* which is inherent to the program CONDUCT. The faces are called I_1 , L_1 , J_1 and M_1 to refer to the nomenclature used in CONDUCT. The model consisted of 10 and 33 elements (implying 12 and 35 nodes) in the x - and y -direction, respectively. One can see that the mesh is not uniform, being more accurate at the optimal sensor location (node $i = 4$ and $j = 11$). The average mesh size in the composite, Δx_{av} and Δy_{av} , were chosen to be homogeneous with the

ratio of the thermal conductivities (κ_{xy}), i.e. $\frac{k_y}{\Delta y_{av}^2} = \frac{k_x}{\Delta x_{av}^2}$. A value of seven for κ_{xy} approximately provided a Δx_{av} of 0.4 mm (7.5 elements for 3 mm) using a Δy_{av} of 1 mm (33 elements for 32 mm). The time step, Δt , was selected to satisfy the Fourier number $\frac{\alpha_x \Delta t}{\Delta x_{av}^2} \leq 1$

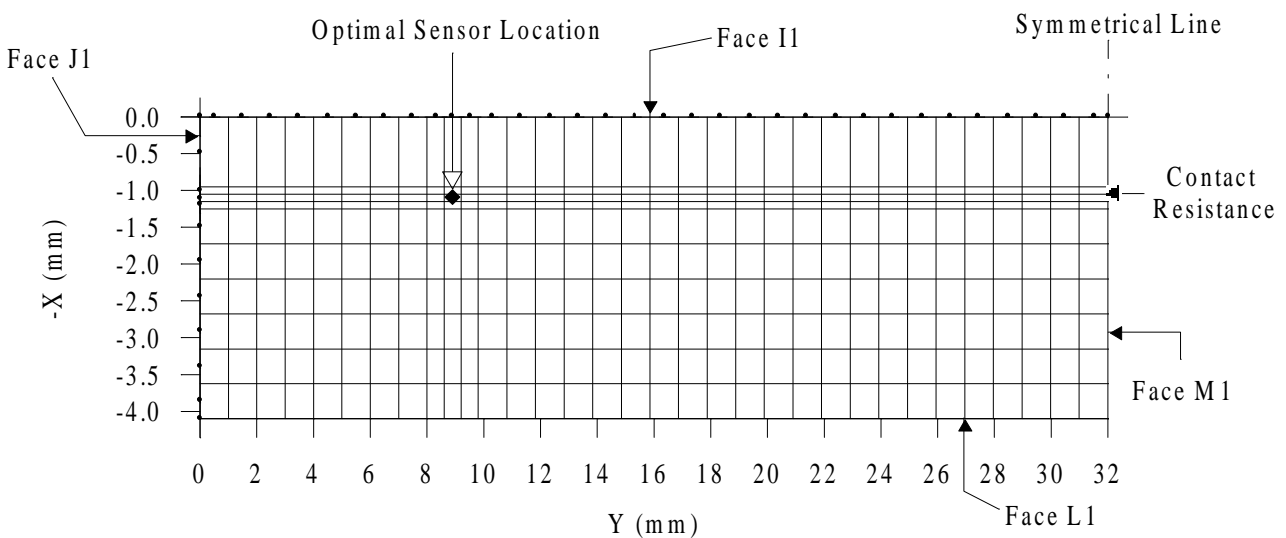


Figure 5.17 Control-volume discretization (grid 10 × 33 elements) from half-sandwich structure (not to scale).

for stability in a control volume of the composite. The use of an initial estimate of $4 \times 10^{-7} \text{ m}^2/\text{s}$ for α_x yielded $\Delta t \leq 0.4 \text{ s}$.

A study was conducted to evaluate the convergence of the model. This included the analysis of the grid size, the time step and the number of iterations used by the solver. It was found that the grid refinement described above was adequate, and that a time step of 0.25 s allowed for a good trade-off between numerical accuracy and the consideration of computational resources. In addition, the number NTIMES which limits the number of inner iterations, NTC, used by the solver in CONDUCT (Patankar, 1991), was set to 10 to allow convergence of the solution, particularly when the heater was turned ON and OFF. Note that this convergence study also permitted investigation of the temperature increase resulting from specified heat flux values. From this, a heat flux value around 1200 W/m^2 was selected as it enabled a maximum temperature increase of about 4°C at high temperature levels, and of about 6°C at room temperature. This then allowed for the estimation of constant properties while maintaining a relatively large signal-to-noise ratio.

- **Specification of the Boundary Conditions**

As discussed previously, the boundary conditions were specified from experimental measurements. The data were treated as follows (refer to Fig. 5.15 for the thermocouple numbering):

- $T_1, T_2, T_9,$ and T_{10} , and t_1, t_2, t_9 and t_{10} were averaged to provide a temperature and time history, respectively, at the location $x_{composite} = 0.75 \text{ mm}$ on face $J1$ of the geometrical model [$T_{J1}(x_{composite} = 0.75)$].
- $T_3, T_4, T_{11},$ and T_{12} , and t_3, t_4, t_{11} and t_{12} were averaged to provide a temperature and time history, respectively, at the location $x_{composite} = 2.25 \text{ mm}$ on face $J1$ of the geometrical model [$T_{J1}(x_{composite} = 2.25)$].
- $T_5, T_6, T_{13},$ and T_{14} , and t_5, t_6, t_{13} and t_{14} were averaged to provide a temperature and time history, respectively, for the face $L1$ of the geometrical model [T_{L1}].

The data associated with the optimal sensor location were subjected to the same treatment, e.g. T_7, T_8, T_{15}, T_{16} , and t_7, t_8, t_{15}, t_{16} were averaged to represent the measured temperature and time $(\tilde{T}_i, \tilde{t}_i)$, respectively, at the optimal sensor. Figure 5.18 illustrates the average experimental histories obtained from the third experiment performed at 50°C .

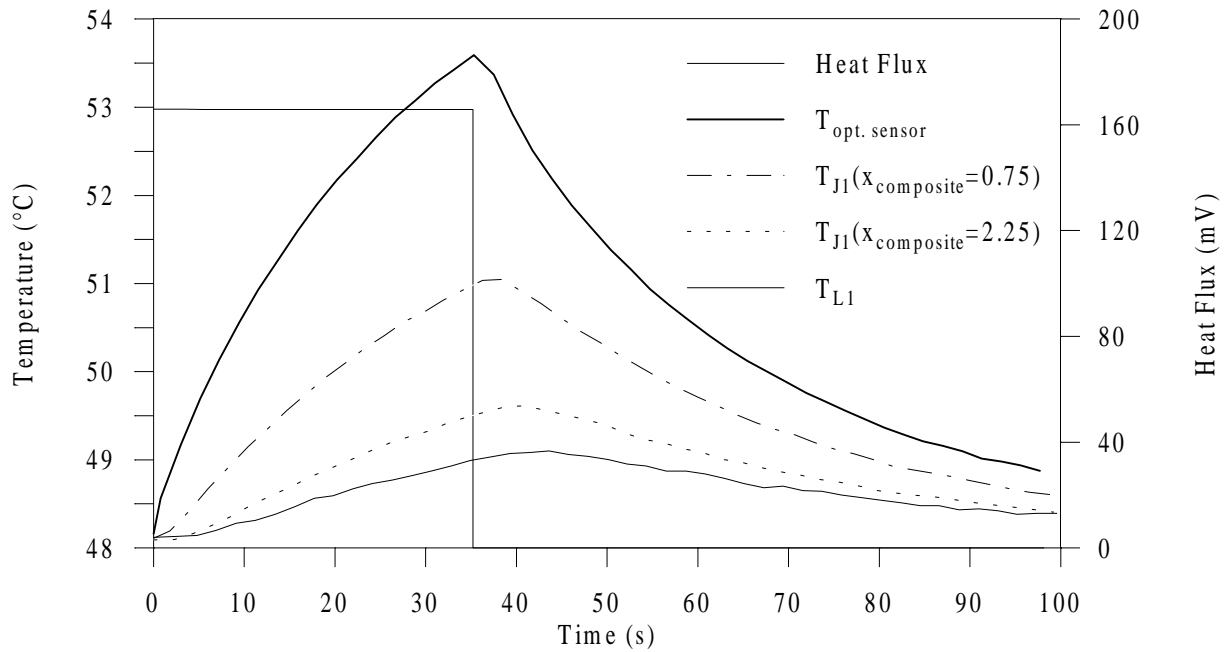


Figure 5.18 Experimental temperature and heat flux histories from experiment #3 at 50°C.

Averaged temperatures used as boundary conditions and heat flux values were then all interpolated in time from a linear regression between two successive data. This was necessary to obtain data at each time step. Finally, a linear regression was realized for the node temperatures on Face $J1$ using the known temperatures at the two locations $x_{composite} = 0.75$ and 2.25 mm. The node temperatures on Face $J1$ were determined based on their $x_{composite}$ -location.

Note that the initial offset generated while the sample was assumed to be at a uniform temperature was slight (on the order of the thermocouple accuracy) and thus was not taken into consideration.

5.1.2.4 Results and Discussion

The objective function to minimize in the estimation methodology implemented in the GACONDUCT was based on simple OLS estimation and was the same as in Eq. (5.2). A temperature history was predicted at the optimal sensor and compared with the measured temperatures at the same location to simultaneously estimate the thermal properties. The

Fortran subroutine GA2DOPT.FOR, written to adapt GACONDUCT to solve this problem, can be found in Appendix E. The properties were estimated for each of the three experiments performed at each temperature level. Note that data from one experiment at 30°C could not be used. The jobs were run on a personal computer P233. For all jobs, the same setting was used for the genetic parameters associated with the convergence criterion and is given in Table 5.18. Recall from Section 4.4 that the setting for the different probabilities associated with the genetic operators was established when analyzing the optimization of the mathematical function **f6** and can be found in Table 4.1. The CPU time was quite costly and therefore, the ideal population size ($n_s = 100 \times n_p$, see Section 4.3.3) could not be used and values for MING, LASTCRITERG and LASTG were minimum. Nevertheless, all jobs were converged before LASTG was reached.

Table 5.18 Genetic convergence parameters setting.

n_s	MING	LASTCRITERG	LASTG	CRITERION
100	5	10	100	0.01 (1%)

Estimation jobs first proceeded at 30°C and 150°C with large ranges for the properties. Then the results gained concerning the estimated properties at these temperature levels were used as a basis for the ranges of study in performing the estimation process at other temperature levels. Figure 5.19 illustrates the estimates obtained along with the linear regressions associated with the properties. The means of the estimates obtained for the three experiments performed at each temperature level and the percentage differences between these means and the values given by the linear regressions were then computed. The 95% confidence intervals associated with the predicted means were not calculated as they would have been meaningless for only three experiments. These results, along with the associated 95% CIs of the estimates [Eq. (3.17)], the least-squares error S , and the Root-Mean-Square values for each of the experiments are given in Table 5.19.

Overall, the small magnitude of S ($S_{max} = 0.0717 \text{ °C}^2$) and the small RMS percentages (of maximum temperature rise; $\text{RMS}_{max} = 0.83\%$) highlight the excellent behavior of the GACONDUCT program. Note that the RMS increase with temperature comes from the fact that the same heat flux was applied at every temperature level, therefore causing smaller temperature rises at higher temperature levels. Figures 5.20 and 5.21 show the calculated and

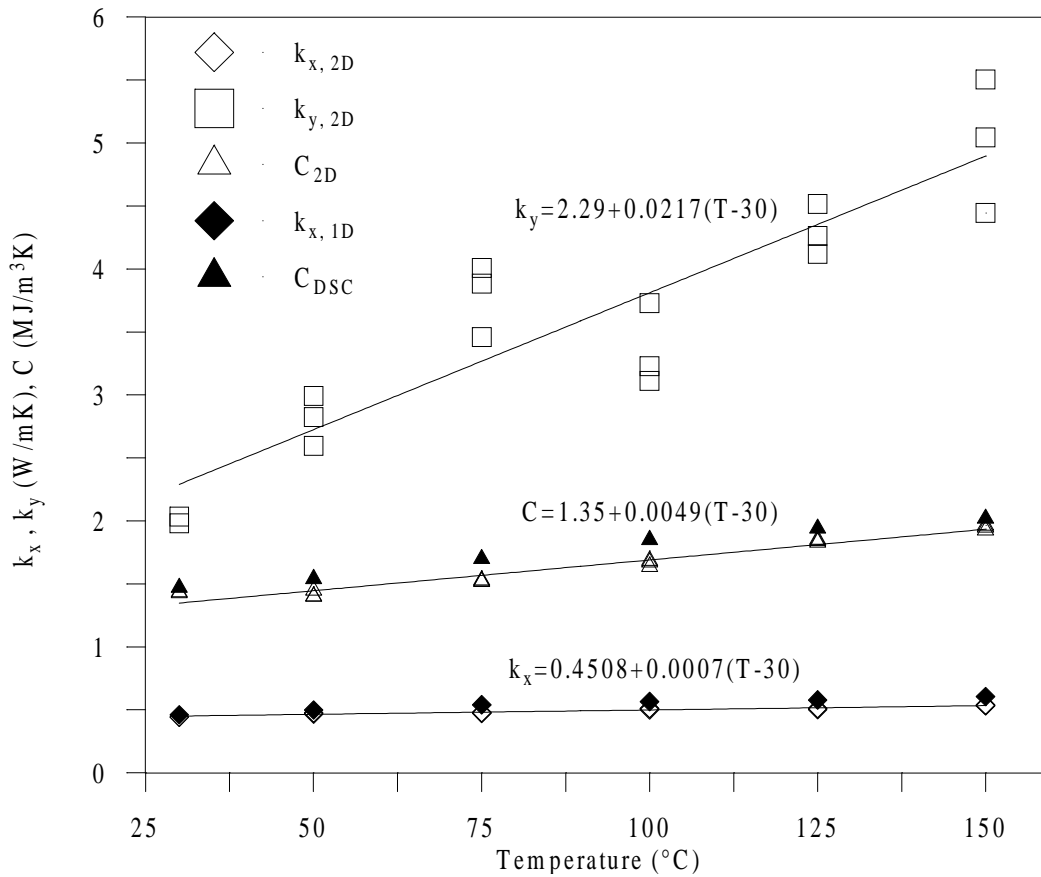


Figure 5.19 Estimated thermal properties and linear regressions (the source for the data regarding $k_{x,1D}$ and C_{DSC} is introduced later).

measured temperatures along with the resulting residuals for the experiment #3 at 50°C and 150°C, respectively. One can see that there is a small bias in the model when the heater is turned on. Indeed, difficulty was encountered in implementing the initial temperature distribution inside the sample. Nevertheless, it is striking that the residuals are small, relatively centered around zero and do not seem to be correlated at different temperature levels after the heater is turned on. Indeed, the shape of the residuals (after the heater is turned on) do not contain a “signature” that would indicate bias or inconsistency in the numerical model. This establishes that the model is satisfactory and provides confidence in the genetic-based estimation methodology. In addition, this “validates” approximation of the standard statistical assumptions (refer to Chapter 3).

Table 5.19 Estimated thermal properties k_x , k_y and C , least square error S , and Root Mean Square error RMS at six different temperature levels in the range [30-150°C].

T (°C)	k_x (W/mK)	k_y (W/mK)	C (MJ/m ³ K)	S (°C) ²	RMS _i (°C) (% ΔT_{max})	
30	0.443±0.029	2.034±1.696	1.435±0.010	0.0211	0.0214	0.37
30	0.442±0.037	1.979±2.202	1.427±0.013	0.0400	0.0291	0.50
<i>Mean</i>	<i>0.443</i>	<i>2.007</i>	<i>1.431</i>	<i>0.0305</i>	<i>0.0252</i>	<i>0.44</i>
Linear Regression	0.450	2.289	1.348	N/A	N/A	N/A
% error Mean/LR	1.749	14.050	5.807	N/A	N/A	N/A
50	0.474±0.021	2.992±1.683	1.448±0.017	0.0129	0.0165	0.30
50	0.466±0.032	2.824±2.437	1.401±0.025	0.0340	0.0275	0.50
50	0.475±0.039	2.596±2.795	1.398±0.029	0.0446	0.0311	0.56
<i>Mean</i>	<i>0.471</i>	<i>2.804</i>	<i>1.416</i>	<i>0.0305</i>	<i>0.0250</i>	<i>0.45</i>
Linear Regression	0.464	2.723	1.446	N/A	N/A	N/A
% error Mean/LR	1.504	2.890	2.129	N/A	N/A	N/A
75	0.479±0.041	3.457±3.408	1.529±0.030	0.0461	0.0313	0.58
75	0.475±0.039	3.883±3.438	1.522±0.027	0.0377	0.0283	0.53
75	0.472±0.039	4.006±3.441	1.517±0.026	0.0370	0.0280	0.52
<i>Mean</i>	<i>0.476</i>	<i>3.782</i>	<i>1.523</i>	<i>0.0402</i>	<i>0.0292</i>	<i>0.55</i>
Linear Regression	0.482	3.265	1.568	N/A	N/A	N/A
% error Mean/LR	1.309	13.661	2.988	N/A	N/A	N/A
100	0.512±0.036	3.227±2.917	1.671±0.032	0.0462	0.0313	0.61
100	0.509±0.031	3.111±2.843	1.685±0.029	0.0324	0.0254	0.52
100	0.499±0.046	3.727±4.020	1.636±0.037	0.0660	0.0378	0.75
<i>Mean</i>	<i>0.507</i>	<i>3.355</i>	<i>1.664</i>	<i>0.0482</i>	<i>0.315</i>	<i>0.63</i>
Linear Regression	0.499	3.808	1.691	N/A	N/A	N/A
% error Mean/LR	1.484	13.492	1.616	N/A	N/A	N/A
125	0.501±0.032	4.260±3.001	1.840±0.031	0.0430	0.0302	0.61
125	0.512±0.034	4.117±3.044	1.830±0.034	0.0589	0.0354	0.72
125	0.508±0.030	4.515±2.879	1.852±0.029	0.0323	0.0264	0.53
<i>Mean</i>	<i>0.507</i>	<i>4.298</i>	<i>1.841</i>	<i>0.0447</i>	<i>0.0306</i>	<i>0.62</i>
Linear Regression	0.517	4.350	1.813	N/A	N/A	N/A
% error Mean/LR	1.964	1.224	1.497	N/A	N/A	N/A
150	0.532±0.028	5.503±2.377	1.924±0.035	0.0717	0.0394	0.83
150	0.535±0.026	5.044±2.630	1.947±0.029	0.0682	0.0385	0.83
150	0.539±0.025	4.443±2.269	1.963±0.029	0.0671	0.0382	0.82
<i>Mean</i>	<i>0.535</i>	<i>4.997</i>	<i>1.945</i>	<i>0.0690</i>	<i>0.0387</i>	<i>0.83</i>
Linear Regression	0.534	4.893	1.936	N/A	N/A	N/A
% error Mean/LR	0.130	2.081	0.458	N/A	N/A	N/A

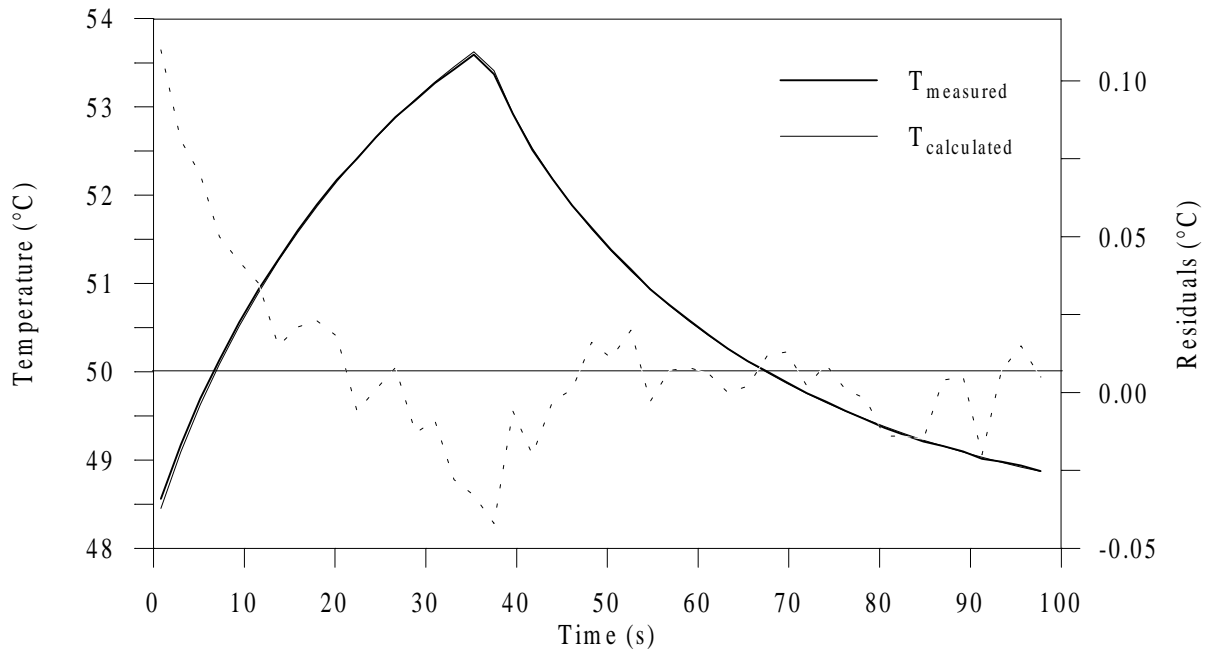


Figure 5.20 Calculated and measured temperature and residual distributions from experiment #3 at 50°C.

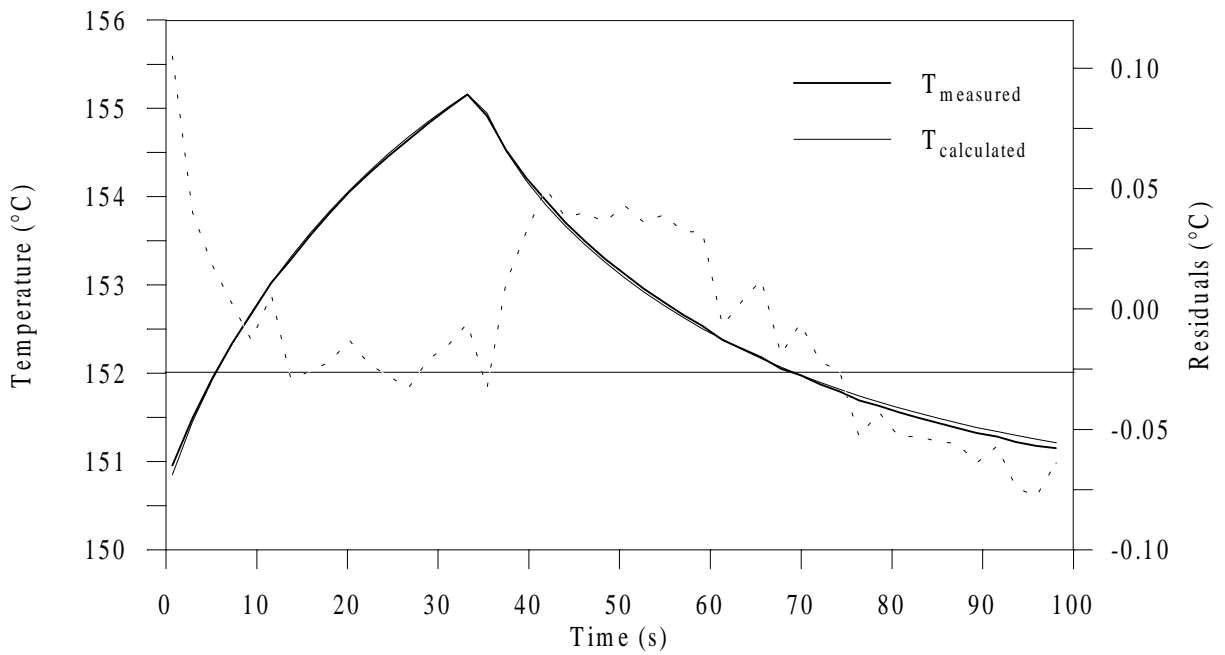


Figure 5.21 Calculated and measured temperature and residual distributions from experiment #3 at 150°C.

Regarding the results of the estimated properties, more variability is observed in the property k_y than in the properties k_x and C . This can be attributed to the much smaller dimensionless sensitivity coefficient of k_y (obtained from finite differences) as illustrated in Fig. 5.22 and Fig. 5.23 for the experiment #3 at 50°C and 150°C, respectively. Indeed, very little information is provided for this thermal property. From the estimation results obtained from the two-dimensional Configuration 1 problem analyzed in the previous study, it was expected that less information would be obtained for the property k_y than for the other two. However, here the sensitivity to k_y is much lower than in the previous study. This comes from the fact that much greater temperature increases at the ideally constant temperature boundaries occurred in the present case (refer to Fig. 5.18). Therefore, the experimental design used is farther from the ideal optimal experiment than in the previous study, causing the higher thermal property variances. As outlined in Chapter 3, this effect stresses the logical need to perform estimation using experimental conditions as close as possible to the ideal ones considered in determining the optimal design. Figure 5.24 shows a typical temperature distribution obtained with the numerical model when the heater is turned off. Obviously, the large temperature variation on the sample sides (also shown in Fig. 5.18) prevent straight two-dimensional heat transfer, therefore not allowing information to be obtained for the accurate estimation of the property k_y .

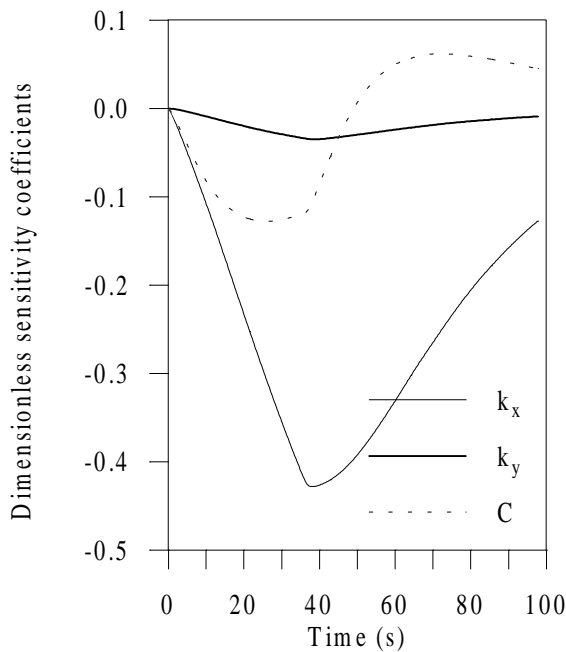


Figure 5.22 Dimensionless sensitivity coefficients from experiment #3 at 50°C.

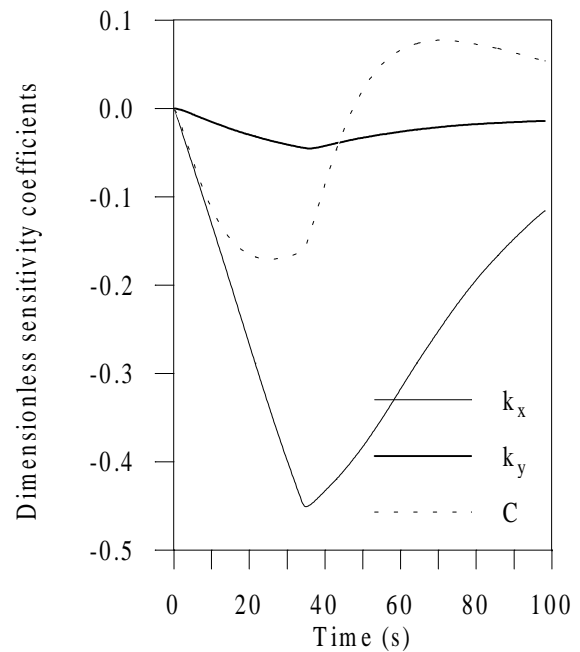


Figure 5.23 Dimensionless sensitivity coefficients from experiment #3 at 150°C.

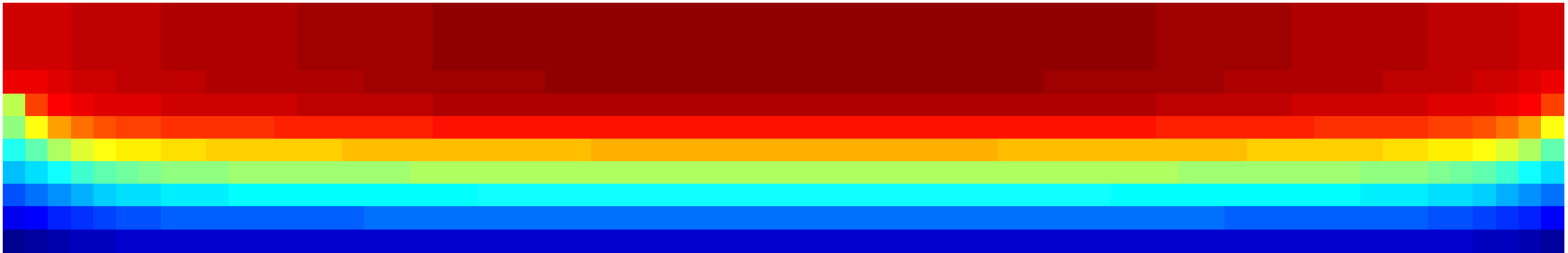


Figure 5.24 Typical two-dimensional temperature distribution obtained when the heater is turned off (at $t = t_h = 35$ s).

As far as correlation between the parameters is concerned, Table 5.20 shows the correlation terms obtained from the estimation performed on the experiment #3 at 50°C and 150°C. One can see that about the same ill defined conditions are found here as in the two-dimensional estimation problem investigated in the previous study.

Table 5.20 Correlation matrices for the simultaneous estimation of k_x , k_y and C from experiment #3 at 50°C and 150°C.

	Exp. 50°C			Exp. 150°C		
	k_x	k_y	C	k_x	k_y	C
k_x	1			1		
k_y	-0.9997	1		-0.9979	1	
C	0.9459	-0.948	1	0.7974	-0.811	1

In measuring the suitability of the experimental design, not only ideal experimental conditions should be taken into account as much as possible, as stated above, but also the initial values used for the variables α_x and κ_{xy} (to determine the optimal values of the experimental design variables) should be verified. The resulting values for the thermal diffusivity, α_x , ranged from 2.8 to 3.4×10^{-7} m²/s, which is not very different from the initial value of 4×10^{-7} m²/s used. Note that the use of an α_x of 3×10^{-7} m²/s would have given a slightly higher dimensional heating time, allowing then to get closer to steady state. Regarding the values obtained for the thermal conductivity ratio, κ_{xy} ($= k_y/k_x$), they ranged from 4.5 at 30°C to 9.3 at 150°C. These values agree approximately with the value of 7 for κ_{xy} that was applied (in association with the aspect ratio L_{xy} of 0.047 of the samples analyzed here) to provide the dimensionless optimal experimental parameter values used.

Based on the linear regression obtained for each property, the thermal conductivity perpendicular to the fibers, k_x , was found to increase approximately 18.7% from 30°C to 150°C, while the thermal conductivity parallel to the fibers, k_y , and the volumetric heat capacity, C , increased approximately 113.8% and 43.6%, respectively, over the same temperature range. The increases for k_y and C are quite high. Table 5.21 shows a comparison of the slopes with temperature obtained here for the properties with previously published results (for carbon/epoxy composite type). The results associated with the present study seem reasonable.

Table 5.21 Comparison of temperature dependence slopes associated with linear regressions for the properties k_x , k_y and C with previously published results (carbon/epoxy composite type).

k_x (W/mK ²)	k_y (W/mK ²)	C (MJ/m ³ K ²)	Temperature Range (°C)	Estimation Method	Reference
0.0016×T	0.0320×T	0.0057×T	[20-100]	2D, Gauss	Loh (1989)
0.0009×T	N/A	0.0045×T	[30-135]	1D, Gauss	Scott & Beck (1992a)
0.0007×T	0.0217×T	0.0049×T	[30-150]	2D, GA	Present Study

In terms of the error introduced from the use of linear regressions for the three properties over the temperature range investigated (compared to the use of the corresponding mean values), on one hand, the error remained below 2% and 6% for k_x and C , respectively. On the other hand, this error is relatively large for k_y and ranges from 1.2% to 14%. One can easily conclude that this is the result of a low magnitude for the sensitivity coefficient X_{k_y} . The confidence intervals of the estimates are consistent from experiment to experiment. Those associated with the property k_y are the largest (in keeping with the variability for this property), while those associated with the property k_x are the smallest.

It is of interest to note all possible sources of errors. These include:

- the uncertainty in the presumably “known” parameters (whose large disruptive effect have been emphasized both in Chapters 2 and 3), namely here the non-uniform thickness of the samples (recall that a discrepancy of up to 10% was found with respect to the average thickness value);
- the assumptions involved in the numerical model (known contact resistance between the aluminum plate and the sample, negligible thermal capacitance of the heater, aluminum property values, ...);
- the procedure for the treatment of experimental data, more particularly of those used to specify the numerical model boundary conditions; and last but not least,
- the data acquisition inaccuracy, the errors due to experimental manipulation and inaccurate calibration of the thermocouples.

As one can see, some of these sources could not be controlled, while the minimization of others was a difficult task.

It should be mentioned that the composite samples investigated in this study were also subject to a one-dimensional analysis with an aim to estimating only the thermal conductivity

perpendicular to the fiber plane, k_x , over the same temperature range as in the two-dimensional analysis. Values for the volumetric heat capacity, C_{DSC} , were provided from a Differential Scanning Calorimetry (DSC) study (C_{DSC} was actually obtained from the product of $c_{p,DSC}$ and the material density). The one-dimensional experiment was performed by Ph. Grandet¹ using the apparatus ALIS. Note that this type of experiment is well established at the LTI and is often applied in the context of industrial contracts as was the case here. A gradient-based procedure (Jurkowski et al., 1997) was used to estimate k_x and it was found that the predicted values from the two-dimensional estimation were in good agreement with the one-dimensional results (see C_{DSC} and $k_{x,1D}$ in Fig. 5.19). The one-dimensional analysis was a good means to verify the validity of the two-dimensional results obtained using the GA-based method.

5.1.2.5 Conclusion

On one hand, this study has stressed how relevant it is to perform experiments that deviate as little as possible from the ideal conditions considered in optimizing the design. On the other hand, the effect of temperature on the thermal properties has been shown to be of great importance and to follow a linear functional relationship. Regarding the procedure applied, estimating the properties as constants at different temperature levels has been illustrated to be tedious, time intensive and experimentally costly. Furthermore, it introduced additional errors between the value of the property estimated at a specific temperature and the linear regression generated over the entire temperature range investigated (Table 5.19). From this, one understands the need to estimate the temperature-dependent properties directly. This is the subject of the following studies.

Another relevant concluding point from this investigation is that the robustness and reliability of the GA-based estimation methodology has been confirmed. Indeed, despite existing correlations between all properties and the little information available for the property k_y , the use of GAs has enabled the unknown thermal properties to be simultaneously identified. Finally, the general-purpose program GACONDUCT has been found to be a powerful algorithm allowing for many interesting applications, as will be shown in the next two subsections.

¹ Mr. Grandet performs measurements associated with industrial services at the LTI/Nantes.

5.2 Case Studies of Mixed Temperature Dependent and Constant Property Estimation

In the following, efforts were undertaken for the characterization of the dependence of the thermal properties on temperature. Both the GA-based optimization and estimation methodologies were modified to include this dependence. Piece-wise linear functions of temperature were used as the functional relationship. For instance, the volumetric heat capacity was expressed as

$$C(T) = C_i + (C_{i+1} - C_i) \frac{T - T_i}{T_{i+1} - T_i}, \quad (5.14)$$

where C_i and C_{i+1} were the parameters to be estimated, corresponding to the values of the property at the temperatures T_i and T_{i+1} , respectively.

Two problems were investigated to demonstrate the performance of the GA-based methodologies. The first was based on the work performed in Section 5.1.2 and involved the optimization of a two-dimensional experimental design for the simultaneous estimation of the thermal properties k_x , k_y and C , as temperature dependent over the range [25-150°C]. In the second problem, the simultaneous estimation of the same properties over the range [100-130°C] from two-dimensional transient experiments in an RTM mold was considered. These problems are described in the next two subsections.

5.2.1 Two-Dimensional Analysis Over the Range [25-150°C]

As mentioned above, this study was built upon the work described previously. Here, the investigation of the D -optimization of the experimental setup described in Section 5.1.2.2 is reported. The objective was to maximize the experimental information for the simultaneous estimation of the three thermal properties, k_x , k_y and C , of the carbon/epoxy composite sample analyzed, directly as temperature dependent over the required range [25-150°C]. In addition, the identification of the contact resistance, R_c , between the sample and the aluminum components used in the setup was taken into consideration. In using D -optimality, the highest accuracy overall for the thermophysical parameters involved was desired. Once the optimization stage was realized, the estimation methodology was demonstrated on simulated data generated from the optimal design.

Details about the estimation and optimization problem are first provided, followed by a description of the control-volume-based finite difference modeling performed. Then, the

results obtained applying the GACONDUCT program in both the optimization and simulated estimation stages are presented and discussed.

5.2.1.1 Problem Description

- **Estimation Problem Formulation**

The dependence on temperature over the range [25-150°C] was characterized using two parameters for both thermal conductivities and four parameters for the volumetric heat capacity, while the contact resistance was assumed as constant. The three thermal properties were expressed by:

$$k_x(T) = k_{x25} + (k_{x150} - k_{x25}) \frac{T - 25}{125}, \quad T \geq 25^\circ \text{C} \quad (5.15)$$

$$k_y(T) = k_{y25} + (k_{y150} - k_{y25}) \frac{T - 25}{125}, \quad T \geq 25^\circ \text{C} \quad (5.16)$$

$$C(T) = C_{25} + (C_{75} - C_{25}) \frac{T - 25}{50}, \quad 25 \leq T < 75^\circ \text{C} \quad (5.17)$$

$$C(T) = C_{75} + (C_{110} - C_{75}) \frac{T - 75}{35}, \quad 75 \leq T < 110^\circ \text{C} \quad (5.18)$$

$$C(T) = C_{110} + (C_{150} - C_{110}) \frac{T - 110}{40}, \quad T \geq 110^\circ \text{C} \quad (5.19)$$

Nine thermophysical parameters (k_{x25} , k_{x150} , k_{y25} , k_{y150} , C_{25} , C_{75} , C_{110} , C_{150} , and R_c) were therefore to be simultaneously estimated by minimizing the least-squares error, S , given in Eq. 5.2. Note that information from only one sensor was considered in the estimation procedure.

- **Optimization Problem Formulation**

The same symmetrical experimental setup (with same dimensions) described in Fig. 5.13 and 5.14, was considered here. Experiments were designed to generate temperatures from 25°C to at least 150°C. Therefore, the plates of the apparatus ALIS were assumed to be maintained at a constant temperature of 25°C (using circulation of a fluid thermally regulated inside the plates), while the increase in temperature to 150°C was sought to be provided from the use of the electric heater (this is discussed later). Regarding the sides of the aluminum

mold in the y -direction, insulation was considered based on the experimental ease of applying and maintaining insulated boundary conditions. Insulation was necessary for the faces of the setup in the z -direction (perpendicular to the page in Fig. 5.13) to meet the restriction of the analysis to two-dimensional heat transfer. In this configuration, the experimental parameters selected to be optimized were the location, x_s and y_s , of the sensor placed on the composite surface, the heating length over the sample, L_p , the heating and cooling times according to a specific heating law introduced next, and the total overall experimental time, t_n . Figure 5.25 provides a schematic of the experimental design to be optimized.

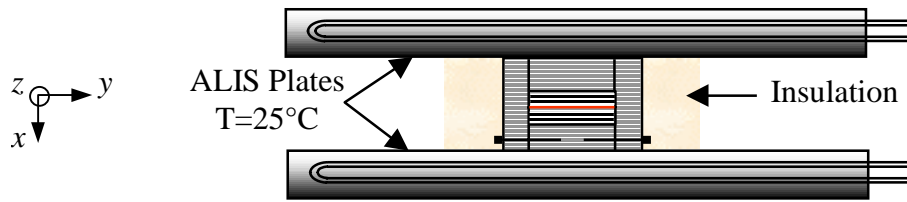


Figure 5.25 Simplified schematic of the experimental setup to be optimized (refer to Fig. 5.13 and 5.14, not to scale).

The heating law was sought to be a double heat flux step, as sketched in Fig. 5.26. Two heating times separated by a cooling period were anticipated to provide more information, particularly for the estimation of the thermophysical parameters associated with the bracket temperatures, 25 and 150°C. In considering such a heating law, the heating time of both heat flux steps, t_{h1} and t_{h2} , and the cooling period t_{12} were considered in the optimization process. Note that integer values were used for these parameters to be consistent with a time step of 0.25 s.

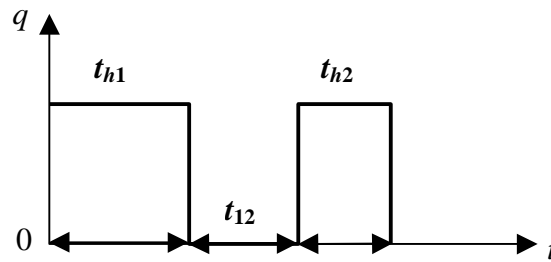


Figure 5.26 Heating law considered in optimization process (heat flux q imposed from the electrical heater).

In using D -optimality, the six experimental parameters, x_s , y_s , L_p , t_{h1} , t_{12} and t_{h2} were optimized by maximizing the determinant D^+ of the dimensionless $\mathbf{X}^T\mathbf{X}$ matrix, which was a 9×9 matrix. Then, using the optimal values found for these parameters, the optimal overall experimental time, t_n , was determined by evaluating the modified determinant D_m^+ . In calculating the coefficients d_{ij}^+ of D^+ [refer to Chapter 3, Eq. (3.23) or Eq. (5.1)], the dimensionless sensitivity coefficients and the term T_{max}^+ were obtained numerically using the control-volume-based finite difference method available in the GACONDUCT.

5.2.1.2 Finite Difference Modeling

In considering thermal properties as temperature dependent, nondimensionalization of the optimization procedure, such as the one performed in Section 5.1.1, was not an easy task, more particularly using a numerical model. Therefore, optimization of the experimental design was performed in dimensional form, which required initial guesses for all unknown thermophysical properties. One can understand that the more complex the estimation problem is, the more iterative the procedure {optimization + estimation} becomes. Table 5.22 displays the values used for the initial estimates. These values were chosen based on the results obtained from the previous study (Section 5.1.2) and on previously reported data on carbon/epoxy composites so that the optimization results could be valuable for similar types of composites having the same dimensions of the sample analyzed here (recall $L_x=3$ mm and $L_y=64$ mm).

Table 5.22 Initial guesses for the parameters to be estimated used in the optimization stage [k in (W/mK), C in (MJ/m³K), and R_c in (10^{-4} m²K/W)].

k_{x25}	k_{x150}	k_{y25}	k_{y150}	C_{25}	C_{75}	C_{110}	C_{150}	R_c
0.5	0.6	2.0	4.0	1.5	1.8	2.0	2.25	1.0

The geometrical discretization is represented in Fig. 5.27. The model included all components of the experimental setup (e.g., including the mold). The two little “holes” on each side of the aluminum plates (Fig. 5. 14) were modeled as air gaps. The resistance between the sample and all aluminum components in contact with it was modeled as four layers of individual thickness 0.1 mm, with thermal conductivity equal to the thickness divided by the estimate for the contact resistance (in the direction perpendicular to the respective layer only) and null thermal capacitance. The thermal capacitance of the heater was

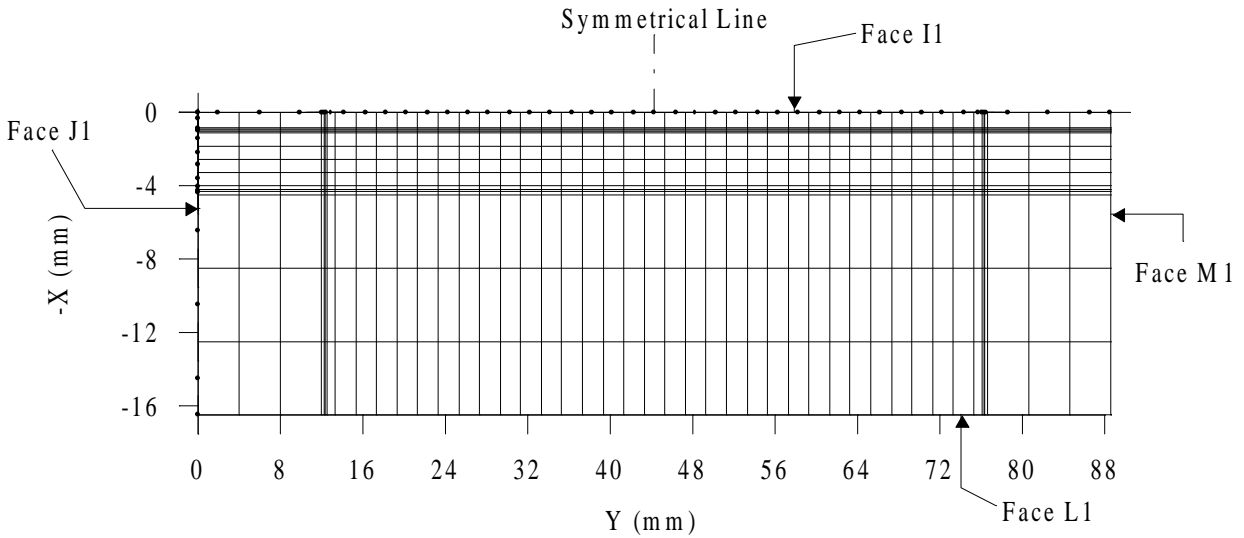


Figure 5.27 Control-volume discretization (grid 15×45 elements) from the complete experimental design (not to scale).

again neglected (due to its very small thickness). The average mesh size inside the composite and the time step were initially selected on the same basis as in the previous study, considering average values for the thermal conductivity ratio and the thermal diffusivity in the x -direction. However, because the computation of the dimensionless (9×9) matrix $\mathbf{X}^T \mathbf{X}$ was excessively time consuming, an important trade-off between numerical accuracy associated with the mesh size in the y -direction and CPU time was realized. A convergence parameter that could not be circumvented was the maximum number of inner iterations, NTIMES , that had to be increased to 40 to account for the dependence on temperature of the thermal properties.

The results from the first run indicated an optimal heating length, L_p , equal to the composite length, L_y . The use of this optimal value for L_p in subsequent runs enabled only half of the experimental design to be modeled, and required a finer mesh size allowing for more confidence in the values for the optimal experimental parameters. Figure 5.28 shows the geometrical discretization associated with the investigation of half of the experimental design. The half-model consisted of 15 and 38 elements in the x - and y -directions, respectively, while the complete model (Fig. 5.27) involved 15 and 45 elements in the same respective directions.

In terms of the optimization of the sensor position and the heating length, it was easier to optimize these experimental parameters in terms of node position than actual location and length, respectively. In doing this, the optimal node i_s, j_s of the sensor was sought, while the

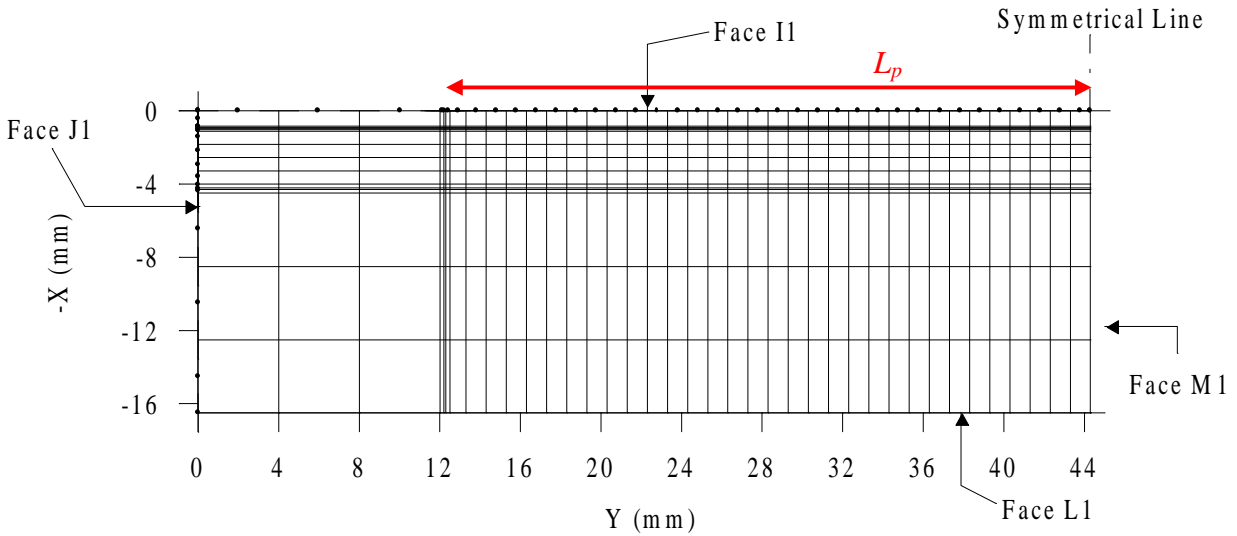


Figure 5.28 Control-volume discretization (grid 15×38 elements) from half-experimental design (not to scale).

optimal position j_p giving the extremity of the heating length on the composite surface ($i=5$) was sought to be optimized. The ranges investigated for these parameters were given by the mesh size; e.g. i fell between 5 and 11, while j fell between 7 and 41 in the complete model and between 7 and 40 in the half-model.

Regarding the power supplied by the heater, its value was selected to provide a maximum temperature reached at steady-state less than 10°C higher than 150°C . Based on this requirement, a value of 28 kW/m^2 was chosen. Note that it was found to take about 150 s to reach steady-state in these conditions. This value was thus used as the heating time limit in the determination of both optimal heating times, t_{h1} and t_{h2} .

One final point worth mentioning deals with the computation of the term T_{max}^+ . In this numerical application, this term was defined to be the maximum temperature increase reached at steady-state in the sample divided by the maximum temperature increase reached at steady-state in the sample if the heat transfer was one-dimensional (allowing application of Fourier's law to the sample thickness and to write $\Delta T_{max,1D} = q_x L_x / k_x$). This definition was found to be in good agreement with the nondimensionalization performed analytically in Section 5.1.1.

5.2.1.3 Results and Discussion

Both optimization and estimation problems were run on a personal computer P400. The Fortran subroutine GA2DLOPT.FOR was written as the adaptation subroutine of the program GACONDUCT to solve these problems, and can be found in Appendix F.

- **Optimization of Experimental Parameters**

Because of the excessive computing cost associated with the 9×9 $\mathbf{X}^T \mathbf{X}$ matrix, the genetic parameters setting relative to the convergence criterion was taken as minimal as possible. The setting applied was similar to the one given in Table 5.18 with the population size (n_s) and maximum allowable number of generations (LASTG) decreased to 50 and 15, respectively. The parameter ranges investigated were the same for the four runs performed and are indicated in Table 5.23 along with the results obtained for the optimal experimental parameter values. Different seeds for the random number generator were however used in each run, thus creating different initial genetic populations. As mentioned earlier, the first run was performed using the complete model shown in Fig. 5.27, while the half-model (Fig. 5.28) was used in the three other runs. Note that the value of D^+ obtained using the complete and half-model cannot be compared since the mesh size was different.

Table 5.23 Optimal experimental parameters for the two-dimensional experiment designed for the simultaneous estimation of the thermal properties as temperature dependent over the range [25-150°C].

	$i_s (=x_s)^a$ [5-11]*	$j_s (=y_s)^a$ [7-41]* [7-40] ^b	$j_p (=L_p)^a$ [7-41]* [7-40] ^b	t_{h1} (s) [0-150]*	t_{12} (s) [0-100]*	t_{h2} (s) [0-150]*	D^+ (10^{+37})	ITERG _r
run 1 complete model	5 (=0)	12 (=8)	41 (= L_y)	109	42	28	1.12	15
run 2 half model	5 (=0)	15 (=7.5)	L_p set to 32 mm	101	41	27	1.09	15
run 3 half model	5 (=0)	15 (=7.5)	L_p set to 32 mm	101	41	27	1.09	12
run 4 half model	5 (=0)	15 (=7.5)	L_p set to 32 mm	101	41	27	1.09	13

* Parameter ranges used to generate the initial population.

^a x_s , y_s and L_p designate dimensions in mm with respect to the composite size.

^b The maximum value for the range of the node position j was 41 and 40 for the complete and half-model, respectively.

Overall, an excellent reproducibility was found in determining the optimal experimental parameters. Note the similarity of the optimal node location with the optimized position found in the study analyzed in Section 5.1.1 ($x_s^+ = 0$, $y_s^+ = 0.14$). Figure 5.29 shows the resulting dimensionless sensitivity coefficients and temperature history from the optimal sensor. One can see that the optimal conditions provide more information for the property k_x than for all other properties. This was expected from the experimental configuration used. Sensitivity to the properties C and k_y is low (less than 0.1), with slightly more information for C than for k_y . Very little information is shown for the contact resistance R_c . Notice that sensitivity coefficients associated with the thermal conductivity parameter values at 25°C present higher slopes when the experiment starts than the coefficients associated with the parameter values at 150°C. This is a logical behavior which is also illustrated in the sensitivity coefficients associated with the different volumetric heat capacity parameters. Among these latter, the coefficient of the parameter value at 75°C has the largest magnitude, as one might expect.

The results for the optimal experimental parameters seem reasonable. However, to verify the goodness of the optimal design, the output from two non-optimal designs defined in Table 5.24 was investigated. Figure 5.30 illustrates the two non-optimal determinants D^+ obtained along with the optimal D^+ . The sensitivity coefficients from the non-optimal design #1 and #2 are shown in Figs. 5.31 and 5.32, respectively. When comparing with Fig. 5.29, one can notice that D -optimization of the experimental design allowed for a global maximization of the sensitivity to all unknown thermophysical parameters.

Table 5.24 Non-optimal experimental designs investigated.

	i_s	j_s	L_p (mm)	t_{h1} (s)	t_{12} (s)	t_{h2} (s)	D^+ (10^{+37})
# 1 half-model	5 (opt.)	15 (opt.)	32 (opt.)	150 (non-opt.)	100 (non-opt.)	150 (non-opt.)	0.046
# 2 half-model	5 (opt.)	15 (opt.)	32 (opt.)	101 (opt.)	0 (non-opt.)	0 (non-opt.)	0.035

Having confidence in the optimized values for the six experimental parameters, the total overall experimental time, t_n , was then determined by evaluating the modified determinant D_m^+ . Figure 5.33 indicates that after a t_n of 435 s, D_m^+ no longer varies, and thus little additional information is being provided for the estimation of the thermophysical parameters (anticipated in Fig. 5.29). Therefore, the experiments can be concluded after this time.

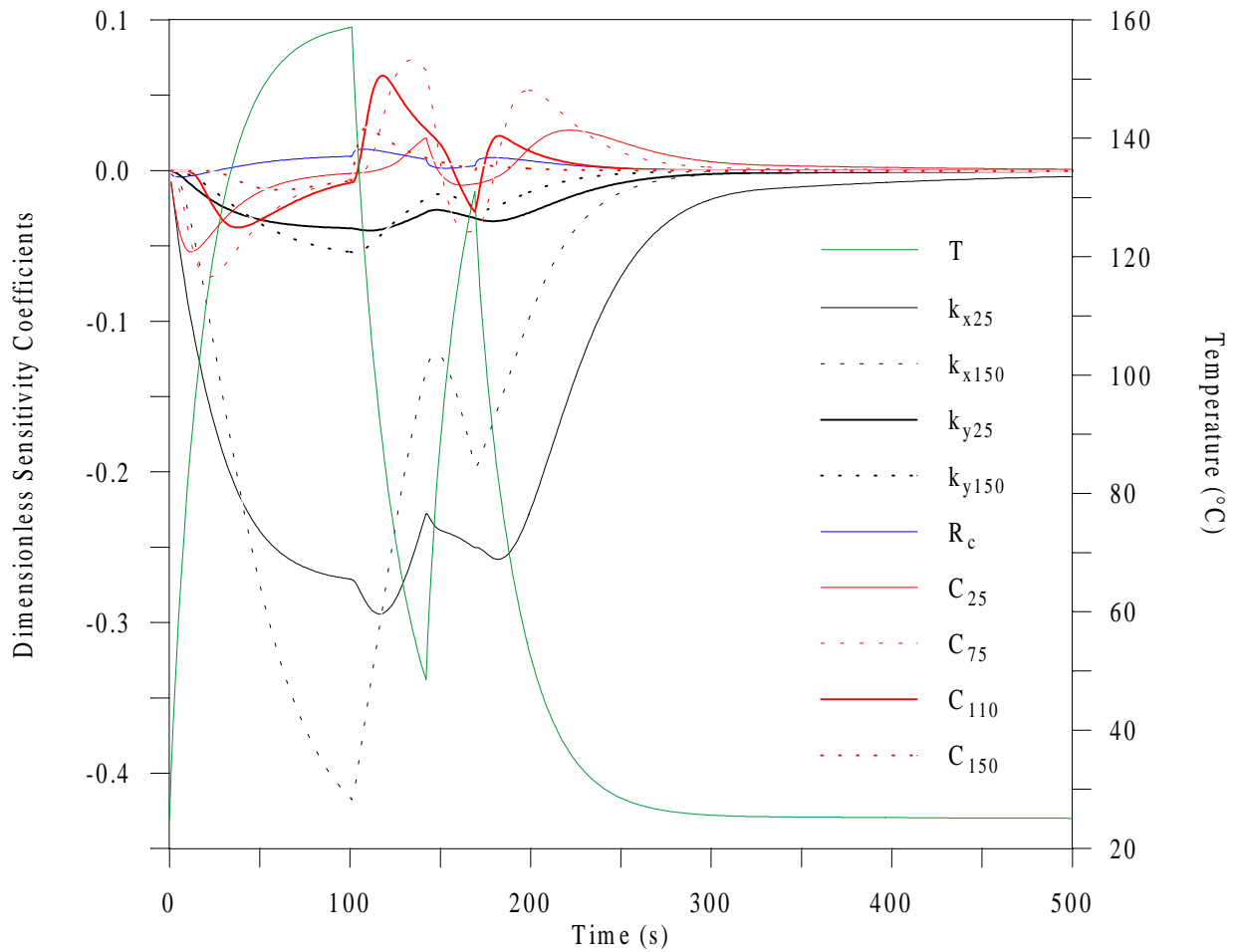


Figure 5.29 Dimensionless sensitivity coefficients and temperature evolution as a function of time from the two-dimensional optimal design for the estimation of temperature-dependent thermal properties.

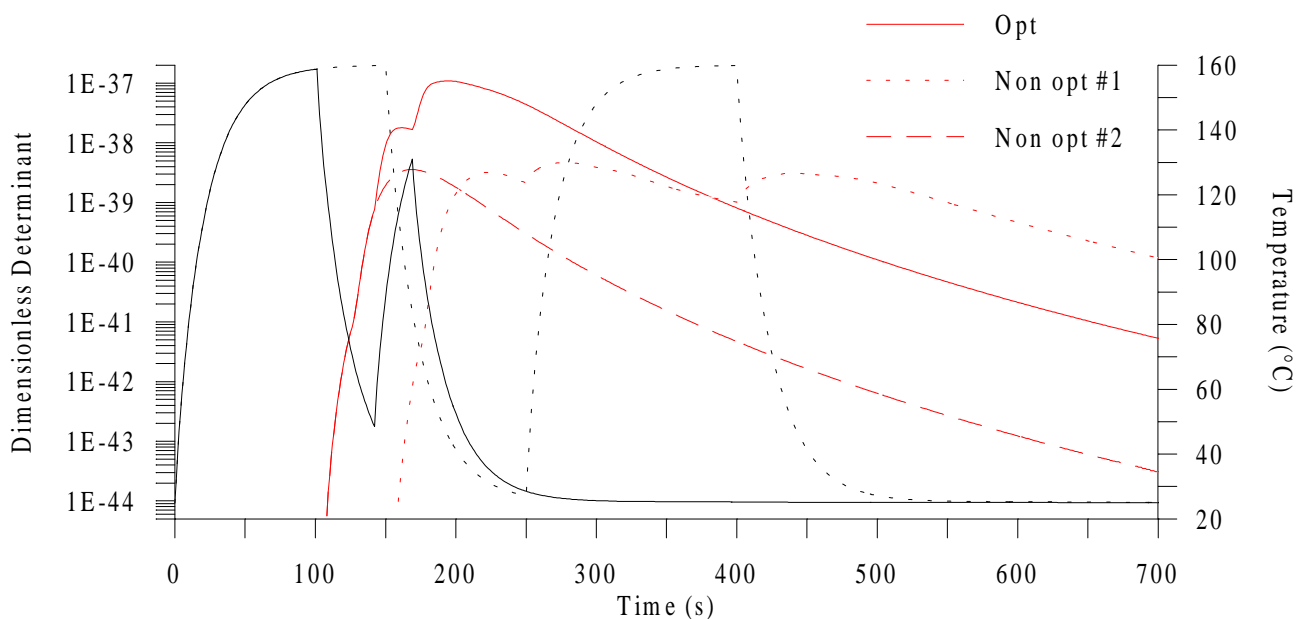


Figure 5.30 Dimensionless determinant and temperature evolution for the optimal and two non-optimal designs.

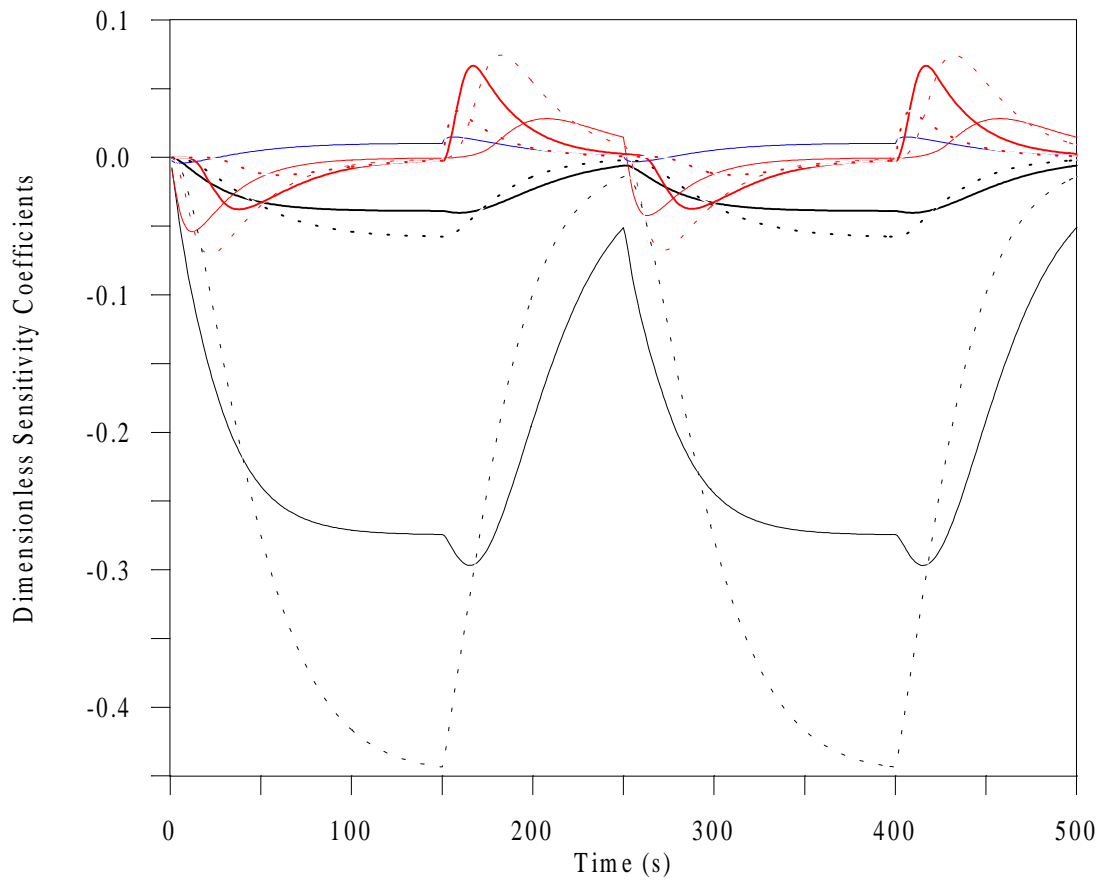


Figure 5.31 Dimensionless sensitivity coefficients from the non-optimal design #1 (same legend as in Fig. 5.32 below).

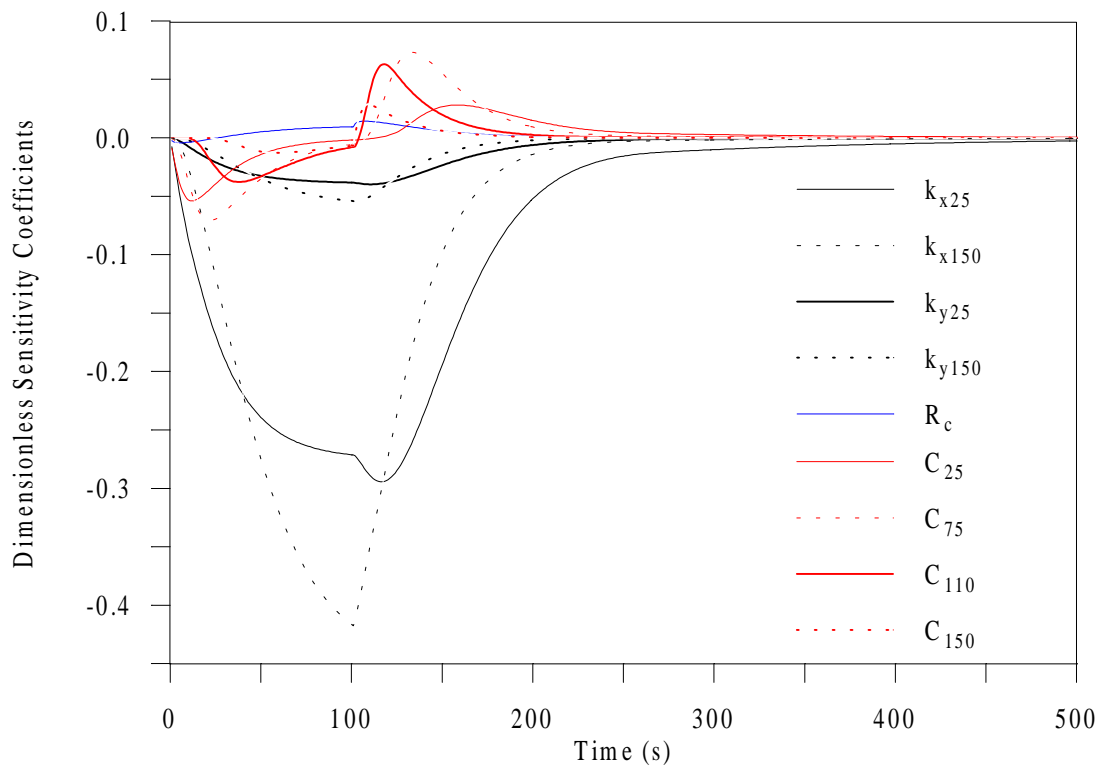


Figure 5.32 Dimensionless sensitivity coefficients from the non-optimal design #2.

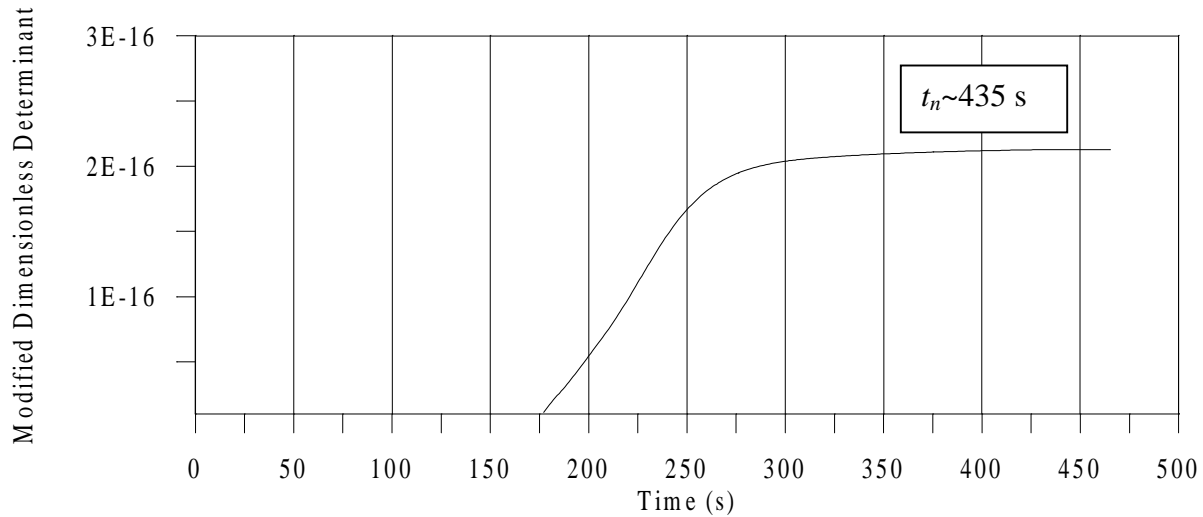


Figure 5.33 Modified dimensionless determinant for the optimal design.

- **Estimation of Properties**

To establish the viability of the optimized experimental design for the simultaneous estimation of the $n_p = 9$ thermophysical parameters, simulated data were utilized as the observation vector in the least-squares error S . These data were generated over the time range 0-450 s by adding some uniformly distributed random errors with a standard deviation 0.1°C to nominal data obtained using the parameter values given in Table 5.24. The overall experimental time value of 450 s was chosen to be a conservative value over the optimal t_n of 435 s. The nominal data were initially used to assess the estimation methodology (common procedure). Then two runs were performed using the data simulated in the time range 0-450 s. A third run was investigated in which data from the time period 130-300 s were used only. This period was chosen to correspond to the interval during which the determinant D is maximized, as one can see from Fig. 5.30. The purpose of this third run was to analyze the effect of restricting to the minimum the experimental data used in the estimation process. Therefore, in the first two runs, 450 data points from the entire time period were used, while in run #3, 170 data point from the time period 130-300 s were employed. Table 5.25 shows the estimates and their 95% CIs [Eq. (3.17)] obtained for these three runs, along with the parameter ranges used to generate the initial population. Note that the minimization of S was not as time intensive as the maximization of D^+ , allowing thus for the use of a population size of 300 (still less than the ideal population size for that problem, which would have been

$100 \times n_p = 900$, as discussed in Section 4.3.3). Different seeds for the random number generator were used in each run.

Table 5.25 Predicted thermophysical parameters, least squares and root mean squares errors, obtained from simulated data using the two-dimensional optimal experiment designed on the temperature range [25-150°C] [k in (W/mK), C in (MJ/m³K), R_c in (10⁻⁴m²K/W), S in (°C)² and RMS in (°C) and (% ΔT_{max})].

	k_{x25} [0.3-0.7]*	k_{x150} [0.3-0.9]*	k_{y25} [1.4-2.5]*	k_{y150} [1.8-6.0]*	C_{25} [1.3-1.8]*	C_{75} [1.5-2.2]*	C_{110} [1.6-2.5]*	C_{150} [1.8-2.6]*	R_c [0.1-10.0]*	S	RMS _i
1^a	0.500 ±0.012	0.615 ±0.013	1.98 ±0.42	3.44 ±0.74	1.53 ±0.02	1.76 ±0.01	2.07 ±0.03	2.26 ±0.05	0.82 ±0.21	6.31	0.118 0.090%
2^a	0.500 ±0.013	0.588 ±0.016	1.93 ±0.49	4.62 ±0.90	1.45 ±0.02	1.85 ±0.01	1.97 ±0.03	2.23 ±0.05	0.94 ±0.19	6.71	0.122 0.092%
3^b	0.499 ±0.011	0.622 ±0.014	1.99 ±0.40	3.29 ±0.67	1.47 ±0.01	1.81 ±0.01	1.93 ±0.02	2.41 ±0.05	1.02 ±0.17	2.18	0.113 0.086%

* Parameter ranges used to generate the initial population.

^a 450 simulated data points from 0-450 s used in the estimation procedure.

^b 170 simulated data points from 130-300 s used in the estimation procedure.

One can see that for the three runs, the results are consistent with the sensitivity coefficient analysis (Fig. 5.29), with the CIs associated with the most variable thermophysical parameters, k_{y25} and k_{y150} , being the largest. One interesting point is that despite the very small sensitivity to the parameter R_c observed in the optimization stage, this parameter is however very well recovered from the GA. The CIs associated with the thermal conductivities k_x and k_y , and with the contact resistance R_c generally consist of the exact data used, but not those associated with the volumetric heat capacity. The approximate formula taken from linear OLS estimation [Eq. (3.17)] gives too small CIs around the four C parameter estimates. Finally, one very relevant result here deals with the output from the third run which allows the same overall accuracy as for runs 1 and 2 in which nearly three times more data points were used for the estimation procedure. This result stresses the benefit of the adequate choice of the time period for accurate parameter estimation. Figures 5.34 and 5.35 show the calculated and simulated temperatures along with the resulting residuals for the second and third run, respectively. The small size of the residuals is noted.

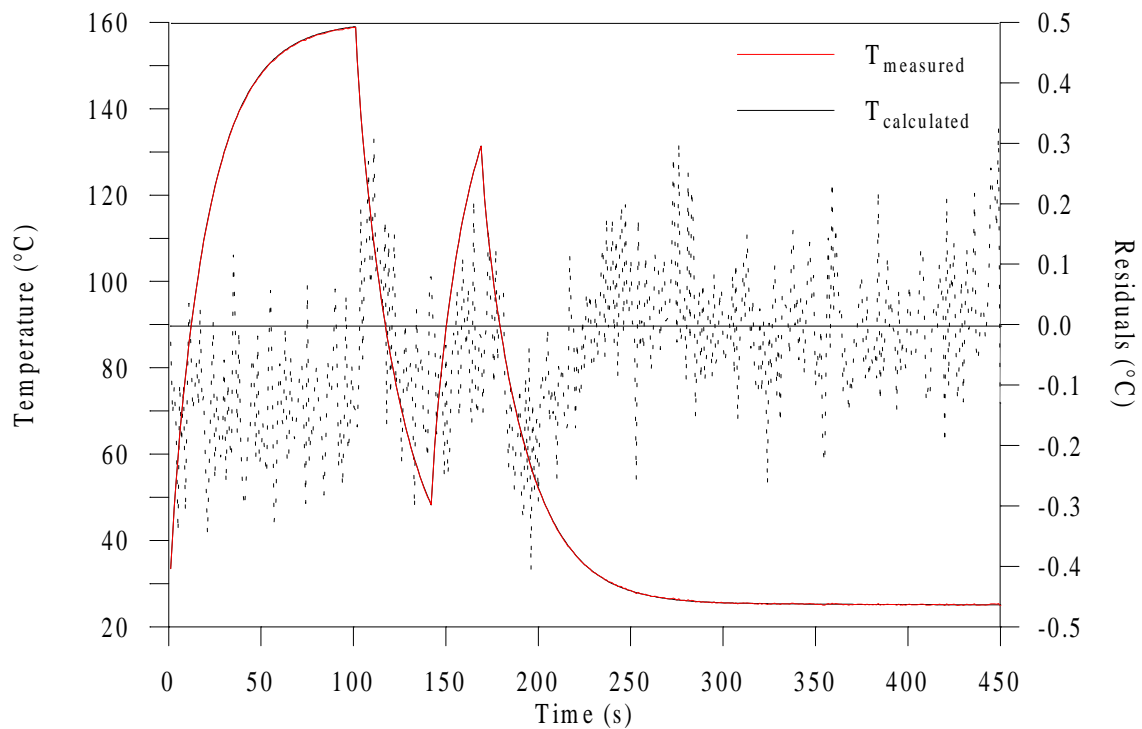


Figure 5.34 Calculated and simulated temperature and residual distributions from run #2 (refer to Table 5.25).

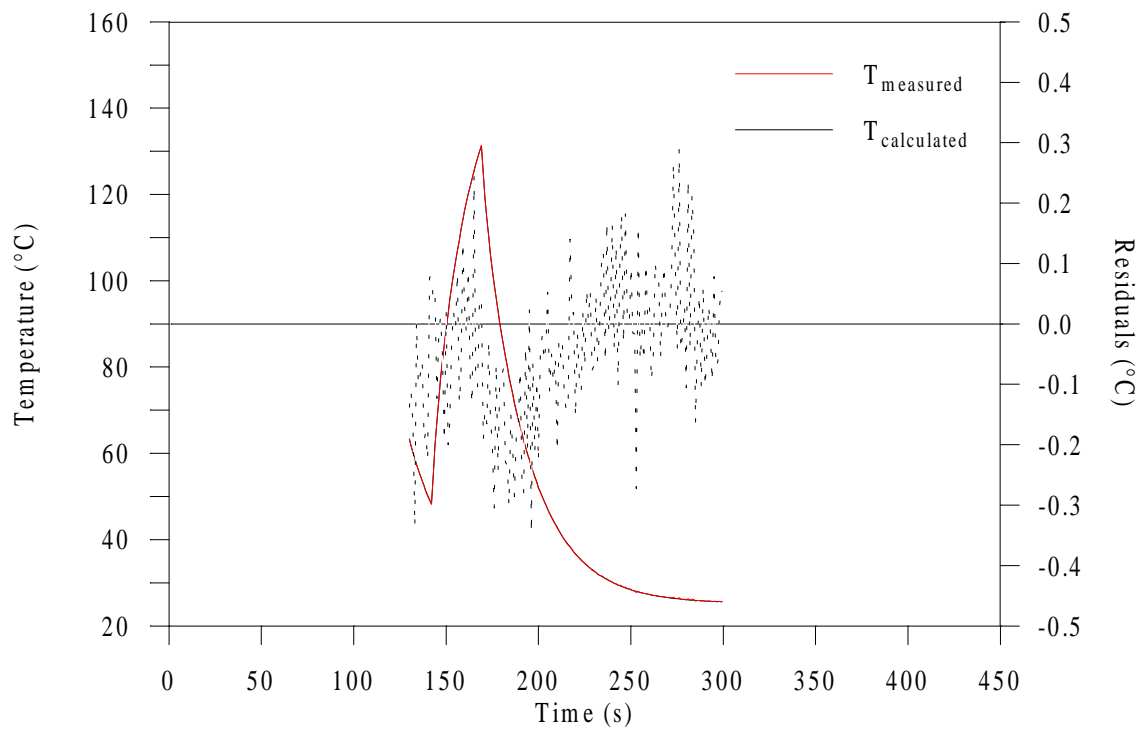


Figure 5.35 Calculated and simulated temperature and residual distributions from run #3 (refer to Table 5.25).

To illustrate the good behavior of the GA-based estimation methodology, Fig. 5.36 displays the minimization of the least-squares error for the second run. Note, however, that for the three runs, the convergence criterion was not satisfied after the 15 generations were performed. This indicates that the estimates for the parameters with low sensitivity would probably need a larger stopping criterion than 1% of their actual value (refer to the description of the convergence criterion used in the GA_3 in Section 4.3.3) and also, that 15 generations were simply not sufficient for this problem which involves the simultaneous estimation of 9 thermophysical parameters.

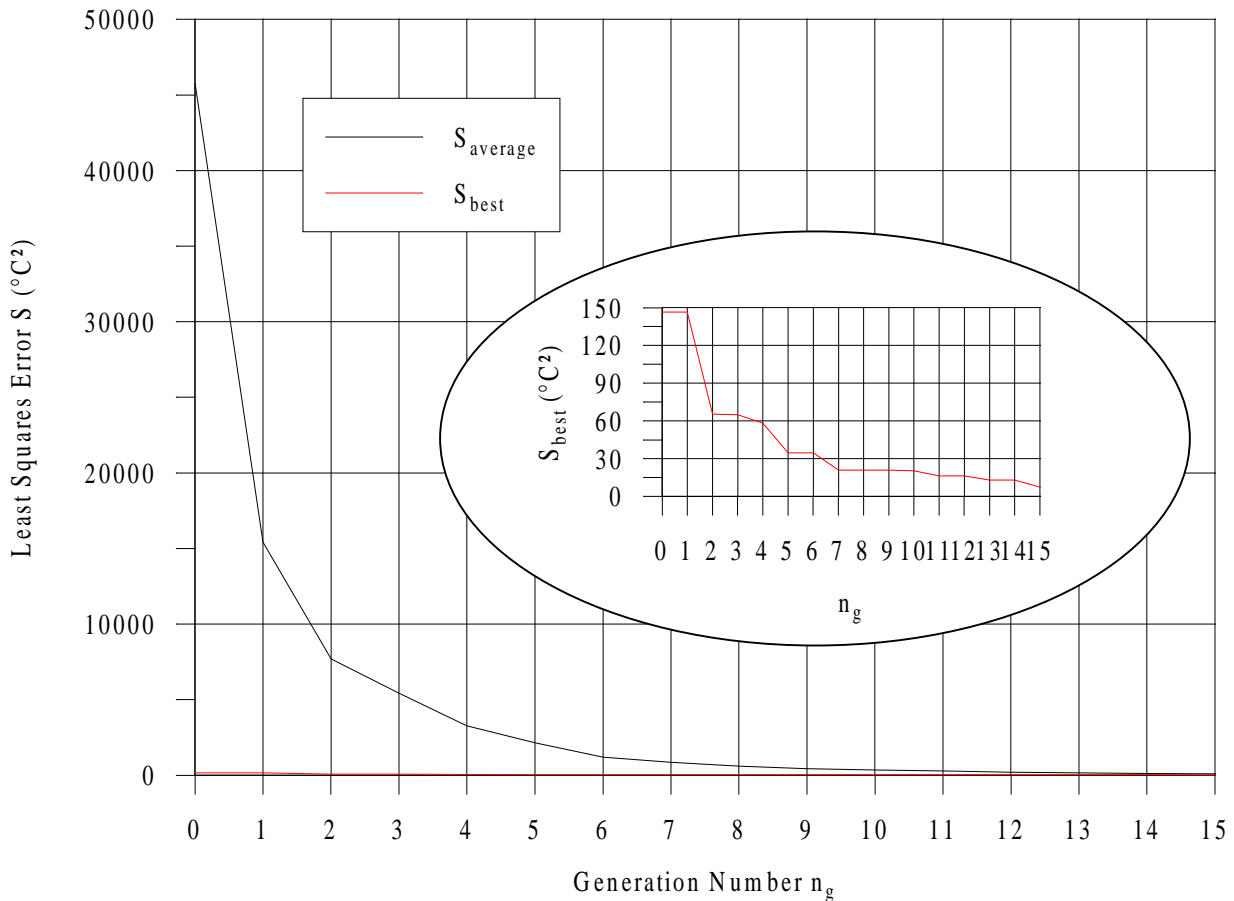


Figure 5.36 Minimization of the least-squares error S from run #2 (refer to Table 5.25).

5.2.1.4 Conclusion

The GA-based optimization methodology has been demonstrated here to be a powerful tool for the optimization of an experimental design to be used for the simultaneous estimation of temperature-dependent thermal properties of an anisotropic composite material. The ability

to optimize such designs is of great importance as their use allows for a drastic decrease in the time spent on both getting experimental data and exploiting those data. In addition, the GA-based estimation methodology has been shown to be valuable for the simultaneous estimation of the nine thermophysical parameters involved. The good results obtained using simulated data give confidence in the capability of GACONDUCT to simultaneously estimate the nine parameters using experimental data. It is however recommended to perform the estimation from several experimental data sets to provide means and associated 95% confidence intervals for the final estimate values.

5.2.2 Two-Dimensional Analysis in RTM Mold Over the Range [100-130°C]

The study presented here was performed in cooperation with D. Lecointe (1999) as part of his PhD project at the LTI. His research work deals with the thermal characterization of composite materials from Resin Transfer Molding (RTM) processing. Here, the application of the GACONDUCT for the simultaneous estimation of the thermal properties (k_x , k_y and C) over the range [100-130°C] along with a contact resistance parameter (R_c) was investigated from a two-dimensional experiment conducted in an RTM mold. The purpose of this complementary study was two-fold. On one hand, it was desired to verify the estimates found by Lecointe who used a parametric study to estimate k_y and R_c assuming both k_x and C to be known. On the other hand, the successful application of the GA-based estimation methodology would definitely establish the use of GAs for complex simultaneous estimation problems.

In the following, the estimation problem is first introduced. Next, the finite difference modeling is described and the experimental data are specified. The results are then shown and compared with those obtained by Lecointe.

5.2.2.1 Problem Description

- **Introduction**

The problem analyzed involves a two-dimensional experimental RTM mold used for the thermal characterization of carbon/epoxy composite materials (Fig. 5.37 discussed later). RTM process consists in the injection of thermosetting resin (epoxy here) inside a closed

mold including a fibrous reinforcement (carbon here). Improvement in productivity and quality of processed composites requires the control of the thermal phenomena and thus, knowledge of the thermal properties. Typically, these latter are determined independently by performing separate and successive analyses. These include the use of:

- Differential Scanning Calorimetry (DSC) to measure the material heat capacity;
 - one-dimensional analysis (Jurkowsky et al., 1997) to measure the thermal conductivity perpendicular to the fiber plane, k_x , using the c_p values obtained from DSC (and the material density) (this step can also be performed from hot guarded plate experiments),
- and finally,
- temperature measurements from an experimental RTM mold instrumented with a set of embedded thermocouples to measure the thermal conductivity parallel to the fiber plane, and other specific heat transfer coefficient such as the contact resistance between the material and a mold component; in this last analysis, the values obtained previously for c_p and k_x are used.

These successive analysis have been performed by Lecoite. For different material configurations including fibrous reinforcements alone and with raw and cured resin, Lecoite determined the thermal conductivities, k_x and k_y , and the contact resistance between the sample and a copper duct inside the mold. Both thermal conductivities were estimated as constants. Note that from the results of the one-dimensional analysis mentioned earlier, Lecoite found that the property k_x could indeed be assumed as constant over the temperature range [100-130°C] which was planned to be investigated in the RTM mold.

The focus of the present study was to use experimental data from the RTM mold with the GACONDUCT to simultaneously estimate all unknown thermophysical parameters, e.g. k_x , k_y , C and R_c . The significance of the capability of solving such an estimation problem is that it would allow for considerable time and cost savings by combining the three analysis reviewed previously into one. Because the objective was not to investigate all material configurations and experimental data analyzed by Lecoite, only one configuration involving a non reticulated composite (e.g. fibrous reinforcement with raw resin) and one data set was considered. The volume fraction of the composite was 60%. Note that this material configuration and the associated experimental data were adequately selected by Lecoite as they had shown to provide him with good results regarding the estimation of k_y and R_c . Therefore, the comparison with the results from the GACONDUCT would allow application of the algorithm to other material configurations and experimental data sets with confidence.

- **Estimation Problem Formulation**

Because the experimental temperatures inside the sample ranged from 100 to 130°C, the dependence on temperature for the properties k_y and C was taken into account. The property k_x was assumed as constant since Lecointe showed that this assumption was appropriate, as discussed earlier. The contact resistance between the sample and the copper duct inside the mold was also considered as constant. The dependence on temperature was characterized using two and three parameters for k_y and C , respectively. These properties were thus expressed by:

$$k_y(T) = k_{y100} + (k_{y130} - k_{y100}) \frac{T - 100}{30}, \quad T \geq 100^\circ\text{C} \quad (5.20)$$

$$C(T) = C_{100} + (C_{115} - C_{100}) \frac{T - 100}{15}, \quad 100 \leq T \leq 115^\circ\text{C} \quad (5.21)$$

$$C(T) = C_{115} + (C_{130} - C_{115}) \frac{T - 115}{15}, \quad T > 115^\circ\text{C} \quad (5.22)$$

Seven thermophysical parameters (k_x , k_{y100} , k_{y130} , C_{100} , C_{115} , C_{130} and R_c) were therefore to be simultaneously estimated. The estimation procedure was based on the minimization of the least-squares error, S , over the same experimental data used by Lecointe when estimating k_y and R_c . Data from 4 thermocouples were involved, which gave for the mathematical expression of S :

$$S(\boldsymbol{\beta}) = \sum_{k=1}^4 \sum_{i=1}^{N_i} [T_{ik}(\boldsymbol{\beta}, \tilde{t}) - \tilde{T}_{ik}]^2 \quad (5.23)$$

5.2.2.2 Experimental Design and Data

With an aim to accurately estimating the property k_y , the experimental mold was designed to emphasize heat transfer in the composite in the direction parallel to the fiber plane. The sample was subject to cooling from 130°C to approximately 100°C. In the following, only a brief description of both the experimental mold and methods used, and the boundary conditions applied, is provided. More in-depth details can be found in the dissertation work of Lecointe (1999).

The experimental mold represented Fig. 5.37 was symmetrical with respect to the x -axis. The mold was made of teflon (PTFE) and was coated with an aluminum thermal guard to favor initial isothermal conditions. The necessary components for RTM injection were included in the mold, namely ducts for the resin input and exit as well as a seal. The temperature gradient was generated from circulation of oil through a copper duct. The fluid was thermally regulated at 80°C using a “Lauda” type apparatus. Therefore, on the contrary to the three previous estimation studies, no heat flux measurements were used here. The composite sample to characterize consisted of two (nearly) identical 5 mm-thick and 60 mm-long planar and rectangular reinforcing phases (carbon fibers). The top center of one of the reinforcing phase was instrumented with five type K thermocouples of diameter $80\ \mu\text{m}$. The thermocouples (TC_1 to TC_5) were placed approximately equally apart in the direction of heat transfer, as shown in Fig. 5.38. An additional thermocouple (TC_0) was located underneath the copper duct. Once the mold was assembled, it was placed between the two heating plates of the experimental press ALIS (described in Section 5.1.2.2) and insulation material (Kerlane) was wrapped around the sides to minimize thermal losses. The use of ALIS enabled, on one hand, the RTM mold to be put under pressure and thus ensured the mold to be closed and, on the other hand, the bottom and top surfaces of the mold to be set to the temperature of 130°C specified by the thermally regulated plates. The complete setup was equipped with a vacuum pump required for RTM injection.

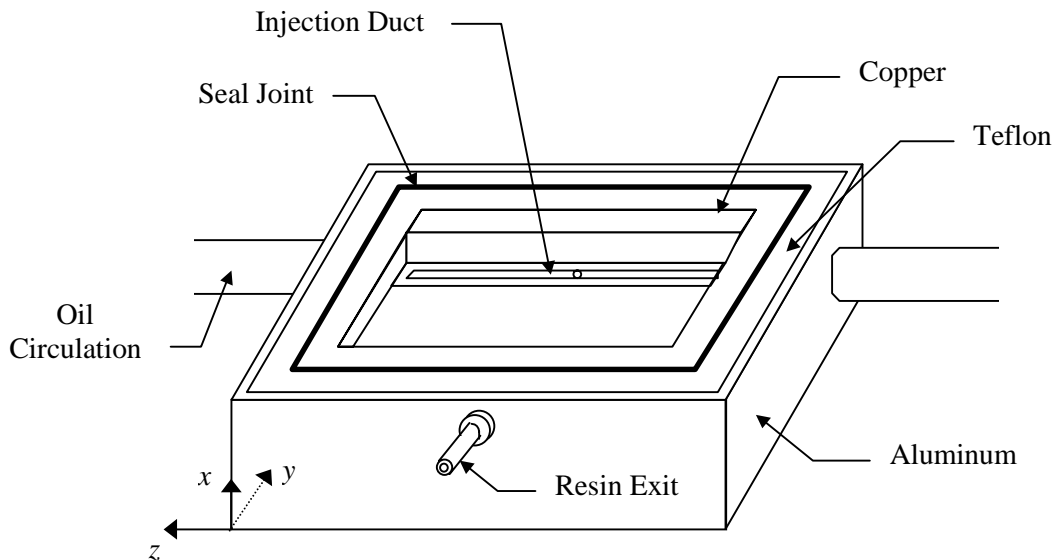


Figure 5.37 Experimental RTM mold.

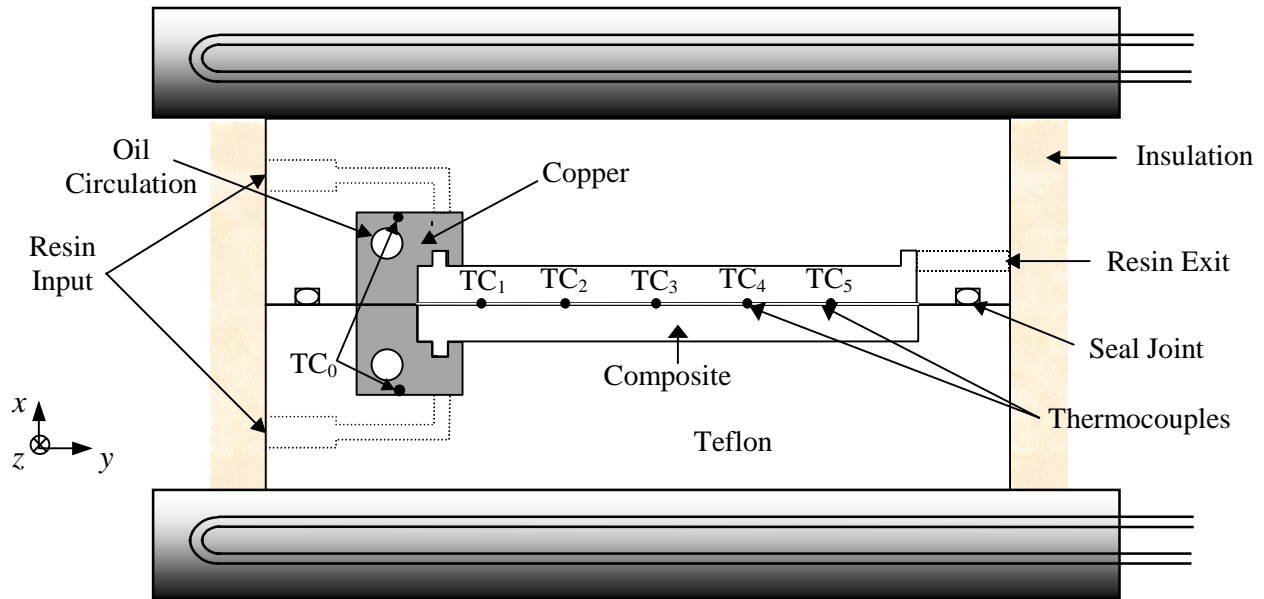


Figure 5.38 Detailed view of the x -symmetrical RTM mold placed between both plates of the experimental press ALIS.

A preliminary numerical study was performed by Lecointe using thermophysical parameters values reported in the literature for the mold components. This study first allowed him determination of the time period during which a two-dimensional analysis was adequate (over a three-dimensional model). Based on this, a total overall experimental time of 500 s was chosen. Then, by comparing the numerical and experimental temperatures obtained on the mold sides (y -direction) before the experiment started, two convective heat transfer coefficients, h_1 and h_2 , were defined to account for the small heat losses observed, as sketched in Fig. 5.39. Finally, the coefficient h_f , was determined to account for the convective heat transfer between the copper duct and the fluid inside (oil). The value for this coefficient was approximated by also comparing numerical and experimental temperatures from the thermocouple TC₀ during cooling. The results from this preliminary numerical study are summarized in Table 5.26.

Table 5.26 Results of the preliminary numerical analysis.

t_n (s)	h_1 (W/m ² K)	h_2 (W/m ² K)	h_f (W/m ² K)
500	1	0.2	3000

The initial temperature field inside the mold was found to be considerably nonhomogeneous. ($\Delta T_x > 5^\circ\text{C}$ while $\Delta T_y \sim 1^\circ\text{C}$). Therefore, in order to best retrieve the initial

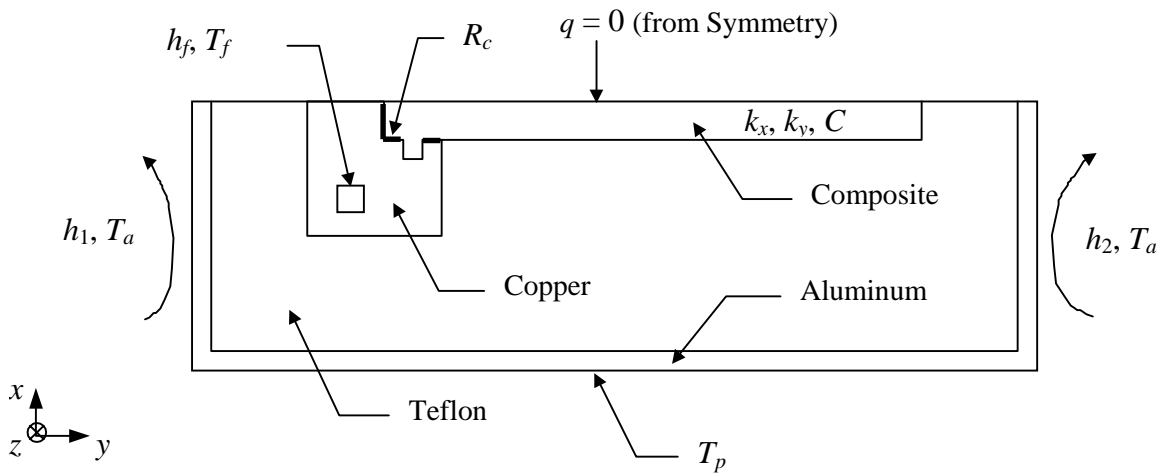


Figure 5.39 Two-dimensional boundary conditions associated with the RTM mold analysis (T_a , T_f and T_p are the ambient, oil fluid and ALIS plate temperatures, respectively).

state, measurements from the thermocouples TC_1 to TC_5 before the experiment started, were used to specify the top boundary condition. In doing this, the temperature on this boundary was defined using a linear functional in the y -position. The same conditions were kept for the other boundaries. The steady-state reached from these conditions was taken as the initial state.

The temperature histories from thermocouples TC_1 to TC_4 were used in the estimation procedure. Lecoite used a numerical method based on finite differences (with the nodes located at the mesh interfaces) to generate the required calculated histories. In using GACONDUCT, however, the discretization equations are solved following a control-volume technique in which the node temperatures prevail over the entire control volumes. Therefore, in this study, the same numerical modeling as the one from Lecoite could not be used. However, nearly the same mesh size and the same time step were applied. This is developed next.

5.2.2.3 Finite Difference Modeling

The geometrical discretization is represented in Fig. 5.40. The contact resistance was modeled on the same basis as in previous studies (Sections 5.1.2 and 5.2.1). Here, three layers of thickness 0.5 mm were defined, with thermal conductivity equal to the thickness divided by the estimate for the contact resistance (in the direction perpendicular to the respective layer only) and null thermal capacitance. The convective heat flux inside the copper component

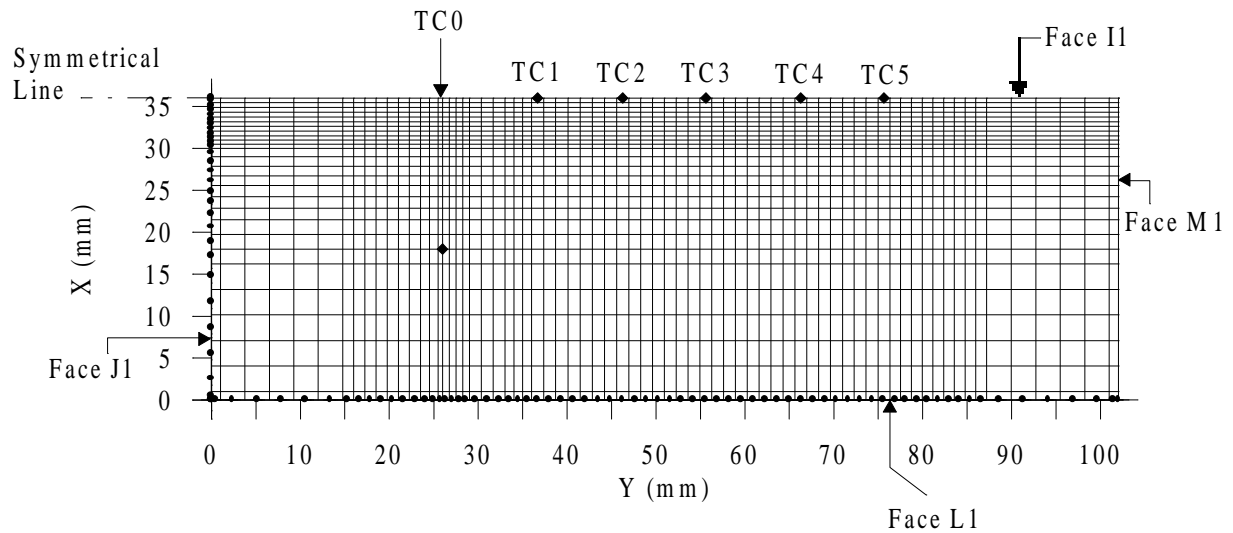


Figure 5.40 Control-volume discretization (grid 27×71 elements) from half-RTM mold (not to scale).

was set into the near-boundary-control volumes via the source terms (Patankar, 1991). The conductivity and thermal capacitance inside the duct were both set to zero. Eventually, the resin injection duct was considered to be full of raw resin (for the particular non reticulated material configuration studied here). The grid included 27 and 71 elements in the x - and y -directions, respectively, while Lecoite used 26 and 68 elements in the same directions. The mesh size and time step ($\Delta t = 0.1$ s) were verified to be adequate for numerical accuracy.

5.2.2.4 Results and Discussion

Two estimation runs with different seeds for the random number generator were performed using a personal computer P233. The genetic parameters setting relative to the convergence criterion was the same as given in Table 5.18, but with a population size of 100. Here again, the investigation of the time-consuming two-dimensional numerical model did not allow for the use of the ideal population size, which would be 700 for seven parameters to be simultaneously estimated. The Fortran subroutine GA2DRTM.FOR was written as the adaptation subroutine of the program GACONDUCT to solve this problem and is provided in Appendix G.

Table 5.27 shows the predicted estimates and their 95% CIs [Eq. (3.17)] from both two genetic runs and the parametric study from Lecoite. Recall that Lecoite identified k_y and R_c assuming k_x and C to be known. Both GA runs were converged before the maximum number

of generations was reached. First of all, notice the adequacy between the thermophysical parameter values predicted by the GA runs and those predicted by Lecointe. Both GA runs gave (nearly) the same estimates. A difference between the GA and parametric study results can be observed in the contact resistance. This difference may be the output from both estimating the property k_y as temperature-dependent and obtaining slightly different volumetric capacity estimates with the GA CONDUCT. Note, however, that the confidence intervals of the predicted C (nearly) consist of the C values used by Lecointe. The temperature-dependence of the predicted C is shown in Fig. 5.41. One can see that the predicted linear regressions approximate the theoretical C relatively closely. The theoretical C was obtained applying the Rule-of-Mixtures [see Eq. (2.1)] with DSC results.

Table 5.27 Predicted thermophysical parameters obtained from experimental data from a non reticulated carbon/epoxy sample in an RTM mold [k in (W/mK), C in (MJ/m³K), R_c in (10⁻³m²K/W), S in (°C)² and RMS in (°C) and (% ΔT_{max})].

	k_x	k_{y100}	k_{y130}	C_{100}	C_{115}	C_{130}	R_c	S	RMS
Run1	0.596 ±0.06	3.39 ±0.18	3.88 ±0.11	2.068 ±0.12	2.130 ±0.09	2.274 ±0.07	1.40 ±0.25	37.6	0.274 0.86%
Run2	0.594 ±0.06	3.34 ±0.17	3.91 ±0.11	2.060 ±0.11	2.122 ±0.09	2.276 ±0.07	1.36 ±0.26	36.3	0.269 0.84%
L (1999)	0.6 ^a	3.4 ±0.06		2.143 ^b	2.220 ^b	2.278 ^b	3.40 ±0.04	105.8	0.460 1.44%

^a obtained from a one-dimensional analysis (Jurkowsky et al., 1997).

^b obtained from applying the Rule-of-Mixtures [Eq. (2.1)] with DSC results.

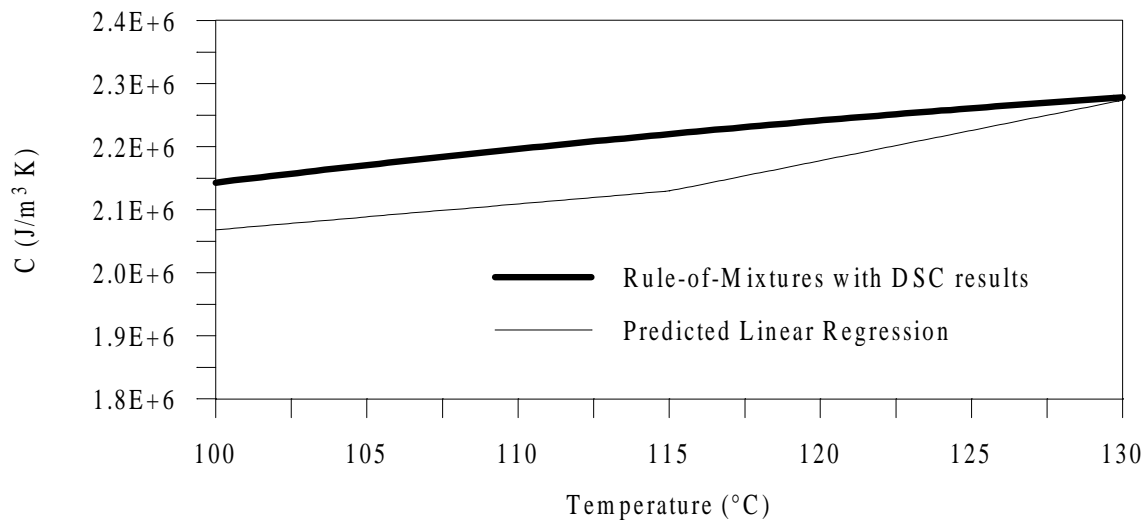


Figure 5.41 Predicted linear regressions for the volumetric heat capacity, C , over the range [100-130°C].

The property k_y was found to increase 14.5% from 100 to 130°C. This is similar as the increase found from 100 to 125°C using the linear regression obtained for the reticulated carbon/epoxy material analyzed in Section 5.1.2. Note that, even though the material considered here was not reticulated, the evolution with temperature of the thermal conductivity parallel to the fibers can be compared with the results for a reticulated material (provided there are both carbon/epoxy composite type), because the value of the property k_y depends mainly on the fiber type. This result gives confidence in the predicted parameters obtained here for k_y .

One important result is that the *RMS* errors for the two GA runs are about half the *RMS* error obtained using the parametric study. The use of GACONDUCT allowed for a lower *S* and, thus a better fit of the experimental temperatures. This is illustrated in Fig. 5.42, which shows the measured temperature histories from the thermocouples TC₁ to TC₅ and the corresponding calculated histories obtained using both the estimates and numerical model from Lecointe and those from this study (second run). More particularly, one can observe that the set of thermophysical parameters predicted from the GA method enabled the correct modeling of the experimental temperature history from the thermocouple TC₅, although information from this sensor was not used in the estimation methodology.

The dimensionless sensitivity coefficients of the seven thermophysical parameters are shown in Fig. 5.43 to 5.46 for the thermocouples TC₁ to TC₄, respectively. One can see that the coefficient associated with the parameter k_{y130} presents a higher initial slope than the coefficient associated with k_{y100} . The same comment applies when comparing C_{130} with C_{115} or C_{100} . This is a logical output since the initial state is about 130°C. Another consistent result is that the thermocouple TC₁ (the closer to the cold copper block) is much more sensitive to both parameters k_x and R_c than the thermocouple TC₄ (the further in the *y*-direction from the cold copper block), while the opposite occurs for both parameters of the thermal property k_y . All thermocouples provide information for the parameters of the volumetric capacity. The appreciable overall sensitivity to the property k_y explains the lower confidence intervals (around the estimates k_{y100} and k_{y130}) obtained in this study compared to the results of the studies described in the previous sections. The CIs obtained for all thermophysical parameters seem consistent with the magnitude of the associated sensitivity coefficients.

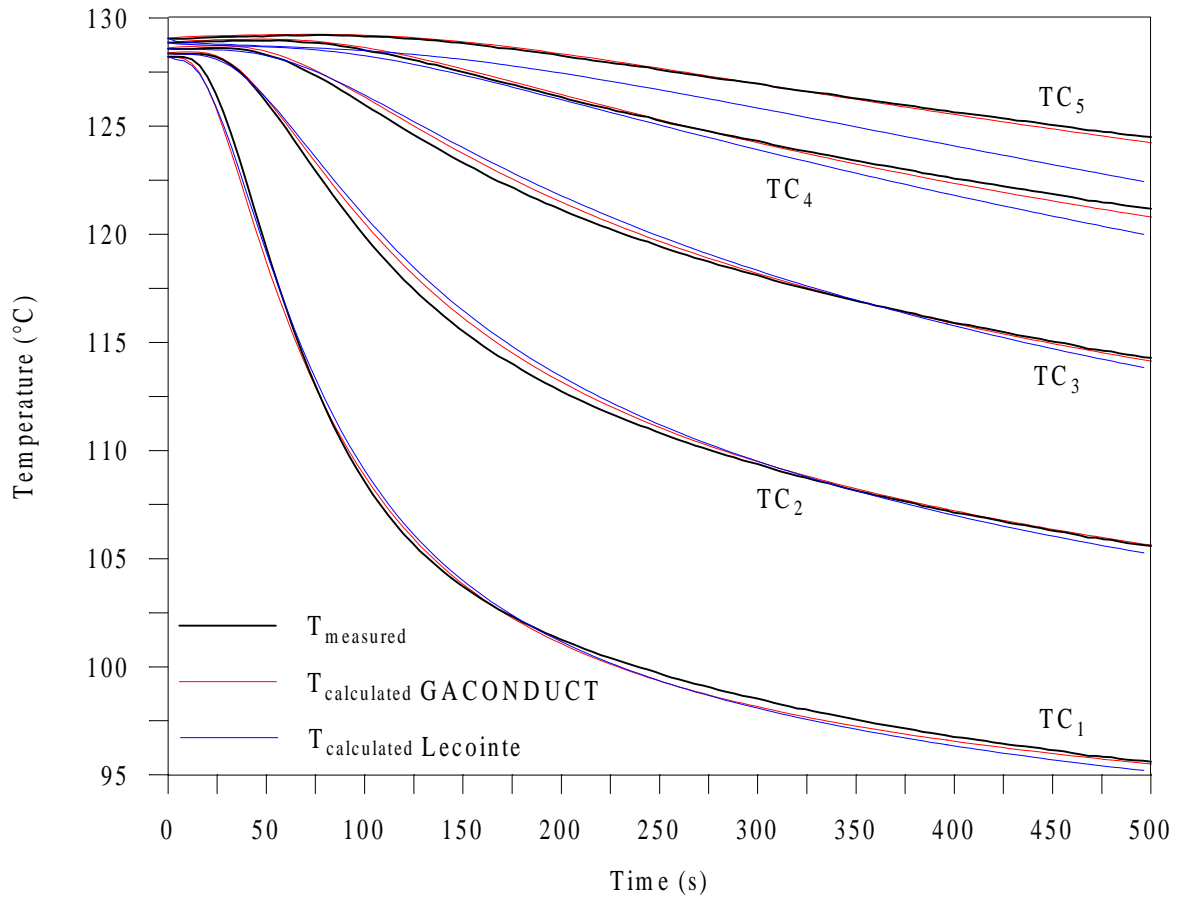


Figure 5.42 Temperature distributions from the five thermocouples embedded in the RTM mold.

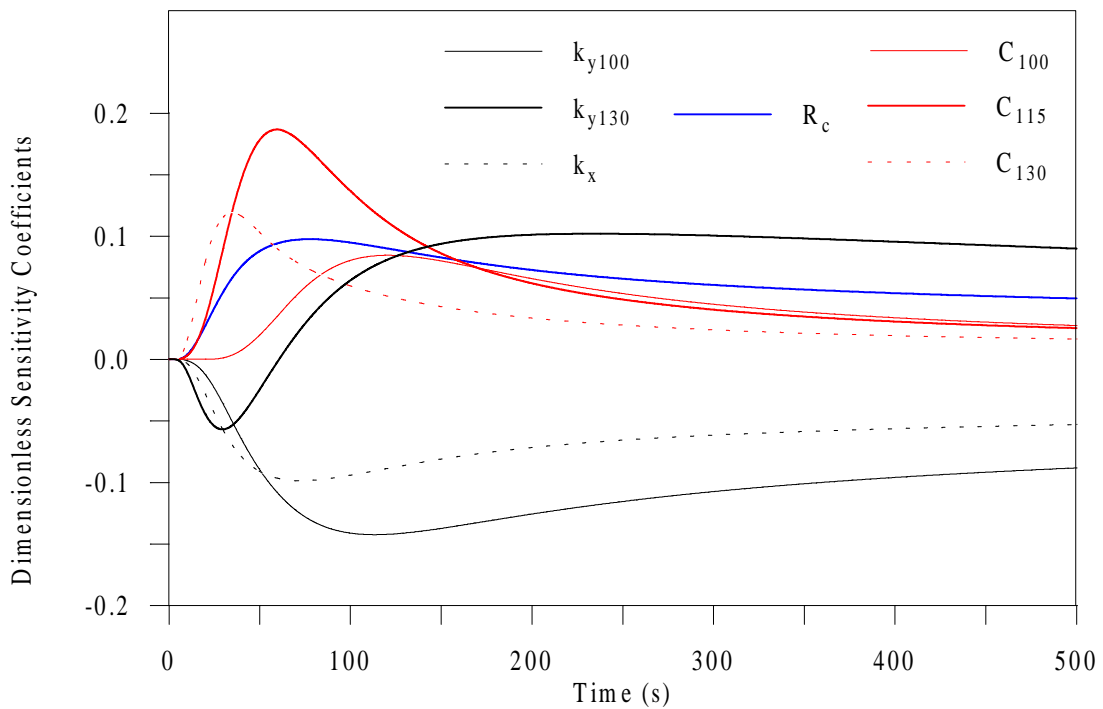


Figure 5.43 Dimensionless sensitivity coefficients from thermocouple TC₁.

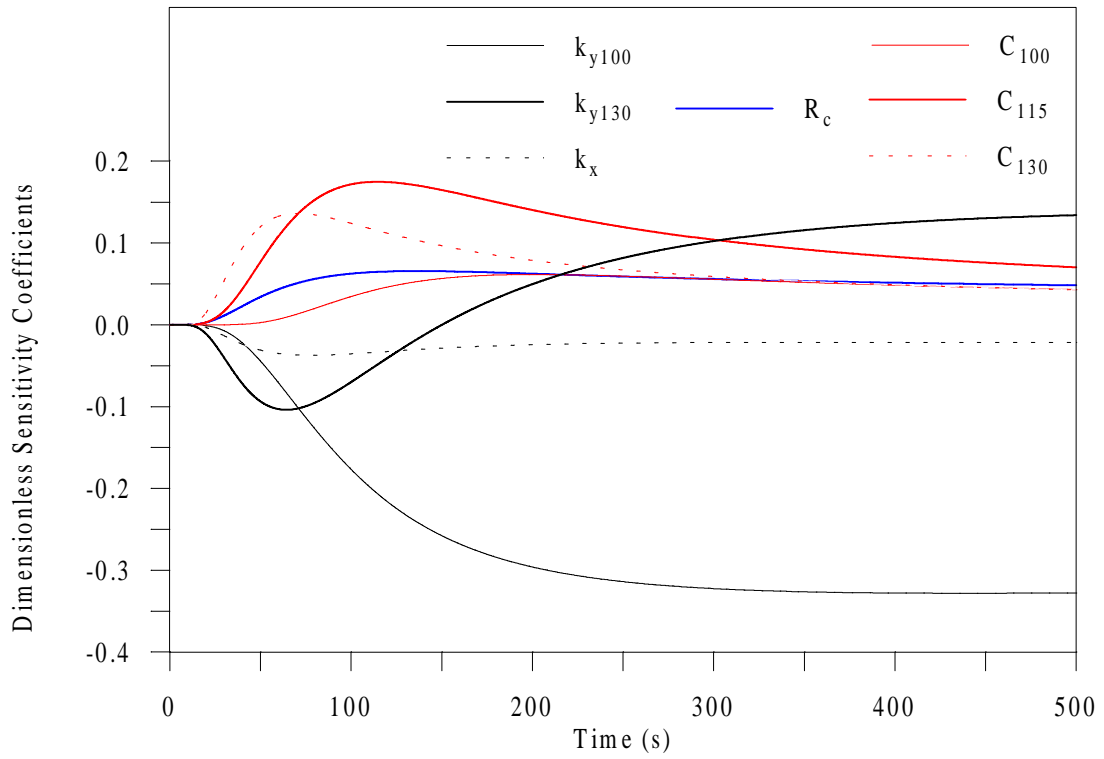


Figure 5.44 Dimensionless sensitivity coefficients from thermocouple TC₂.

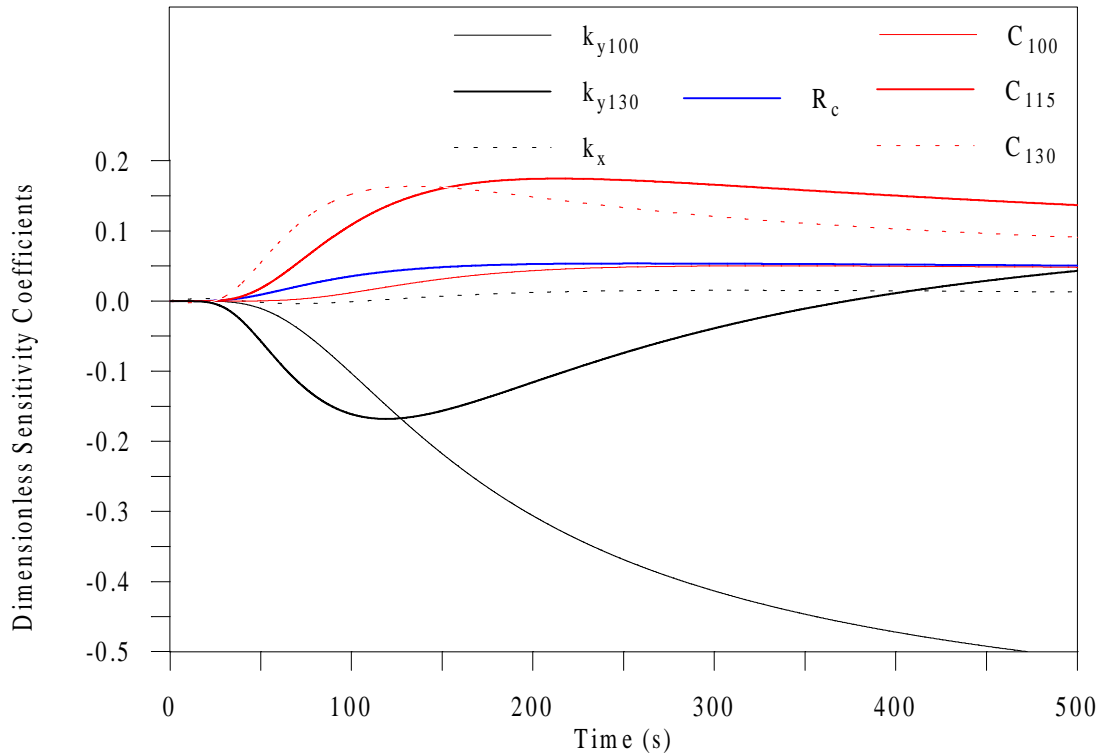


Figure 5.45 Dimensionless sensitivity coefficients from thermocouple TC₃.

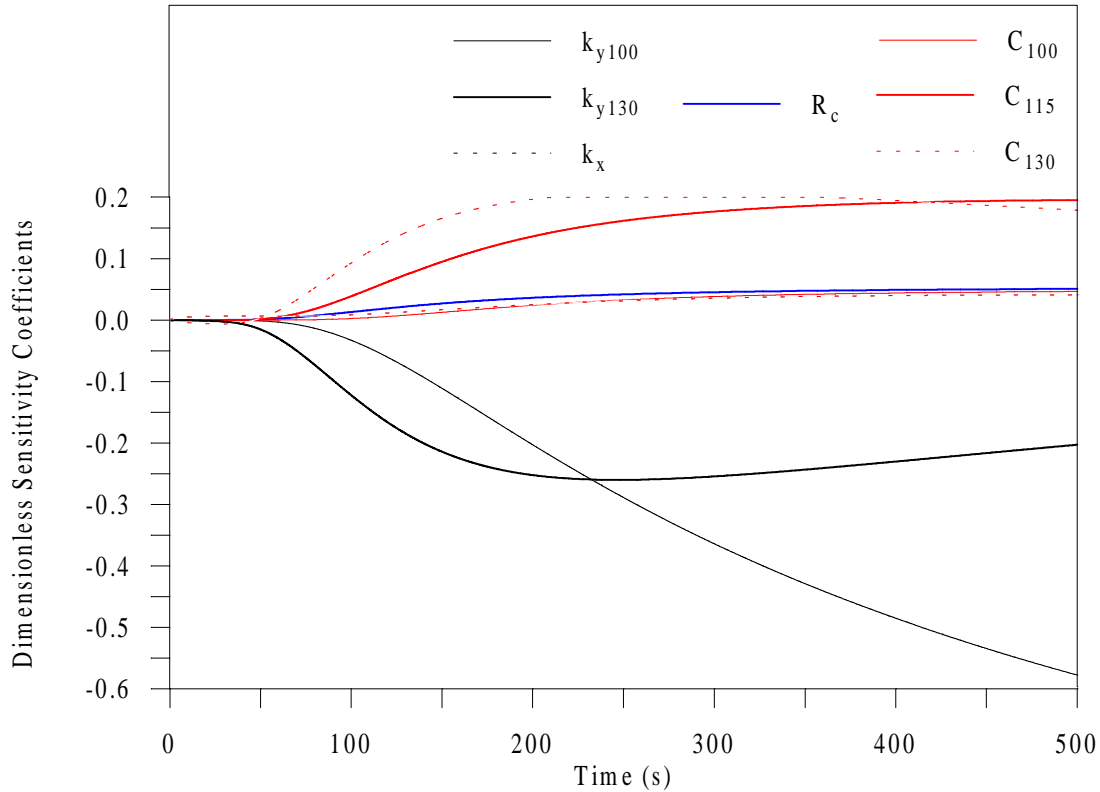


Figure 5.46 Dimensionless sensitivity coefficients from thermocouple TC₄.

Before concluding this section, it should be recalled from theoretical considerations discussed in chapter 3, that the setting of presumably known parameters to nominal values involves a bias in the estimation procedure (this bias being obviously function of the accuracy of the nominal values and the correlation between the known parameters and the unknown ones to be estimated). From the results presented here, one may conclude that the setting of the property k_x and C to known nominal values did generate a small bias on the final estimates, which resulted in a larger least-squares error than if the properties were taken into account in the estimation procedure (refer to Fig. 5.42 and Table 5.27). Note that the restriction of the estimation of the property k_y as a constant can be considered as a form of “nominal value knowledge” and is also thought to have generated bias in the present case.

5.2.2.5 Conclusion

This study allows for the definitive assessment of the use of GAs for the simultaneous estimation of several thermophysical parameters. Both the robustness and reliability of the

GA method have been demonstrated. The tremendous capabilities of GAs are relevant here as their use are associated with considerable experimental and time cost savings. In addition, it has been shown that, by enabling the simultaneous estimation of several parameters, the use of GAs thus allows bias induced by setting presumably known parameters to nominal values to be avoided.

CHAPTER 6

Kinetic Characterization of the Curing of Thermosetting Materials

This chapter is dedicated to presenting the analysis performed for the kinetic characterization of the curing process of composite matrix materials, namely thermosetting resins. The model from Kamal and Sourour (K&S) (1973) was used in the prediction of the curing of an epoxy, a polyester and a rubber mixture. This model involves six kinetic parameters which were simultaneously estimated applying the general-purpose program GAMAIN.

The first section provides an overview of the K&S model and the motivation for studying it. In the following section, the estimation problem is formulated according to three strategies. For the kinetic characterization to be complete, a model for the determination of the inhibition time was constructed based on the model described by Bailleul (1997; also in Bailleul et al., 1996), and is detailed in the third section. Then, the three thermosetting resins investigated and the experimental data obtained from Differential Scanning Calorimetry (DSC) and used in the estimation procedure are described. Finally, the results of the analysis are presented and discussed in the last section.

6.1 Kamal and Sourour (K&S) Model

6.1.1 Description

The model from K&S (1973) is referred to as describing an autocatalyzed reaction rate mechanism. It is a very well known empirical model that allows for the analysis of complex substances. Its mathematical form is:

$$v = \frac{d\alpha}{dt} = (K_1 + K_2 \times \alpha^m)(1 - \alpha)^n \quad (6.1)$$

where v is the cure (reaction) rate, α , the degree of cure and K_1 and K_2 , the two rate constants that represent the catalytic and autocatalytic nature of the cure mechanism, respectively. The order of curing for each mechanism is given by the two exponents m and n . The rate constants depend on absolute temperature from the Arrhenius law, then involving each two Arrhenius parameters A_i and E_i according to:

$$K_i = A_i \exp\left[-\frac{E_i}{RT}\right], \quad i = 1,2 \quad (6.2)$$

The mathematical form of the K&S model can be generalized into $v=F(T,\alpha,\beta)$. The true parameter vector β to be estimated here involves the six parameters (A_1 , E_1 , A_2 , E_2 , m and n) inherent to the K&S model.

6.1.2 Motivation for Using the K&S Model

A question then comes: why use the K&S model for the kinetic study of thermoset resins while some of these materials have been shown to either be well characterized with a simpler model (Bailleul, 1993 and 1997; Amiaud, 1993; and Mouchnino, 1997) or follow a three phase law (Garnier, 1990)? The following outlines the two main points that have provided the motivation for studying this model.

- Its simplicity and its intensive use in kinetic analysis of the curing of thermosetting materials. This model is generally the one available in software packages that simulate the coupling between exothermal effects from autocatalyzed curing and conduction heat transfer within the material. Recall that such simulation is necessary to control the thermal phenomena during composite fabrication processes.
- There is no knowledge in the literature of methods capable of solving the simultaneous estimation of the six K&S parameters without setting assumptions regarding the parameters m and n . Therefore, the study of the K&S model is an excellent test of robustness for the GA-based estimation methodology developed in this work.

6.2 K&S Estimation Problem Formulation

The estimation methodology implemented in the GAMAIN program is based on Ordinary Least-Squares (OLS). The objective function is the sum-of-squares function simply defined by the error between experimental and calculated data, as introduced in Chapter 3.

Differential Scanning Calorimetry (DSC) data are to be used in the kinetic analysis. Because the rate of heat generation is measured directly in DSC experiments, one can logically think of using cure rate information in the estimation procedure. Two strategies (I and II) were then considered for the computation of v :

- In Strategy I, illustrated in Fig. 6.1, it is assumed that the degree of cure and temperature are known at each observation and Eq. (6.1) is used to directly compute the cure rate.
- The cure rate is calculated in two steps in Strategy II, assuming time and temperature to be the known data; first, the degree of cure is determined [using a numerical procedure to solve the first order differential equation given by Eq. (6.1); this is discussed later] and then, its value is used in Eq. (6.1) to find the cure rate. Figure 6.2 displays a schematic of Strategy II (see Fig. 3.1 as a reference).

Considering the cure rate, v , as the measured quantity, two estimation Strategies, I and II, were thus investigated for the identification of the true parameter vector $\boldsymbol{\beta}$. The mathematical expressions for the two objective functions S_1 and S_2 associated with Strategy I and II, respectively, are for N_i measurements and N_j experiments:

$$S_1(\boldsymbol{\beta}) = \sum_{i=1}^{N_i} \sum_{j=1}^{N_j} \left[v_{ij}(\boldsymbol{\beta}, \tilde{\alpha}_{ij}, \tilde{T}_{ij}) - \tilde{v}_{ij} \right]^2 \quad (6.3)$$

$$S_2(\boldsymbol{\beta}) = \sum_{i=1}^{N_i} \sum_{j=1}^{N_j} \left[v_{ij}(\boldsymbol{\beta}, \tilde{t}_{ij}, \tilde{T}_{ij}) - \tilde{v}_{ij} \right]^2 \quad (6.4)$$

Furthermore, a third estimation strategy, Strategy III, was analyzed assuming that the measured quantity is now the degree of cure α . The determination of α is similar to the first step of Strategy II. The schematics of this strategy is provided in Fig. 6.3. This third strategy was defined after the work from Scott and Saad (1993) who indicated that in their study, the degree of cure provided more information than the cure rate. The mathematical expression for the objective function S_3 associated with estimation Strategy III is:

$$S_3(\boldsymbol{\beta}) = \sum_{i=1}^{N_i} \sum_{j=1}^{N_j} \left[\alpha_{ij}(\boldsymbol{\beta}, \tilde{t}_{ij}, \tilde{T}_{ij}) - \tilde{\alpha}_{ij} \right]^2 \quad (6.5)$$

To perform the three estimation strategies, one therefore needs the set $\{\tilde{t}_{ij}, \tilde{\alpha}_{ij}, \tilde{v}_{ij}, \tilde{T}_{ij}\}$ of experimental data where t is time, $i=1, \dots, N_i$ measurements, and $j=1, \dots, N_j$ experiments. These data can be either isothermal or dynamic.

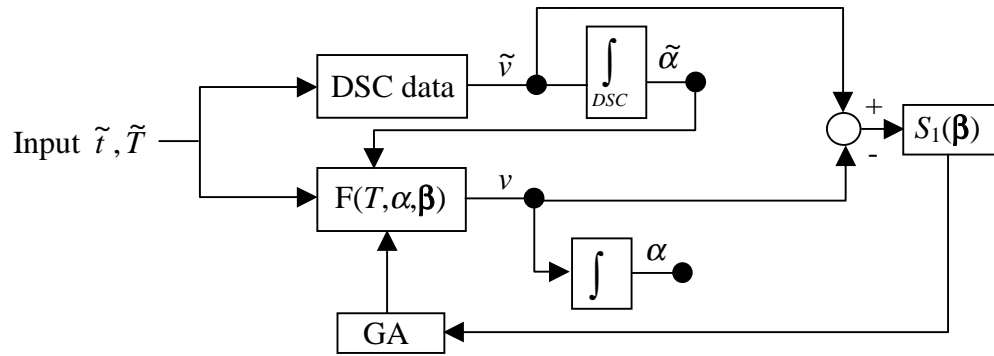


Figure 6.1 Schematic of estimation Strategy I.

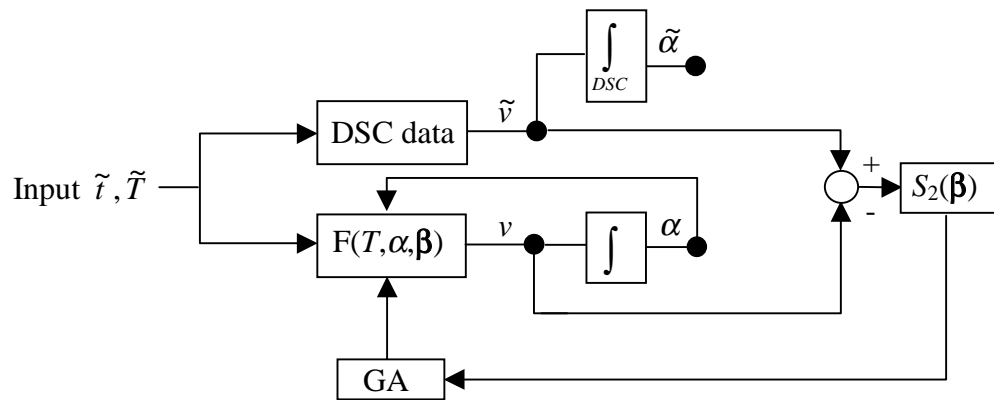


Figure 6.2 Schematic of estimation Strategy II.

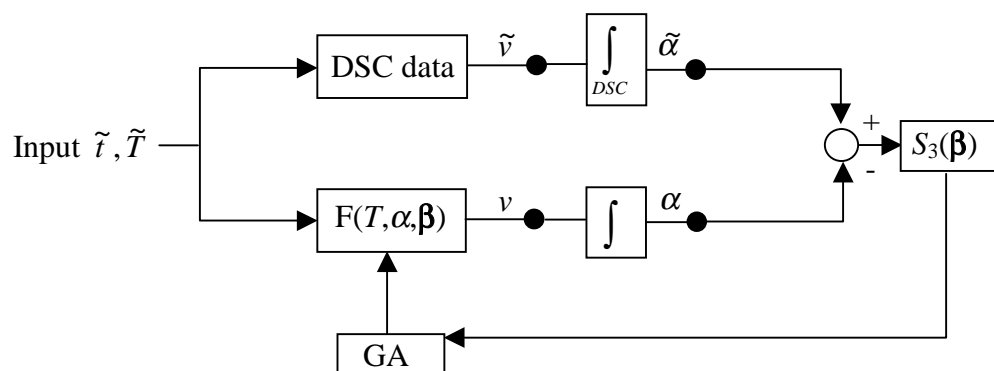


Figure 6.3 Schematic of estimation Strategy III.

As mentioned previously, the computation of the degree of cure α requires the use of a numerical method to solve a first order differential equation assuming time and temperature are given. Two schemes were initially investigated and included a second-order Runge-Kunta analysis and a Crank-Nicholson technique. In short, to determine a solution at the iteration $i+1$, the q^{th} order Runge Kutta method is based on the evaluation of a function q times between the successive time iterations t^i and t^{i+1} . In the Crank-Nicholson scheme, a central finite-difference analysis is realized. Both schemes requires an initial value for the degree of cure. The detailed mathematical foundation and the Fortran coding translation for both procedures can be found in Numerical Recipes (Press et al., 1990). These schemes were selected because they provide good compromise between accuracy and convergence speed. They both gave similar convergent results on simulated data. Because of its ability to converge a little faster, the second-order Runge Kunta technique was retained and subsequently applied. Note that the work of Sommier (1998) also advised for the use of this scheme.

Analytical expressions were obtained for the sensitivity coefficients of the parameters associated with estimation Strategy I by differentiating Eq. (6.1) with respect to each kinetic parameter. The resulting equations are given below:

$$X_{A_1} = \exp\left[-\frac{E_1}{RT}\right](1-\alpha)^n \quad (6.6)$$

$$X_{A_2} = \exp\left[-\frac{E_2}{RT}\right]\alpha^m(1-\alpha)^n \quad (6.7)$$

$$X_{E_1} = -\frac{K_1}{RT}(1-\alpha)^n \quad (6.8)$$

$$X_{E_2} = -\frac{K_2}{RT}\alpha^m(1-\alpha)^n \quad (6.9)$$

$$X_m = K_2\alpha^m(1-\alpha)^n \ln(\alpha) \quad (6.10)$$

$$X_n = [K_1 + K_2\alpha^m](1-\alpha)^n \ln(1-\alpha) \quad (6.11)$$

In the case of both Strategies II and III, sensitivity coefficients were evaluated numerically using the simple, but adequate, finite-differences, as described in Chapter 3. Recall that the estimation methodology based on GAs does not use sensitivity information. Nevertheless, it is meaningful to analyze the coefficients to obtain some insight in the estimation procedure.

The program GAMAIN, described in Chapter 4, was used to estimate the true parameter vector β . The choice for the GA method was supported by the presence of strong correlations between the sensitivity coefficients of the parameters, as it is shown in the results section. The Fortran subroutine GAKINETIC.FOR, written as the adaptation subroutine of the program GAMAIN, is provided in Appendix H along with its dependent subroutines.

6.3 Inhibition Time Estimation Problem Formulation

The K&S characterization is sought to start at a null degree of cure value. The induction period t_{ind} represents the time during which the reaction is inhibited, that is while $\tilde{v}_{ij} = 0$. This occurs because the materials contain inhibition substances. The determination of this period must take into account the material “thermal history” before curing actually starts, that is $T(t)$ for $t < t_{ind}$. The procedure used here for such determination is based on a model applied by Bailleul (1997) in which the inhibition period is considered over when the function $h(T)$, defined next, becomes null.

$$h(T) = t_{ref} - \int_0^{\tilde{t}_{ind}} \exp \left[-B \times \left(\frac{T_{ref}}{T(t)} - 1 \right) \right] dt \quad (6.12)$$

In Bailleul’s work, the reference temperature T_{ref} is arbitrarily selected within the range investigated. Then, knowing the experimental induction time \tilde{t}_{ind} and the thermal history $T(t)$ for $t < \tilde{t}_{ind}$, the objective is to identify the two parameters t_{ref} and B that best minimize the function $[h(T)]^2$ for all experiments. Note that these parameters are strongly correlated and in his study, Bailleul used a parametric graphical procedure to provide true estimates. The test of this objective function with the estimation methodology based on GAs resulted in an unstable behavior. Indeed, using different initial parameter ranges, the estimate for t_{ref} would always be the smallest value available from the range investigated, thus giving different estimates for B . Therefore, even though the function $[h(T)]^2$ was nearly null using the final estimates, it was clear the procedure was not stable. From the results obtained in this test the estimation criterion was modified to be based on the error between the calculated and measured inhibition times. This gives a new sum-of-squares S_{ind} for the objective function:

$$S_{ind} = \sum_{j=1}^{N_j} \left[t_{ind\ j}(\underline{\beta}) - \tilde{t}_{ind\ j} \right]^2 \quad (6.13)$$

where the inhibition time for each experiment j , $t_{ind\ j}$, can be obtained from the numerical solution of:

$$t_{ref} = \int_0^{t_{ind,j}} \exp\left[-B \times \left(\frac{T_{ref}}{T_j(t)} - 1\right)\right] dt \quad (6.14)$$

where $T_j(t)$ is known for $t < t_{ind,j}$. Even though the estimation criterion has changed, the goal is still to minimize the function $h(T)$ given in Eq. (6.12). One method to perform this is to set t_{ref} to the average value of the integrals calculated for the N_j experiments, as shown below.

$$t_{ref} = \frac{1}{N_j} \sum_{j=1}^{N_j} \left[\int_0^{\tilde{t}_{ind,j}} \exp\left[-B \times \left(\frac{T_{ref}}{T_j(t)} - 1\right)\right] dt \right] \quad (6.15)$$

The parameter vector β involves now the unknown T_{ref} and B . As seen in the results section, the estimation methodology still conducted to different estimates for these two parameters due to the non-uniqueness of the solution. However, all solutions resulted to the same value for S_{tind} , thus stressing the stability of the procedure.

The adaptation subroutine to solve this estimation problem with the program GAMAIN is also GAKINETIC.FOR, with some slight changes (from its use in the K&S model study). These changes obviously include a different data input file, number of parameters to estimate, ..., but also the setting of the key parameter KTIMEINHI to 1 (instead of 0 if the K&S estimation is desired). The functioning of GAKINETIC.FOR along with the possibilities of analysis are detailed through several explanative comments in the subroutine.

6.4 Materials and Experimental Procedures

6.4.1 Description of Materials

Three thermoset resins were investigated. These include an epoxy, a polyester and a rubber mixture. The epoxy mixture consists of an epoxy resin with a DGEBA/3DCM prepolymer system and about 60% unidirectional glass fiber. The elastomer is a complex mixture with 58% (in weight) natural rubber of SMR type, 32% black carbon, 2% sulfur and 8% of accelerating/inhibiting/protecting agents. No specific details about the polyester can be provided here based on confidentiality considerations.

Differential Scanning Calorimetry (DSC) was selected as the experimental procedure and it is described in the next subsection. It is relevant to recall here that while epoxy and polyester resins present strong exothermal reticulation transformations (300 to 600 J/g), the exothermal effects from the vulcanization of rubber compounds is relatively small (~ 20 J/g)

(Garnier, 1990), making calorimetric measurements more difficult for these latter. Therefore, it is anticipated that the kinetic parameter estimation for the characterization of the rubber be more sensible to experimental errors than for the characterization of the two other resins.

6.4.2 DSC Experimental Procedures

- **Fundamentals**

The Perkin-Elmer DSC-7 apparatus was used for the analysis of both the epoxy and the rubber samples. The device consists of two identical temperature-regulated furnaces, as simplified in Fig. 6.4. One contains the sample to be characterized and the other an empty reference pan. The fundamental principle behind DSC is based on power compensation; that is, the apparatus records the heat flux difference (in heating or cooling) between both furnaces that are assumed to be isothermal. The difficulty in using DSC is that small samples are required to validate the main assumptions of isothermal conditions and negligible contact resistance between the pan and the sample. A detailed description of general DSC theory and the possibilities of application are given by McNaughton and Mortimer (1975). Several studies have also been conducted with the DSC-7 to define experimental methodologies that minimize the effects of perturbing parameters such as the contact resistances between the pan and the sample and the pan and the furnace (Garnier, 1990; Ollivier, 1991; and Lalouana, 1992, to name a few).

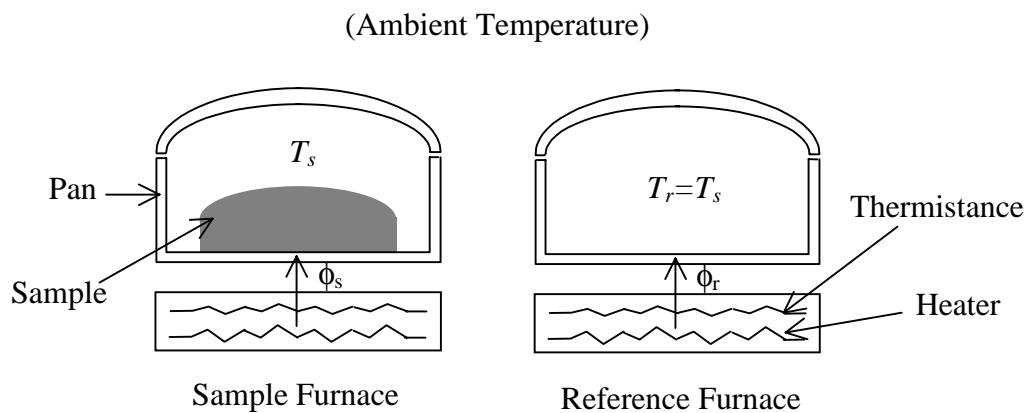


Figure 6.4 Simplified schematic of DSC-7 apparatus.

This paragraph briefly summarizes the principles associated with DSC. Considering the thermal losses to be identical from each furnace and the sample temperature to rigorously follow the prescribed temperature, the differential heat flow between both furnaces can then be expressed by:

$$\Delta\phi = \phi_s - \phi_r = -mc_p \frac{dT}{dt} + m \frac{dh}{dt}, \quad \frac{dh}{dt} = \Delta H \frac{d\alpha}{dt}, \quad (6.16)$$

where m is the sample mass, c_p , the specific heat, $h(t)$, the enthalpy function represented in Fig. 6.5, ΔH , the total heat of reaction and $\frac{d\alpha}{dt}$ (or ν), the reaction rate. The total heat

generated (also total enthalpy of the reaction) is given by $\Delta H = \int_0^{t_f} \left(\frac{dh}{dt} \right) dt$, where t_f is the total

curing time. The reaction rate, $\frac{d\alpha}{dt}$, is the ratio of the rate of heat generated to the total heat generated. The determination of ΔH and ν is possible by total and partial numerical integration of the exothermal peak recorded by DSC. In doing this, one must properly define the bound points (m_1 and m_2) of the reaction, as illustrated in Fig. 6.5. Then, by selecting a sigmoidal curve for the baseline of the exothermal peak, the variations of specific heat with curing in the case of dynamic experiments are taken into account (Hemminger and Hohne, 1984). The calculation procedure to determine the sigmoid is an iterative process which computes the baseline so that the variation of specific heat due to the transformation ends up to be proportional to the degree of cure. This procedure is usually implemented in DSC softwares. Eventually, the degree of cure α is obtained from numerical integration of the rate of cure.

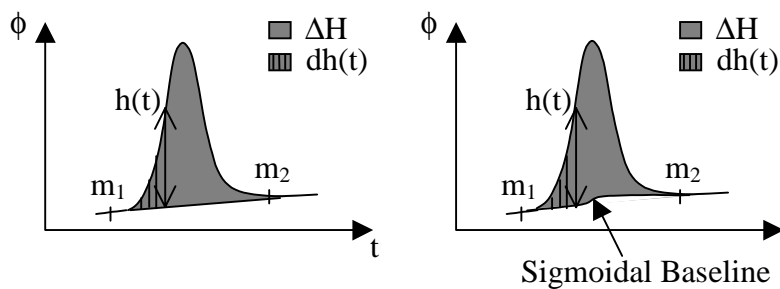


Figure 6.5 Numerical integration of the exothermal peak measured with DSC.

After treatment of the experimental heat fluxes recorded by DSC, one ends up with the set $\{\tilde{t}_{ij}, \tilde{\alpha}_{ij}, \tilde{\nu}_{ij}, \tilde{T}_{ij}\}$, where t is time, and i and j are the number of measurements and experiments recorded, respectively. In this work, data obtained by DSC before the cure started were used for the determination of the two parameters associated with the inhibition time model, while the rest of the data were used in the three estimation Strategies, I, II and III. The cure starting point corresponding to the experimental inhibition time was taken as the time preceding the first degree of cure value different than zero and followed by a consistent increase. This point selection method obviously depends on the precision of the DSC data acquisition system. Note that the use of a small percentage of the maximum value reached by the cure rate as the value of the cure starting point would have allowed for the kinetic analysis to be performed independently of the apparatus bias level.

- **Experiments Performed**

Because curing started quickly for the three resins (in the time period corresponding to the apparatus response), isothermal experiments were not feasible. Therefore, estimation was proceeded using dynamic experimental data only. For each resin, several cycles for which the temperature increased linearly with time and at different rates, V_T , were realized. The upper temperature value was chosen to ensure that the curing process was complete but still remaining below a temperature level which could cause material degradation. As part of a collaboration project, Dr. B. Garnier¹ performed the experiments on both the epoxy and rubber samples using the Perkin Elmer DSC-7. Data associated with the polyester resin were provided by another doctoral student of the LTI/Nantes as part of an industrial contract. Table 6.1 summarizes the number (N_j) and conditions of experiments for each resin. One can see that six cycles were realized on both the epoxy and rubber samples and, sixteen on the polyester compound. Also, note that the smaller the temperature rate V_T , the larger the number of recorded data points N_i . The maximum increase in cure rate for each cycle is given by Δv_{max} (min^{-1}) and, $[\Delta v_{max}]_{av}$ designates the corresponding averaged-maximum increase for each resin.

¹ CNRS Researcher at the LTI/Nantes.

Table 6.1 Conditions of experiments performed using DSC.

Epoxy $N_j=6, T \in [40-220 \text{ }^\circ\text{C}]$			Rubber $N_j=6, T \in [40-200 \text{ }^\circ\text{C}]$			Polyester $N_j=16, T \in [40-200 \text{ }^\circ\text{C}]$		
V_T ($^\circ\text{C}/\text{min}$)	N_i	Δv_{max} (min^{-1})	V_T ($^\circ\text{C}/\text{min}$)	N_i	Δv_{max} (min^{-1})	V_T ($^\circ\text{C}/\text{min}$)	N_i	Δv_{max} (min^{-1})
2.5	447	0.1248	2.5	212	0.4374	3	2186	0.2259
5	270	0.2325	5	474	0.8237	5	1470	0.3060
7.5	186	0.3278	7.5	89	0.9024	7	1044	0.4271
10	140	0.4165	10	195	1.2337	10	675	0.5380
12.5	118	0.4962	12.5	49	1.2721	12	547	0.6659
15	93	0.5692	15	82	1.2652	15	471	0.7666
$N_{tot} = 1254$		$[\Delta v_{max}]_{av} = 0.3612$	$N_{tot} = 1101$		$[\Delta v_{max}]_{av} = 0.9891$	17	425	0.8684
						20	329	1.001
						25	234	1.2134
						30	207	1.4008
						35	190	1.5837
						40	169	1.2324
						45	136	1.8552
						50	131	2.0179
						55	117	2.1766
						60	106	2.3846
						$N_{tot} = 8437$		$[\Delta v_{max}]_{av} = 1.1665$

6.5 Results and Discussion

6.5.1 K&S Estimation

In the following, the estimation procedure is described. Next, the results are discussed in terms of first, the individual analysis of each estimation strategy and, then, the comparison between the three strategies.

6.5.1.1 Estimation Procedure

Recall that three procedures were investigated as defined by Eq. 6.3, 6.4 and 6.5. Using Strategy I, one considers the measured quantity to be the cure rate and assumes the degree of cure and temperature to be known at each observation (independent variables). With Strategy II, one also considers the measured quantity to be the cure rate, but assumes time and

temperature to be the known data. Finally, in Strategy III, the measured variable is the degree of cure, and time and temperature are assumed to be the independent variables. For these three methods, the estimation of the kinetic parameters was carried out as follows. Using large ranges for the kinetic parameters, two estimations were run for each of the three procedures, considering six (run 1) and four parameters (run 2 without K_7), successively. The second run thus corresponded to the study of the simplified K&S model, which has a similar form to the equation suggested by Piloyan et al. (1966). Note that the computation of the degree of cure without the rate constant K_1 in the model required an initial value (very small number) to be input in the numerical scheme.

The objective function values obtained for these two initial runs (runs 1 and 2) were compared and the setting (6 or 4 parameters) which provided the smallest sum-of-squares error was retained for subsequent trials. Note that even though the improvement of studying the complete K&S model (6 parameters) over the simplified model (4 parameters) was very small, the simultaneous estimation of the six parameters was further investigated. Although such decision was “against” the principle of parsimony which states that one should employ the smallest number of parameters (Beck and Arnold, 1977), this was in agreement with the motivation behind this work, which was the analysis of the complete K&S model.

Following the choice between the complete and simplified model, four additional trials were conducted with the GA method (run # 3, 4, 5 and 6 in the result tables introduced later), decreasing each time the parameter ranges used to generate the initial population. This insured convergence towards the global minimum of the objective functions associated with the three estimation strategies. Finally, the last run was considered to provide the best possible estimates, e.g. to provide a model close to the optimal model that can be reached with the K&S form.

For all estimation trials performed, the same setting, given in Table 6.2, was used for the genetic parameters associated with the convergence criterion (refer to Chapter 4). All jobs were run on a personal computer P233. As the CPU time requirement was not costly, the ideal population size could, therefore, be investigated, in association with substantial values for MING, LASTCRITERG and LASTG.

Table 6.2 Genetic convergence parameters setting.

N_S	MING	LASTCRITERG	LASTG	CRITERION
$N_p \times 100$	100	100	500	0.01 (1%)

6.5.1.2 Results and Discussion

The results obtained from application of the three estimation Strategies, I, II and III, are introduced beforehand for convenience.

Tables 6.3 to 6.5 show the detailed results obtained for the three strategies applied on the experimental data recorded for the epoxy, rubber and polyester compound, respectively. In order to gain insight into the estimation problems, the dimensionless sensitivity coefficients associated with each set of final estimate values were carefully examined. Recall from Chapter 3 that a dimensionless coefficient represents the product of the coefficient by its parameter value and scaled with respect to the measured variable by dividing by the maximum increase in the variable (Δv_{max} , given in Table 6.1, or $\Delta \alpha_{max} = 1$). Note that the superscript ⁽⁺⁾ that usually denotes “dimensionless” was omitted for convenience. The experiments performed at 15°C/min were used as the basis for the sensitivity analysis. Figures 6.6 to 6.11 are associated with the sensitivity study realized on the epoxy sample (using estimates obtained with Strategy I, II and III), while Figs. 6.12 to 6.14 and 6.15 to 6.17 are related to the polyester and rubber mixture, respectively. As an alternative to appreciate the relative linear-dependence between the sensitivity coefficients, the correlation matrices were computed for the experiments at 15°C/min. The correlation matrices are shown in Table 6.6, for the three compounds. This table also includes the condition number of the $\mathbf{X}^T\mathbf{X}$ matrix associated with each estimation problem. The condition number which represents the largest eigenvalue of the $\mathbf{X}^T\mathbf{X}$ matrix divided by the smallest, was also calculated with an aim to measuring the ill-conditionness of the estimation problems.

Finally, to illustrate the physical significance of the final estimate values (run 6) obtained with each strategy, simulated isothermal cure rate data were generated as a function of degree of cure. Note that the goal was to simulate cure rate data of magnitude approximately similar to that encountered in the experiments (Δv_{max}). The simulated plots are represented in Figs. 6.18 to 6.20 for the epoxy, 6.21 to 6.23 for the polyester and 6.24 to 6.26 for the rubber compound.

Table 6.3 K&S detailed estimation results - Epoxy resin.

		Run					
		1	2	3	4	5	6
Estimation Strategy I	A_1 (min^{-1})	6.74 $\times 10^{27}$	N/A				
	E_1 (kJ/mol)	4569.7	N/A				
	$A_2 \times 10^{-8}$ (min^{-1})	9.41	9.60	9.59	9.59	9.57	9.54
	E_2 (kJ/mol)	71.45	71.52	71.51	71.52	71.51	71.50
	m	0.653	0.653	0.653	0.653	0.653	0.653
	n	1.567	1.567	1.567	1.567	1.567	1.567
	S_1 (min^{-1}) ²	0.0714	0.0708	0.0708	0.0708	0.0707	0.0707
	ITERG _f	500	218	235	267	226	396
Estimation Strategy II	A_1 (min^{-1})	3.20 $\times 10^{14}$	N/A	9.57 $\times 10^6$	1.35 $\times 10^{20}$	7.84 $\times 10^{10}$	1.37 $\times 10^{15}$
	E_1 (kJ/mol)	148.29		84.74	192.35	111.20	144.03
	$A_2 \times 10^{-8}$ (min^{-1})	80.8	116.3	76.9	51.4	62.8	58.9
	E_2 (kJ/mol)	78.61	80.00	78.35	76.94	78.12	77.40
	m	0.673	0.647	0.686	0.689	0.694	0.694
	n	1.774	1.771	1.790	1.787	1.786	1.786
	S_2 (min^{-1}) ²	0.0734	0.0825	0.0730	0.0717	0.0708	0.0707
	ITERG _f	500	261	500	500	500	500
Estimation Strategy III	A_1 (min^{-1})	4.71 $\times 10^{45}$	N/A	1.00 $\times 10^{40}$	0.92 $\times 10^{37}$	1.00 $\times 10^{37}$	1.05 $\times 10^{37}$
	E_1 (kJ/mol)	406.31		358.6	350.00	334.47	338.24
	$A_2 \times 10^{-8}$ (min^{-1})	137	149	136	135	135	135
	E_2 (kJ/mol)	80.68	80.95	80.66	80.64	80.66	80.66
	m	0.651	0.659	0.652	0.652	0.651	0.651
	n	1.586	1.594	1.586	1.586	1.584	1.584
	S_3	0.0954	0.0984	0.0953	0.0953	0.0952	0.0952
	ITERG _f	500	446	500	500	500	500

Table 6.4 K&S detailed estimation results - Polyester resin.

		Run					
		1	2	3	4	5	6
Estimation Strategy I	A_1 (min^{-1})	9.7 $\times 10^{12}$	N/A				
	E_1 (kJ/mol)	6.83 $\times 10^9$	N/A				
	$A_2 \times 10^{-13}$ (min^{-1})	6.18	6.15	6.18	6.2	6.21	6.21
	E_2 (kJ/mol)	98.35	98.33	98.35	98.36	98.36	98.37
	m	0.575	0.575	0.575	0.574	0.574	0.574
	n	2.373	2.373	2.373	2.372	2.373	2.373
	S_1 (min^{-1}) ²	18.87	18.87	18.87	18.87	18.87	18.87
	ITERG _f	500	284	312	254	217	246
Estimation Strategy II	A_1 (min^{-1})	2.65 $\times 10^{45}$	N/A	3.26 $\times 10^{50}$	1.90 $\times 10^{47}$	1.92 $\times 10^{47}$	1.92 $\times 10^{47}$
	E_1 (kJ/mol)	352.79		394.17	376.02	367.92	368.10
	$A_2 \times 10^{-13}$ (min^{-1})	50.1	47.1	42.4	37.2	24.4	24.9
	E_2 (kJ/mol)	104.02	103.80	103.44	102.96	101.57	101.63
	m	0.703	0.696	0.704	0.711	0.715	0.715
	n	2.980	2.971	2.886	2.931	2.927	2.927
	S_2 (min^{-1}) ²	16.68	16.87	16.28	16.19	16.13	16.13
	ITERG _f	500	452	500	500	500	500
Estimation Strategy III	A_1 (min^{-1})	8.21 $\times 10^{58}$	N/A	5.90 $\times 10^{62}$	4.73 $\times 10^{62}$	1.00 $\times 10^{62}$	1.37 $\times 10^{62}$
	E_1 (kJ/mol)	467.09		491.07	489.04	484.80	485.93
	$A_2 \times 10^{-13}$ (min^{-1})	1080	1726	1130	1120	1110	1100
	E_2 (kJ/mol)	114.37	115.87	114.04	114.01	113.94	113.94
	m	0.658	0.652	0.691	0.691	0.693	0.693
	n	2.605	2.631	2.806	2.807	2.812	2.812
	S_3	2.585	2.962	2.300	2.300	2.298	2.298
	ITERG _f	500	250	500	500	500	500

Table 6.5 K&S detailed estimation results - Rubber compound.

		Run					
		1	2	3	4	5	6
Estimation Strategy I	A_1 (min^{-1})	4.37 $\times 10^8$	N/A				
	E_1 (kJ/mol)	302.67	N/A				
	$A_2 \times 10^{-6}$ (min^{-1})	93.6	64.9	64.8	64.6	64.7	64.8
	E_2 (kJ/mol)	61.10	59.71	59.70	59.69	59.69	59.70
	m	0.966	0.975	0.975	0.975	0.975	0.975
	n	1.623	1.630	1.630	1.630	1.630	1.630
	S_1 (min^{-1}) ²	4.716	4.706	4.706	4.706	4.706	4.706
	ITERG _f	500	211	458	446	498	362
Estimation Strategy II	A_1 (min^{-1})	8.68 $\times 10^{49}$	N/A	4.93 $\times 10^{51}$	2.40 $\times 10^{52}$	4.95 $\times 10^{52}$	4.96 $\times 10^{52}$
	E_1 (kJ/mol)	439.4		457.27	462.64	465.66	465.76
	$A_2 \times 10^{-6}$ (min^{-1})	1000	5.52 $\times 10^7$	1050	821	800	802
	E_2 (kJ/mol)	71.16	111.43	70.41	69.39	69.20	69.16
	m	0.888	0.818	0.919	0.929	0.932	0.934
	n	1.548	2.072	1.667	1.825	1.861	1.868
	S_2 (min^{-1}) ²	16.12	20.6	15.16	14.62	14.55	14.55
	ITERG _f	500	270	500	500	500	500
Estimation Strategy III	A_1 (min^{-1})	2.9 $\times 10^{62}$	N/A	8.11 $\times 10^{67}$	9.93 $\times 10^{67}$	7.98 $\times 10^{67}$	8.50 $\times 10^{67}$
	E_1 (kJ/mol)	543.90		590.00	590.22	589.40	589.62
	$A_2 \times 10^{-6}$ (min^{-1})	8.32	36000	3.42	1.25	1.01	1.00
	E_2 (kJ/mol)	53.27	85.40	49.64	45.86	45.04	45.02
	m	0.918	0.764	0.934	0.945	0.949	0.949
	n	1.462	1.205	1.551	1.572	1.583	1.582
	S_3	2.260	7.13	2.105	2.061	2.058	2.058
	ITERG _f	500	252	500	500	500	500

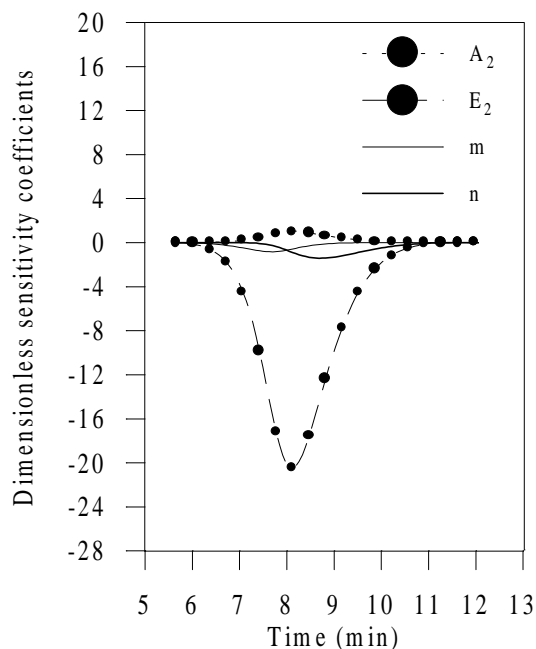


Figure 6.6 Dimensionless sensitivity coefficients with respect to the cure rate for the epoxy experiment at 15°C/min and using estimates obtained with Strategy I.

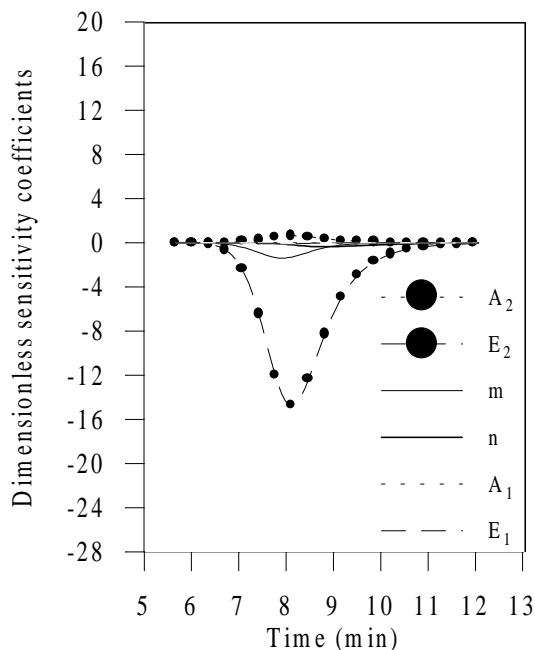


Figure 6.7 Dimensionless sensitivity coefficients with respect to the degree of cure for the epoxy experiment at 15°C/min and using estimates obtained with Strategy III.

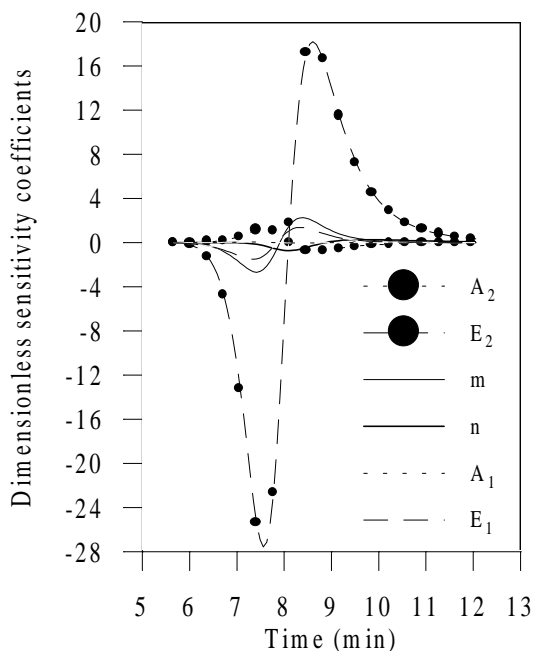


Figure 6.8 Dimensionless sensitivity coefficients with respect to the cure rate for the epoxy experiment at 15°C/min and using estimates obtained with Strategy II.

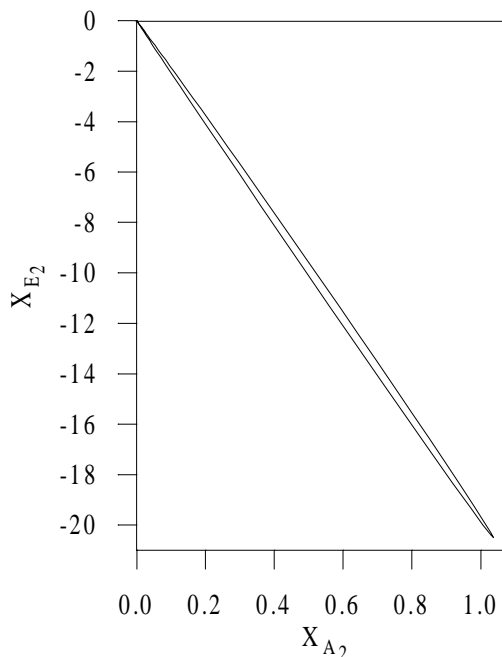


Figure 6.9 Linear dependence between dimensionless sensitivity coefficients with respect to the cure rate for the epoxy experiment at 15°C/min and using estimates obtained with Strategy I.

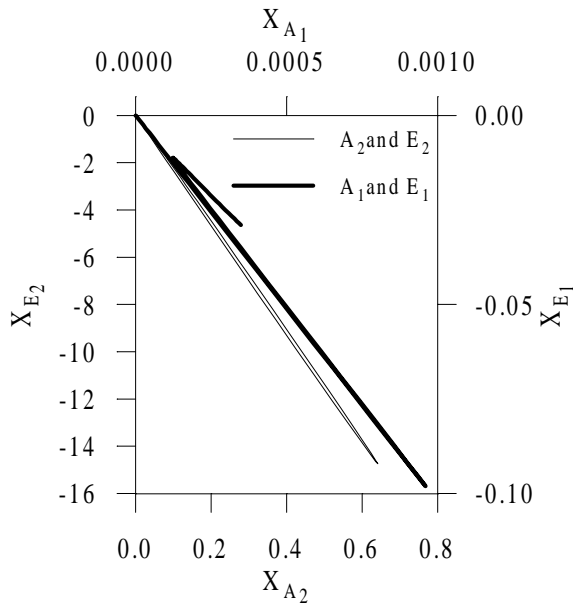


Figure 6.10 Linear dependence between dimensionless sensitivity coefficients with respect to the degree of cure for the epoxy experiment at 15°C/min and using estimates obtained with Strategy III.

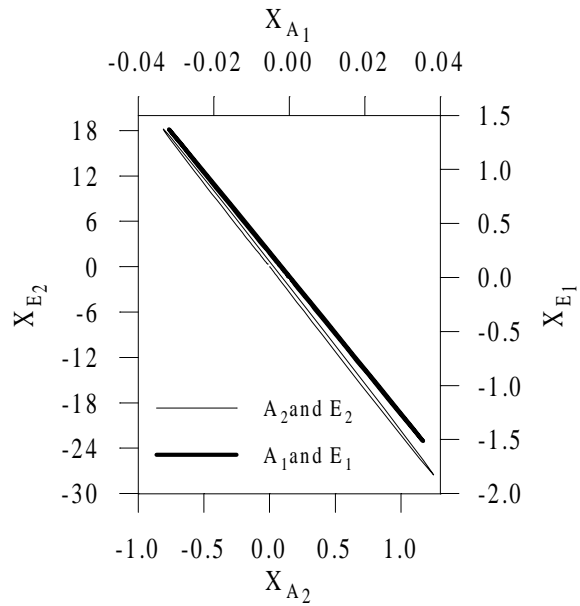


Figure 6.11 Linear dependence between dimensionless sensitivity coefficients with respect to the cure rate for the epoxy experiment at 15°C/min and using estimates obtained with Strategy II.

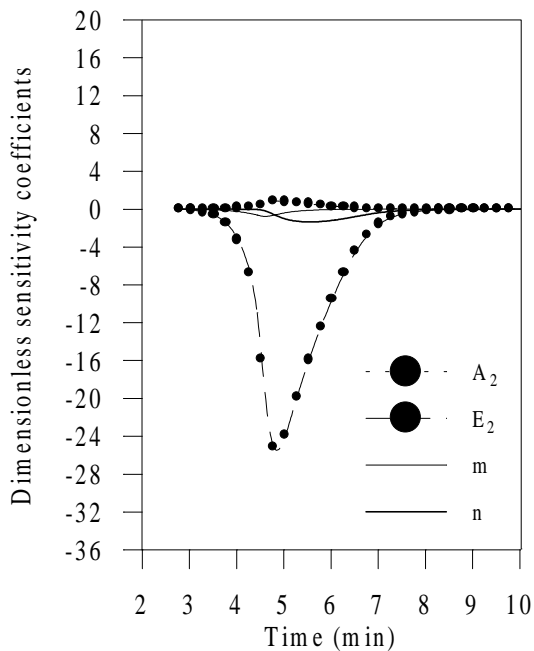


Figure 6.12 Dimensionless sensitivity coefficients with respect to the cure rate for the polyester experiment at 15°C/min and using estimates obtained with Strategy I.

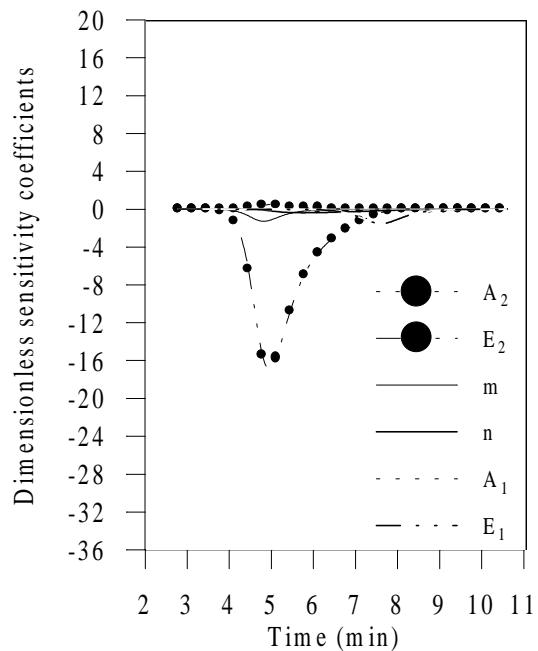


Figure 6.13 Dimensionless sensitivity coefficients with respect to the degree of cure for the polyester experiment at 15°C/min and using estimates obtained with Strategy III.

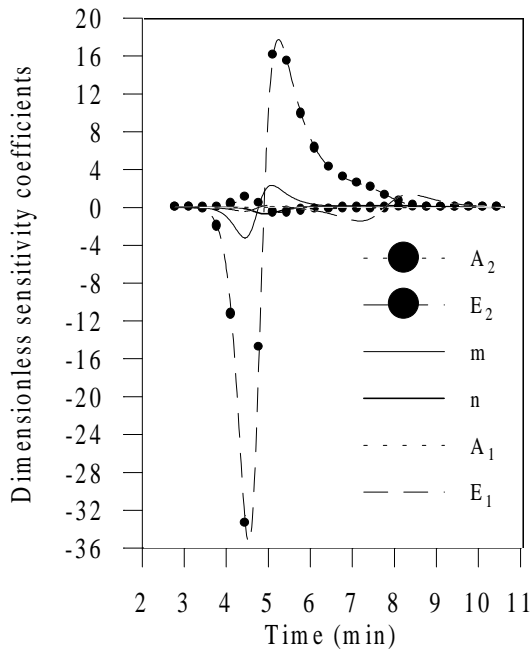


Figure 6.14 Dimensionless sensitivity coefficients with respect to the cure rate for the polyester experiment at 15°C/min and using estimates obtained with Strategy II.

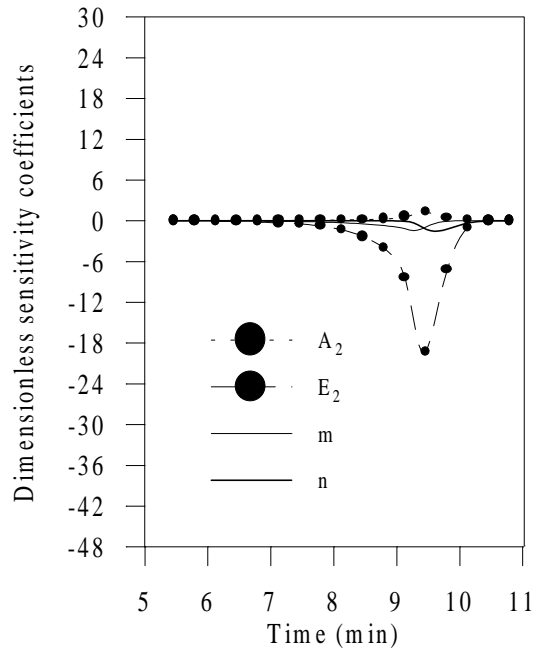


Figure 6.15 Dimensionless sensitivity coefficients with respect to the cure rate for the rubber experiment at 15°C/min and using estimates obtained with Strategy I.

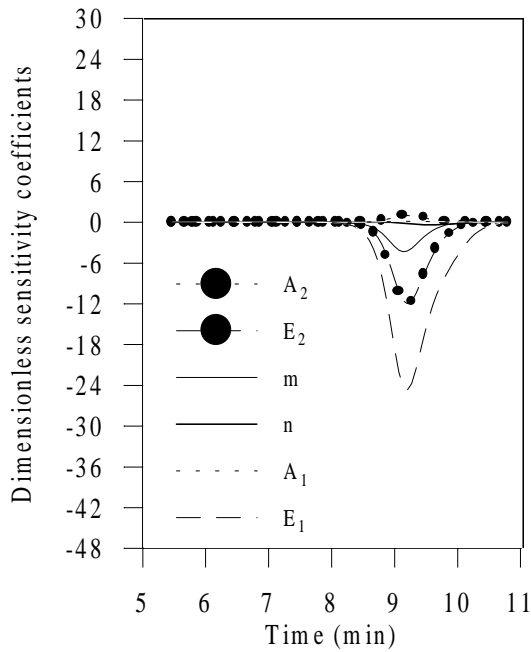


Figure 6.16 Dimensionless sensitivity coefficients with respect to the degree of cure for the rubber experiment at 15°C/min and using estimates obtained with Strategy III.

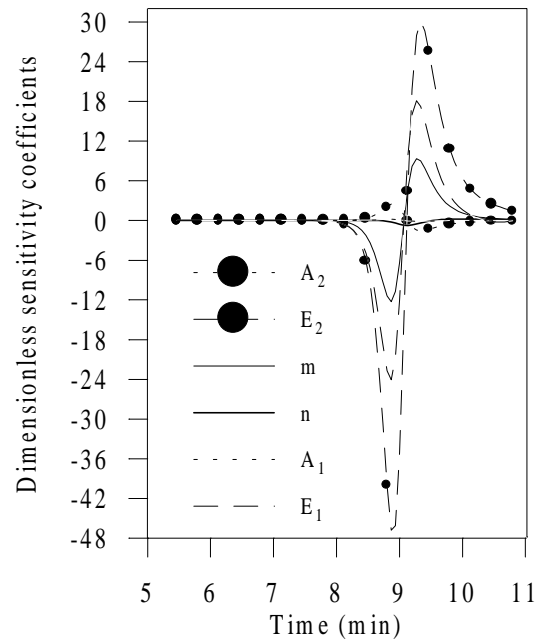


Figure 6.17 Dimensionless sensitivity coefficients with respect to the cure rate for the rubber experiment at 15°C/min and using estimates obtained with Strategy II.

Table 6.6 Correlation matrices for the experiment at 15°C/min using the final estimates for A_2 , E_2 , m and n obtained with Strategy I, and for A_2 , E_2 , m , n , A_1 and E_1 obtained with Strategies III and II.

		Correlation Matrices						$X^T X$
		A_2	E_2	m	n	A_1	E_1	Condition Number
		(same parameter order in successive rows)						
Strategy I	Epoxy	1						2.2×10^{25}
		0.99999987	1					
		-0.99952504	-0.99953946	1				
		0.99976909	0.99975897	-0.99877226	1			
Strategy I	Rubber	1						1.3×10^{21}
		0.99993299	1					
		-0.85545951	-0.86100699	1				
		0.31595407	0.30575324	0.12948831	1			
Strategy I	Polyester	1						5.1×10^{33}
		0.99998703	1					
		-0.84328080	-0.84578450	1				
		0.99279303	0.99222073	-0.78687505	1			
Strategy III	Epoxy	1						1.5×10^{86}
		0.99999985	1					
		-0.99956251	-0.99957820	1				
		0.99975756	0.99974559	-0.99872098	1			
		0.98760610	0.98767961	-0.99155235	0.98468336	1		
		0.98754912	0.98762392	-0.99155332	0.98456435	0.99997955	1	
Strategy III	Rubber	1						5.3×10^{145}
		0.99999978	1					
		-0.96573745	-0.96575413	1				
		0.45631421	0.45619001	-0.21787876	1			
		0.83250834	0.83247622	-0.94089368	-0.34664105	1		
		0.82178858	0.82176005	-0.93563001	-0.58837947	0.99969320	1	
Strategy III	Polyester	1						2.5×10^{133}
		0.99999841	1					
		-0.99771348	-0.99783054	1				
		0.99775175	0.99764037	-0.99150643	1			
		0.93441283	0.93462117	-0.94011339	0.92132442	1		
		0.92960404	0.92982551	-0.93579450	0.91590186	0.99989531	1	
Strategy II	Epoxy	1						1.2×10^{42}
		0.99999889	1					
		-0.99292060	-0.99295367	1				
		0.98725702	0.98722365	-0.96308618	1			
		-0.97647893	-0.97636123	0.99062039	-0.93522729	1		
		-0.97662716	-0.97650803	0.99059672	-0.93553850	0.99999848	1	
Strategy II	Rubber	1						6.0×10^{114}
		0.99997263	1					
		-0.37566816	-0.38216480	1				
		0.91963533	0.91686833	-0.41734366	1			
		-0.55217443	-0.54658623	-0.52979213	-0.76562909	1		
		-0.54297776	-0.53731499	-0.54594706	-0.76011437	0.99949438	1	
Strategy II	Polyester	1						9.1×10^{102}
		0.99999652	1					
		-0.99440854	-0.99467224	1				
		0.98503697	0.98465311	-0.96395214	1			
		0.86643686	0.86695768	-0.89091614	0.81518906	1		
		0.85752856	0.85807330	-0.88325712	0.80489092	0.99974650	1	

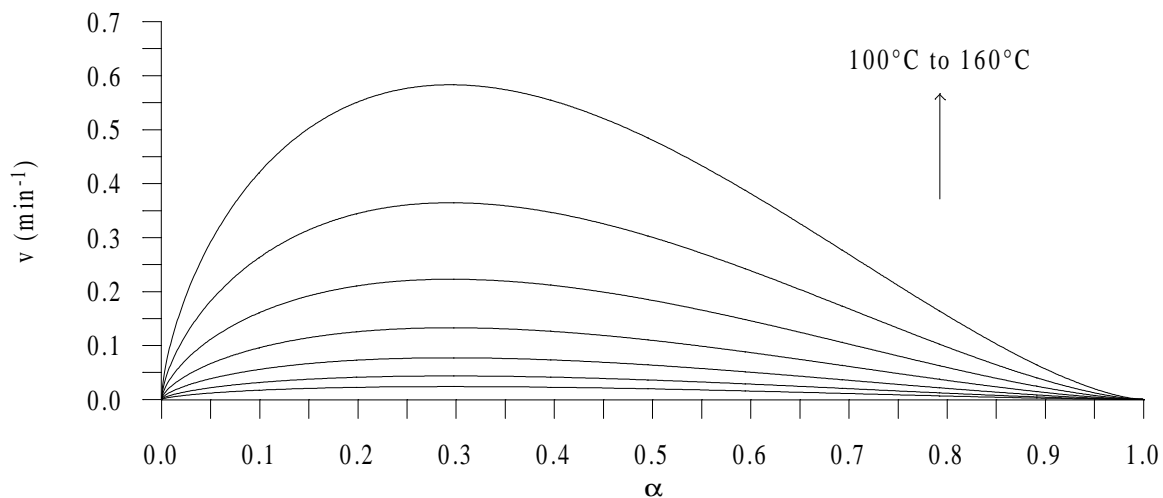


Figure 6.18 Simulation of isothermal cure rates using estimates obtained with Strategy I
– Epoxy compound.

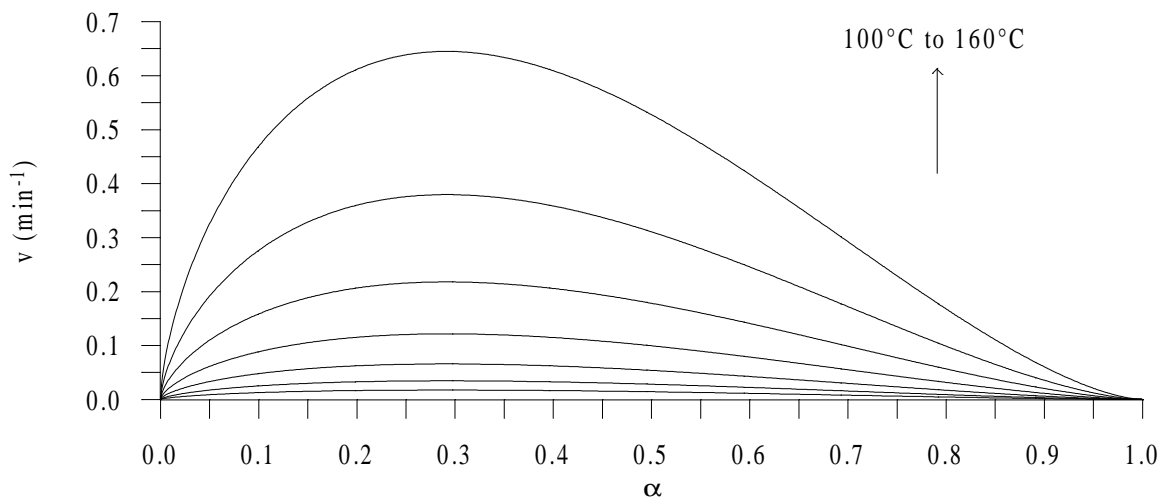


Figure 6.19 Simulation of isothermal cure rates using estimates obtained with Strategy III
– Epoxy compound.

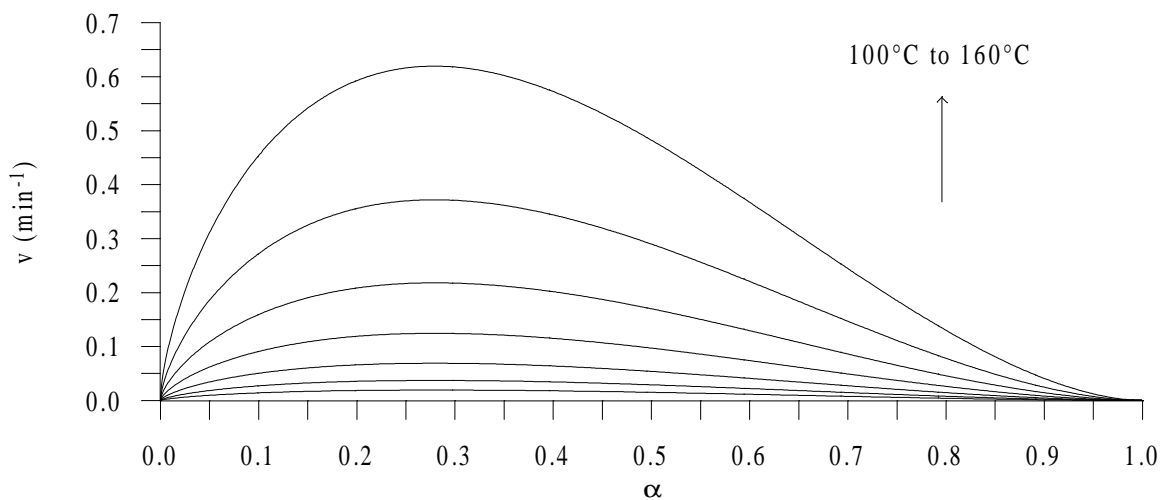


Figure 6.20 Simulation of isothermal cure rates using estimates obtained with Strategy II
– Epoxy compound.

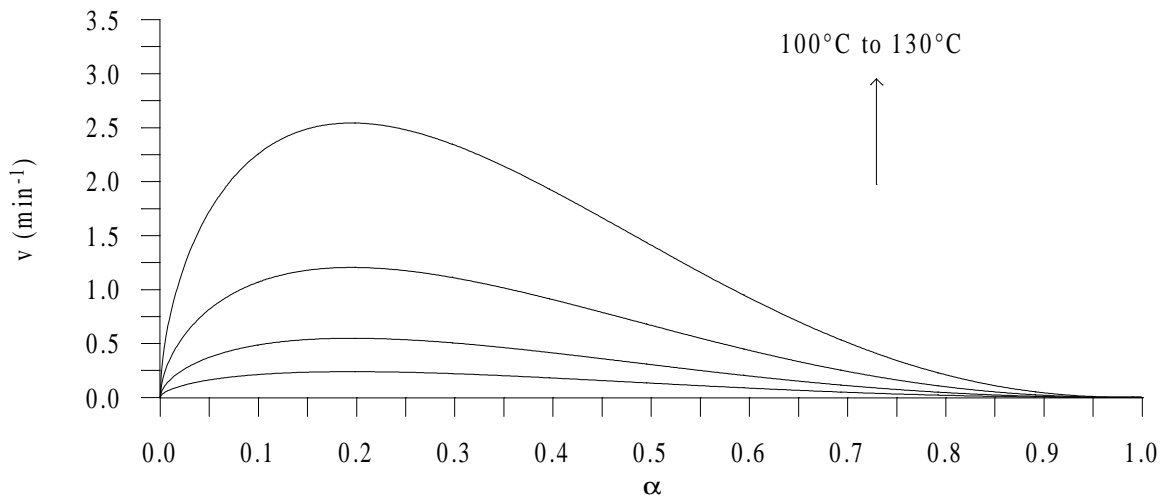


Figure 6.21 Simulation of isothermal cure rates using estimates obtained with Strategy I – Polyester compound.

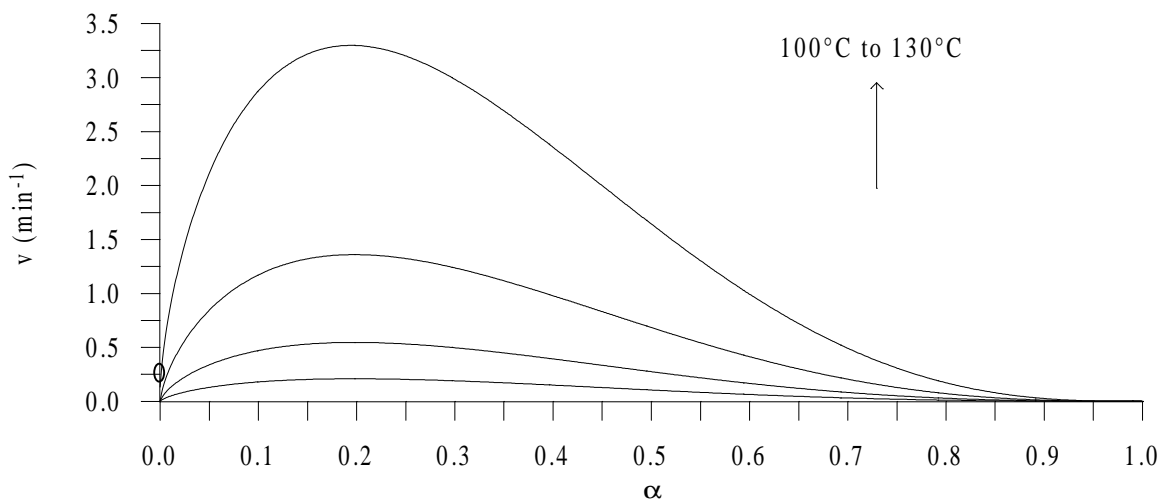


Figure 6.22 Simulation of isothermal cure rates using estimates obtained with Strategy III – Polyester compound.

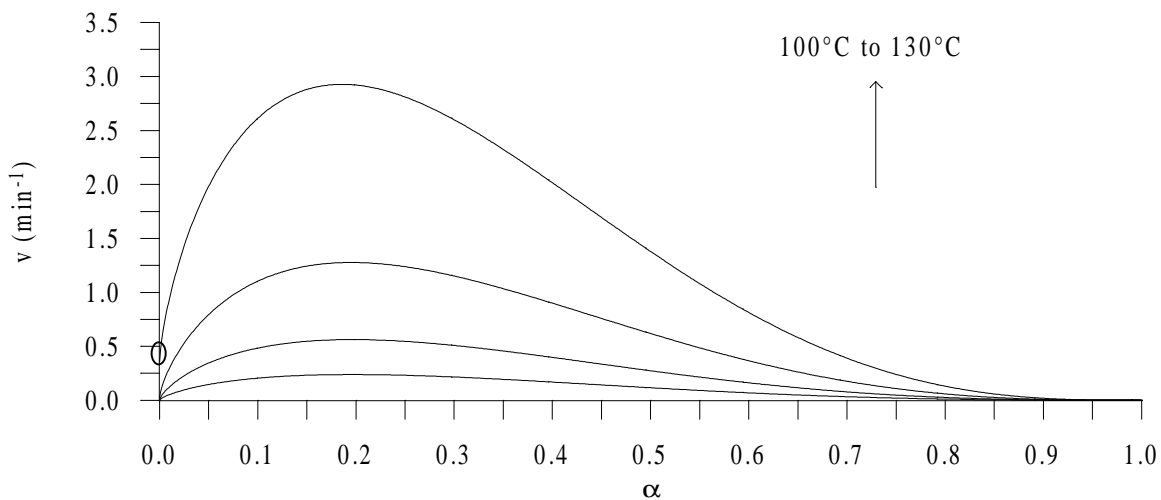


Figure 6.23 Simulation of isothermal cure rates using estimates obtained with Strategy II – Polyester compound.

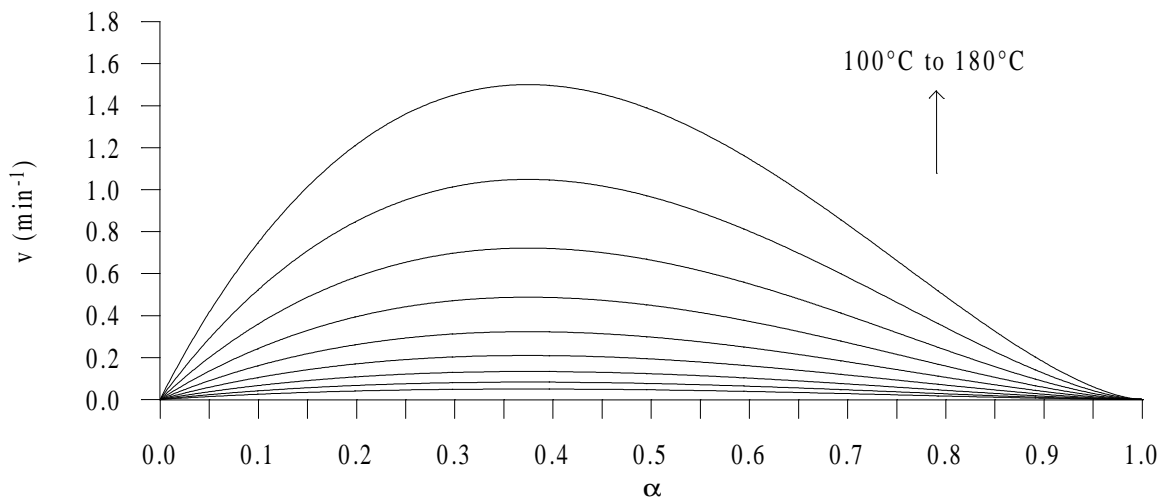


Figure 6.24 Simulation of isothermal cure rates using estimates obtained with Strategy I – Rubber compound.

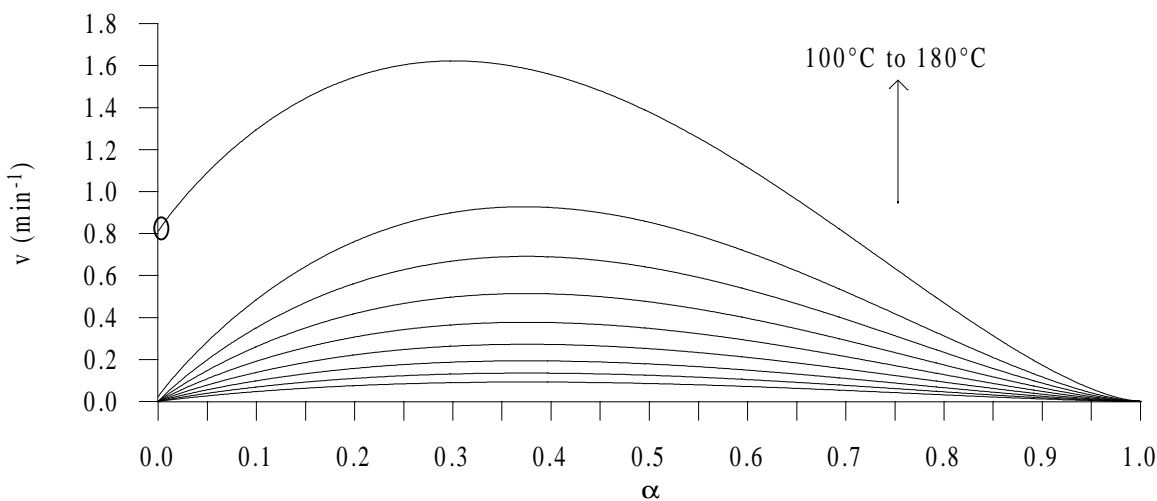


Figure 6.25 Simulation of isothermal cure rates using estimates obtained with Strategy III – Rubber compound.

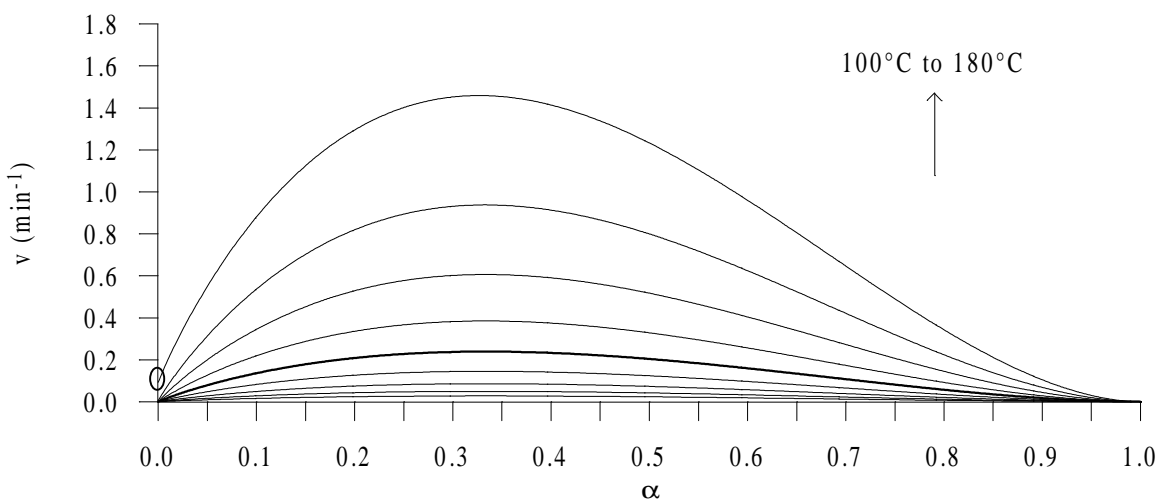


Figure 6.26 Simulation of isothermal cure rates using estimates obtained with Strategy II – Rubber compound.

- **Strategy I**

In all first runs conducted according to the estimation Strategy I, the rate constant K_1 appeared to take a null value and the second and further runs concentrated on the estimation of A_2 , E_2 , m and n provided the same or slightly smaller sum-of-squares errors. This indicates a negligible effect of K_1 which was supported by the imperceptible sensibility of the cure rate computed using Strategy I to the parameters A_1 and E_1 during a preliminary sensitivity analysis (prior to the implementation of the estimation procedure). The dimensionless sensitivity coefficients show a much higher magnitude for the parameter E_2 for the three mixtures (Figs. 6.6, 6.12 and 6.15), but sufficient information is provided for the estimation of the three other parameters with magnitudes much greater than the rule-of-thumb limit 0.1. The correlation matrices (Table 6.6) reveal a strong linear dependence between the two parameters of the rate constant K_2 , which is illustrated Fig. 6.9 in the epoxy case. This behavior can actually be understood if Eq. (6.2) is rewritten as:

$$K_i = \exp\left[A_i - \frac{E_i}{RT}\right], A = \exp(A_i), \quad i = 1,2 \quad (6.17)$$

Eq. 6.17 obviously indicates that if temperature does not vary much, the values of A_i and E_i are not unique. From Table 6.1, one can see that the temperature range investigated for each material was quite large.

The high condition numbers of the $\mathbf{X}^T\mathbf{X}$ matrices obtained for the three mixtures (Table 6.6) are another means for stressing how ill-conditioned the estimation is. Indeed, both the correlations and the large magnitude difference between the sensitivity coefficients of the parameters E_2 and m result in a large magnitude difference between the largest and smallest eigenvalue. Note that this sensitivity difference and the predominance of the Arrhenius constant E was reported by Bournez et al. (1999), as mentioned in Chapter 2. One can see that despite these conditions, the GA method demonstrates excellent convergence (Table 6.3). This is possible because GAs do not use derivative information. In addition, sufficient information is provided by the smallest sensitivity coefficient. The final estimates resulting from run 6 can be considered to be the best estimates that can be obtained with Strategy I.

- **Strategy III**

Regarding estimation Strategy III, the presence of the rate constant K_1 resulted in better modeling of the degree of cure. The improvement was considerable for the rubber and

worthwhile for the polyester sample, but it was minor in the epoxy case. The sensitivity coefficients corroborate these results. Indeed, the sensibility of the degree of cure to the parameter E_1 is nearly negligible for the epoxy compound (Fig. 6.7), while substantial for the polyester (Fig. 6.13), and larger than the corresponding sensitivity coefficients of E_2 for the rubber mixture (Fig. 6.16). Note that the parameter A_1 shows a negligible sensitivity coefficient for all mixtures. Correlations are present (among the six parameters in both the epoxy and polyester cases), as shown in Table 6.6 and illustrated in Fig. 6.10 for the epoxy case. Combined with the negligible sensitivity of the measured variable to the parameter A_1 , this makes the GA method unable to converge before 500 generations, which is the value for LASTG, the fixed maximum number of generations. An important point related to convergence should be outlined here. Recall from Chapter 4 that the convergence criterion implemented in the GA_3 algorithm (and, thus, the GAMAIN version) is based on a small percentage change (1%) in both all gene values and the objective function value of the best-so-far chromosome. In extreme cases where very little sensitivity of the measured quantity to some parameters is observed, large variations in these parameters do not affect the objective function (least-squares error). Therefore, one can understand that in those extreme cases, which correspond to the present case, the best-so-far chromosome may involve parameters that vary greatly and, thus, no convergence, according to the criterion used, can be achieved. The results obtained here are an illustration of the weakness of the convergence criterion defined for the GA_3. Consequently, it is believed that the solution achieved using Strategy III is “converged” towards a solution close to the global minimum of the function S_3 .

The huge condition number of the $\mathbf{X}^T\mathbf{X}$ matrices show how ill-defined the estimation problem is when the complete K&S model is investigated. Note that the much larger condition number values obtained here than when applying Strategy I must result from the increase in magnitude difference between the largest and smallest sensitivity coefficients. Indeed, the smallest sensitivity coefficient, which is associated with the parameter A_1 , is nearly null for the three thermosetting materials.

A comparison of the simulated isothermal cure rate data illustrates the differences between the sets of final estimates obtained using Strategies I and III (Figs. 6.18 and 6.19, 6.21 and 6.22, and 6.24 and 6.25, for the epoxy, polyester and rubber compound, respectively). For the three mixtures, one notices that Strategy III provides higher maximum cure rate values (at the same temperature). In addition, the relative effect of the rate constant K_1 can be seen. The deviation observed in the initial cure rate values as temperature increases (which is typically encountered when this constant has some effect) is considerable for the

rubber, significant for the polyester and negligible for the epoxy compound. This is in good agreement with the information provided by the sensitivity coefficients.

- **Strategy II**

As with Strategy III, the use of the complete K&S model with Strategy II allowed a better minimization of the sum-of-squares error. The improvement is mostly significant for the rubber compound for which the sensitivity of the cure rate to the parameter E_I (Fig. 6.17) is, indeed, much larger than for the two other compounds (Fig. 6.8 and 6.14). The sensitivity to the parameter A_I is still very small for the three mixtures, but not negligible any more (Figs. 6.11, 6.14 and 6.17). The sensitivity coefficients are actually all magnified compared to the plots obtained with the two previous strategies. Note that since the independent variable used here (v) is the derivative of the one used in Strategy III (α), the sensitivity coefficients here are likewise derivatives of the sensitivity coefficient curves shown for Strategy III. Correlations are still present, as illustrated in Table 6.6 and in Fig. 6.11 for the epoxy case as an example. One again notices the inability of the GA method to converge, which is due to the very small sensitivity to the parameter A_I . This results in different combinations of the parameters that provide similar values for the sum-of-squares error. As seen with Strategy III, this effect illustrates again the weakness of the convergence criterion defined for the GA_3. Therefore, one should understand that the nonconvergence shown here is related to the definition of the convergence criterion used for the stopping condition of the GA run. It is believed that the solution achieved in run 6 for the objective function is near the global minimum of the function S_2 .

The ill-conditionness of the estimation problem indicated by the condition number of the $\mathbf{X}^T\mathbf{X}$ matrices (Table 6.6) is slightly improved compared with Strategy III, apparently because the magnitudes of the smallest sensitivity coefficient (associated to the parameter A_I) are higher.

In terms of the physical significance of the sets of final estimates obtained using Strategy II, the simulated isothermal cure rate data show two different behaviors. On one hand, in both the epoxy and polyester case (Figs. 6.20 and 6.23, respectively), the maximum values are comprised between the maximum values produced (at the same temperature) by the simulated data using the two other estimation strategies. On the other hand, in the rubber case (Fig. 6.26), the maximum values are smaller than when using the two other strategies. Note in this latter case the larger effect of the rate constant K_I using estimates obtained with Strategy

III (Fig. 6.25) than with those obtained with Strategy II. Regarding the relevance of using the constant K_I in the model when applying Strategy II, Fig. 6.20 confirms that it could have been neglected for the epoxy mixture.

- **Comparison of the Three Estimation Strategies**

From the analysis conducted previously for the three estimation strategies, one can observe the following points:

- There is no best strategy regarding correlation. Indeed, sensitivity coefficients were shown to be linearly dependent for all strategies used.
- With the estimation restricted to four parameters, Strategy I led to better condition numbers of the $\mathbf{X}^T\mathbf{X}$ matrices and to converged final estimates. However, this approach could be dangerous because it seems to hide any possible effect of the rate constant K_I although this latter could be needed in the kinetic model. The results obtained for the rubber mixture supports this conclusion. On the contrary, the use of the two other strategies enhanced the fact whether the constant K_I should or not appear in the model by, for instance, showing sensitivity coefficient of the parameter E_I of magnitude proportional to the effect of K_I . In addition, simulated isothermal cure rate data obtained with both Strategies II and III enable confirmation of the relative effect of K_I .
- When estimating for the six parameters, Strategy II magnifies all sensitivity coefficients compared to Strategy III. Besides, it resulted in a decrease in the magnitude difference between the largest and smallest coefficient, thus decreasing the condition number.
- Estimates from Strategy III provided higher magnitudes for the simulated isothermal cure rate data than those from Strategy I (at equal temperatures). Using estimates from Strategy II, the magnitudes reached by the simulated isothermal cure rate data depended on the mixture investigated.

These observations provide some insight into the three estimation strategies. In addition, one may deduce that Strategy I should be avoided. However, these conclusions do not allow for the determination of the procedure that reproduces experimental data most accurately. Therefore, with an aim of recommending which estimation strategy should be used, for each set of final estimates (run 6) obtained for each of the three strategies, the sum-of-squares errors S_1 , S_2 and S_3 (associated with each of the three strategies) were computed, along with the associated Root-Mean-Square errors. A summary of the results is given in Table 6.7. Note

that the RMSs are also given as a percent of the maximum increase in the measured variable. The best estimation strategy is the one that globally minimizes the three objective functions, e.g. minimizes the sum of RMSs defined by Σ RMS in Table 6.7.

Table 6.7 K&S estimation results – Summary (S_1 , S_2 and S_3 are the OLS errors resulting from application of Strategies I, II, and III, respectively).

Using estimates obtained with Strategies: →	Epoxy			Rubber			Polyester		
	I	II	III	II	II	III	I	II	III
S_1 (min^{-1}) ²	0.07*	0.19	0.24	4.71*	8.52	8.35	18.87*	17.24	380
RMS₁ (min^{-1})	0.0075	0.0123	0.0138	0.0654	0.0880	0.0871	0.0473	0.0452	0.2122
RMS₁ (% [Δv_{max}] _{av})	2.07	3.41	3.81	6.61	8.89	8.80	4.05	3.88	18.19
S_2 (min^{-1}) ²	0.201	0.07*	0.147	112	14.55*	10.50	35.5	16.13*	22.1
RMS₂ (min^{-1})	0.0127	0.0075	0.0108	0.3189	0.1150	0.0978	0.0649	0.0437	0.0512
RMS₂ (% [Δv_{max}] _{av})	3.51	2.07	3.00	32.25	11.62	9.87	5.56	3.75	4.39
S_3	0.85	0.35	0.10*	434	6.74	2.06*	22.9	5.57	2.3*
RMS₃	0.0261	0.0167	0.0087	0.6278	0.0782	0.0433	0.0521	0.0257	0.0165
RMS₃ (% $\Delta\alpha_{max}=1$)	2.61	1.67	0.87	62.78	7.82	4.33	5.21	2.57	1.65
ΣRMS (%)	8.19	7.15	7.68	101.64	28.33	23.00	14.82	10.20	24.23

* Values of the errors S_1 , S_2 and S_3 shown in **bold** were the output of the runs # 6 in Tables 6.3 to 6.5.

Comparing the values of the sum of RMSs among each other, one can distinguish that the kinetic parameter values estimated applying Strategy II globally allow for the best errors in the case of the epoxy and polyester samples. The RMS errors generated are all below four percent of the corresponding maximum increase in the measured variable. Those values indicate that the models simulate experimental cures relatively well for both materials. Figures 6.27 to 6.30 illustrate for these two thermosetting materials the reaction rate and degree of cure simulated using the K&S estimates obtained applying Strategy II. As one can see, the K&S model (which could have been simplified in the epoxy case, as discussed in the results associated with Strategy II) is an appropriate choice for the kinetic characterization of both resin compounds. The model is not as suitable for the polyester than for the epoxy compound due to the much higher increase in cure rate developed during curing in that case.

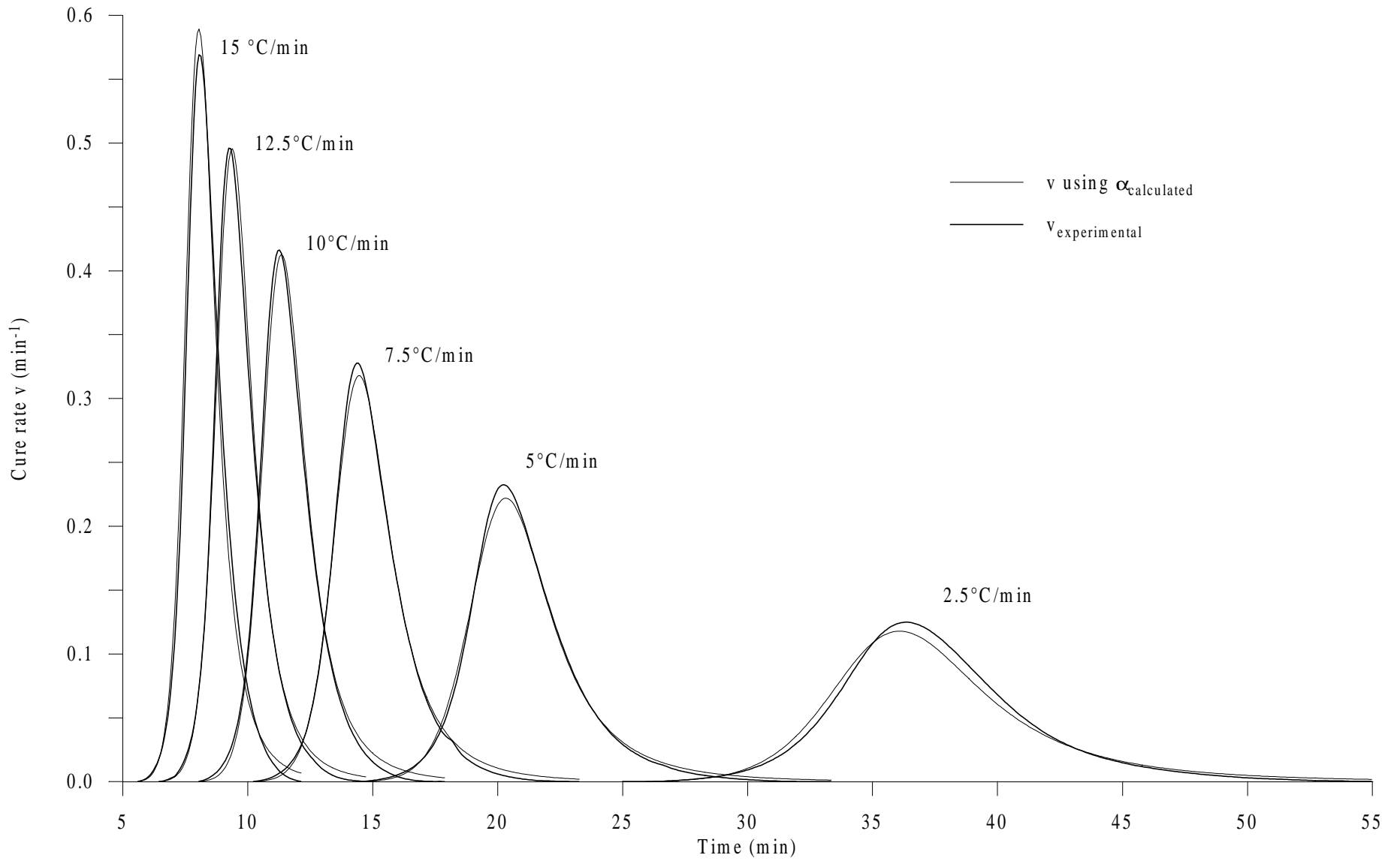


Figure 6.27 Simulation of the cure rate using estimates obtained with Strategy II - Epoxy compound.

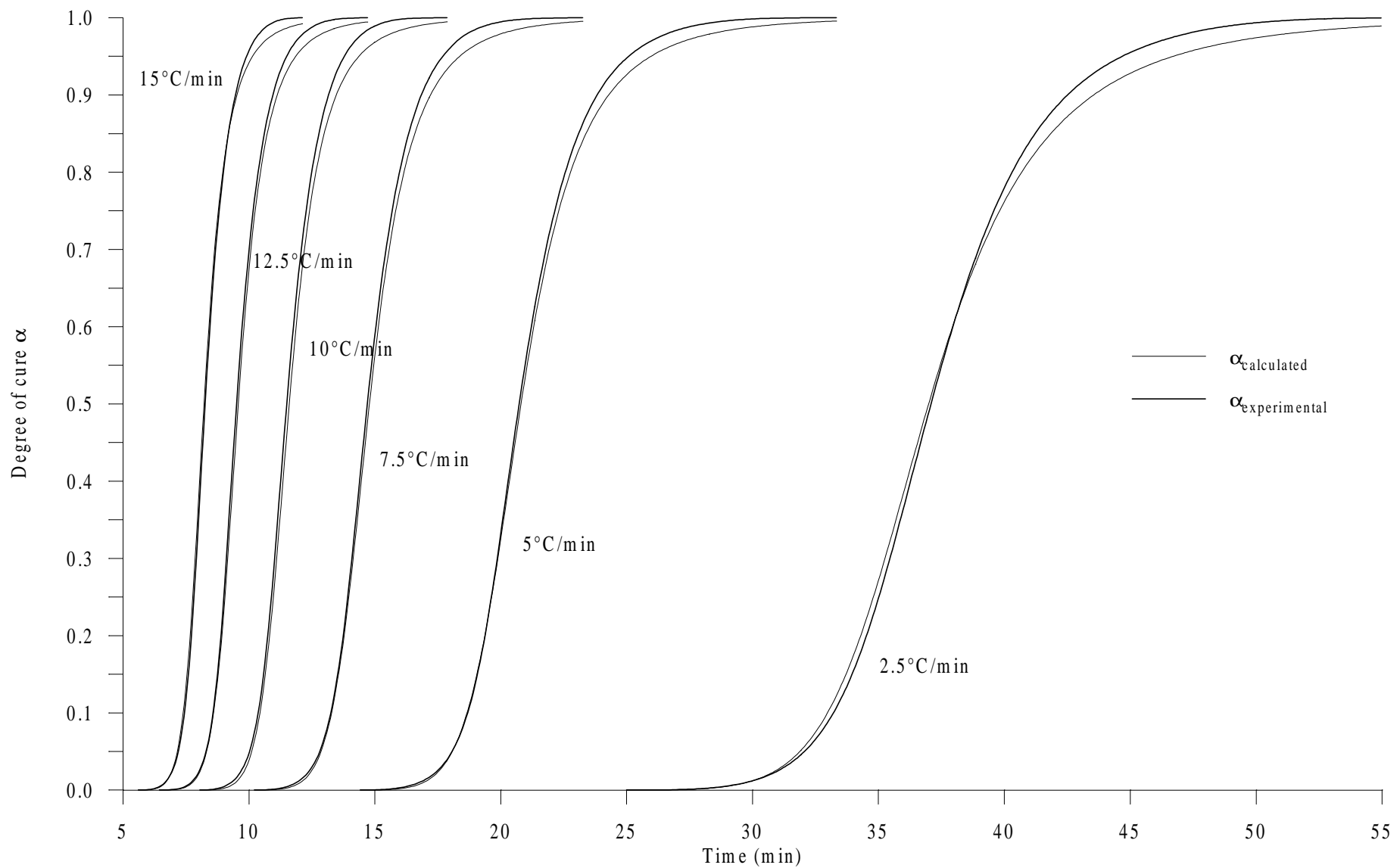


Figure 6.28 Simulation of the degree of cure using estimates obtained with Strategy II - Epoxy compound.

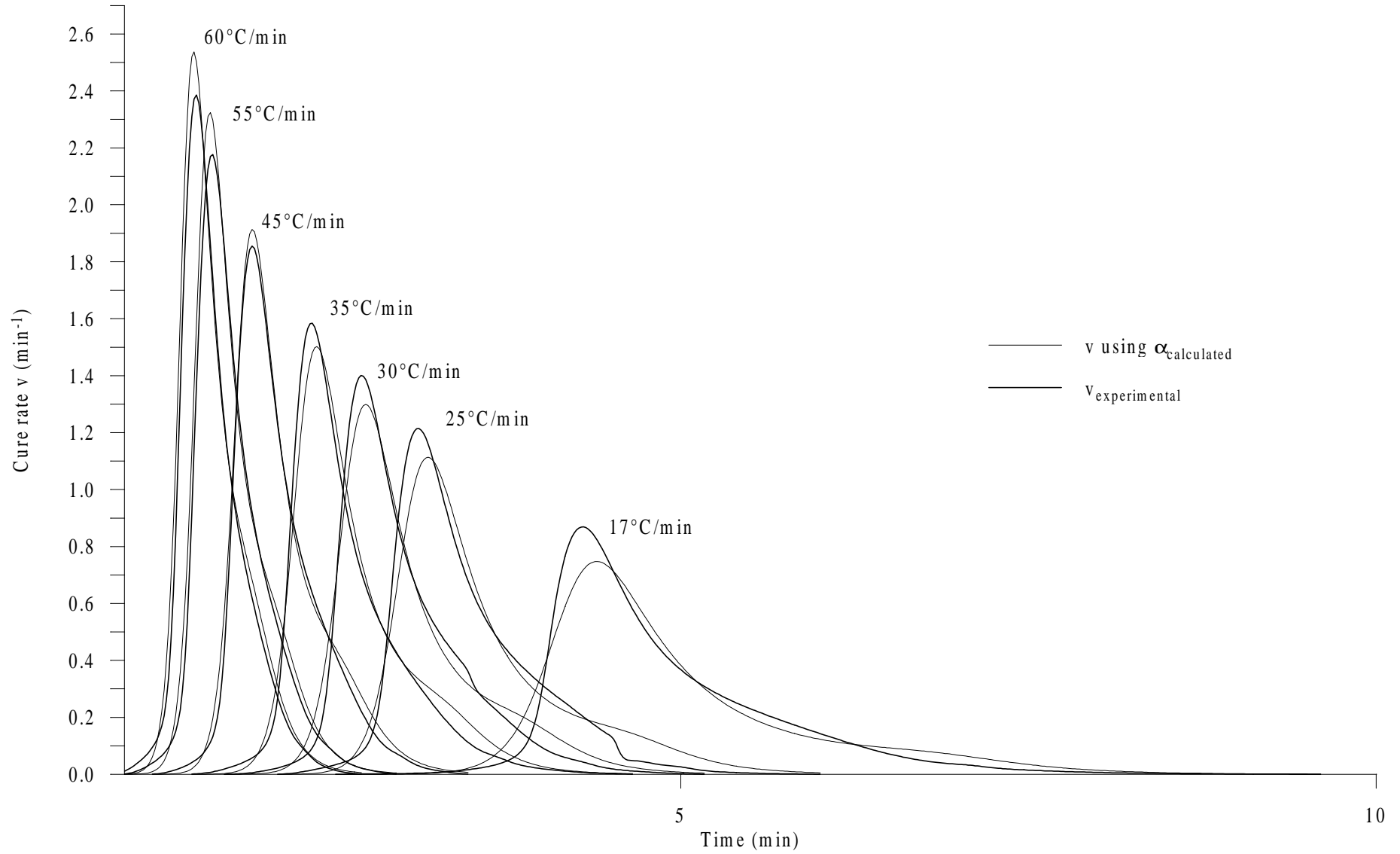


Figure 6.29a Simulation of the cure rate using estimates obtained with Strategy II - Polyester compound (Experiments from 60°C/min to 17°C/min).

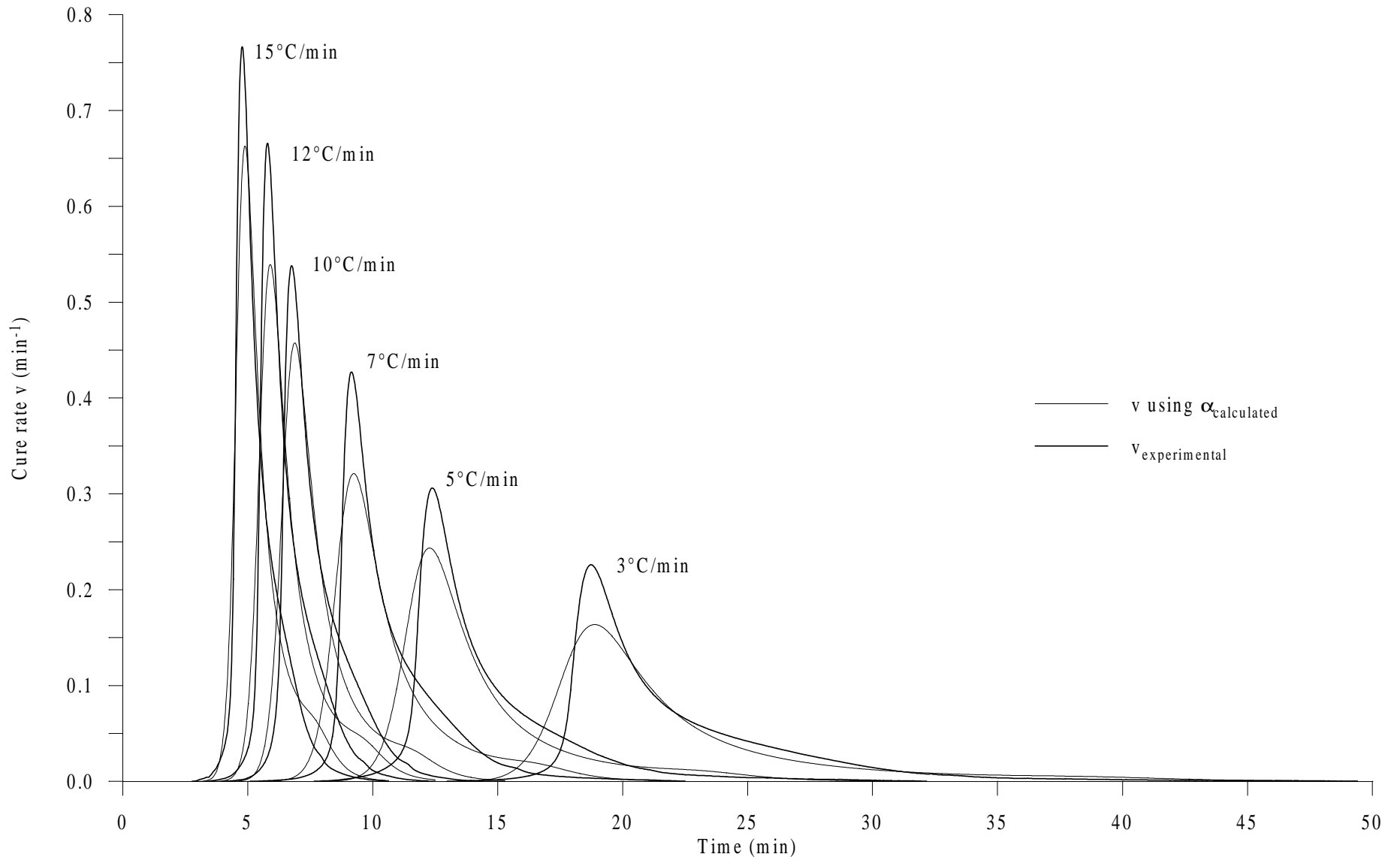


Figure 6.29b Simulation of the cure rate using estimates obtained with Strategy II - Polyester compound (Experiments from $15^\circ\text{C}/\text{min}$ to $3^\circ\text{C}/\text{min}$).

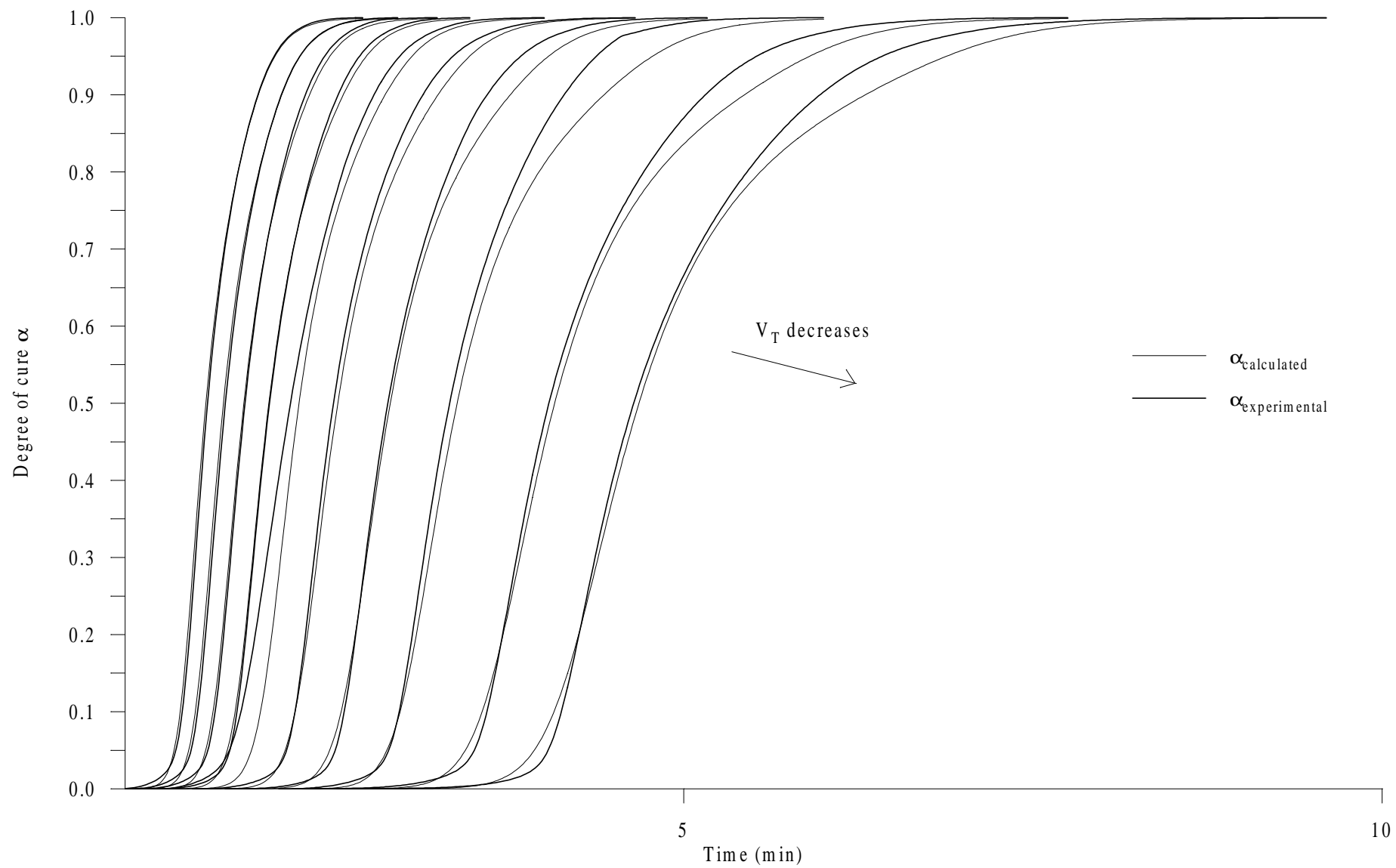


Figure 6.30a Simulation of the degree of cure using estimates obtained with Strategy II - Polyester compound (Experiments from 60°C/min to 17°C/min).

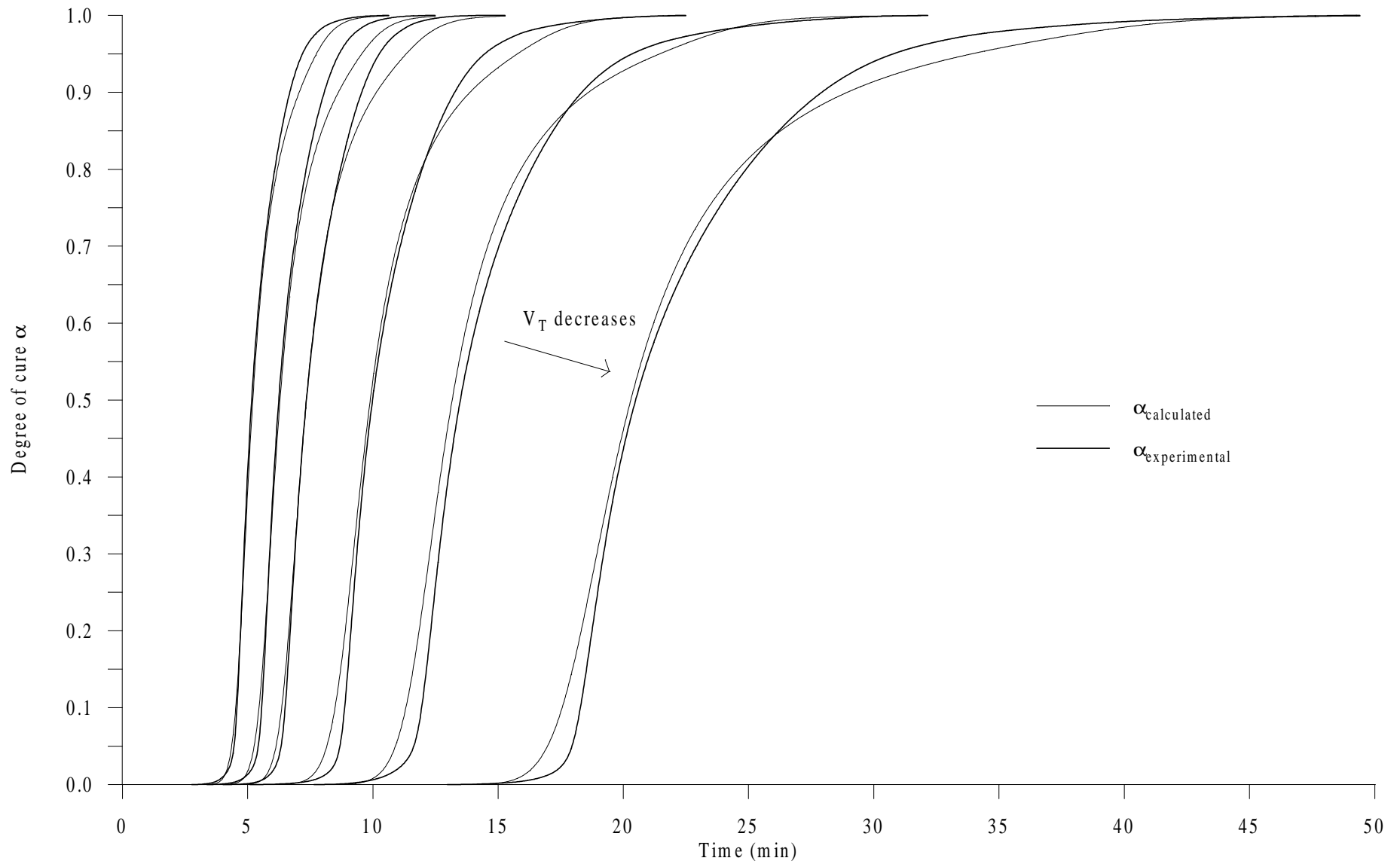


Figure 6.30b Simulation of the degree of cure using estimates obtained with Strategy II - Polyester compound (Experiments from 15°C/min to 3°C/min).

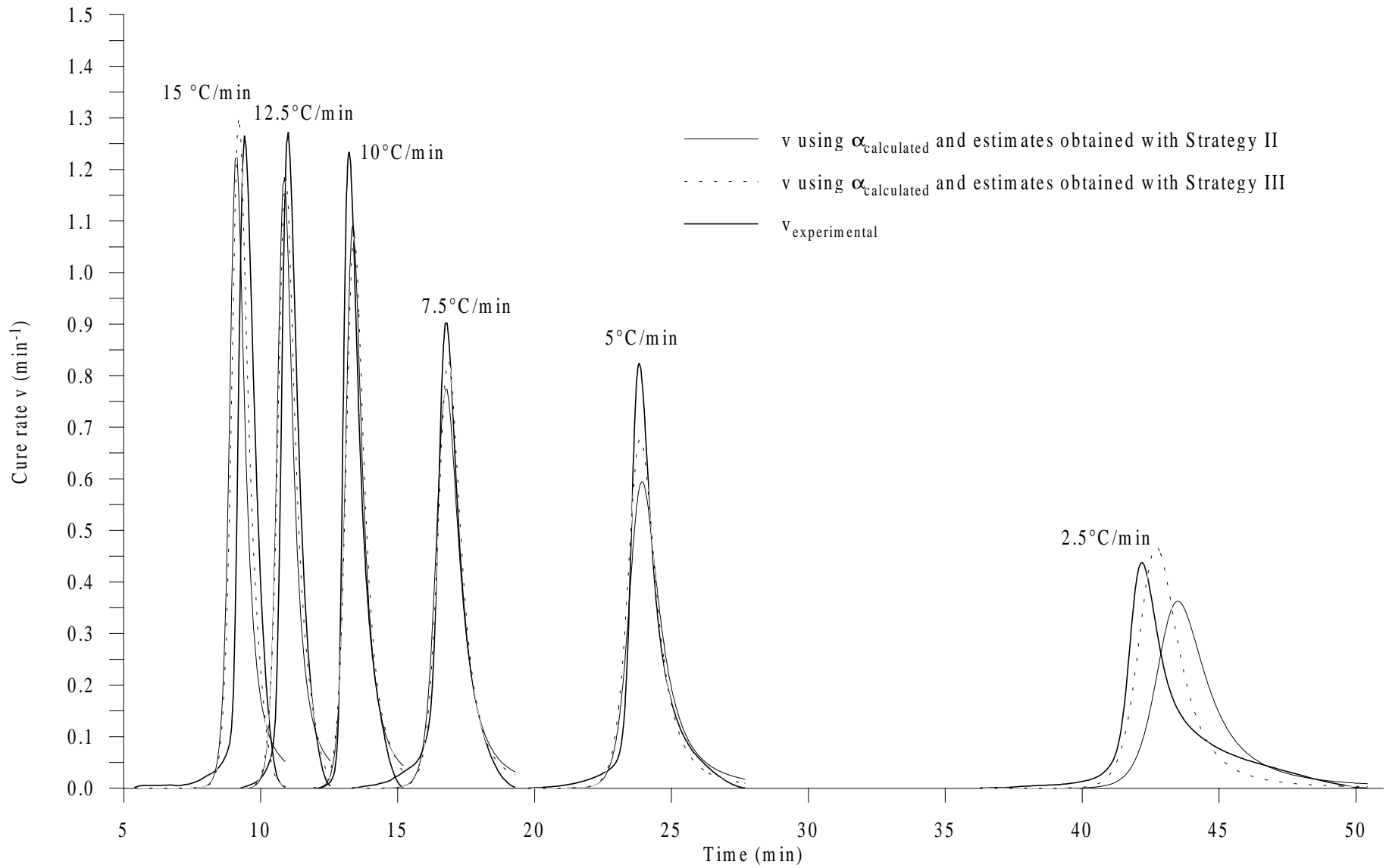


Figure 6.31 Simulation of the cure rate using estimates obtained with Strategy II and III - Rubber compound.

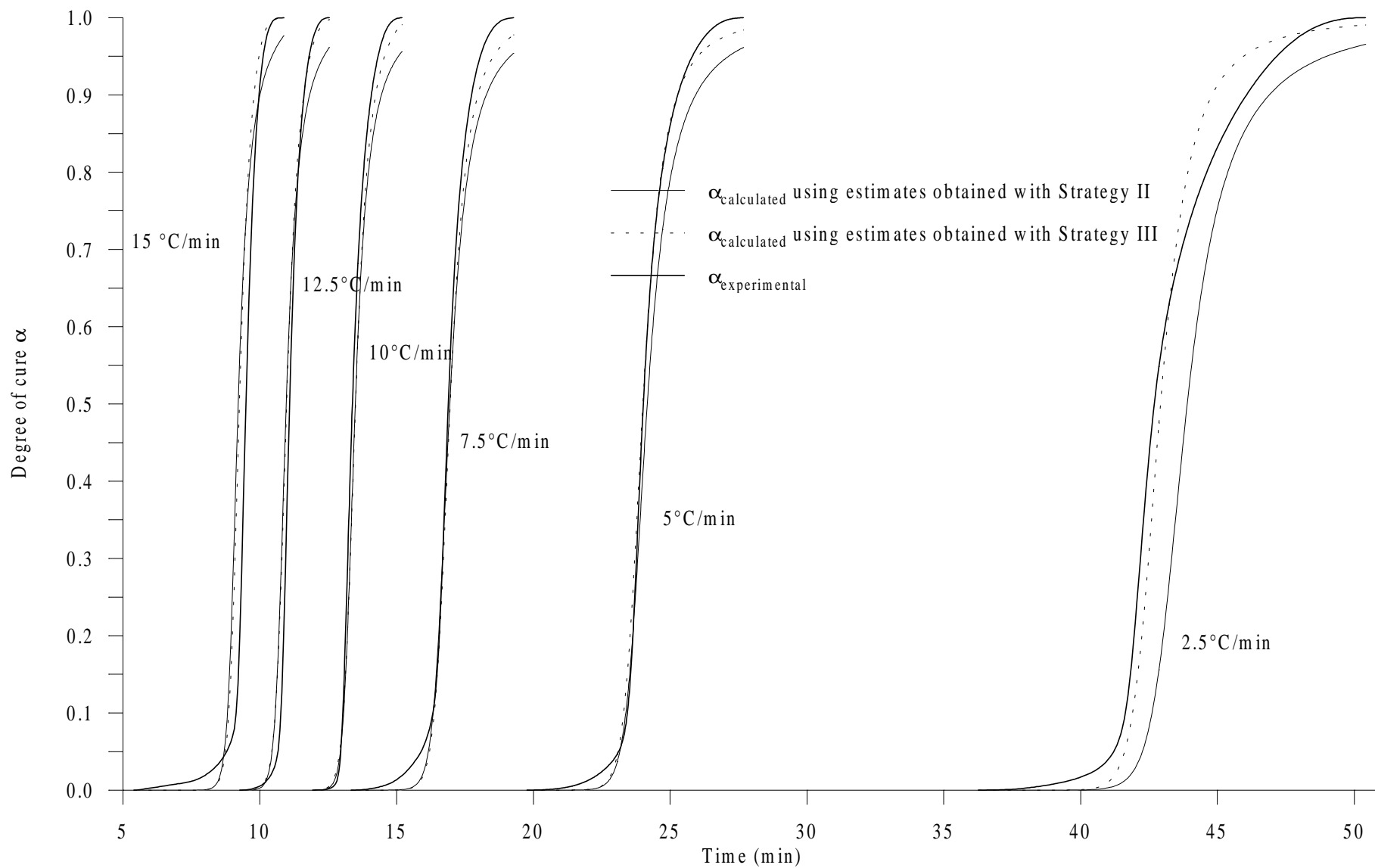


Figure 6.32 Simulation of the degree of cure using estimates obtained with Strategy II and III - Rubber compound.

For the rubber compound, the use of estimates from Strategy III gives smaller errors than the use of those from Strategy II. The RMS errors are substantially larger than for the epoxy and polyester mixtures and go up to nearly 10% of the maximum increase in cure rate when considering Strategy II to compute the dependent variable. This confirms the fact that the K&S model is generally inappropriate for the curing characterization of rubber mixtures (Garnier, 1990). Note that the results from Strategy II are consistent for the three sum-of-squares errors, which is not the case for those from Strategy I. The maximum error generated from using estimates obtained with Strategy II reaches 12% of the maximum increase in the measured quantity. The reaction rate and degree of cure simulated using both sets of estimates obtained applying Strategy III and II are compared with the experimental data in Figs. 6.31 and 6.32. One can see in the rubber case the larger discrepancies between simulated and experimental data than in the epoxy or polyester case.

- **Conclusion**

This work shows that the estimation strategy associated with the study of the K&S model should be based on the rate of cure as the measured quantity and on the assumption that only time and temperature are known (Strategy II). This strategy has demonstrated its efficiency on the curing characterization of both the epoxy and polyester mixtures, for which the K&S model seems adequate. Note that when the goal is to perform a numerical simulation of thermal fields inside a composite material being cured, the procedure used to resolve the kinetic equation (which is coupled to the energy equation) also follows Strategy II. The estimation strategy recommended here is, therefore, in good agreement with the latter use of the estimated kinetic parameters.

In the case of the kinetic characterization of the rubber mixture, the recommended procedure provided consistent but higher errors than the estimation strategy based on the degree of cure measurements. This might indicate that the K&S model is not appropriate.

Regarding the significance of using the complete K&S model, this study reveals that the rate constant K_I could have been neglected with nearly no lost in accuracy for the epoxy compound. In other words, a model based on the separation of the dependent variables T and α could have been used for this compound. In this particular type of model, the one from Jarny et al. (1993) has been shown to take into account small deviations encountered in cure rate initial values as temperature increases. As this was the case for the polyester compound,

the model from Jarny et al. is therefore anticipated to be suitable for both the epoxy and the polyester kinetic characterization. Because this is a simpler model than the K&S form, it is thought to be a potential alternative.

6.5.2 Inhibition Time Estimation

Recall that the objective here was to minimize the sum-of-squares, S_{ind} , defined in Eq. (6.13) for the determination of the parameters T_{ref} and B governing the inhibition time model. In performing the minimization of S_{ind} several combinations of T_{ref} and B provided the same optimal value for the objective function. One GA run was performed only to generate a set of optimal solutions. Figures 6.33 to 6.35 show for the three thermosetting materials the linear regressions obtained between the two parameters. Then, using one possible solution, simulations of inhibition time and temperature were generated and are illustrated in Figs. 6.36 to 6.38. The values for the inhibition times calculated for all experiments associated with the three resins are given in Table 6.8. One can see that the inhibition models are quite good for both the epoxy and the polyester compounds. The average error between experimental and calculated induction periods is only 6.6 s and 12.6 s for the first and second resin, respectively. In the case of the rubber compound, this error attains an average value of 44.4 s. The major source of error is the difference between the experimental and calculated inhibition time for the experiment at 15°C/min. It is believed that the experimental data contains a large bias. Furthermore, in all experiments, it is possible that several chemical reactions are taking place within the sample before curing actually starts, causing then the model not to be adequate and thus inducing biases attached to the determination of the experimental inhibition time. Those effects have been underlined by Garnier (1990).

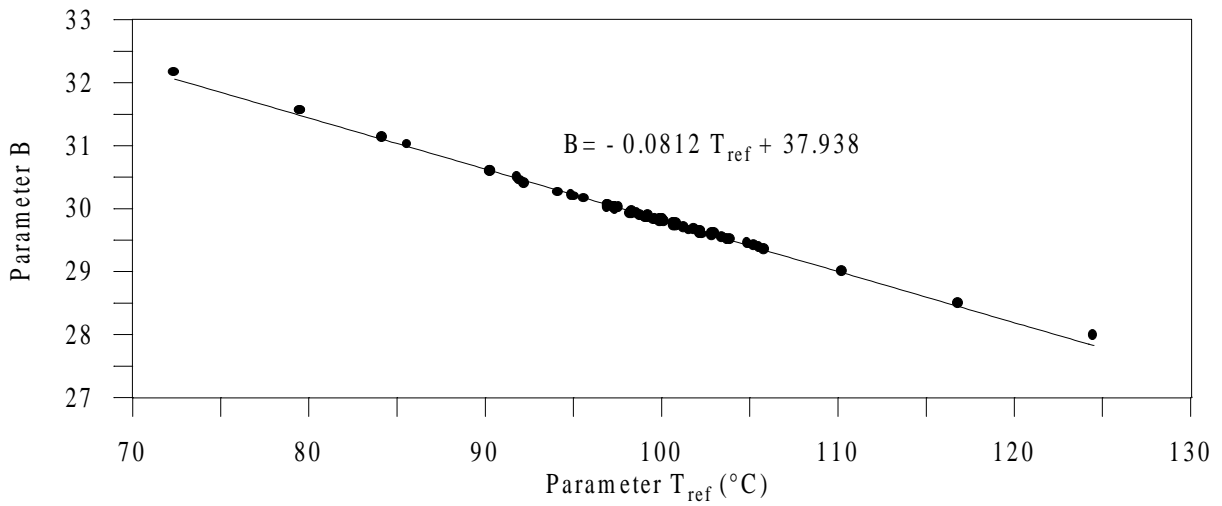


Figure 6.33 Linear regression between the inhibition time model parameters - Epoxy compound.

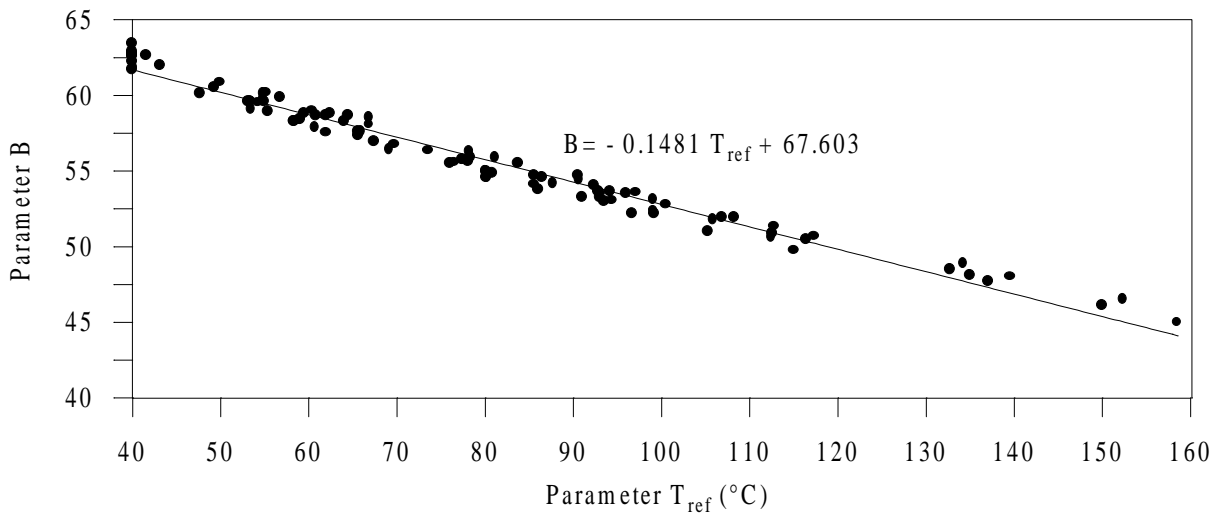


Figure 6.34 Linear regression between the inhibition time model parameters - Polyester compound.

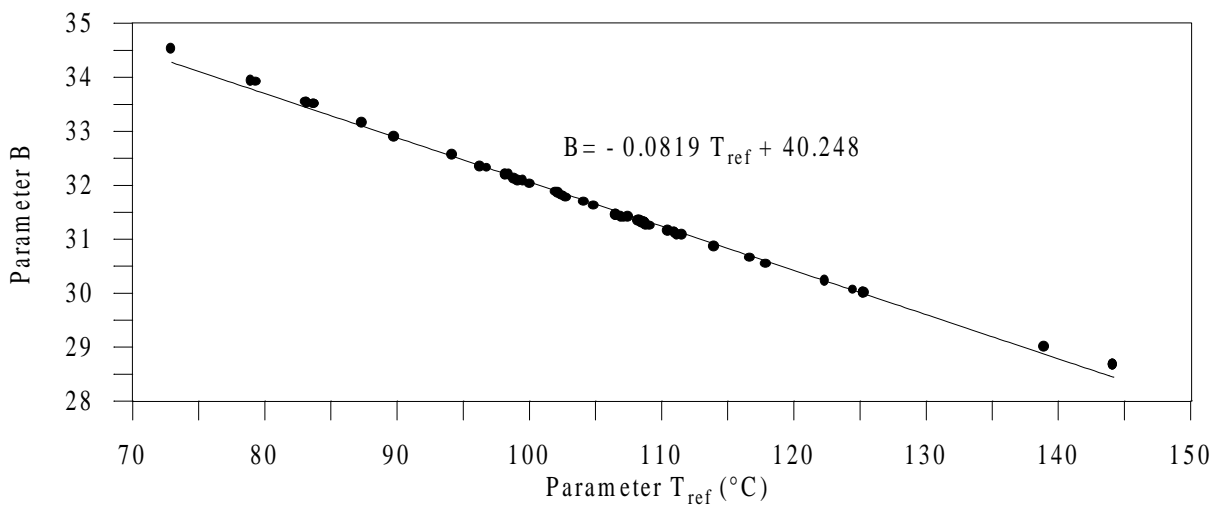


Figure 6.35 Linear regression between the inhibition time model parameters - Rubber compound.

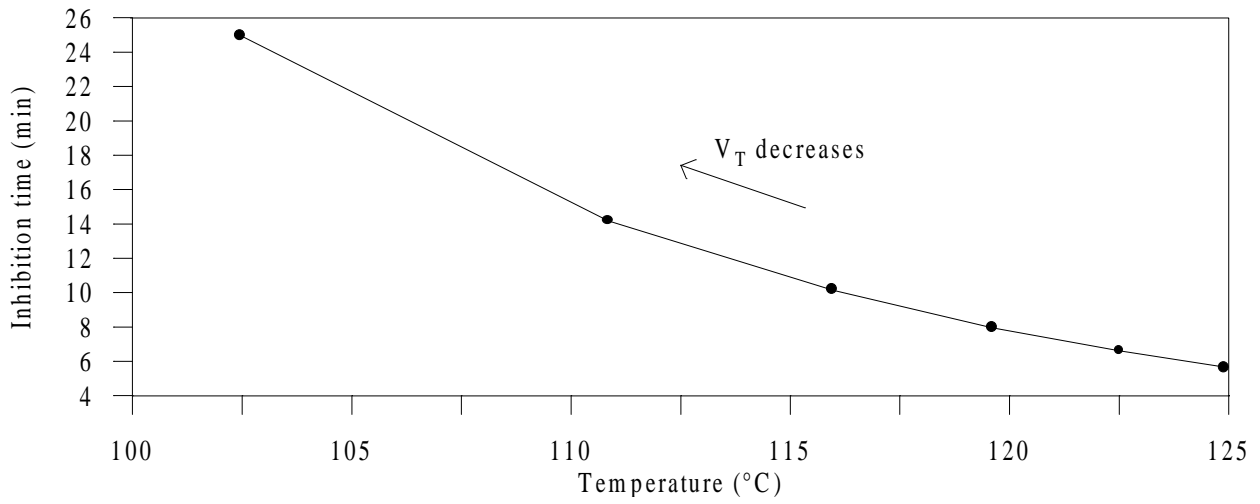


Figure 6.36 Simulation of inhibition time vs. temperature – Epoxy compound.

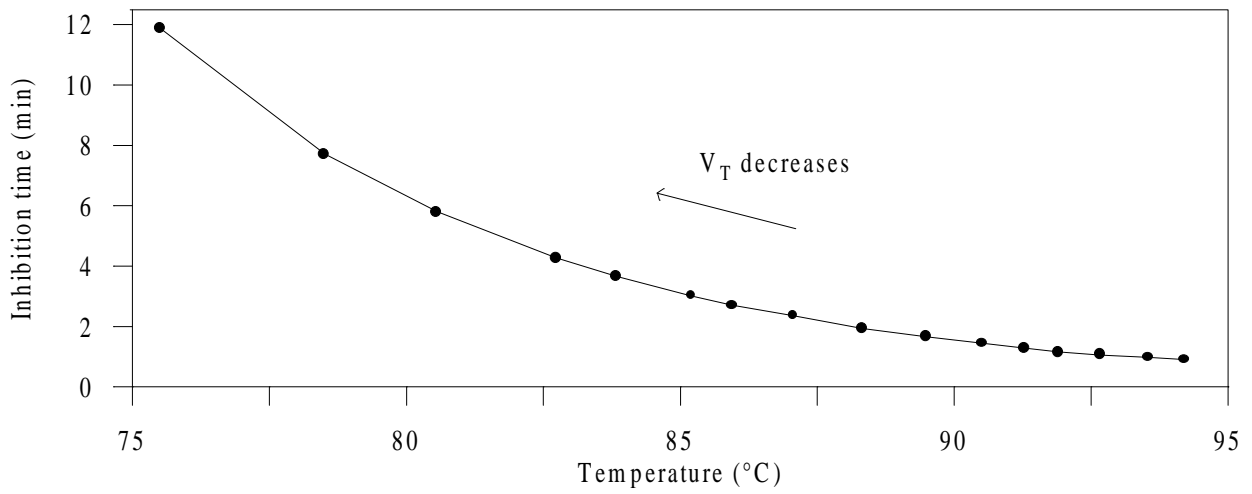


Figure 6.37 Simulation of inhibition time vs. temperature – Polyester compound.

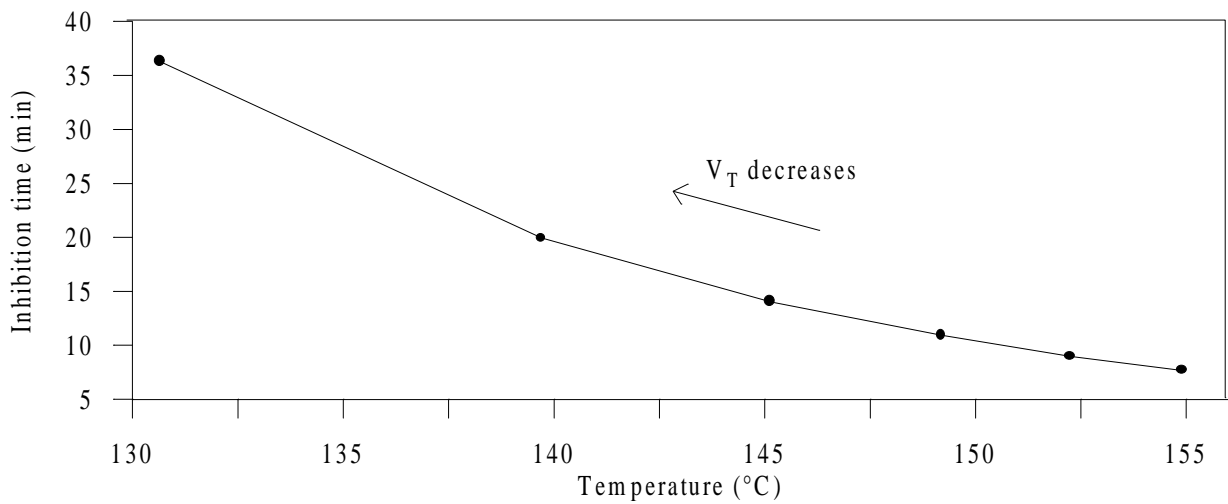


Figure 6.38 Simulation of inhibition time vs. temperature – Rubber compound.

Table 6.8 Inhibition time estimation results.

Epoxy			Rubber			Polyester		
V_T (°C/min)	$t_{ind\ exp.}$ (min)	$t_{ind\ calc.}$ (min)	V_T (°C/min)	$t_{ind\ exp.}$ (min)	$t_{ind\ calc.}$ (min)	V_T (°C/min)	$t_{ind\ exp.}$ (min)	$t_{ind\ calc.}$ (min)
2.5	24.99	24.98	2.5	36.27	36.26	3	12.97	11.88
5	14.42	14.17	5	19.77	19.94	5	7.65	7.70
7.5	10.22	10.13	7.5	13.33	14.02	7	5.08	5.79
10	8.05	7.96	10	11.3	10.92	10	4.02	4.27
12.5	6.44	6.60	12.5	9.27	8.98	12	3.37	3.65
15	5.60	5.66	15	5.40	7.66	15	2.77	3.01
$(\Delta t_{ind})_{average}$ (min)		0.11	$(\Delta t_{ind})_{average}$ (min)		0.74	17	2.52	2.70
		6.6			44.4			
						20	2.27	2.35
						25	2.10	1.93
						30	1.72	1.65
						35	1.48	1.44
						40	1.19	1.28
						45	1.20	1.15
						50	1.05	1.05
						55	1.00	0.97
						60	0.93	0.90
						$(\Delta t_{ind})_{average}$ (min)		0.21
								12.6
								(s)

6.5.3 Conclusion

Overall, the results illustrate that the proposed GAMAIN program is an effective tool in the simultaneous determination of kinetic parameters involved in both the K&S model and the associated inhibition time model. The fact that the GA did not converge when the six kinetic parameters of the K&S model were simultaneously estimated (Strategies II and III) should be taken care of by defining a more suitable convergence criterion; that is, a criterion adapted to the extreme cases of very small magnitude for the lowest sensitivity coefficient, and large magnitude difference between the highest and lowest sensitivity coefficients. The definition of such adapted convergence criterion is one of the recommendations of this research.

An important advantage for the use of GAs in the application presented here is its attribute to overcome difficulties due to correlation(s) inherent to the models investigated.

CHAPTER 7

Conclusions and Recommendations

The focus of this study was on the development of systematic and reliable methodologies for both Experimental Design Optimization (EDO) for thermal property estimation, and Simultaneous Parameter Estimation (SPE) for thermophysical characterization of composite materials. With an aim to overcoming the limits of commonly used techniques in EDO and SPE, parametric studies and gradient-based methods, respectively, Genetic Algorithms (GAs) were investigated for use as a strategy for both areas of interest. The overall objectives were on developing a robust GA-based methodology allowing for practical applications and general use of EDO and SPE. This work was associated with a dual US-French PhD program between the Mechanical Engineering Department of Virginia Tech (VT), USA, and the Laboratoire de Thermocinétique de l'ISITEM (LTI) of the University of Nantes, France.

Note that it is not intended to assert that the applications reported in this dissertation were thoroughly analyzed in terms of EDO and SPE theoretical considerations. Rather, the emphasis was on illustrating the potential of GAs on various applications. All optimization and estimation problems treated involved the maximization of the D -optimality criterion, and the minimization of the Ordinary Least-Squares (OLS) estimator, respectively. The following provides summary and conclusions of the work accomplished for this dual program in terms of the Genetic Algorithms developed and the thermophysical characterizations performed for different composite materials. Then, other thermophysical characterizations of various material types, which have been performed using the Genetic Algorithms developed in the current work, are reported. Finally, the overall conclusions are specified, and some recommendations are suggested.

7.1 Genetic Algorithms

Three different real-encoding GAs were developed over the course of this work, each time improving the last version over the previous one. The first algorithm developed was a standard GA featuring a Basic Elitist strategy (BEGA). The second algorithm implemented an Extended Elitist strategy (EEGA). Finally, the third algorithm (GA_3) benefited from the knowledge gained in the GA field, as, for instance, more appropriate genetic operators (particularly for the real-encoding used) were applied. GA_3 was designed as a general-purpose computer program constructed in two parts, an invariant and an adaptation part, following the structure of the program CONDUCT developed by Patankar (1991). Two versions were developed. The GAMAIN version was written for the analysis of any optimization/estimation problems for which a mathematical direct model is to be provided by the user. Its performance were illustrated on the optimization of a highly multimodal mathematical function. The second version, GA_CONDUCT, combines the GA_3 with a finite-difference program based on an extension of the program CONDUCT. This version allows for any optimization/estimation problems in the field of conduction and duct flow heat transfer in two-dimensional rectangular or cylindrical geometry.

The results obtained using the GA_3 showed that this algorithm performed very well. However, the weakness of the convergence criterion was stressed in estimation applications in which the sensitivity to some parameters was very small.

7.2 Thermophysical Characterization of Composite Materials

Towards the appraisal of using GAs as both EDO and SPE methodologies, two optimization/estimation test problems previously solved in the literature were first investigated, using successively the BEGA and EEGA (Garcia and Scott, 1998; Garcia et al., 1998). These problems involved the thermal characterization of anisotropic carbon/epoxy composite materials. The experiments analyzed included one- and two-dimensional optimal designs performed by Moncman (1994) and Hanak (1995), respectively. In the one-dimensional design (Moncman, 1994), sensor location and heating time were optimized for the simultaneous estimation at ambient temperature of the thermal conductivity through the fiber plane, k_x , and the volumetric heat capacity, C . In the two-dimensional design (Hanak, 1995), four parameters involving sensor location, heating time and heating area, were

optimized in experiments used to simultaneously estimate at ambient temperature both thermal conductivities perpendicular and parallel to the fibers, k_x and k_y , and the volumetric heat capacity, C . In both EDOs, the BEGA and EEGA were found to outperform the traditionally used parametric study. The simple one-dimensional estimation problem provided a good basis to gain confidence in using the EEGA to perform SPE. The following conclusion can be made regarding the two-dimensional estimation results: because of strong correlations between the thermal conductivities k_x and k_y , the modified Box-Kanemasu method was found not to converge (even though three sensors and initial estimates of the unknown properties very close to their “true” values were used); whereas the EEGA allowed the simultaneous estimation of the three thermal properties, k_x , k_y and C , from the use of one sensor.

A study was also conducted to evaluate the effects of the optimality criterion used for the experimental design on the accuracy of the estimated thermal properties. The one- and two-dimensional experimental designs were optimized using the A -, D -, and E -criteria. Based on these optimal designs, simulated data were generated using an analytical mathematical model of the design. The thermal properties were then estimated from the simulated data from each experimental design, and the confidence intervals of the resulting estimates were compared. Based on the obtained results, D -optimality was confirmed to provide the highest accuracy overall. A further analysis was performed to show the benefit from optimizing experimental designs. From this analysis, the following conclusions were drawn: 1) optimality criteria based on the D -criterion and on the condition number of the Fisher information matrix ($\mathbf{X}^T\mathbf{X}$) are equivalent; 2) minimum correlation does not imply maximum accuracy; and 3) large magnitude difference between the sensitivity coefficients has more negative effect on the accuracy of the estimates than correlation between the parameters

A variety of advanced EDO and SPE problems for the thermal characterization of anisotropic carbon/epoxy composite materials were then investigated using the GACONDUCT general-purpose program. As part of an industrial contract, the thermal properties k_x , k_y and C , were simultaneously estimated over the temperature range [30-150°C] (Garcia et al., 1999a). Taking advantage of the estimation problem similarities with the two-dimensional transient heat transfer analysis performed by Hanak (1995), the experimental setup was based on the same basic experimental design, and the same nondimensional optimal experimental parameters were used. The experiments were conducted at different initial temperatures ranging from 30 to 150°C. The properties were estimated as constants and linear

regressions were generated to express the properties as functions of temperature. The results agreed very well with both a one-dimensional analysis performed apart on the same materials, and previous published results for similar composites.

This study was then used as a basis to investigate the optimization of the experimental design for the simultaneous estimation over the range [25-150°C] of the thermal properties k_x , k_y and C , as temperature-dependent, and the contact resistance between the composite sample and the aluminum components used in the setup (R_c). The dependence on temperature was characterized by piece-wise linear functions with temperature, using two parameters for both thermal conductivities and four parameters for the volumetric heat capacity. Nine thermophysical parameters (k_{x25} , k_{x150} , k_{y25} , k_{y150} , C_{25} , C_{75} , C_{110} , C_{150} , and R_c) were therefore defined to be simultaneously estimated. The experimental parameters optimized were the location of the sensor placed on the composite, the heating length over the sample, the heating and cooling times according to a specific heating law, which was designed as a double heat flux step, and the overall total experimental time. The optimal setting was verified to provide the best information against two non-optimal designs. The nine thermophysical parameters were then simultaneously estimated from simulated data with noise generated from the optimal design. The estimates were found to be in adequacy with the initial values used to generate the simulated data.

The last application dealing with the thermal characterization of anisotropic carbon/epoxy composites involved the simultaneous estimation over the range [100-130°C] of seven thermophysical parameters (k_x , k_{y100} , k_{y130} , C_{100} , C_{115} , C_{130} , and R_c) associated with the processing of composite materials in two-dimensional RTM (Resin Transfer Molding) mold (Garcia et al., 1999b). This work was performed in cooperation with D. Lecoite (1999) as part of his PhD project at the LTI. The dependence on temperature for both the thermal conductivity parallel to the fibers, k_y , and the volumetric heat capacity, C , was characterized by piece-wise linear functions with temperature using two and three parameters for k_y and C , respectively. The results obtained were compared with those from Lecoite who used a parametric study to estimate k_y and R_c , assuming both k_x and C to be known. The simultaneous estimation of the seven thermophysical parameters was found to provide a set of estimates that allowed for a better fit of all experimental data from the different thermocouples than using the set of estimates from the parametric study.

From the applications described above, the following general conclusions can be drawn:
1) the properties k_x , k_y and C , were found to increase with temperature; and 2) the thermal

conductivity parallel to the fiber plane, k_y , was found to be larger and to increase more with temperature than the transverse to the fiber plane, k_x .

The analysis of SPE problems dealing with the kinetic characterization of the curing of composite matrix materials, namely thermosetting materials, was another specific objective of this research. The model from Kamal and Sourour (1973) was investigated for the prediction of the curing process of three thermosetting resins, an epoxy, a polyester and a rubber mixture (Garcia et al., 1999c). The GAMAIN general-purpose program was used for the simultaneous estimation of the six parameters involved in the kinetic model. Such an estimation has not previously been attempted. The estimation problem was formulated according to three strategies that differed from the measured quantity considered (rate of cure or degree of cure) and/or the experimental input (time and temperature or degree of cure and temperature). For the kinetic characterization to be complete, a model for the determination of the inhibition time was constructed based on the model described by Bailleul (1997). The following conclusion was drawn from the obtained results: the estimation strategy associated with the study of the Kamal and Sourour model should be based on the rate of cure as the measured quantity and on the assumption that only time and temperature are known.

7.3 Other Thermophysical Characterizations Using GAs

The GAs developed in this work have been applied to various thermophysical characterizations in cooperation with other researchers. In these studies, the use of GAs was necessitated from the existence of strong correlations that were found to make gradient-based methods not to converge. Note that these studies were not described in this dissertation. Only brief overviews are given below and references are provided for more in-depth descriptions.

The EEGA was used for the simultaneous estimation of four thermal and radiative properties of an insulative foam material (polystyrene) (Guynn, 1996; Garcia et al., 1998). This study was realized in cooperation with J. Guynn as part of his master's thesis in the Mechanical Engineering Department at VT. The properties included the (effective) thermal conductivity, volumetric heat capacity and extinction coefficient of the material, and the volumetric heat capacity of the heater. The properties were estimated as constants at ambient

temperature from a one-dimensional transient analysis of combined conduction and radiation heat transfer.

The EEGA was also used for the thermal analysis of a complex aerospace structure which involved composite/honeycomb panels (Hanuska, 1998; Hanuska et al., 1999). One- and two-dimensional models were optimized for the simultaneous estimation of up to eight thermal properties of the different components forming the structure. The properties were estimated as constants at different temperature levels.

The estimation methodology featured in GAMAIN is currently being used for the thermophysical characterization of thin layers (Orain et al., 1999). Here, the coating material thermal conductivity as well as two contact resistances are to be estimated for different values of the coating thickness. This study is realized in cooperation with S. Orain as part of his PhD at the LTI.

7.4 Overall Conclusions

This study has provided demonstrative examples that showed that both areas of interest in this research, EDO and SPE, can definitely benefit from the robustness and efficiency of GAs. In the EDO field, the use of GAs allows for a reliable approach that outperforms the parametric study as the number of design variables increases. In the SPE field, the most tangible artifact of this work is the successful simultaneous estimation of correlated parameters. The use of GAs actually finds all its rationale for such ill-conditioned estimation problems. In addition, by enabling the SPE of several parameters, the use of GAs implies considerable experimental and time cost savings, along with the possibility to avoid bias induced by setting presumably known parameters to nominal values. However, compared to traditional parameter estimation inverse methods, GAs present a highly time consuming nature, stressing thus the use of these algorithms as the alternative when the traditional inverse methods do not work.

7.5 Recommendations

This research represents a large step forward using a probabilistic GA-based method for the thermophysical characterization of composite materials. The following recommendations are made to improve and broaden the scope of this research.

- In SPE applications, when there was very little sensitivity of the measured quantity to one parameter, the GA run would generally not converge, e.g. the run would terminate because the maximum allowable number of generations was reached. It is therefore necessary to define a convergence criterion that is appropriately weighted by the sensitivity to the parameters. This could also apply for EDO applications.
- The Confidence Intervals (CIs) of the final estimates should include uncertainties in all other “presumably” known parameters that are set to nominal values. The subroutine that computes the CIs according to Eq. (3.16), could be adequately modified to translate such uncertainties (which, for instance, could be given by the user as a percentage of the nominal value) into uncertainties in the unknown parameters. If no functional between unknown and known parameters exist, then, an approximate mathematical relation could be defined.
- Efforts could be taken for the analysis of EDO for the most accurate estimation of kinetic parameters. Ultimately, the goal would be to be capable of performing the unique EDO that would allow for the most accurate simultaneous estimation of both the thermal properties and the kinetic parameters.
- The GA_3 genetic scheme is by no means exhaustive. Other GAs could be used but more particularly, it is believed that the combination of the GA_3 scheme with a local approach could be very powerful. The local approach could be performed using either a gradient-based method or a zeroth-order method like, for instance, the sequential simplex method [which is also derivative free calculation and is therefore not limited by correlated parameters (Haftka and Gurdal, 1992)]. The use of such hybrid GA would exploit the

advantages of both the GA and the local methods and seems a promising strategy for solving complex SPE problems with interesting computation cost. The hybridization between both methods could be either sequentially or in batch.

Bibliography

- Alifanov O. M., Artyukhin E. A. and Rumyantsev S. V., 1995, *Extreme Methods for Solving Ill-Posed Problems with Applications to Inverse Problems*, Begell House, Wallingford, UK.
- Amiaud S., 1993, "La cuisson du caoutchouc: étude de la cinétique de réticulation," Rapport de DEA Thermique, ISITEM/LTI, Université de Nantes, France.
- André S. and Maillet D., 1999, "Méthode Flash et Estimation de Paramètres", *Proc. (atelier) Ecole d'hiver METTI'99*, Bolquère, France.
- Arora J. S., 1989, *Introduction to Optimum Design*, McGraw-Hill, NY, USA.
- Autrique L. and Souza de Cursi J. E., 1997, "On Stochastic Modification for Global Optimization Problems: An Efficient Implementation for the Control of the Vulcanization Process," *Int. Journal of Control*, Vol. 67, No. 1, pp. 1-21.
- Back T., 1994, "Evolutionary Algorithm: Comparisons of Approaches," in R. Paton, (ed.), *Computing with Biological Metaphors*, Chapman and Hall, Cambridge, UK.
- Bailleuil J. L., 1993, "Détermination de la Cinétique de Réticulation de la Résine DGEBA/DDA/BDMA," Rapport de DEA Thermique, ISITEM/LTI, Université de Nantes, France.
- Bailleuil J. L., 1997, "Optimisation du Cycle de Cuisson de Pièces Epaissees en Matériau Composite. Application à un Préimprégné Résine Epoxyde / Fibres de Verre," Thèse de Doctorat, ISITEM/LTI, Université de Nantes, France.
- Bailleuil J. L., Delaunay D. and Jarny Y., 1996, "Determination of Temperature Variable Properties of Composite Materials: Methodology and Experimental Results", *J. of Reinforced Plastics and Composites*, Vol. 15, pp. 479-496.
- Bard Y., 1974, *Nonlinear Parameter Estimation*, Academic Press, NY, USA.
- Beck J. V., 1966, "Transient Determination of Thermal Properties," *Nuclear Engineering and Design*, Vol. 3, pp. 373-381.
- Beck J. V., 1969, "Determination of Optimum, Transient Experiments for Thermal Contact conductance," *Int. J. Heat Mass Transfer*, vol. 12, pp.621-633.
- Beck J. V. and Arnold K. J., 1977, *Parameter Estimation in Engineering and Science*, John Wiley, NY, USA.
- Beck J. V., Blackwell B. and St. Clair C. R., 1985, *Inverse Heat Conduction – Ill Posed Problems*, Wiley-Interscience, NY, USA.

- Belegundu A. D., Murthy D. V., Salagame R. R. and Constans E. W., 1994, "Multi-Objective Optimization of Laminated Ceramic Composites Using Genetic Algorithms," *AIAA-94-4364-CP*, pp. 1015-1022.
- Bournez E., Raynaud M., Dupuy J. and Nicolle P., 1999, "Experimental Determination of Properties of a Thermoset Resin," *Proc. 24th Int. Thermal Cond. Conf & 12th Int. Thermal Expansion Symp.*, pp. 695-706.
- Box M. J. and Draper N. J., 1971, "Factorial Designs, the $X^T X$ Criterion and Some Related Matters," *Technometrics*, Vol. 13, No. 4, pp. 731-742.
- Box G. E. P. and Kanemasu H., 1972, "Topics in Model Building, Part II, on Nonlinear Least Squares," Tech. Report No. 321, University of Wisconsin, Dept. of Statistics, Madison, Wisconsin, USA.
- Brown L. D., Olkin I., Sacks J. and Wynn H. P., ed., 1985, *Jack Carl Kiefer Collected Papers III - Design of Experiments*, Springer-Verlag, NY, USA.
- Carroll D. L., 1996a, "Chemical Laser Modeling with Genetic Algorithms," *AIAA Journal*, Vol. 34, No. 2, pp. 338-346.
- Carroll D. L., 1996b, "Genetic Algorithms and Optimizing Chemical Oxygen-Iodine Lasers," *Development in Theoretical and Applied Mechanics*, Vol. 18.
- Copenhaver D. C., 1996, "Thermal Characterization of Honeycomb Core Sandwich Structures," M.S. Thesis, Department of Mechanical Engineering, Virginia Polytechnic Institute and State University, Blacksburg, VA, USA.
- Copenhaver D. C., Scott E. P. and Hanuska A., 1998, "Thermal Characterization of Honeycomb Sandwich Structures," *AIAA Journal of Spacecraft and Rockets*, Vol. 35, No. 4, 1998, pp. 539-545.
- Davalos R. V. and Rubinsky B., 1996, "An Evolutionary-Genetic Approach to Heat Transfer Analysis," *Journal of Heat Transfer*, Vol. 118, pp. 528-531.
- Davis L., 1991, *Handbook of Genetic Algorithms*, Van Nostrand Reinhold Pub., NY, USA.
- Degiovanni A., 1994, "Conductivité et Diffusivité Thermique des Solides," *Techniques de l'Ingénieur, Traité Mesures et Contrôle*, R2850, France.
- Doyle J. F., 1995, "Determining the Size and Location of a Crack in a Frame Structure," *Proc. of the 7th Inverse Problems in Engineering Seminar*, OSU, USA.
- Dowding K. J., Beck J. V. and Blackwell B. F., 1996, "Estimation of Directional-Dependent Thermal Properties in a Carbon-Carbon Composite," *International Journal of Heat and Mass Transfer*, Vol. 39, No. 15, pp. 3157-3164.
- Draper N. R. and Smith H., 1981, *Applied Regression Analysis*, John Wiley, NY, USA.

- Eschenauer H., Koski J. and Osyczka A., 1990, *Multicriteria Design Optimization - Procedures and Applications*, Springer-Verlag, NY, USA.
- Fabbi G., 1997, "A Genetic Algorithm for Fin Profile Optimization," *Int. Journal of Heat and Mass Transfer*, Vol. 40, No. 9, pp. 2165-2172.
- Field P., 1996, "A Multary Theory for Genetic Algorithms: Unifying Binary and Nonbinary Problem Representations," Ph.D. Dissertation, Computer Science Department, Queen Mary and Westfield College, Univ. London, London, UK.
- Furuya H. and Haftka R. T., July 17-22, 1993, "Genetic Algorithms for Placing Actuators on Space Structures," *Proc. of the 5th International Conference on Genetic Algorithms*, Urbana, IL., pp. 536-542.
- Garcia S, 1994, "Analysis of a Space Experimental Design For High-Tc Superconductive Thermal Bridges," M.S. Thesis, Department of Mechanical Engineering, Virginia Polytechnic Institute and State University, Blacksburg, VA, USA.
- Garcia S. and Scott E. P., 1998, "Use of Genetic Algorithms in Thermal Property Estimation: Part I - Experimental Design Optimization", *Num. Heat Transfer, Part A*, vol. 33, pp. 135-147.
- Garcia S., Guynn J. and Scott E. P., 1998, "Use of Genetic Algorithms in Thermal Property Estimation: Part II - Simultaneous Estimation of Thermal Properties ", *Num. Heat Transfer, Part A*, vol. 33, pp. 149-168.
- Garcia S., Garnier B. and Jarny Y., May 1999a, "Utilisation des Algorithmes Génétiques pour la Caractérisation Thermique de Matériaux Composites," *Proc. Congrès SFT'99 Thermique et Matériaux*, Elsevier pub., pp. 33-38, Arcachon, France.
- Garcia S., Lecointe D., Jarny Y. and Delaunay D., September 5-9 1999b, "Simultaneous Estimation of Thermophysical Parameters from Experimental Measurements in RTM Mold Using Genetic Algorithms," to be published in *Proc. 15th Eur. Conf. on Thermophysical Properties*, Würzburg, Germany.
- Garcia S., Garnier B. and Jarny Y., June 1999c, "Simultaneous Estimation of Kinetic Parameters Using Genetic Algorithms," *Proc. 3rd Int. Conf. Inverse Problems in Eng.: Theory & Practice*, in press, Port Ludlow, Washington, USA.
- Garnier B., 1990, "Etude du Couplage Entre Transferts Thermiques et une Réaction Chimique. Application à la Vulcanisation du Caoutchouc," ISITEM/LTI, Université de Nantes, France.
- Garnier B., 1996, "Estimation des Propriétés Thermophysiques de Matériaux à Faible Conductivité Thermique en Géométrie 1D Cylindrique," *Proc. Congrès SFT'96*, France.
- Garnier B., Delaunay D. and Beck J. V., 1992, "Estimation of Thermal Properties of Composite Materials Without Instrumentation Inside The Samples," *International Journal of Thermophysics*, Vol. 13, No. 6, pp. 1097-1111.

- Garnier B., Danès F. and Delaunay D., 1993, "Effet du Degré de Dispersion du Soufre sur la Cinétique de Vulcanisation," *Thermochimica Acta*, Vol. 222, pp. 115-125.
- Garnier B. and Danès F., 1994, "Critères de Choix d'un Appareil de Type Calorimètre Différentiel à Balayage (DSC) pour l'Etude des Cinétiques Chimiques et du Terme Source dans l'Equation de la Chaleur," *Journal of Thermal Analysis*, Vol. 41, pp. 1619-1627.
- Gen M. and Cheng R., 1997, *Genetic Algorithms and Engineering Designs*, John Wiley, NY, USA.
- Goldberg D. E., 1989., *Genetic Algorithms in Search, Optimization and Machine Learning*, Addison-Wesley, Reading, MA, USA.
- Grimstadt A. A. and Mannseth T., 1998, "Nonlinearity, Scale, and Sensitivity for a Class of Parameter Estimation Problems," *Proc. 9th Conf. Inverse Problems in Eng.*, in press, Muncie, IN.
- Guyonwarch G., 1995, "Analyse et Optimisation des Transferts Thermiques Couplés lors du Moulage de Matériaux Composites par Transferts de Résine (Procédé RTM) – Application à la Pièce Automobile d'Aspect en Polyester / Fibre de Verre," Thèse de Doctorat, ISITEM/LTI, Université de Nantes, France.
- Guyonwarch G., Garnier B. and Delaunay D., 1995, "Thermal Characteristics and Kinetic Parameter Estimation of a Low-Profile Polyester Resin-Based Composite", 2nd Int. Thermal Energy Congress, Agadir.
- Guynn J. H., 1996, "Estimation of Thermal Properties in a Medium With Conduction and Radiation Heat Transfer," M.S. Thesis, Department of Mechanical Engineering, Virginia Polytechnic Institute and State University, Blacksburg, VA, USA.
- Haftka R. T. and Gurdal Z., 1992, *Elements of Structural Optimization*, Kluwer Academic Pub., The Netherlands.
- Haftka R. T., Scott E. P. and Cruz J., 1998, "Optimization and Experiments - A Survey," *Applied Mechanical Reviews*, Vol. 51, No. 7, pp. 435-448.
- Hanak J. P., 1995, "Experimental Verification of Optimal Experimental Designs for the Estimation of Thermal Properties of Composite Materials," M.S. Thesis, Department of Mechanical Engineering, Virginia Polytechnic Institute and State University, Blacksburg, VA, USA.
- Hanuska A. R., 1998, "Thermal Characterization of Complex Aerospace Structures," M.S. Thesis, Department of Mechanical Engineering, Virginia Polytechnic Institute and State University, Blacksburg, VA, USA.
- Hanuska A. R., Scott E. P. and Daryabeigi K., 1999, "Thermal characterization of complex aerospace structures," Presented at the A.I.A.A. 35th Aerospace Sciences Meeting & Exhibit, Reno, NV, A.I.A.A. Paper No. 99-1953.

- Hemminger and Hohne, 1984, *Fundamentals and Practice*, Verlag Chemie.
- Heitkoetter J. and Beasley D., (Eds), 1994, *The Hitch-Hiker's Guide to Evolutionary Computation: A List of Frequently Asked Questions (FAQ)*, Usenet: comp.ai.genetic.
- Holland J. H., 1975, *Adaptation in Natural and Artificial Systems: An Introductory Analysis with Applications to Biology, Control and Artificial Intelligence*, University of Michigan Press, Ann Arbor, MI, USA.
- Incropera F. P. and DeWitt D. P., 1996, *Fundamentals of Heat and Mass Transfer*, 4th ed., John Wiley, NY, USA.
- Jarny Y. and Maillet D., 1999, "Problèmes Inverses en Dimension Finie," *Proc. (cours) Ecole d'hiver METTI'99*, Bolquère, France.
- Jarny Y., Delaunay D. and Le Brizaut J. S., 1993, "Inverse Analysis of the Elastomer Cure Control of the Vulcanization Degree," ISITEM/LTI, Université de Nantes, France.
- Jones M. R., Brewster M. Q. and Yamada Y., 1996, "Application of Genetic Algorithms to the Optical Characterization of Propellant Smoke," *Journal of Thermophysics and Heat Transfer*, Vol. 10, No. 2, pp. 372-377.
- Jurkowski T., Jarny Y. and Delaunay D., 1992, "Simultaneous Identification of Thermal Conductivity and Thermal Contact Resistance Without Internal Temperature Measurements," *Institution of Chemical Engineers Symposium Series*, Vol. 2, No. 129, pp. 1205-1211.
- Jurkowski T., Jarny Y. and Delaunay D., 1997, "Estimation of Thermal Conductivity of Thermoplastics Under Molding Conditions: an Apparatus and an Inverse Algorithm," *Int. Journal Heat Mass Transfer*, Vol. 40, No. 17, pp. 4169- 4181.
- Kamal M. R. and Sourour S., 1973, "Kinetics and Thermal Characterization of Thermoset Cure," *Polymer Engineering & Science*, Vol. 13, No. 1.
- Kamal M. R., Sourour S. and Ryan M., 1973, *Proc. of the 31st SPE Technical Conference*, Vol. 19, p187.
- Kiefer J., 1974, "General Equivalence Theory for Optimum Designs (Approximate Theory)," *The Annals of Statistics*, Vol. 2, No. 5, pp. 849-879.
- Kiefer J., 1975a, "Variation in Structure and Performance Under Change of Criterion," *Biometrika*, 62, 2, pp. 277-288.
- Kiefer J., 1975b, "Optimality Criteria for Designs," Unpublished paper prepared under NSF Grant GP35816X, Dept. of Math., Cornell University, Ithaca, NY, USA.
- Kiefer J., 1981, "The interplay of Optimality and Combinatorics in Experimental Design," *The Canadian Journal Of Statistics*, Vol. 9, No. 1, pp. 1-10.

- Kirkpatrick S., Gelatt C. D. Jr. and Vecchi M. P., 1983, "Optimization by Simulated Annealing," *Science*, Vol. 220, pp. 671-680.
- Krottmaier J., 1993, *Optimizing Engineering Designs*, McGraw-Hill Book Company, London, UK.
- Lalouana S, 1992, "Etude du Couplage entre les Transferts Thermiques et la Cinétique de Cristallisation d'un Thermoplastique Injecté," Thèse de Doctorat, ISITEM/LTI, Université de Nantes, France.
- Lecoite D., "Simulation du Processus d'Écoulement lors d'Injection de Résine du Procédé Resin Transfer Molding (RTM)," Thèse de Doctorat, ISITEM/LTI, Université de Nantes, France, (Expected date of graduation: July 1999).
- Li H. Y. and Yang C. Y., 1997, "A Genetic Algorithm for Inverse Radiation Problems," *Int. Journal of Heat and Mass Transfer*, Vol. 40, No. 7, pp. 1545-1549.
- Loh M. H., 1989, "Two-Dimensional Heat Transfer Studies in Carbon Composite Materials," M.S. Thesis, Department of Mechanical Engineering, Michigan State University, East Lansing, MI, USA.
- Loh M. H. and Beck J. V., 1991, "Simultaneous Estimation of Two Thermal Conductivity Components From Transient Two-Dimensional Experiments," *ASME Paper No. 91-WA/HT-11*, ASME, NY, USA.
- Lohman T., Bock H. G. and Schlöder J. P., 1992, "Numerical Methods for Parameter Estimation and Optimal Experiment Design in Chemical Reaction Systems," *Ind. Eng. Chem. Res.*, Vol. 31, pp. 54-57.
- Lorion R., Chabriat J. P., Bessafi M. and Herve P., May 1999, "Identification de la Diffusivité Thermique par Algorithme Génétique. Application au Cas Multicouche," *to be published in Proc. SFT'99*, Bordeaux, France.
- McMahon M. T., 1998, "A Distributed Genetic Algorithm with Migration for the Design of Composite Laminate Structures," M.S. Thesis, Department of Computer Science, Virginia Polytechnic Institute and State University, Blacksburg, VA, USA.
- McNaughton J. C. and Mortimer C. T., 1975, "La Calorimétrie Différentielle à Balayage," Perkin Elmer Corporation.
- Michalewicz Z., 1996, *Genetic Algorithms + Data Structures = Evolution Programs*, 3rd Ed., Springer-Verlag, NY, USA.
- Mitchell M., 1996, *An Introduction to Genetic Algorithms*, Complex Adaptive System Series, Bradford Publishing.
- Mitchell T. J., 1974, "An Algorithm for the Construction of 'D-Optimal' Experimental Designs," *Technometrics*, Vol. 16, pp. 203-210.

- Moncman D. A., 1994, "Optimal Experimental Designs for the Estimation of Thermal Properties of Composite Materials," M.S. Thesis, Department of Mechanical Engineering, Virginia Polytechnic Institute and State University, Blacksburg, VA, USA.
- Moncman D.A., Hanak J. P., Copenhaver D.C. and Scott E P., 1995, "Optimal experimental designs for estimating thermal properties," Proceedings of the 4th A.S.M.E.-J.S.M.E. Thermal Engineering Joint Conference, Maui, HI, Vol. 3, pg. 461-468.
- Mouchnino C., 1997, "Caractérisation d'un BMC et Suivi du Retrait en Cours de Transformation," Rapport de DEA Thermique, ISITEM/LTI, Université de Nantes, France.
- Nakamura M. and Taomoto N., 1996, "Shape Determination of Structural Components for Minimum Weight Design Using Genetic Algorithms," *Proc. 2nd Int. Conf. Inverse Problems in Eng.: Theory & Practice*, in press.
- Nenarokomov A. V., Emery A. F. and Fadale T. D., 1998, "Optimal Experiment Design With Uncertainties in Mathematical Model," *Proc. Inv. Problems*, Moscow, Russia.
- Ollivier F., 1991, "Contribution à l'Etude du Calorimètre Différentiel à Balayage," Rapport de DEA Thermique, ISITEM/LTI, Université de Nantes, France.
- Olsommer B., Von Spakovsky M. R. and Favrat D., 1997, "An Approach for the Time-Dependent Thermo-economic Modeling and Optimization of Energy System Synthesis, Design and Operation," *Proc. TAIES'97*, pp. 321-339.
- Orain S., Garcia S. and Scudeller Y., "Simultaneous Estimation of Thin Film Thermal Properties Using Genetic Algorithms," *Journal of Heat & Mass Transfer* (Expected date of submission: July 1999).
- Patankar S. V., 1991, *Computation of Conduction and Duct Flow Heat Transfer*, Innovative Research, Maple Grove, MN, USA.
- Piloyan G. P., Ryabchikov I. D. and Novikova O. S., 1966, *Nature*, 212, 1229.
- Press W. H., Flannery B. P., Teukolsky S. A. and Vetterling W. T., 1990, *Numerical Recipes, the art of scientific computing (Fortran version)*, Cambridge University Press, NY, USA.
- Pronzato L. and Walter E., 1989, "Experiment Design in a Bounded-Error Context: Comparison with D-Optimality," *Automatica*, Vol.25, pp. 383-391.
- Queipo N., Devarakonda R. and Humphrey J. A. C., 1994, "Genetic Algorithms for thermosciences Research: Application to the Optimized Cooling of Electronic Components," *Int. Journal of Heat and Mass Transfer*, Vol. 37, No. 6, pp. 893-908.
- Raudenský M., Woodbury K. A., Kral J. and Brezina T., 1995, "Genetic Algorithm in Solution of Inverse Heat Conduction Problems," *Num. Heat Transfer, Part B*, Vol. 28, pp. 293-306.
- Raynaud M., 1999, "Conception Optimale d'Expériences," *Proc. (cours) Ecole d'hiver METTI'99*, Bolquère, France.

- Raynaud M., 1999, "Strategy for Experimental Design and the Estimation of Parameters," *High Temp. – High Pressures*, Vol. 31, pp. 1-15.
- Rigollet F., Papini F., Boisson D. and Petit D., "Caractérisation Thermophysique d'un Dépôt Métallique par une Méthode Photothermique Impulsionnelle. Conception et Réalisation d'Expériences," *Proc. SFT'98*, pp. 338-343.
- Robinson P. S., 1998, "Development of Methodologies for the Noninvasive Estimation of Blood Perfusion," M.S. Thesis, Department of Mechanical Engineering, Virginia Polytechnic Institute and State University, Blacksburg, VA, USA.
- Sakait J. and Chang Gea H., 1996, "PCB Layout Design Using a Genetic Algorithm," *J. Electronic Packaging*, vol.118, pp. 11-15.
- Schaffer J. D., Caruana R. A., Eshelman L. J. and Das R., 1989, "A Study of Control Parameters Affecting Online Performance of Genetic Algorithms for Function Optimization," *Proc. 3rd Int. Conf. on GAs*, Morgan Kaufmann Publishers, San Mateo, CA, USA.
- Schwefel H. P., 1995, *Evolution and Optimization Seeking*, John Wiley, NY, USA.
- Scott, E. P. 1994, "An Analytical Solution and Sensitivity Study of Sublimation-Dehydration Within a Porous Medium With Volumetric Heating," *Journal of Heat Transfer*, Transactions of the ASME, Vol. 116, pp. 686-693.
- Scott E. P. and Beck J. V., 1992a, "Estimation of Thermal Properties in Epoxy Matrix/Carbon Fiber Composite Materials," *Journal of Composite Materials*, Vol. 26, No. 1, pp. 132-149.
- Scott E. P. and Beck J. V., 1992b, "Estimation of Thermal Properties in Carbon/Epoxy Composite Materials During Curing," *Journal of Composite Materials*, Vol. 26, No. 1, pp. 20-36.
- Scott E. P. and Saad Z., 1993a, "Estimation of Kinetic Parameters Associated with the Curing of Thermoset Resins. Part I: Theoretical Investigation," *Polymer Engineering & Science*, Vol. 33, No. 18, pp.1157-1164.
- Scott E. P. and Saad Z., 1993b, "Estimation of Kinetic Parameters Associated with the Curing of Thermoset Resins. Part II: Experimental Results," *Polymer Engineering & Science*, Vol. 33, No. 18, pp.1165-1169.
- Sommier A., 1998, "Mesure des Propriétés Thermophysiques des Résines Thermodurcissables au Cours de leur Mise en Forme et Suivi de leur Polymérisation par Microdiélectrométrie," Thèse de Doctorat, ISITEM/LTI, Université de Nantes, France.
- Soremekum G. A. E., 1997, "Genetic Algorithms for Composite Laminate Design and Optimization," M.S. Thesis, Department of Engineering Science and Mechanics, Virginia Polytechnic Institute and State University, Blacksburg, VA, USA.

- Taktak R., Scott E. P. and Beck J. V., 1991, "Optimal Experimental Designs for Estimating the Thermal Properties of Composite Materials," *Proc. of the 3rd ASME - JSME Thermal Engineering Joint Conference*, ASME, Vol. 3, pp. 481-488.
- Tortorelli D. A. and Michaleris P., 1994, "Design Sensitivity Analysis: Overview and Review," *Inverse Problems in Engineering*, Vol. 1, pp. 71-105.
- Walpole R. E. and Myers R. H., 1993, *Probability and Statistics for Engineers and Scientists*, 5th Ed., Macmillan Publishing Co., NY, USA.
- Walter E. and Pronzato L., 1990, "Qualitative and Quantitative Experiment Design for Phenomenological Models – A Survey," *Automatica*, Vol. 26, pp. 195-213.
- Walter E. and Pronzato L., 1994, *Identification de Modèles Paramétriques à partir de Données Expérimentales*, Masson, Paris, France.
- Welch W. J., 1982, "Branch-and-Bound Search for Experimental Designs Based on *D*-Optimality and Other Criteria," *Technometrics*, Vol. 24, pp. 41-48.
- Whetstone W. D., 1983, *EISI-EAL Engineering Analysis Language*, Engineering Information Systems, Inc., San Jose, CA, USA.
- Wright A. D., 1996, "Acoustic Boundary Condition Estimation in a Near-Scale Gas-Turbine Combustor," M.S. Thesis, Department of Mechanical Engineering, Virginia Polytechnic Institute and State University, Blacksburg, VA, USA.

APPENDIX A

Mechanisms of a Standard Simple Genetic Algorithm

This appendix provides, as an introductory tutorial, a step-by-step description of the mechanisms behind the genetic operator variants of the standard simple GA presented in Fig. 4.2. For this purpose, a simple function optimization example is used. One will see that the mechanisms of such a standard simple GA are simple, involving nothing more complex than copying chromosomal strings and swapping partial strings. This example is an extension of an example found in Goldberg's book (1989).

Function optimization example: maximizing the function $g(x) = x^2$, where x is an integer and $0 \leq x \leq 31$.

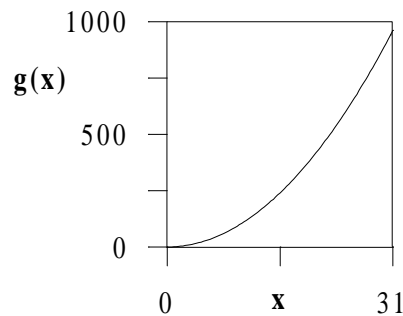


Figure A.1 Function g vs. x .

Encoding Scheme

To obtain numbers between 0 and 31, a 5-bit binary chromosome is used to code the integer x ($n_{gene} = 5$). (Recall that in base 2 arithmetic, 00000 and 11111 decodes to the base 10 number 0 and 31, respectively; for instance, 11111 is decoded to $1 \cdot 2^4 + 1 \cdot 2^3 + 1 \cdot 2^2 + 1 \cdot 2^1 + 1 \cdot 2^0 = 31$.)

Initialization

The initial population of arbitrary size $n_s = 4$ is randomly generated through 20 successive flips of an unbiased coin (head = 1, tail = 0):

⇒ 01101 11000 01000 10011

Evaluation

The chromosome are decoded to base 10 numbers in the solution space. The fitness f_i is chosen as the objective function value given by $g(x)$. Results of the evaluation and ranking processes are summarized in Table A.1. The average fitness of the initial population is 293.

Table A.1 Summary of evaluation and ranking processes over the initial population.

String #	Chromosome	x	$g(x)$	Rank	Selection probability
1	01101	13	169	3	5.5 %
2	11000	24	576	1	49.2 %
3	01000	8	64	4	14.4 %
4	10011	19	361	2	30.9 %

Selection

Four parents are selected by pairs for breeding using the proportionate selection scheme. The selection probability of a chromosome is equal to its fitness divided by the total fitness of the population. The selection probabilities of the chromosomes in the current population are: $p_1 = 49.2\%$, $p_2 = 30.9\%$, $p_3 = 14.4\%$ and $p_4 = 5.5\%$, as given in Table A.1. The mating pool of the next generation is selected by spinning the weighted roulette wheel shown in Fig. A.2, where each chromosome has a roulette wheel slot sized in proportion to its selection probability.

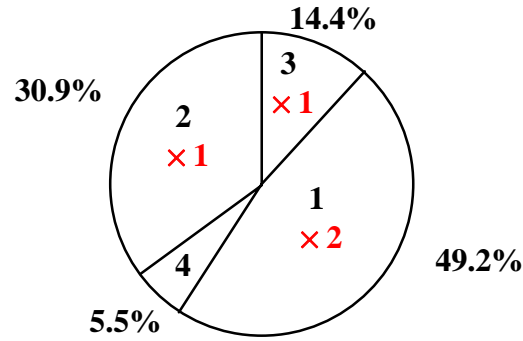


Figure A.2 Weighted roulette wheel with slots sized according to the chromosomes' fitness of the initial population.

To “numerically” spin the roulette wheel, one calculates the cumulated probability, q_i , defined by $q_i = \sum_1^i p_i$. Then, one draws a random number, R , uniformly distributed in $[0,1]$. The chromosome j is selected if $q_{j-1} < R \leq q_j$.

Actual simulation of this process results in selecting successively the chromosomes 3 and 1 (1st pair), and 1 and 2 (2nd pair); e.g. chromosomes 2 and 3 receiving one copy in the mating pool, chromosome 1 receiving two copies, and chromosome 4 receiving no copy, as shown in Fig. A.2. Note that comparing this with the expected number of copies ($n_s \cdot p_i$), one obtains what one should expect: the best get more copies, the average stay even, and the worst die off.

Crossover

Both pairs of parents are crossed according to the single-point crossover with a probability of 1 (no parent can be cloned). First, a crossover point is randomly chosen in $[1, n_{gene}-1]$ and the partial strings of the two chromosomes are swapped. Say the crossing site is 4 for the first pair and 2 for the second, and the resulting children can be checked in Table A.2.

Table A.2 Summary of crossover process over the parent population, and mutation, evaluation and ranking processes over the children population.

Current Rank #	Parents	Crossing site	Children	Mutation	x	$g(x)$	Rank
3	$P_1 = 0110\underline{1}$	4	$C_1 = 01100$	01101	13	169	4
1	$P_2 = 1100\underline{0}$	4	$C_2 = 11001$	-	25	625	2
1	$P_3 = 11\underline{000}$	2	$C_3 = 11011$	-	27	729	1
2	$P_4 = 10\underline{011}$	2	$C_4 = 10000$	-	16	256	3

Mutation

This operator is performed on a bit-by-bit basis, with a low probability (usually between 0.001 and 0.01 for binary encoding). Actual simulation of this process indicates that the 5th bit of Parent 1 is changed from 0 to 1 (Table A.2).

Replacement

Basic elitism is applied and the new population consists of the 1st chromosome of the previous generation, e.g. chromosome 11000, and the (n_s-1) best children, e.g. C₃, C₂, and C₄. Table A.3 displays the new ranked population.

Table A.3 New ranked population at generation 1.

String #	Chromosome	x	$g(x)$	Rank
1	11000	24	576	3
2	11011	27	729	1
3	11001	25	625	2
4	10000	16	256	4

The average fitness of the generation 1 population is 546.5. One can note how both the maximal and average fitness have improved in the new population. From this, one starts to see how the mechanics behind this standard simple genetic algorithm can allow achievement of better performance through generations.

Remarks

- 1) Standard simple GAs using binary encoding, single-point crossover and binary mutation are robust algorithms, but they are almost never the best algorithms to use for any problem.
- 2) Using real-number encoding, a chromosome would only consist of one gene for the variable x . Crossover and mutation operators adapted to real-number encoding should be applied (such as the arithmetic crossover and the jump mutation used in the GA_3 which was defined in Chapter 4).

APPENDIX B

GAMAIN.FOR Program and GACOMMON_MAIN.FOR Subroutine

This program is based on the genetic algorithm GA_3 described in Chapter 4. It is structured in analogy with the program CONDUCT developed by Patankar (1991), e.g. it consists of an adapt and an invariant part. The following provides the invariant part that contains the general calculation scheme. The GAMAIN version was written for the analysis of experimental design optimization and/or simultaneous parameter estimation problems for which a mathematical direct solution is to be provided by the user. The default values of the key parameters that control the program are specified in the subroutine DEFAULT.

Appendices C and G provide two adapt subroutines that work with GAMAIN.

The GACOMMON_MAIN subroutine includes all variable declaration. It is provided at the end of GAMAIN.

```
c*****
PROGRAM GAMAIN

c Numerical optimizer based on GAs
c
c Needs a user subroutine (adaptation part)
c - Sandrine Garcia,
c Laboratoire de Thermocinetique de l'ISITEM, France, 29/9/98
c
c HP77 or PC
c*****
INCLUDE 'gacommon_main.for'
c*****

CALL DEFLT
CALL INIT
CALL SETVAR
CALL READY      !start calculations

c --- Generate initial generation + compute OF
CALL INIGEN

10 CONTINUE

c ----- Generation (= parent population) analysis -----
CALL GENANA
IF (KSTOPF.NE.0) GOTO 20

c ----- Breeding process -----
CALL BREED

c ----- Elitism process + compute OF of new generation -----
CALL ELITISM

GOTO 10

20 CONTINUE

c ----- Results analysis -----
1000 CALL RESULT

STOP 'GAMAIN done'
END

C_____
C_____

SUBROUTINE DEFAULT
```

```
c Default subroutine SG 29/09/98
c HP77 or PC

c*****
INCLUDE 'gacommon_main.for'
c*****

ENTRY DEFLT

COME HERE TO SET THE DEFAULT VALUES

c set initial clock time at start of run
TIME0=SECNDS(0.0)
c set cpu time for each generation loop to 0
CPUG=TIME0
KCPU=0

c set parameter adimensionalization marker
DO J=1,NPMAX
FACTADIM(J)='LIN'
ENDDO

c set iteration and convergence markers to 0
NCRITERG=0
ITERG=0
KSTOPF=0
NFEVAL=0
OFFLINE=0.D0
ONLINE=0.D0
KCONT=0  !=1 or 2 to apply constraints (to be defined by the user)
NCONTMIN=0 !# of times parmin constraint is applied
NCONTMAX=0 !# of times parmax constraint is applied

c set user markers to 0 (!associated w/ ...)
KPAR=0  !=1 to calculate OF for a particular parameter
KXPRINT=0 !=1 to print sensitivity coefficient; (to be used w/
KPAR=1)
KPRINT=0 !=1 to print T; to be used w/ KPAR=1
KSENS=0 !becomes 1 when sensof called for sensitivity analysis
!or when KETA=2
KMINMAX=0 !=0/1 associated w/ min/max of the OF
KETA=0 !compute ETA only.
c If KETA>1 : iterations on ETA and compute RES=ETA-YARR
!KETA=1 to perform estimation (OLS)
SIGMA=1.D0 !standard deviation for OLS estimation
DO I=1,NEXPMAX
IDATA0(I)=1 !number of the first data to use for OLS estimation
```



```

10 CONTINUE

c if OLS estimation (KETA=1) or experimental design optimization
(KETA=2) then
c reset OF value and iteration on experiment #
15 PAR(NP+1)=0.D0
JEXP=1

CCCCCCCCCCCCCCCCCCCCCCCCCCCCCCCCCCCCCCCCCCCCCCCCCCCC
IF (KETA.EQ.1) THEN
ITERETA=0
c start the iteration or time-step loop
20 CONTINUE
CALL MODELETA
IF (KSS.EQ.1.OR.ITERETA.EQ.0) GOTO 30
IF (ITERETA.GE.IDATA0(JEXP)) THEN
c compute residu at ITERETA associated w/ time t
RES=YARR(JEXP,ITERETA)-ETA
c compute S=sum of least-square errors
PAR(NP+1)=PAR(NP+1)+(RES/SIGMA)**2
ENDIF
30 ITERETA=ITERETA+1
IF (ITERETA.GT.LASTETA(JEXP)) THEN
JEXP=JEXP+1
IF (JEXP.GT.NEXP) GOTO 80
ITERETA=0
ENDIF
GOTO 20

ELSE
IF (KETA.EQ.2) THEN
JEXP=JEXPCI
KSENS=1
CALL MODELXI
ITERETA=1
IF (KTN.EQ.1) OPTOFMOD=0.D0 !searching for the total exp time
40 CONTINUE
CALL COMPTXOPT(XTXOPT)
CALL JACOBI(XTXOPT,NPEST,NPEST,EIG)
CALL RANGER(NPEST,EIG)
SUMEIG=0.D0
PRODEIG=1.D0
DO 50 J=1,NPEST
SUMEIG=SUMEIG+EIG(J)
PRODEIG=PRODEIG*EIG(J)
50 CONTINUE

IF (OPTCRIT.EQ.'D') THEN
OPTOF=PRODEIG
ELSE
IF (OPTCRIT.EQ.'A') THEN
OPTOF=SUMEIG
ELSE
OPTOF=EIG(1)
ENDIF
ENDIF

IF (KTN.EQ.0) THEN
IF (OPTOF.GT.PAR(NP+1)) PAR(NP+1)=OPTOF
ELSE
RATIO=ABS((OPTOF-OPTOFMOD)/(OPTOFMOD+1.D-30))
IF (ITERETA*PASDT(JEXP).GT.TIMEHEAT.AND.
RATIO.LE.1.D-4) THEN
PAR(NP+1)=ITERETA*PASDT(JEXP) !optimal total exp time
GOTO 80
ELSE
OPTOFMOD=OPTOF
ENDIF
ENDIF

IF (KXPRINT.EQ.1) WRITE(IUEIG,60)ITERETA*PASDT(JEXP),
OPTOF,(EIG(J),J=1,NPEST)
60 FORMAT(F16.3,11(1X,E16.8))

70 ITERETA=ITERETA+1

```

```

IF (ITERETA.GT.LASTETA(JEXP)) THEN
IF (KTN.EQ.1) PAR(NP+1)=ITERETA*PASDT(JEXP)
GOTO 80
ENDIF

GOTO 40

ELSE !KETA=0
CALL MODELETA
PAR(NP+1)=ETA
ENDIF
ENDIF
CCCCCCCCCCCCCCCCCCCCCCCCCCCCCCCCCCCCCCCCCCCCCCCCCCCC

80 ARR(ITERID,NP+1)=PAR(NP+1)
NFEVAL=NFEVAL+1
ONLINE=ONLINE+ARR(ITERID,NP+1)

c come here only for a particular chromosome
IF (KPAR.EQ.1) THEN
IF (KSS.EQ.1) THEN
WRITE(99,(A8,F13.6))'ETAMAX=',ETA
WRITE(*,(A8,F13.6))'ETAMAX=',ETA
STOP 'ETAMAX calculated w/ KSS=1 & KETA=1'
ENDIF
c results of the particular set of thermal properties
JBEG=1
JEND=NP+1
JREP=(JEND-JBEG+10)/10
DO 90 JWRITE=1,JREP
INCRJ=MIN(9,JEND-JBEG)
JSTOP=JBEG+INCRJ
WRITE(99,(/10(1X,E16.8)/'))(PAR(J),J=JBEG,JSTOP)
WRITE(*,(/10(1X,E10.3)/'))(PAR(J),J=JBEG,JSTOP)
JBEG=JSTOP+1
90 CONTINUE
IF (KETA.EQ.1) CALL COMPCI
WRITE(*,*)
STOP 'Particular set of genes analyzed'
ENDIF

100 CONTINUE

RETURN
END
C_____

SUBROUTINE COMPYSIM(STDDV)

c generate simulated temperatures by adding random normal errors
to calculated ETA
c HP77 or PC - SG 11/3/98

C*****
INCLUDE 'gacommon_main.for'
C*****
REAL*8 DATA(20000)
COMMON NDAT
C-----
c CAREFUL, if NEXP>1 is used, the user must define for which
experiment J(=1) the Yarr(1,i), timeexp(1,i) and Xi(i,np) must be
determined

CALL RANDOM(DATA,LASTETA(1),STDDV)

ITERETA=0

c start the iteration or time-step loop
10 CONTINUE
CALL MODELETA
IF (ITERETA.EQ.0) THEN
WRITE(1,20)
20 FORMAT(/2X,'ITERETA',8X,'TIME',9X,'ETA',8X,
'YARR(1,ITERETA),')
ENDIF
IF (ITERETA.GT.LASTETA(1)) GOTO 30

```



```

10 v1=2.*ran1(idum)-1.
v2=2.*ran1(idum)-1.
R=v1**2+v2**2
if (R.ge.1..or.R.eq.0.) goto 10
fac=sqrt(-2.*LOG(R)/R)
gset=v1*fac
gasdev=v2*fac
ISET=1
else
gasdev=gset
ISET=0
endif

return
END
C_____

```

SUBROUTINE GABODY

c HP77 or PC - SG 25/09/98

```

c*****
INCLUDE 'gacommon_main.for'
c*****
DIMENSION CHILDRAND(NSMAX,NPMAX+1)
C-----

```

ENTRY INIGEN

c initialize the random generator
CALL RMARIN(ISEED1,ISEED2)

c create the initial normalized population
CALL INITPOP

*c if the rank-based selection is applied, determine
c the fitness and probability of breeding of each parent*
IF (SELECT.EQ.'R') CALL RANKFIT

c compute OF of initial pop
CALL COMPOF(NS,CP)

```

RETURN
c*****

```

ENTRY GENANA

c rank the population at generation iterg
CALL RANKNS

c compute OFavg of the population at generation iterg
CALL OFAVE

c check if convergence criterion is met
CALL CHECKCONV

```

RETURN
c*****

```

ENTRY BREED

c make ns children
DO 20 ICHILD=1,NS/2

```

IF (SELECT.EQ.'R') THEN
c select 2 parents according to rank selection
CALL SELRANK(ICHILD)
ELSE
c select 2 parents according to tournament selection
CALL SELTOURMT
ENDIF

```

c make 2 children by crossing the 2 selected parents
CALL CROSS

c mutate the child according to jump mutation

CALL MUTJUMP

c mutate the child according to jump AND creep mutations
IF (MUT.EQ.'JC') CALL MUTCREEP

```

DO 10 J=1,NP
CC(ICHILD,J)=CHILD(1,J)
CC(ICHILD+NS/2,J)=CHILD(2,J)
10 CONTINUE

```

20 CONTINUE

IF (KCONT.NE.0) CALL CHECKCONT(NS,CC)

```

RETURN
c*****

```

ENTRY ELITISM

c compute OF of children population
CALL COMPOF(NS,CC)

c apply basic elitism
IF (ELIT.EQ.'B') THEN

c keep best parent by destroying last child made -arbitrarily
DO 30 I=2,NS
DO 30 J=1,NP+1
CP(I,J)=CC(I-1,J)
30 CONTINUE

ELSE
IF (ELIT.EQ.'SS') THEN

c apply SS elitism
c 1. compute OF of children population that mutated
IF (MUT.EQ.'J') THEN
NMUT=NMUTJUMP
ELSE
NMUT=NMUTJUMP+NMUTCREEP
ENDIF

IF (KCONT.NE.0) CALL CHECKCONT(NMUT,CHILDMUT)

CALL COMPOF(NMUT,CHILDMUT)

*c 2. combine both children populations and rank the combined
children population*

```

NTOT=NS+NMUT
DO 60 J=1,NP+1
DO 40 I=1,NS
CHILDTOT(I,J)=CC(I,J)
40 CONTINUE
DO 50 I=1,NMUT
CHILDTOT(I+NS,J)=CHILDMUT(I,J)
50 CONTINUE
60 CONTINUE
CALL RANK2NS

```

c 3. keep the best parents
NPKEPT=INT(NS*(1.D0-PR))
IF (NPKEPT.EQ.0) NPKEPT=1 !to preserve at least the best parent
~ B elitism

IF (KILLTWIN.EQ.'N') THEN

*c 4. replace a fraction of the parent population with ns*pr children*
70 CONTINUE
DO 80 I=NPKEPT+1,NS
DO 80 J=1,NP+1
CP(I,J)=CHILDTOT(I-NPKEPT,J)
80 CONTINUE

ELSE
c 5. kill the twins; note that NTOT will change
CALL KTWINS

```

IF (NTWINS.LE.(NPKEPT+NMUT)) THEN
GOTO 70
ELSE

NCHILDRAND=NS-NPKEPT-NTOT
WRITE(99,'(A25,I3/)')!!!Need random children: ',NCHILDRAND
DO 100 I=1,NCHILDRAND
DO 90 J=1,NP
CHILD RAND(I,J)=URAND()
90 CONTINUE
CHILD RAND(I,NP+1)=0.DO
100 CONTINUE

CALL COMPOF(NCHILDRAND,CHILD RAND)

DO 110 I=NPKEPT+1,NPKEPT+NTOT
DO 110 J=1,NP+1
CP(I,J)=CHILDTOT(I-NPKEPT,J)
110 CONTINUE
DO 120 I=NPKEPT+NTOT+1,NS
DO 120 J=1,NP+1
CP(I,J)=CHILD RAND(I-NPKEPT-NTOT,J)
120 CONTINUE
ENDIF

ENDIF
ELSE
WRITE(*,*)SR elitism is not set up yet!
ENDIF
ENDIF

RETURN
C*****

ENTRY RESULT

c list the final parent population and measure the GA performance
WRITE(99,130)
130 FORMAT(/75('='),2X,'RESULTS'/50('-'))

WRITE(99,'(A36)')Elapsed CPU time since start of run:
WRITE(99,'(1X,A8,F10.1/)')CPU (s)='KCPU*86400-
TIME0+SECNDS(0.0)

IF (KSTOPF.EQ.2) THEN
WRITE(99,'(A28)')Stopped because iterg=lastg!
ELSE
WRITE(99,'(A34,I4)')Convergence criterion met @ iterg=' ,iterg
ENDIF

c denormalize all genes
DO 150 I=1,NS
DO 150 J=1,NP
IF (FACTADIM(J).EQ.'LIN') THEN
CP(I,J)=(PARMAX(J)-PARMIN(J))*CP(I,J)+PARMIN(J)
ELSE
CP(I,J)=10**(DLOG10(PARMAX(J)/PARMIN(J))*
1 CP(I,J)+DLOG10(PARMIN(J)))
ENDIF
150 CONTINUE

c write the final population to the ouput file
JEND=NP+1
JBEG=1
JREP=(JEND-JBEG+10)/10
DO 160 I=1,NS
JBEG=1
DO 160 JWRITE=1,JREP
INCRJ=MIN(9,JEND-JBEG)
JSTOP=JBEG+INCRJ

WRITE(10,'(I4,2X,10(E16.8,1X))')I(CP(I,J),J=JBEG,JSTOP)
JBEG=JSTOP+1
160 CONTINUE

WRITE(99,170)

```

```

170 FORMAT(/2X,'*** Measure of the GA performance ***')

WRITE(99,'(//A28/)')1) "BEST SO FAR" cp(1,np+1):
JBEG=1
DO 180 JWRITE=1,JREP
INCRJ=MIN(9,JEND-JBEG)
JSTOP=JBEG+INCRJ
WRITE(99,'(10(1X,E16.8/)'))(CP(1,J),J=JBEG,JSTOP)
WRITE(*, '(10(1X,E10.3/)'))(CP(1,J),J=JBEG,JSTOP)
JBEG=JSTOP+1
180 CONTINUE

c EST run: calculate 95% CI of best design+compute correlation
matrix
IF (KETA.EQ.1) THEN
DO 200 J=1,NP+1
PAR(J)=CP(1,J)
200 CONTINUE
CALL COMPCI
ENDIF

WRITE(99,'(//A26/)')2) "OFF LINE" convergence:
WRITE(99,* )'=moyenne courante des bests sur ITERG+1
generations'
WRITE(99,* )'-limite de la convergence'
OFFLINE=OFFLINE/(ITERG +1)
WRITE(99,'(1X,E16.8,2X,A8,I4)')OFFLINE, 'ITERG+1=' ,ITERG+1
WRITE(99,'(//A25/)')3) "ON LINE" convergence:
WRITE(99,* )'=moyenne de toutes les evaluations sur NFEVAL eval.'
WRITE(99,* )'-facon dont la convergence est atteinte'
ONLINE=ONLINE/NFEVAL
WRITE(99,'(1X,E16.8,2X,A7,I6)')ONLINE, 'NFEVAL=' ,NFEVAL

WRITE(99,'(A18,2(1X,I4))')NCONTMIN/NCONTMAX=' ,NCON
TMIN,NCONTMAX

WRITE(99,210)
210 FORMAT(/2X,'*** Statistical analyses on final Nst ***')
c perform statistical calculations on 5 best
IF (NS.GE.5) CALL STATIST(5)
c perform statistical calculations on 10 best
IF (NS.GE.10) CALL STATIST(10)
c perform statistical calculations on NS best
CALL STATIST(NS)

WRITE(99,'(A45)')4a) Elapsed CPU time since gen. loop stopped:
IF (SECNDS(0.0).GT.CPUG) THEN
WRITE(99,'(1X,A24,F10.1)')CPU (s) /Sub. RESULT/ =',
SECNDS(CPUG)
ELSE
WRITE(99,'(1X,A24,F10.1)')CPU (s) /Sub. RESULT/ =',
86400.-CPUG+SECNDS(0.0)
KCPU=KCPU+1
ENDIF

WRITE(99,'(A40)')4b) Elapsed CPU time since start of run:
WRITE(99,'(1X,A8,F10.1)')CPU (s)=' ,KCPU*86400-
TIME0+SECNDS(0.0)

CLOSE(99)
CLOSE(10)
CLOSE(11)
CLOSE(12)

RETURN
END
C_____

SUBROUTINE GAINV

c includes invariant "entry subroutines" dealing with a GA
c HP77 or PC - SG 11/3/98

C*****
INCLUDE 'gacommon_main.for'
C*****

```


c COMMON include file for GAMAIN
c SG 1998

IMPLICIT DOUBLE PRECISION (a-h,o-z)
IMPLICIT INTEGER*4 (i-n)

REAL*4 TIME0,CPUG

PARAMETER (BIG=1.d+52,SMALL=1.d-52)
!if too high use 1.d+/-32
PARAMETER (NSMAX=1000,NPMAX=10,
LASTETAMAX=2200,NEXPMAX=16)

CHARACTER*18 TITLE
CHARACTER*64 HEADER,PRINTF
CHARACTER*4
SELECT,MUT,KILLTWIN,ELIT,OPTCRIT,FACTADIM

COMMON /OFCHARAC/
TITLE,HEADER,PRINTF,OPTCRIT,FACTADIM(NPMAX)

COMMON /OFINT/
ITERETA,NPEST,NEXP,JEXPCI,JEXP,KPAR,KETA,KXPRINT,
KYSIM,KOUT,IU1,IU2,KPRINT,KMINMAX,KSCREEN,KCONT,
KSS,KTN,KSSENS,NCONTMIN,NCONTMAX,IUXI,IUEIG

COMMON /OFINARR/
LASTETA(NEXPMAX),IDATA0(NEXPMAX)

COMMON /OFREAL/
ETA,SIGMA,TIME,TIMEHEAT,ETAMAX,ETAMAXP

COMMON /OFREARR/ PARMIN(NPMAX),PARMAX(NPMAX),
PAR(NPMAX+1),XI(LASTETAMAX,NPMAX),
TIMEEXP(NEXPMAX,LASTETAMAX),
YARR(NEXPMAX,LASTETAMAX),PASDT(NEXPMAX)

COMMON /GACHARAC/ SELECT,MUT,KILLTWIN,ELIT

COMMON /GAIN/ ITERG,MING,LASTG,NMUT,NMUTJUMP,
NMUTCREEP,NTWINS,NTOT,NCHILDRAND,NPKEPT,
NCRITERG,LASTCRITERG,NFEVAL,NS,NP,
KSTOPF,ISEED1,ISEED2,KCPU

COMMON /GAREAL/ PC,PMJ,PMC,PR,PT,CRITERION,
OFFLINE,ONLINE,TIME0,CPUG

COMMON /GAREARR/
CP(NSMAX,NPMAX+1),CC(NSMAX,NPMAX+1),
CHILD(2,NPMAX),CHILDMUT(NSMAX,NPMAX+1),
CHILDTOT(2*NSMAX,NPMAX+1),BEST(NPMAX+1)

APPENDIX C

GACONDUCT.FOR Program and GACOMMON_CONDUCT.FOR Subroutine

This program combines the features of the genetic algorithm GA_3 described in Chapter 4 with those of an extension of the program CONDUCT developed by Patankar (1991). The extension consists in modifications that allow for the analysis of orthotropic properties in rectangular geometry. These modifications were made by Prof. D. J. Nelson (Virginia Tech, Mechanical Engineering Department). The structure of the GACONDUCT follows the one from CONDUCT, e.g. it consists of an adapt and an invariant part. The following provides the invariant part that contains the general calculation scheme. The GACONDUCT version allows for the analysis of experimental design optimization and/or simultaneous parameter estimation problems that deal with the computation of conduction and duct flow heat transfer in two-dimensional rectangular and cylindrical geometry. The default values of the key parameters that control the program are specified in the subroutine DEFRD.

Appendices D, E and F provide three adapt subroutines that work with GACONDUCT.

The GACOMMON_CONDUCT subroutine includes all variable declaration. It is provided at the end of GACONDUCT.

```
c*****
```

```
PROGRAM GACONDUCT
```

```
c Control Volume Method solution of 2D heat conduction combined  
with a GA tool for optimization/estimation analysis
```

```
c
```

```
c Needs a user subroutine (adaptation part)
```

```
c - Sandrine Garcia,
```

```
c Laboratoire de Thermocinetique de l'ISITEM, France, 11/3/98
```

```
c
```

```
c 2D heat conduction solution similar to the computer program  
'conduct' detailed in "Computation of Conduction and Duct Flow  
Heat Transfer", Suhas V. Patankar, Maple Grove, MN: Innovative  
Research, Inc., 1991.
```

```
c Orthotropic Gamma version, double precision
```

```
c - Doug J. Nelson, Virginia Tech, USA, 7/12/93
```

```
c <can also use for isotropic gamma/ single precision - see  
gacommon_conduct.for>
```

```
c HP77 or PC
```

```
c*****
```

```
INCLUDE 'gacommon_conduct.for'
```

```
SAVE
```

```
c*****
```

```
CALL DEFLT
```

```
CALL INIT
```

```
CALL GRID
```

```
CALL READY1
```

```
CALL SETVAR
```

```
CALL READY2
```

```
c --- Generate initial generation + compute OF
```

```
CALL INIGEN
```

```
10 CONTINUE
```

```
c ----- Generation (= parent population) analysis -----
```

```
CALL GENANA
```

```
IF (KSTOPF.NE.0) GOTO 20
```

```
c ----- Breeding process -----
```

```
CALL BREED
```

```
c ----- Elitism process + compute OF of new generation -----
```

```
CALL ELITISM
```

```
GOTO 10
```

```
20 CONTINUE
```

```
c ----- Results analysis -----
```

```
1000 CALL RESULT
```

```
STOP 'GACONDUCT done'
```

```
END
```

```
C_____
```

```
SUBROUTINE DEFRD
```

```
c 2D version, dp - DJN 7/7/93 + additions SG 11/3/98; update 4/06/98
```

```
c HP77 or PC
```

```
c*****
```

```
INCLUDE 'gacommon_conduct.for'
```

```
SAVE
```

```
c*****
```

```
c
```

```
ENTRY DEFLT
```

```
COME HERE TO SET THE DEFAULT VALUES
```

```
c set initial clock time at start of run
```

```
TIME0=SECNDS(0.0)
```

```
c set cpu time for each generation loop to 0
```

```
CPUG=TIME0
```

```
KCPU=0
```

```
c set parameter adimensionalization marker
```

```
DO J=1,NPMAX
```

```
FACTADIM(J)='LIN'
```

```
ENDDO
```



```

c set iteration and convergence markers to 0
NCRITERG=0
ITERG=0
KSTOPF=0
KSTOP=0
ITERT =0
NFEVAL=0
OFFLINE=0.D0
ONLINE=0.D0

c set marker to check the constraints; =1 or 2 for constraints to be
applied
KCONT=0
NCONTMIN=0 !# of times parmin constraint is applied
NCONTMAX=0 !#      parmax

c set GRID marker;
c KXYGRID turns 1 if X(I) & Y(J) provided by the user
c KPRGRID turns 1 to print the grid only
KXYGRID=0
KPRGRID=0

c to look at a particular set of thermal properties:
c=====
c set parameter marker to 0;
c use 1 only to study a particular chromosome (promp gene values in
BEGIN)
KPAR=0
KPARSTOP=0

c set marker to print the XI for a particular chromosome to 0;
associated w/ KPAR=1
KXPRINT=0
KXADIM=0 !use 1 to print dimensionless X even w/ KESTOPT=0

c set marker for the sensor position(s) determination;
c use 1 to evaluate the sensor position for each chromosome;
(associated w/ KESTOPT=1)
c use 2 to evaluate the sensor position in Ready1; (associated w/
KESTOPT=0)
c leave to 0 if grid is fixed and sensor node (isensor, jsensor) is/are
searched or fixed
KSENSOR=0

c set the number of experiment
NEXP=1

c set the experiment number for which to compute the XI
JEXPC=1

c set XTX computation marker to 0; turns 1 to compute the XI
KXTX=0

c set the number of sensor to 1
NSENSOR=1

c set marker for estimation/optimization (0/1) to estimation
c ESTimation:
c min OF=sum of squares S for ML estimator (or OLS: sigma=1)
c set SIGMA (standard deviation for OLS estimation) in SETVAR
c set the thermocouple position(s) in GRID
c OPTimisation: use KSENSOR=1 in "GRID" if sensor's position is
unknown in terms of lenght
c define NPEST in INIT
c max OF=determinant of the Fisher information matrix for D-opt:
use OPTCRIT='D'
c max OF=trace of the Fisher information matrix for A-opt: use
OPTCRIT='A'
c max OF=min eigenvalue of the Fisher information matrix for E-
opt: use OPTCRIT='E'
KESTOPT=0
OPTCRIT='D'
SIGMA=1.D0

```

```

c set the number of the first data to use for S computation
(KESTOPT=0) to 1
IDATA0=1
TI=0.d0

c set marker to study the steady state T distribution and to determine
the SS Tmax; works w/ KPAR=1
KSS=0
TMAX=1.d0
TMAXP=1.D0 !ratio TMAX/correct adim; required in COMPXTXOPT
when KESTOPT=1

c set marker to plot the Tdist at a particular t; turns 1 when time-t in
OUTPUT; works w/ KPAR=1
KTHPRINT=0

c set marker to determine the optimal total experimental time TN
c associated w/ KESTOPT=1 and requires to know TIMEHEAT
(TN>TIMEHEAT)
KTN=0
TIMEHEAT=0.d0

c set marker to simulate data to 0
KYSIM=0

c set marker to use DT
c TIMEEXP ARRAY used: KDT=0; read measured T in SETVAR
c DT used      : KDT=1; set DT in SETVAR
c if KESTOPT=0 and KDT=1 generate simulated T in SETVAR
c (if KSS=1 KDT=1 and DT=BIG)
KDT=0

HEADER='USE THE CHARACTER VARIABLE HEADER TO
SPECIFY A PROBLEM TITLE'
PRINTF='PRINT.DAT'
PLOTf='PLOT.OUT'
KORD =2
MODE =1 !for cartesian coordinate system
KPGR =1
KOUT =2
c if KOUT=3 IU1=6,IU2=7 both on PRINTF and screen
c if KOUT=2 IU1=IU2=7=PRINTF
c if KOUT=1 IU1=IU2=6=on screen
KSCREEN=0 !=1 to print 'ITERG=...' on screen

C
-----
TIME = 0.0d0
DT = BIG
R(1) = 0.0d0
POWERX = 1.0d0
POWERY = 1.0d0

DO 10 NZ=1,NZMAX
POWRX(NZ)=1.0d0
10 POWRY(NZ)=1.0d0

DO 20 N=1,NFMAX
CRIT(N)=1.d-5
KSOLVE(N)=0
NTIMES(N)=40
KBLOC(N)=1
RELAX(N)=1.0d0
TITLE(N)=' '
KPRINT(N)=0 !to print temperature in PRINTF when PRINT
called at a particular t
KPLOT(N)=0 !to plot "      PLOTf  PLOT

DO 30 I=2,NI
FLUXJ1(I,N)=0.0d0
30 FLUXM1(I,N)=0.0d0

DO 40 J=2,NJ
FLUXI1(J,N)=0.0d0
40 FLUXL1(J,N)=0.0d0

20 CONTINUE

```



```

IF(KBC11(J),EQ.1) THEN
CON(2,J)=CON(2,J)+AIM(2,J)*F(1,J,NF)
ELSE
AP(1,J)=AIP(1,J)-FLXPI1(J)
CON(1,J)=FLXC11(J)
TEMP=AIM(2,J)/AP(1,J)
AP(2,J)= AP(2,J)-AIP(1,J)*TEMP
AIP(2,J)=AIP(2,J)-AIM(1,J)*TEMP
CON(2,J)=CON(2,J)+CON(1,J)*TEMP
ENDIF
AP(2,J)=AP(2,J)+AIM(2,J)
AIM(2,J)=0.0d0
CONSIDER I=L1 BOUNDARY
DIFF=GAMX(L2,J)/(0.5d0*XCX(L2)*SX(J))+SMALL
AIP(L2,J)=BETA*DIFF
AIM(L1,J)=AIP(L2,J)
AIP(L2,J)=AIP(L2,J)*ARX(J)
AIP(L1,J)=(BETA-1.0d0)*AIM(L2,J)/ARX(J)
AIM(L2,J)=AIM(L2,J)+AIP(L1,J)*ARX(J)
IF(KBCL1(J),EQ.1) THEN
CON(L2,J)=CON(L2,J)+AIP(L2,J)*F(L1,J,NF)
ELSE
AP(L1,J)=AIM(L1,J)-FLXPL1(J)
CON(L1,J)=FLXCL1(J)
TEMP=AIP(L2,J)/AP(L1,J)
AP(L2,J)= AP(L2,J)-AIM(L1,J)*TEMP
AIM(L2,J)=AIM(L2,J)-AIP(L1,J)*TEMP
CON(L2,J)=CON(L2,J)+CON(L1,J)*TEMP
ENDIF
AP(L2,J)=AP(L2,J)+AIP(L2,J)
AIP(L2,J)=0.0d0
30 CONTINUE

COEFFICIENTS FOR Y-DIRECTION DIFFUSION
DO 40 J=2,M3
DO 40 I=2,L2
AREA=RV(J+1)*XCX(I)
DIFF=AREA*2.0d0*GAMY(I,J)*GAMY(I,J+1)/(YCV(J)
*GAMY(I,J+1)+
1 YCV(J+1)*GAMY(I,J)+SMALL)
AJP(I,J)=DIFF+SMALL
AJM(I,J+1)=AJP(I,J)
40 CONTINUE

DO 50 I=2,L2
CONSIDER J=1 BOUNDARY
AREA=RV(2)*XCX(I)
DIFF=GAMY(I,2)/(0.5d0*YCV(2))+SMALL
AJM(I,2)=BETA*DIFF
AJP(I,1)=AJM(I,2)
AJM(I,2)=AJM(I,2)*AREA
AJM(I,1)=(BETA-1.0d0)*AJP(I,2)/(RV(3)*XCX(I))
AJP(I,2)=AJP(I,2)+AJM(I,1)*AREA
IF(KBCJ1(I),EQ.1) THEN
CON(I,2)=CON(I,2)+AJM(I,2)*F(I,1,NF)
ELSE
AP(I,1)=AJP(I,1)-FLXPJ1(I)
CON(I,1)=FLXCJ1(I)
TEMP=AJM(I,2)/AP(I,1)
AP(I,2)= AP(I,2)-AJP(I,1)*TEMP
AJP(I,2)=AJP(I,2)-AJM(I,1)*TEMP
CON(I,2)=CON(I,2)+CON(I,1)*TEMP
ENDIF
AP(I,2)=AP(I,2)+AJM(I,2)
AJM(I,2)=0.0d0
CONSIDER J=M1 BOUNDARY
AREA=RV(M1)*XCX(I)
DIFF=GAMY(I,M2)/(0.5d0*YCV(M2))+SMALL
AJP(I,M2)=BETA*DIFF
AJM(I,M1)=AJP(I,M2)
AJP(I,M2)=AJP(I,M2)*AREA
AJP(I,M1)=(BETA-1.0d0)*AJM(I,M2)/(RV(M2)*XCX(I))
AJM(I,M2)=AJM(I,M2)+AJP(I,M1)*AREA
IF(KBCM1(I),EQ.1) THEN
CON(I,M2)=CON(I,M2)+AJP(I,M2)*F(I,M1,NF)
ELSE

```

```

AP(I,M1)=AJM(I,M1)-FLXPM1(I)
CON(I,M1)=FLXCM1(I)
TEMP=AJP(I,M2)/AP(I,M1)
AP(I,M2)= AP(I,M2)-AJM(I,M1)*TEMP
AJM(I,M2)=AJM(I,M2)-AJP(I,M1)*TEMP
CON(I,M2)=CON(I,M2)+CON(I,M1)*TEMP
ENDIF
AP(I,M2)=AP(I,M2)+AJP(I,M2)
AJP(I,M2)=0.0d0
50 CONTINUE

```

```

COME HERE TO INTRODUCE UNDERRELAXATION
CONSTRUCT AP(I,J) AND CON(I,J) IN THEIR FINAL FORM
DO 60 J=2,M2
DO 60 I=2,L2
ANB=AIP(I,J)+AIM(I,J)+AJP(I,J)+AJM(I,J)
AINR=ANB*RLX
AP(I,J)=AP(I,J)+ANB+AINR
CON(I,J)=CON(I,J)+AINR*F(I,J,NF)
60 CONTINUE

```

```

CALL THE SOLVE ROUTINE TO OBTAIN THE SOLUTION OF
THE DISCRETIZATION EQUATIONS
CALL SOLVE
100 CONTINUE

```

```

ITERT=ITERT+1
IF(ITERT.GE.LASTT) KSTOP=1 !also exists in OUTPUT if used
IF (KDT.EQ.0) THEN
TIME=TIMEEXP(1,ITERT)
ELSE
TIME=TIME+DT
ENDIF

```

```

RETURN
END

```

```

c*****

```

```

SUBROUTINE SOLVE

```

```

c 2D version, dp - DJN 7/7/93
c HP77 or PC

```

```

c*****

```

```

INCLUDE 'gaccommon_conduct.for'

```

```

c*****

```

```

DIMENSION RT(6)

```

```

SAVE

```

```

C-----

```

```

BIG1=1.d+10
SMALL1=1.0d-5
LL2=2*L2
LL=LL2-2
MM2=2*M2
MM=MM2-2
N=NF
NTM=NTIMES(N)

```

```

DO 200 NT=1,NTM
NTT=NT
ICON=1

```

```

COME HERE TO PERFORM THE I-DIRECTION BLOCK
CORRECTION

```

```

C-----

```

```

PTX(1)=0.0d0
QTX(1)=0.0d0

```

```

DO 10 I=2,L2
BL=SMALL
BLP=0.0d0
BLM=0.0d0
BLC=0.0d0

```

```

DO 20 J=2,M2
IF(AP(I,J).LT.BIG1) THEN

```

```

BL=BL+AP(I,J)
IF(AP(I,J+1).LT.BIG1) BL=BL-AJP(I,J)
IF(AP(I,J-1).LT.BIG1) BL=BL-AJM(I,J)
IF(AP(I+1,J).LT.BIG1) BLP=BLP+AIP(I,J)
IF(AP(I-1,J).LT.BIG1) BLM=BLM+AIM(I,J)
CONVERGENCE CRITERION FOR THE SOLUTION ROUTINE
RT(1)=AIP(I,J)*F(I+1,J,N)
RT(2)=AIM(I,J)*F(I-1,J,N)
RT(3)=AJP(I,J)*F(I,J+1,N)
RT(4)=AJM(I,J)*F(I,J-1,N)
RT(5)=-AP(I,J)*F(I,J,N)
RT(6)=CON(I,J)
RES=0.0d0
TERM=1.0d-8

DO 30 IRT=1,6
RES=RES+RT(IRT)
30 TERM=MAX(TERM,ABS(RT(IRT)))

```

```

IF(ABS(RES/TERM).GT.CRIT(N))ICON=0
BLC=BLC+RES

```

```

ENDIF
20 CONTINUE

```

```

DENOM=BL-PTX(I-1)*BLM
IF(ABS(DENOM/BL).LT.SMALL1) DENOM=BIG
PTX(I)=BLP/DENOM
QTX(I)=(BLC+BLM*QTX(I-1))/DENOM
10 CONTINUE

```

```

IF(NTT.NE.1.AND.ICON.EQ.1) GO TO 210
IF(KBLOC(NF).EQ.0) GO TO 80
BL=0.0d0

```

```

DO 40 I=L2,2,-1
BL=BL*PTX(I)+QTX(I)
DO 40 J=2,M2
IF(AP(I,J).LT.BIG1) F(I,J,N)=F(I,J,N)+BL
40 CONTINUE

```

```

COME HERE TO PERFORM THE J-DIRECTION BLOCK
CORRECTION

```

```

C-----
PTY(1)=0.0d0
QTY(1)=0.0d0

```

```

DO 50 J=2,M2
BL=SMALL
BLP=0.0d0
BLM=0.0d0
BLC=0.0d0

```

```

DO 60 I=2,L2
IF(AP(I,J).LT.BIG1) THEN
BL=BL+AP(I,J)
IF(AP(I+1,J).LT.BIG1) BL=BL-AIP(I,J)
IF(AP(I-1,J).LT.BIG1) BL=BL-AJM(I,J)
IF(AP(I,J+1).LT.BIG1) BLP=BLP+AJP(I,J)
IF(AP(I,J-1).LT.BIG1) BLM=BLM+AJM(I,J)
BLC=BLC+CON(I,J)+AIP(I,J)*F(I+1,J,N)+AIM(I,J)*F(I-1,J,N)
1+AJP(I,J)*F(I,J+1,N)+AJM(I,J)*F(I,J-1,N)-AP(I,J)*F(I,J,N)
ENDIF
60 CONTINUE

```

```

DENOM=BL-PTY(J-1)*BLM
IF(ABS(DENOM/BL).LT.SMALL1) DENOM=BIG
PTY(J)=BLP/DENOM
QTY(J)=(BLC+BLM*QTY(J-1))/DENOM
50 CONTINUE

```

```

BL=0.0d0

```

```

DO 70 J=M2,2,-1
BL=BL*PTY(J)+QTY(J)
DO 70 I=2,L2

```

```

IF(AP(I,J).LT.BIG1) F(I,J,N)=F(I,J,N)+BL
70 CONTINUE

```

```

80 CONTINUE

```

```

CARRY OUT THE I-DIRECTION TDMA

```

```

C-----
DO 90 JJ=2,MM
J=MIN(JJ,MM2-JJ)
PTX(1)=0.0d0
QTX(1)=0.0d0

```

```

DO 100 I=2,L2
DENOM=AP(I,J)-PTX(I-1)*AIM(I,J)
PTX(I)=AIP(I,J)/DENOM
TEMP=CON(I,J)+AJP(I,J)*F(I,J+1,N)+AJM(I,J)*F(I,J-1,N)
QTX(I)=(TEMP+AIM(I,J)*QTX(I-1))/DENOM
100 CONTINUE

```

```

DO 110 I=L2,2,-1
110 F(I,J,N)=F(I+1,J,N)*PTX(I)+QTX(I)

```

```

90 CONTINUE

```

```

CARRY OUT THE J-DIRECTION TDMA

```

```

C-----
DO 120 II=2,LL
I=MIN(II,LL2-II)
PTY(1)=0.0d0
QTY(1)=0.0d0

```

```

DO 130 J=2,M2
DENOM=AP(I,J)-PTY(J-1)*AJM(I,J)
PTY(J)=AJP(I,J)/DENOM
TEMP=CON(I,J)+AIP(I,J)*F(I+1,J,N)+AIM(I,J)*F(I-1,J,N)
QTY(J)=(TEMP+AJM(I,J)*QTY(J-1))/DENOM
130 CONTINUE

```

```

DO 140 J=M2,2,-1
140 F(I,J,N)=F(I,J+1,N)*PTY(J)+QTY(J)

```

```

120 CONTINUE

```

```

C-----
200 CONTINUE

```

```

NTC(N)=NTT
GO TO 220
210 NTC(N)=NTT-1
220 CONTINUE

```

```

CALCULATE THE UNKNOWN BOUNDARY VALUES AND
FLUXES

```

```

C-----
DO 160 I=2,L2

```

```

TEMP=AJM(I,1)*(F(I,3,N)-F(I,2,N))
IF(KBCJ1(I).EQ.2)
1 F(I,1,N)=(AJP(I,1)*F(I,2,N)-TEMP+CON(I,1))/AP(I,1)
FLUXJ1(I,N)=AJP(I,1)*(F(I,1,N)-F(I,2,N))+TEMP
TEMP=AJP(I,M1)*(F(I,M3,N)-F(I,M2,N))
IF(KBCM1(I).EQ.2)
1 F(I,M1,N)=(AJM(I,M1)*F(I,M2,N)-
TEMP+CON(I,M1))/AP(I,M1)
160 FLUXM1(I,N)=AJM(I,M1)*(F(I,M1,N)-F(I,M2,N))+TEMP

```

```

DO 170 J=2,M2
TEMP=AIM(1,J)*(F(3,J,N)-F(2,J,N))
IF(KBCI1(J).EQ.2)
1 F(1,J,N)=(AIP(1,J)*F(2,J,N)-TEMP+CON(1,J))/AP(1,J)
FLUXI1(J,N)=AIP(1,J)*(F(1,J,N)-F(2,J,N))+TEMP
TEMP=AIP(1,J)*(F(1,3,N)-F(1,2,N))
IF(KBCL1(J).EQ.2)
1 F(1,1,N)=(AIM(1,1)*F(1,2,N)-TEMP+CON(1,1))/AP(1,1)
170 FLUXL1(J,N)=AIM(1,1)*(F(1,1,N)-F(1,2,N))+TEMP

```

```

COME HERE TO RESET CON,AP,KBC,FLXC, AND FLXP
C-----

```

```
DO 180 J=2,M2
KBCI1(J)=1
KBCL1(J)=1
FLXCI1(J)=0.0d0
FLXCL1(J)=0.0d0
FLXPI1(J)=0.0d0
FLXPL1(J)=0.0d0
```

```
DO 180 I=2,L2
CON(I,J)=0.0d0
AP(I,J)=0.0d0
180 CONTINUE
```

```
DO 190 I=2,L2
KBCJ1(I)=1
KBCM1(I)=1
FLXCJ1(I)=0.0d0
FLXCM1(I)=0.0d0
FLXPJ1(I)=0.0d0
FLXPM1(I)=0.0d0
190 CONTINUE
```

```
RETURN
END
c*****
```

SUBROUTINE TOOLS

*c 2D version, dp - DJN 7/7/93 - SG /3/98
c HP77 or PC*

```
c*****
INCLUDE 'gacommon_conduct.for'
SAVE
c*****
```

ENTRY EZGRID

CONSTRUCT THE X-DIRECTION GRID

```
L1=NCVLX+2
XU(2)=0.0d0
XU(L1)=XL
L2=L1-1
FCVLX =FLOAT(NCVLX)
```

```
DO 20 I=3,L2
DD=FLOAT(I-2)/FCVLX
IF(POWERX.GT.0.d0) THEN
XU(I)=XL*DD**POWERX
ELSE
XU(I)=XL*(1.d0-(1.d0-DD)**(-POWERX))
ENDIF
20 CONTINUE
```

CONSTRUCT THE Y-DIRECTION GRID

```
M1=NCVLY+2
YV(2)=0.0d0
YV(M1)=YL
M2=M1-1
FCVLY =FLOAT(NCVLY)
```

```
DO 30 J=3,M2
DD=FLOAT(J-2)/FCVLY
IF(POWERY.GT.0.d0) THEN
YV(J)=YL*DD**POWERY
ELSE
YV(J)=YL*(1.d0-(1.d0-DD)**(-POWERY))
ENDIF
30 CONTINUE
```

```
RETURN
c*****
```

ENTRY ZGRID

CONSTRUCT THE GRID ZONE-BY-ZONE

CONSIDER THE X DIRECTION

```
XU(2)=0.0d0
I2=2
```

```
DO 40 NZ=1,NZX
FCVLX=FLOAT(NCVX(NZ))
ILAST=I2
I1 =ILAST+1
I2 =ILAST+NCVX(NZ)
```

```
DO 40 I=I1,I2
DD=FLOAT(I-ILAST)/FCVLX
IF(POWRX(NZ).GT.0.) THEN
XU(I)=XU(ILAST)+XZONE(NZ)*DD**POWRX(NZ)
ELSE
XU(I)=XU(ILAST)+XZONE(NZ)*(1.d0-(1.d0-DD)**(-
POWRX(NZ)))
ENDIF
40 CONTINUE
```

L1=I2

CONSIDER THE Y DIRECTION

```
YV(2)=0.0d0
J2=2
```

```
DO 50 NZ=1,NZY
FCVLY=FLOAT(NCVY(NZ))
JLAST=J2
J1 =JLAST+1
J2 =JLAST+NCVY(NZ)
```

```
DO 50 J=J1,J2
DD=FLOAT(J-JLAST)/FCVLY
IF(POWRY(NZ).GT.0.) THEN
YV(J)=YV(JLAST)+YZONE(NZ)*DD**POWRY(NZ)
ELSE
YV(J)=YV(JLAST)+YZONE(NZ)*(1.d0-(1.d0-DD)**(-
POWRY(NZ)))
ENDIF
50 CONTINUE
```

M1=J2

```
RETURN
c*_*_*_*_*_*_*_*_*_*_*_*_*_*_*_*_*_*_*_*_*_*_*_*_*_*_*_*_*_*_*_*_*_*_*_*_*_*
```

ENTRY XYGRID

CONSTRUCT THE GRID KNOWING THE NODE POSITIONS

CONSIDER THE X DIRECTION

```
XU(2)=X(1)
DO 60 I=3,L1
XU(I)=XU(I-1)+2.D0*(X(I)-XU(I-1))
60 CONTINUE
```

CONSIDER THE Y DIRECTION

```
YV(2)=Y(1)
DO 70 J=3,M1
YV(J)=YV(J-1)+2.D0*(Y(J)-YV(J-1))
70 CONTINUE
```

```
RETURN
c*_*_*_*_*_*_*_*_*_*_*_*_*_*_*_*_*_*_*_*_*_*_*_*_*_*_*_*_*_*_*_*_*_*_*_*_*
```

ENTRY PRINT

```
DO 199 IUNIT=IU1,IU2
```

COME HERE TO ARRANGE THE PRINTOUT OF TWO-DIMENSIONAL FIELDS

```
IF(KPGR.NE.0) THEN
CREATE PRINTOUT FOR GRID
```



```

READ(*,*)(PAR(J),J=1,NP)
WRITE(*,*)
WRITE(*,*)KADIM? Note that 0=w/o dimensions and 1=w/ dim.'
WRITE(*,*)
READ(*,*)KADIM
IF (KADIM.EQ.1) THEN
GOTO 15
ELSE
DO J=1,NP
ARR(1,J)=PAR(J)
ENDDO
ENDIF
ENDIF

```

```

c denormalize the genes = dimensionalize the parameters
DO 10 J=1,NP
IF (FACTADIM(J).EQ.'LIN') THEN
PAR(J)=(PARMAX(J)-PARMIN(J))*ARR(ITERID,J)+PARMIN(J)
ELSE
PAR(J)=10.D0**(DLOG10(PARMAX(J)/PARMIN(J))
*ARR(ITERID,J)+DLOG10(PARMIN(J)))
ENDIF
10 CONTINUE

```

```

c reset OF value to 0
15 PAR(NP+1)=0.D0

```

```

c*****
IF (KESTOPT.EQ.0) THEN
c EST run: reset statements for new T and S computation
CALL BEGIN
c start the iteration or time-step loop
20 CONTINUE
CALL OUTPUT
IF (ITERT.EQ.0.OR.ITERT.GT.LASTT.OR.KSS.EQ.1) GOTO 40
IF (ITERT.GE.IDATA0) THEN
DO 30 NSENS=1,NSENSOR
IF (KTS(NSENS).EQ.1) THEN
c compute residu at time t
RES=YARR(NSENS,KDATA(NSENS))-TSENSOR(NSENS)
c compute S=sum of least-square errors
PAR(NP+1)=PAR(NP+1)+(RES/SIGMA)**2
KTS(NSENS)=0
!deactivate S comp. (KTS=1 when time=timeexp)
KDATA(NSENS)=KDATA(NSENS)+1
ENDIF
30 CONTINUE
ENDIF
40 IF (KSTOP.NE.0) GOTO 80
CALL HEART
GOTO 20

```

```

c*****
ELSE
c OPT run: determine sensitivity coefficients and matrix XTX for
OPTCRIT computation
CALL COMPMX
DO 60 IXTX=1,LASTT
IF (IXTX.EQ.1.AND.KTN.EQ.1) OPTOFMOD=0.D0 !searching
for the total exp time
CALL COMPMXTXOPT(IXTX,XTXOPT)
CALL JACOBI(XTXOPT,NPEST,NPEST,EIG)
CALL RANGER(NPEST,EIG)
SUMEIG=0.D0
PRODEIG=1.D0
DO 50 J=1,NPEST
SUMEIG=SUMEIG+EIG(J)
PRODEIG=PRODEIG*EIG(J)
50 CONTINUE
c compute optimality criterion:
c D- = det. XTX matrix = -a(1)/a(4) = product of eigenvalues
c E- = max the min eigenvalue
c A- = trace XTX matrix = -a(3)/a(4) = sum of eigenvalues
IF (OPTCRIT.EQ.'D') THEN
OPTOF=PRODEIG
ELSE

```

```

IF (OPTCRIT.EQ.'A') THEN
OPTOF=SUMEIG
ELSE
OPTOF=EIG(1)
ENDIF
ENDIF
IF (KTN.EQ.0) THEN
IF (OPTOF.GT.PAR(NP+1)) PAR(NP+1)=OPTOF
ELSE
RATIO=ABS((OPTOF-OPTOFMOD)/(OPTOFMOD+1.D-30))
IF (IXTX*DT.GT.TIMEHEAT.AND.RATIO.LE.1.D-4) THEN
PAR(NP+1)=IXTX*DT
GOTO 70
ELSE
OPTOFMOD=OPTOF
ENDIF
ENDIF
IF (KXPRINT.EQ.1) WRITE(IUEIG,55)IXTX*DT,OPTOF,
(EIG(J),J=1,NPEST)
55 FORMAT(F16.3,11(1X,E16.8))
60 CONTINUE

```

```

IF (KTN.EQ.1) PAR(NP+1)=IXTX*DT
70 CONTINUE
ENDIF

```

```

c*****

```

```

80 ARR(ITERID,NP+1)=PAR(NP+1)
NFEVAL=NFEVAL+1
ONLINE=ONLINE+ARR(ITERID,NP+1)

```

```

c come here only for a particular chromosome
IF (KPARSTOP.EQ.1) THEN
c results of the particular set of thermal properties
JBEG=1
JEND=NP+1
JREP=(JEND-JBEG+11)/11
DO 90 JWRITE=1,JREP
INCRJ=MIN(10,JEND-JBEG)
JSTOP=JBEG+INCRJ
WRITE(*,(11(1X,E16.8)/'))(PAR(J),J=JBEG,JSTOP)
WRITE(99,(11(1X,E16.8)/'))(PAR(J),J=JBEG,JSTOP)
JBEG=JSTOP+1
90 CONTINUE
IF (KESTOPT.EQ.0) THEN
KPARSTOP=0
CALL COMPMX
ENDIF
WRITE(*,*)
STOP 'Particular set of genes analyzed'
ENDIF

```

```

100 CONTINUE

```

```

RETURN
END

```

```

c*****

```

```

SUBROUTINE RMARIN(IJ,KL)

```

```

c HP77 or PC

```

C This is the initialization routine for the random number generator RANMAR(). C NOTE: The seed variables can have values between: 0 <= IJ <= 31328 0 <= KL <= 30081 C The random number sequences created by these two seeds are of sufficient length to complete an entire calculation with. For example, if several different groups are working on different parts of the same calculation, each group could be assigned its own IJ seed. This would leave each group with 30000 choices for the second seed. That is to say, this random number generator can create 900 million different subsequences -- with each subsequence having a length of approximately 10^30. Use IJ = 1802 & KL = 9373 to test the random number generator. The subroutine RANMAR should be used to generate 20000 random

SUBROUTINE GABODY

c HP77 or PC - SG 25/9/98

```
c*****  
INCLUDE 'gacommon_conduct.for'  
c*****  
DIMENSION CHILDRAND(NSMAX,NPMAX+1)  
CHARACTER*24 FDATE  
SAVE  
C-----
```

ENTRY INIGEN

c initialize the random generator
CALL RMARIN(ISEED1,ISEED2)

c create the initial normalized population
CALL INITPOP

*c if the rank-based selection is applied, determine
c the fitness and probability of breeding of each parent*
IF (SELECT.EQ.'R') CALL RANKFIT

c compute OF of initial pop
CALL COMPOF(NS,CP)

RETURN

```
c*****
```

ENTRY GENANA

c rank the population at generation iterg
CALL RANKNS

c compute OFavg of the population at generation iterg
CALL OFAVE

c check if convergence criterion is met
CALL CHECKCONV

RETURN

```
c*****
```

ENTRY BREED

c make ns children
DO 20 ICHILD=1,NS/2

IF (SELECT.EQ.'R') THEN
c select 2 parents according to rank selection
CALL SELRANK(ICHILD)

ELSE
c select 2 parents according to tournament selection
CALL SELTOURMT
ENDIF

c make 2 children by crossing the 2 selected parents
CALL CROSS

c mutate the child according to jump mutation
CALL MUTJUMP

c mutate the child according to jump AND creep mutations
IF (MUT.EQ.'JC') CALL MUTCREEP

DO 10 J=1,NP
CC(ICHILD,J)=CHILD(1,J)
CC(ICHILD+NS/2,J)=CHILD(2,J)
10 CONTINUE

20 CONTINUE

IF (KCONT.NE.0) CALL CHECKCONT(NS,CC)

RETURN

```
c*****
```

ENTRY ELITISM

c compute OF of children population
CALL COMPOF(NS,CC)

c apply basic elitism
IF (ELIT.EQ.'B') THEN

c keep best parent by destroying last child made -arbitrarily
DO 30 I=2,NS
DO 30 J=1,NP
CP(I,J)=CC(I-1,J)
30 CONTINUE

ELSE
IF (ELIT.EQ.'SS') THEN

c apply SS elitism
c 1. compute OF of children population that mutated
IF (MUT.EQ.'J') THEN
NMUT=NMUTJUMP
ELSE
NMUT=NMUTJUMP+NMUTCREEP
ENDIF

IF (KCONT.NE.0) CALL CHECKCONT(NMUT,CHILDMUT)

CALL COMPOF(NMUT,CHILDMUT)

*c 2. combine both children populations and rank the combined
children population*

NTOT=NS+NMUT
DO 60 J=1,NP+1
DO 40 I=1,NS
CHILDTOT(I,J)=CC(I,J)
40 CONTINUE
DO 50 I=1,NMUT
CHILDTOT(I+NS,J)=CHILDMUT(I,J)
50 CONTINUE
60 CONTINUE
CALL RANK2NS

c 3. keep the best parents
NPKEPT=INT(NS*(1.D0-PR))
IF (NPKEPT.EQ.0) NPKEPT=1 *!to preserve at least the best
parent ~ B elitism*

IF (KILLTWIN.EQ.'N') THEN

*c 4. replace a fraction of the parent population with ns*pr children*
70 CONTINUE
DO 80 I=NPKEPT+1,NS
DO 80 J=1,NP+1
CP(I,J)=CHILDTOT(I-NPKEPT,J)
80 CONTINUE

ELSE
c 5. kill the twins; note that NTOT will change
CALL KTWINS
IF (NTWINS.LE.(NPKEPT+NMUT)) THEN
GOTO 70
ELSE

NCHILDRAND=NS-NPKEPT-NTOT
WRITE(99,'(A25,I3)')!!!Need random children: ',
+NCHILDRAND
DO 100 I=1,NCHILDRAND
DO 90 J=1,NP
CHILDRAND(I,J)=URAND()
90 CONTINUE
CHILDRAND(I,NP+1)=0.D0
100 CONTINUE

CALL COMPOF(NCHILDRAND,CHILDRAND)

```

DO 110 I=NPKEPT+1,NPKEPT+NTOT
DO 110 J=1,NP+1
CP(I,J)=CHILDTOT(I-NPKEPT,J)
110 CONTINUE
DO 120 I=NPKEPT+NTOT+1,NS
DO 120 J=1,NP+1
CP(I,J)=CHILDRAND(I-NPKEPT-NTOT,J)
120 CONTINUE
ENDIF

ENDIF
ELSE
WRITE(*,*)'SR elitism is not set up yet!'
ENDIF
ENDIF

RETURN
c*****

ENTRY RESULT

c list the final parent population and measure the GA performance
WRITE(99,130)
130 FORMAT(/75('=')/2X,'RESULTS'/50('-'))

WRITE(99,'(//A36)')'Elapsed CPU time since start of run:'
WRITE(99,'(1X,A8,F10.1)')'CPU (s)=' ,KCPU*86400-
TIME0+SECNDS(0.0)

IF (KSTOPF.EQ.2) THEN
WRITE(99,'(A28)')'Stopped because iterg=lastg!'
ELSE
WRITE(99,'(A34,I3)')'Convergence criterion met @ iterg=' ,iterg
ENDIF

DO 150 I=1,NS
DO 150 J=1,NP
IF (FACTADIM(J).EQ.'LIN') THEN
CP(I,J)=(PARMAX(J)-PARMIN(J))*CP(I,J)+PARMIN(J)
ELSE
CP(I,J)=10**(DLOG10(PARMAX(J)/PARMIN(J))
*CP(I,J)+DLOG10(PARMIN(J)))
ENDIF
150 CONTINUE

c write the final population to the output file
JEND=NP+1
JBEG=1
JREP=(JEND-JBEG+11)/11
DO 160 I=1,NS
JBEG=1
DO 160 JWRITE=1,JREP
INCRJ=MIN(10,JEND-JBEG)
JSTOP=JBEG+INCRJ
WRITE(10,'(I3,2X,I1(G16.8,1X))',I,(CP(I,J),J=JBEG,JSTOP)
JBEG=JSTOP+1
160 CONTINUE

WRITE(99,170)
170 FORMAT(/2X,'*** Measure of the GA performance ***')

WRITE(99,'(//A28/)')1 "BEST SO FAR" cp(1,np+1):'
JBEG=1
DO 180 JWRITE=1,JREP
INCRJ=MIN(10,JEND-JBEG)
JSTOP=JBEG+INCRJ
WRITE(99,'(11(1X,G16.8/))',CP(1,J),J=JBEG,JSTOP)
PRINT*, (CP(1,J),J=JBEG,JSTOP)
JBEG=JSTOP+1
180 CONTINUE

c EST run: calculate 95% CI of best design + compute correlation matrix
c OPT run: calculate total experimental time (when Dmod+ unchanged)
IF (KESTOPT.EQ.1) THEN

```

```

KTN=1
CALL COMPOF(1,BEST)
WRITE(99,190)
190 FORMAT(/2X,'Nondimensional total experimental time:')
WRITE(99,'(G16.8/)'BEST(NP+1)
ELSE
DO 200 J=1,NP+1
PAR(J)=CP(1,J)
200 CONTINUE
CALL COMPCCI
ENDIF

WRITE(99,'(//A26/)')2) "OFF LINE" convergence:'
WRITE(99,'*')='moyenne courante des bests sur ITERG+1 generations'
WRITE(99,'*')='limite de la convergence'
OFFLINE=OFFLINE/(ITERG +1)
WRITE(99,'(1X,G16.8,2X,A8,I3)')OFFLINE,'ITERG+1=' ,ITERG+1
WRITE(99,'(//A25/)')3) "ON LINE" convergence:'
WRITE(99,'*')='moyenne de toutes les evaluations sur NFEVAL eval.'
WRITE(99,'*')='facon dont la convergence est atteinte'
ONLINE=ONLINE/NFEVAL
WRITE(99,'(1X,G16.8,2X,A7,I6)')ONLINE,'NFEVAL=' ,NFEVAL

WRITE(99,210)
210 FORMAT(/2X,'*** Statistical analyses on final Nst ***')
c perform statistical calculations on 5 best
IF (NS.GE.5) CALL STATIST(5)
c perform statistical calculations on 10 best
IF (NS.GE.10) CALL STATIST(10)
c perform statistical calculations on NS best
CALL STATIST(NS)

WRITE(99,'(//A45)')4a) Elapsed CPU time since gen. loop stopped:'
IF (SECNDS(0.0).GT.CPUG) THEN
WRITE(99,'(1X,A24,F10.1)')'CPU (s) /Sub. RESULT/ =' ,
1 SECNDS(CPUG)
ELSE
WRITE(99,'(1X,A24,F10.1)')'CPU (s) /Sub. RESULT/ =' ,
1 86400.-CPUG+SECNDS(0.0)
KCPU=KCPU+1
ENDIF

WRITE(99,'(//A40)')4b) Elapsed CPU time since start of run:'
WRITE(99,'(1X,A8,F10.1)')'CPU (s)=' ,KCPU*86400-
TIME0+SECNDS(0.0)

CLOSE(99)
CLOSE(10)
CLOSE(11)
CLOSE(12)
CLOSE(8)
CLOSE(9)

RETURN
END
c*****

SUBROUTINE GAINV
c includes invariant "entry subroutines" dealing with a GA
c HP77 or PC - SG 11/3/98

c*****
INCLUDE 'gacommon_conduct.for'
c*****
COMMON/PROBGA/P(NSMAX),IPARENT(2)
DIMENSION IPLACE(2)
SAVE
c-----

ENTRY RANKFIT

c determine the probability of breeding of a population of size ns
c based on a ranked fitness

P(1)=2.D0/(NS*1.D0+1.D0)
DO 10 I=2,NS

```



```

DO 280 I=1,N
RMEAN(J)=RMEAN(J)+CP(I,J)
280 CONTINUE
RMEAN(J)=RMEAN(J)/RN
290 CONTINUE

WRITE(99,300)
300 FORMAT(/'RMEAN(CP(1:N,NP+1)):')
JBEG=1
JEND=NP+1
JREP=(JEND-JBEG+11)/11
DO 310 JWRITE=1,JREP
INCRJ=MIN(10,JEND-JBEG)
JSTOP=JBEG+INCRJ
WRITE(99,'(11(1X,G16.8))')(RMEAN(J),J=JBEG,JSTOP)
JBEG=JSTOP+1
310 CONTINUE

c compute the standard deviations:
DO 330 J=1,NP+1
DO 320 I=1,N
DEV(J)=DEV(J)+(CP(I,J)-RMEAN(J))**2
320 CONTINUE
DEV(J)=SQRT(DEV(J)/(RN-1.D0))
330 CONTINUE

WRITE(99,340)
340 FORMAT(/'STANDARD DEVIATIONS:')
JBEG=1
DO 350 JWRITE=1,JREP
INCRJ=MIN(10,JEND-JBEG)
JSTOP=JBEG+INCRJ
WRITE(99,'(11(1X,G16.8))')(DEV(J),J=JBEG,JSTOP)
JBEG=JSTOP+1
350 CONTINUE

c compute the 95% confidence intervals for the mean values:
IF (N.LE.5) TCOEF=2.776D0
IF (N.EQ.10) TCOEF=2.262D0
IF (N.EQ.25) TCOEF=2.064D0
IF (N.EQ.30) TCOEF=2.045D0
IF (31.LE.N.AND.N.LE.41) TCOEF=2.042D0-0.0021D0*(RN-31.D0)
IF (41.LT.N.AND.N.LE.61) TCOEF=2.021D0-0.00105D0
*(RN-41.D0)
IF (61.LT.N.AND.N.LE.121) TCOEF=2.D0-3.333D-4*(RN-61.D0)
IF (N.GT.121) TCOEF=1.96D0

DO 360 J=1,NP+1
CI(J)=TCOEF*DEV(J)/SQRT(RN)
360 CONTINUE

WRITE(99,370)
370 FORMAT(/'95% CONFIDENCE INTERVALS:')
JBEG=1
DO 380 JWRITE=1,JREP
INCRJ=MIN(10,JEND-JBEG)
JSTOP=JBEG+INCRJ
WRITE(99,'(11(1X,G16.8))')(CI(J),J=JBEG,JSTOP)
JBEG=JSTOP+1
380 CONTINUE

RETURN
END
c*****

SUBROUTINE SENSOF

c includes invariant "entry subroutines" dealing with an OF
c HP77 or PC - SG modified 25/09/98

c*****
INCLUDE 'gacommon_conduct.for'
c*****
COMMON/PROBMATP/
XI(LASTTMAX,NPMAX),XTX(NPMAX,NPMAX)
DIMENSION P(NPMAX,NPMAX),RI(NPMAX,NPMAX),

```

```

AUG(NPMAX,NPMAX+1),T1(LASTTMAX),T2(LASTTMAX),
SUMXTX(NPMAX,NPMAX),XTXOPT(NPMAX,NPMAX)
SAVE
c-----

ENTRY COMPMI

c compute sensibility coefficients of parameters to be estimated

KXTX=1
KDB=0

c reset statements for new T computation
10 CALL BEGIN

IF (KDB.EQ.0.AND.KSENSOR.EQ.1) THEN
c define the sensor(s) position(s) with the design parameters xs and ys
NSENS=1
11 CONTINUE
I=1
J=1
XS=XSENSOR(NSENS)
YS=YSENSOR(NSENS)
IF (X(I).LE.XS.AND.XS.LE.X(I+1)/2.D0) THEN
IS=I
ELSE

I=I+1
IF (X(I)/2.D0.LT.XS.AND.XS.LE.XU(I+1)) THEN
IS=I
ELSE

12 I=I+1
IF (XU(I).LT.XS.AND.XS.LE.XU(I+1)) THEN
IS=I
ELSE
IF (I.LT.L3) GOTO 12

I=I+1
IF (XU(I).LT.XS.AND.XS.LT.(X(I)+(X(I+1)-X(I))/2)) THEN
IS=I
ELSE

IS=I+1
ENDIF
ENDIF
ENDIF
ENDIF

IF (Y(J).LE.YS.AND.YS.LE.Y(J+1)/2.D0) THEN
JS=J
ELSE

J=J+1
IF (Y(J)/2.D0.LT.YS.AND.YS.LE.YV(J+1)) THEN
JS=J
ELSE

13 J=J+1
IF (YV(J).LT.YS.AND.YS.LE.YV(J+1)) THEN
JS=J
ELSE
IF (J.LT.M3) GOTO 13
J=J+1
IF (YV(J).LT.YS.AND.YS.LT.(Y(J)+(Y(J+1)-Y(J))/2)) THEN
JS=J
ELSE
JS=J+1
ENDIF
ENDIF
ENDIF
ENDIF

ISENSOR(NSENS)=IS
JSENSOR(NSENS)=JS
IF (KXPRINT.EQ.1) THEN

```


c COMMON include file for GACONDUCT
c SG 3/11/98; update 4/06/98

IMPLICIT DOUBLE PRECISION (a-h,o-z)
IMPLICIT INTEGER*4 (i-n)

REAL*4 TIME0,CPUG

PARAMETER (BIG=1.d+52, SMALL=1.d-52) *!double precision*
PARAMETER (NI=102,NJ=102,NFMAX=1,NZMAX=15)
PARAMETER (NSMAX=500,NPMAX=9,LASTTMAX=10001,
NEXPMAX=5,NSENSORMAX=1)

CHARACTER*18 TITLE
CHARACTER*64 HEADER,PRINTF,PLOTF
CHARACTER*4 SELECT,MUT,KILLTWIN,ELIT,OPTCRIT,
FACTADIM

C _____

COMMON F(NI,NJ,NFMAX),ALAM(NI,NJ),
GAM(NI,NJ), *!Isotropic gamma*
GAMX(NI,NJ),GAMY(NI,NJ), *!Orthotropic gamma*
CON(NI,NJ),AP(NI,NJ),AIP(NI,NJ),
AIM(NI,NJ),AJP(NI,NJ),AJM(NI,NJ),
FLUXI1(NJ,NFMAX),FLUXJ1(NI,NFMAX),
FLUXL1(NJ,NFMAX),FLUXM1(NI,NFMAX),
X(NI),XU(NI),XCV(NI),ARX(NJ),Y(NJ),YV(NJ),
YCV(NJ),YCVR(NJ),R(NJ),RV(NJ),SX(NJ),
PTX(NI),QTX(NI),PTY(NJ),QTY(NJ)

COMMON/BCarray/
FLXCI1(NJ),FLXC11(NJ),FLXCJ1(NI),FLXCM1(NI),
FLXPI1(NJ),FLXPL1(NJ),FLXPJ1(NI),FLXPM1(NI),
KBCI1(NJ),KBCL1(NJ),KBCJ1(NI),KBCM1(NI)

COMMON/GENL/NF,L1,L2,L3,M1,M2,M3,ITER,T,LASTT,
MODE,KORD,KOUT,IU1,IU2,KPGR,KSTOP,
IBLOCK(NI,NJ),TIME,DT

COMMON/NFF/RELAX(NFMAX),CRIT(NFMAX),
KPRINT(NFMAX),KSOLVE(NFMAX),KBLOC(NFMAX),
KPLOT(NFMAX),NTIMES(NFMAX),NTC(NFMAX)

COMMON/TTL/TITLE(NFMAX),HEADER,PRINTF,PLOTF

COMMON/EZG/XL,YL,POWERX,POWERY,NCVLX,NCVLY

COMMON/ZG/XZONE(NZMAX),YZONE(NZMAX),
POWRX(NZMAX),POWRY(NZMAX),
NCVX(NZMAX),NCVY(NZMAX),NZX,NZY
C _____

COMMON/OFCHARAC/OPTCRIT,FACTADIM(NPMAX)

COMMON/OFINT/KPAR,KPARSTOP,KXADIM,
KSTOPT,KSS,KTHPRINT,KXPRINT,KDT,KXTX,
KSENSOR,KTN,NPEST,NEXP,JEXP,JEXPCI,KYSIM,
KCONT,NCONTMIN,NCONTMAX,IUX1,IUEIG,KSCREEN,
KPRGRID,KXYGRID

COMMON/OFINARR/SENSOR,IDATA0,KTS(NSENSORMAX),
KDATA(NSENSORMAX),ISENSOR(NSENSORMAX),
JSENSOR(NSENSORMAX)

COMMON/OFREAL/SIGMA,TMAX,TMAXP,TI,TIMEHEAT,
DELTAB

COMMON/OFREARR/PARMIN(NPMAX),PARMAX(NPMAX),
PAR(NPMAX+1),DB(NPMAX),
TIMEEXP(NSENSORMAX,LASTTMAX),
YARR(NSENSORMAX,LASTTMAX),
TSENSOR(NSENSORMAX),XSENSOR(NSENSORMAX),
YSENSOR(NSENSORMAX)

COMMON/GACHARAC/SELECT,MUT,KILLTWIN,ELIT

COMMON/GAINT/ITERG,MING,LASTG,NMUT,NMUTJUMP,
NMUTCREEP,NTWINS,NTOT,NCHILDRAND,NPKEPT,
NCRITERG,LASTCRITERG,NFEVAL,NS,NP,
KSTOPF,ISEED1,ISEED2,KCPU

COMMON/GAREAL/PC,PMJ,PMC,PR,PT,CRITERION,
OFFLINE,ONLINE,TIME0,CPUG

COMMON/GAREARR/CP(NSMAX,NPMAX+1),
CC(NSMAX,NPMAX+1),CHILD(2,NPMAX),
CHILDMUT(NSMAX,NPMAX+1),
CHILDTOT(2*NSMAX,NPMAX+1),BEST(NPMAX+1)

DIMENSION SC(NI,NJ), SP(NI,NJ)
EQUIVALENCE (CON,SC), (AP,SP)

c To use as an isotropic gamma version, uncomment the next 2 lines
c and change the commented-out line in the first COMMON block.

CCC DIMENSION GAMX(NI,NJ), GAMY(NI,NJ)
CCC EQUIVALENCE (GAMX,GAM), (GAMY,GAM)

APPENDIX D

GADAVISF6.FOR Subroutine

This subroutine was written as the adapt part of the program GAMAIN given in Appendix A. It was used to solve the mathematical test function **f6** (Section 4.4).

SUBROUTINE GAPROBLEM

c HP77 or PC - SG 1998

C ATTENTION: THE USER MUST DEFINE VARIABLES USED THROUGHOUT GAPROBLEM (BETWEEN ENTRY STATEMENTS) IN THE COMMON/PROB. VARIABLES THAT ARE USED ELSEWHERE THAN GAPROBLEM MUST BE DEFINED IN THE FILE GACOMMON_MAIN.FOR. DEFAULT VALUES FOR USER MARKERS ARE SET IN DEFLT (KPAR,KYSIM,KXPRINT,KEST, ...)

```
c*****
INCLUDE 'gacomon_main.for'
c*****
CHARACTER*24 FDATE
COMMON/PROB/DELTAB,DB(NPMAX)
DIMENSION ARR(NSMAX,NPMAX+1)
c-----
```

ENTRY INIT

c give printing informations
!iunit=output file PRINTF only (dependent variable output file='ETAPRINT.DAT' in DEFLT)
!main title for file PRINTF
HEADER='GA test using F6 evaluation function'

c come here to change the default values of the following key parameters [KSCREEN, KMINMAX, KETA, NPEST, OPTCRIT, KTN, KSS, ETAMAX, KCONT, KYSIM, SIGMA, IDATA0, NEXP?]
KMINMAX=1 *!OF maximization*
KSCREEN=1
NPEST=2

c to look at a particular set of properties:

```
c=====
cKPAR=1
```

c general output file:

```
c=====
OPEN(UNIT=99,FILE='df6.out') !general GAoutput file
WRITE(99,20)
20 FORMAT(2X,'GA test using F6 evaluation function'/50(1H*)/1) !GAoutput file title!
IF (KPAR.NE.1) THEN
OPEN(UNIT=10,FILE='POPPRINT.dat')
OPEN(UNIT=11,FILE='OFPRINT.dat')
OPEN(UNIT=12,FILE='MTCPRINT.dat')
ENDIF
IF (KSCREEN.EQ.1) THEN
PRINT *,'GAMAIN running ...'
PRINT *,'ITERG=',ITERG
ENDIF
WRITE(99,(2X,A24)) FDATE() !initial date and time
```

RETURN

```
c-----
```

ENTRY SETVAR

c set GA variables:

```
c=====
OPEN(UNIT=25,FILE='INPUT.DAT')
READ(25,*)ISEED1
READ(25,*)ISEED2
IF (KETA.EQ.2) THEN
NP=1 != Number of parameters optimized
ELSE
NP=NPEST != Number of parameters estimated
ENDIF
READ(25,*)NS
READ(25,*)SELECT
READ(25,*)PT
READ(25,*)PC
READ(25,*)MUT
READ(25,*)PMJ
READ(25,*)PMC
READ(25,*)ELIT
READ(25,*)PR
READ(25,*)KILLTWIN
READ(25,*)CRITERION
READ(25,*)LASTCRITERG
READ(25,*)MING
READ(25,*)LASTG
CLOSE(25)
```

c set OF variables:

```
c=====
c set initial ranges + adimensionalization factor of unknown parameters to be determined
PARMIN(1)=-100.D0
PARMAX(1)=100.D0
FACTADIM(1)='LIN'

PARMIN(2)=-100.D0
PARMAX(2)=100.D0
FACTADIM(2)='LIN'
```

LASTETA(NEXP)=1

c output:

```
c=====
WRITE(99,30)
30 FORMAT(/2X,'GA VARIABLES:'/30('-'))
WRITE(99,(A7,I5))'iseed1=',ISEED1
WRITE(99,(A7,I5))'iseed2=',ISEED2
WRITE(99,(A3,I4))'ns=',NS
WRITE(99,(A3,I3))'np=',NP
WRITE(99,(A3,F15.6))'pmj (jump)=',PMJ
WRITE(99,(A3,F15.6))'pmc (creep)=',PMC
WRITE(99,(A3,F15.6))'pc=',PC
WRITE(99,(A3,F15.6))'pr=',PR
WRITE(99,(A3,F15.6))'pt=',PT
WRITE(99,(A10,F15.6))'criterion=',CRITERION
WRITE(99,(A12,I3))'lastcriterg=',LASTCRITERG
WRITE(99,(A5,I3))'ming=',MING
WRITE(99,(A6,I4))'lastg=',LASTG
IF (SELECT.EQ.'R') WRITE(99,(A14))'rank selection'
```

```

IF (SELECT.EQ.'T') WRITE(99,'(A20)')'tournament selection'
IF (MUT.EQ.'J') WRITE(99,'(A13)')'jump mutation'
IF (MUT.EQ.'JC') WRITE(99,'(A21)')'jump + creep mutation'
IF (KILLTWIN.EQ.'Y')WRITE(99,'(A8)')'killtwin'
IF (ELIT.EQ.'SS') WRITE(99,'(A20)')'steady state elitism'

```

```

WRITE(99,40)
40 FORMAT(/2X,'OF VARIABLES:'/30('-')/
DO I=1,NP
WRITE(99,'(2(A7,I2,A3,E14.3,1X),A9,A3)')
1 'parmin(',I,')=' ,PARMIN(I),
2 'parmax(',I,')=' ,PARMAX(I),
3 'Factadim=' ,FACTADIM(I)
ENDDO
IF (KCONT.EQ.0) THEN
WRITE(99,'(/A18)')'PAS DE CONTRAINTES'
ELSE
IF (KCONT.EQ.1) WRITE(99,'(/A26)')'CONTRAINTES 0/1
appliquées'
IF (KCONT.EQ.2) WRITE(99,'(/A26)')'CONTRAINTES 1/2
appliquées'
ENDIF

```

```

WRITE(99,*)'-----'
RETURN
c-----

```

ENTRY MODELETA

```
IF (ITERETA.EQ.0.AND.KETA.EQ.1) RETURN
```

```

c find x and y that optimizes ETA
X=PAR(1)
Y=PAR(2)
ETA=0.5D0-((SIN(SQRT(X**2+Y**2))))**2-0.5D0)
/(1.D0+0.001D0*(X**2+Y**2))**2
RETURN
c-----

```

ENTRY MODELXI !USE NPEST

```
c find NONDIMENSIONAL XI
```

```
RETURN
```

```
c-----
```

ENTRY CHECKCONT(N,ARR)

```

c check that the children generation satisfy the constraints
inherent to the model (subroutine MODELETA).
c this procedure can also be used to force the children to stay
within the ranges defined

```

```

DO 100 I=1,N
DO 100 J=1,NP
IF (ARR(I,J).LT.0.D0) THEN
IF (KCONT.EQ.1) ARR(I,J)=0.D0
IF (KCONT.EQ.2) ARR(I,J)=0.5D0
NCONTMIN=NCONTMIN+1
ENDIF
IF (ARR(I,J).GT.1.D0) THEN
IF (KCONT.EQ.1) ARR(I,J)=1.D0
IF (KCONT.EQ.2) ARR(I,J)=0.5D0
NCONTMAX=NCONTMAX+1
ENDIF
100 CONTINUE

```

```
RETURN
```

```
END
```

```
c*****
```

```
c include main program
```

```
INCLUDE 'gamain.for'
```

APPENDIX E

GA2DOPT.FOR Subroutine

This subroutine was written as the adapt part of the program GACONDUCT given in Appendix B. It was used to determine the thermophysical parameters k_x , k_y and C as constant at six different temperature levels in the range [30-150°C] of a carbon/epoxy composite material analyzed in Section 5.1.2.

SUBROUTINE GAPROBLEM

c HP77 or PC - SG 1998

C ATTENTION: THE USER MUST DEFINE VARIABLES USED THROUGHOUT GAPROBLEM.FOR (BETWEEN ENTRY STATEMENTS) IN THE COMMON/PROB/ NOTE THAT VARIABLES THAT ARE USED ELSEWHERE THAN GAADAPT MUST BE DEFINED IN THE FILE GACOMMON_CONDUCT.FOR

C THE USER SHOULD REMEMBER TO CHECK FOR VALIDITY OF CONVERGENCE:

*- REASONABLE ASPECT RATIO DX/DY
- GRID REFINEMENT DX, DY OK (GOOD COMPROMISE WITH COMPUTATION COST)
- FOR TRANSIENT ANALYSIS: TIME STEP DT OK
- FOR STEADY STATE ANALYSIS: EBAL=0
- NTC SMALLER THAN NTIMES (10 BY DEFAULT) AT EACH ITERATION*

*c******

INCLUDE 'gacommon_conduct.for'

*c******

*CHARACTER*24 FDATE
COMMON/PROB/CDX,CDY,RHOC,XP,CDP,RHOCPP,THK,
CDTHK,RHOCPTHK,KBC12,KBC34,KBC5,KBCV,KQAV,
RHEATER,QAV,YHEAT,LASTDATA,DTINIT,TI12,TI34,TI5,
YARRI,TIME12(100),T12(100),TIME34(100),T34(100),
TIME5(100),T5(100),TIMEV(100),VOLT(100),
TIMEARR(1,100),XSAMPLE,YSAMPLE*

c-----

DIMENSION T(NI,NJ),ARR(NSMAX,NPMAX+1)

EQUIVALENCE (F(1,1,1),T(1,1))

SAVE

c-----

ENTRY INIT

c give printing informations

*HEADER='Transient 2D Cond. [25-150C] w/ Tconst / Matra
sample1'*

PRINTF='run.pr'

TITLE(1)='TEMPERATURE'

KSOLVE(1)=1 ! enable to solve for the T

*c come here to change the default values of the following key
parameters (KCONT?KSCREEN?KESTOPT?TI?TMAX?
NPEST?OPTCRIT?KSENSOR?NSENSOR?KSS?KTN?
TIMEHEAT?MODE?)*

possible to define TIMEHEAT in BEGIN

KCONT=1

KSCREEN=1

KESTOPT=0

TMAX=53.88d0 !max found at symmetry

NPEST=3

KSENSOR=2

c to look at a particular set of thermal properties:

c=====

KPAR=1

KPRINT(1)=1 ! enable to print T; open PRINTF

KXPRINT=1

KXADIM=1

KOUT=2

KPLOT(1)=1 ! enable to plot T; open PLOTF

c general output file:

c=====

IF (KESTOPT.EQ.0) THEN

OPEN(UNIT=99,FILE='Estrun.out')

WRITE(99,1)

FORMAT(2X,'MATRA1 ESTIMATION using the 2D1-opt

design'/50(1H)') !EST title!*

*PRINT *,'MATRA1 ESTIMATION using the 2D1-opt design'*

IF (KSS.EQ.0.AND.KPAR.EQ.1)

OPEN(UNIT=199,FILE='TYrun.dat')

!TSENSOR(s) & YARR(s) file output

ENDIF

IF (KPAR.NE.1) THEN

OPEN(UNIT=10,FILE='POPPRINT.dat')

OPEN(UNIT=11,FILE='OFPRINT.dat')

OPEN(UNIT=12,FILE='MTCPRINT.dat')

ENDIF

IF (KSCREEN.EQ.1) THEN

*PRINT *,'GAMAIN running ...'*

*PRINT *,'ITERG=',ITERG*

ENDIF

c write initial date and time

WRITE(99,'(2X,A24)') FDATE()

RETURN

c-----

ENTRY GRID

c come here to change the default value for KXYGRID

THK=0.1D-3

XP=1.D-3

XSAMPLE=3.D-3

YSAMPLE=32.D-3

NZX=3

NCVX(1)=1

XZONE(1)=XP-THK/2.D0

NCVX(2)=3

*XZONE(2)=3.D0*THK*

NCVX(3)=6

*XZONE(3)=XSAMPLE-1.5D0*THK*

```

NZY=3 !only half studied because of symmetry
NCVY(1)=8
YZONE(1)=8.D-3
NCVY(2)=3
YZONE(2)=1.8D-3
NCVY(3)=22
YZONE(3)=22.2D-3
CALL ZGRID !refine grid for homogeneous orthotropic material

```

```

c give info about thermocouple position if the node(s) # (IS,JS) is
(are) to be found

```

```

IF (KESTOPT.EQ.0) THEN
XSENSOR(1)=0.D0*XSAMPLE+XP+THK
!SENSORS POSITION DETERMINED IN READY1
YSENSOR(1)=0.14D0*(2.D0*YSAMPLE)
ENDIF

```

```

RETURN

```

```

c-----

```

```

ENTRY SETVAR

```

```

c come here to change the default values of the following key
parameters

```

```

c (KYSIM?KDT?DELTAB?SIGMA?IDATA0?KPRGRID?)
KDT=0
DELTAB=1.d-6
KPRGRID=1

```

```

c print grid if asked

```

```

IF (KPRGRID.EQ.1) THEN
OPEN(UNIT=299,FILE='GRIDTEST.DAT')
DO I=1,L2
WRITE(299,'(4(F15.6))')X(I)*1000.,Y(1)*1000.,XU(I+1)*1000.,
1 Y(M1)*1000.
ENDDO
WRITE(299,'(2(F15.6))')X(L1)*1000.,Y(1)*1000.
DO J=1,M2
WRITE(299,'(4(F15.6))')X(1)*1000.,Y(J)*1000.,X(L1)*1000.,
1 YV(J+1)*1000.
ENDDO
WRITE(299,'(2(F15.6))')X(1)*1000.,Y(M1)*1000.
STOP
ENDIF

```

```

c set GA variables:

```

```

c=====
ISEED1=492 !random number seeds
ISEED2=27
NS=50 !CHOOSE NS EVEN TO MAKE NS/2 CHILDREN
IF (KESTOPT.EQ.0) THEN
NP=NPEST
ENDIF
PMJ=2.D0/(1.D0*NS)
PMC=PMJ/2.D0
PC=0.9D0
PR=0.9D0
PT=0.9D0
CRITERION=0.01D0
LASTCRITERG=5 !at least (MING + LASTCRITERG)
MING=5
LASTG=20
SELECT='T' !rank (R) or tournament (T) selection
MUT='JC' !Jump mutation alone (J) or {Jump+Creep}
mutation (JC)
KILLTWIN='N' !kill or not the twins (Y/N)
ELIT='SS' !steady state (SS) or basic (B) or "similar
replacement" (SR) elitism NOT SET UP yet

```

```

c set OF variables:

```

```

c=====
PARMIN(1)=0.3
PARMAX(1)=0.8
FACTADIM(1)='LIN'

PARMIN(2)=1.5

```

```

PARMAX(2)=6.0
FACTADIM(2)='LIN'

```

```

PARMIN(3)=1.2D6
PARMAX(3)=2.3D6
FACTADIM(3)='LIN'

```

```

CDTHK=1.D0
CDP=177.D0 !alu alloy plate thermal property values @ 300K
RHOCPP=2.42375D6 !(pure alu. @ 300K: 237. & 2.439906d6)
RHEATER=359.6D0
YHEAT=YSAMPLE

```

```

IF (KESTOPT.EQ.0) THEN
IF (KYSIM.EQ.0) THEN
OPEN(UNIT=1,FILE='matra2d_0598_150b3.in')
READ(1,*)LASTDATA, YARRI,TI12,TI34,TI5,TIMEHEAT
TI=(YARRI+TI12+TI34+TI5)/4.d0
DO I=1, LASTDATA
READ(1,10)TIMEARR(1,I),YARR(1,I),TIME12(I),TI2(I),
1 TIME34(I),TI34(I),TIME5(I),T5(I),TIMEV(I),VOLT(I)
ENDDO
READ(1,'(I3)')LASTT
DO I=1,LASTT
READ(1,'(F6.2)')TIMEEXP(1,I)
ENDDO
CLOSE(1)
10 FORMAT(5(F6.2,1X,F7.3,2X))

```

```

ELSE
PAR(1)=0.6D0 !define thermal properties for simulation
PAR(2)=3.0D0
PAR(3)=1.6D6
KDT=1
DT=0.2D0
LASTT=500

```

```

STDDV=0.1D0 !normal error standard deviation of
simulated data
OPEN(UNIT=2,FILE='Ysim.in') !Tsimulated file output
WRITE(2,15)
15 FORMAT('Simulated T /2D1-opt design/ for MATRA EST
/50(1H*)/) !title!
WRITE(2,'(1X,A4,3(1X,F15.3)/)')PAR=',PAR(1),PAR(2),PAR(3)
WRITE(2,'(1X,A6,F4.2/)')STDDV=',STDDV
CALL COMPYSIM(STDDV) !generate simulated T
CLOSE(2)
STOP 'Ysim.dat generated'
ENDIF
ENDIF

```

```

c write in general output file:

```

```

c=====
WRITE(99,20)
20 FORMAT(2X,'GEOMETRICAL DIMENSIONS AND
GRID:/30('-))
WRITE(99,'(A3,F12.5)')XL=',X(L1)
WRITE(99,'(A3,F12.5)')YL=',Y(M1)
WRITE(99,'(A5,I3,A1,I2)')GRID=',L1,'x',M1
WRITE(99,'(A12)')ZGRID called'

WRITE(99,30)
30 FORMAT(//2X,'GA VARIABLES:/30('-))
WRITE(99,'(A7,I5)')iseed1=',ISEED1
WRITE(99,'(A7,I5)')iseed2=',ISEED2
WRITE(99,'(A3,I3)')ns=',NS
WRITE(99,'(A3,I3)')np=',NP
WRITE(99,'(A3,F12.5)')pmj (jump)=',PMJ
WRITE(99,'(A3,F12.5)')pmc (creep)=',PMC
WRITE(99,'(A3,F12.5)')pc=',PC
WRITE(99,'(A3,F12.5)')pr=',PR
WRITE(99,'(A3,F12.5)')pt=',PT
WRITE(99,'(A10,F12.5)')criterion=',CRITERION
WRITE(99,'(A12,I3)')lastcriterg=',LASTCRITERG
WRITE(99,'(A5,I3)')ming=',MING
WRITE(99,'(A6,I3)')lastg=',LASTG

```



```

IF (SELECT.EQ.'R') WRITE(99,'(A14)')'rank selection'
IF (SELECT.EQ.'T') WRITE(99,'(A20)')'tournament selection'
IF (MUT.EQ.'J') WRITE(99,'(A13)')'jump mutation'
IF (MUT.EQ.'JC') WRITE(99,'(A21)')'jump + creep mutation'
IF (KILLTWIN.EQ.'Y')WRITE(99,'(A8)')'killtwin'
IF (ELIT.EQ.'SS') WRITE(99,'(A20)')'steady state elitism'

```

```

WRITE(99,40)
40 FORMAT(/2X,'OF VARIABLES:/'30('-')/)
DO I=1,NP
WRITE(99,'(2(A7,I2,A3,E14.3,1X),A9,A3)')
'parmin(',I,')=',PARMIN(I),
'parmax(',I,')=',PARMAX(I),
'Factadim=',FACTADIM(I)
ENDDO
IF (KESTOPT.EQ.0) THEN
WRITE(99,'(/A28)')'2D1- optimal design variables:'
WRITE(99,'(A3,G18.8)')'xs=',XSENSOR(1)
WRITE(99,'(A3,G18.8)')'ys=',YSENSOR(1)
WRITE(99,'(A6,G18.8)')'yheat=',YHEAT
WRITE(99,'(A9,G18.8)')'timeheat=',TIMEHEAT
IF (KYSIM.EQ.0) THEN
WRITE(99,50)
50 FORMAT(/'Arrays read: timearr and Yarr')
!EXPERIMENTAL ARRAYS READ!
WRITE(99,'(A9,I4)')'lastdata=',LASTDATA
WRITE(99,'(A6,I4)')'lastt=',LASTT
ELSE
WRITE(99,60)
60 FORMAT(/'Arrays(last) simulated: Yarr')
!ARRAYS SIMULATED!
ENDIF
ENDIF

```

```
WRITE(99,'(A7,E10.1)')DELTAB=',DELTAB
```

```
IF (KDT.EQ.1) WRITE(99,'(A3,F10.5)')DT=',DT
```

```

WRITE(99,65)
65 FORMAT(2X,'SAMPLE DIMENSIONS AND GRID:
/30('-')/)
WRITE(99,'(A13,G10.3)')'XP ALU PLATE=',XP
WRITE(99,'(A37,G10.3)')'THK to model the contact resist.=', THK
WRITE(99,'(A8,G10.3)')'XSAMPLE=',XSAMPLE
WRITE(99,'(A8,G10.3)')'YSAMPLE=',YSAMPLE
WRITE(99,'(2(A4,I2,1X))')'NZX=',NZX,'NZY=',NZY
WRITE(99,66)'NCVX(1)=',NCVX(1),'XZONE(1)=',XZONE(1)
WRITE(99,66)'NCVX(2)=',NCVX(2),'XZONE(2)=',XZONE(2)
WRITE(99,66)'NCVX(3)=',NCVX(3),'XZONE(3)=',XZONE(3)
WRITE(99,66)'NCVY(1)=',NCVY(1),'YZONE(1)=',YZONE(1)
WRITE(99,66)'NCVY(2)=',NCVY(2),'YZONE(2)=',YZONE(2)
WRITE(99,66)'NCVY(3)=',NCVY(3),'YZONE(3)=',YZONE(3)
66 FORMAT(A8,I2,2X,A9,G10.3)
WRITE(99,'(A12)')'ZGRID called'

```

```

IF (KCONT.EQ.0) THEN
WRITE(99,'(/A18)')'PAS DE CONTRAINTES'
ELSE
IF (KCONT.EQ.1) WRITE(99,'(/A26)')'CONTRAINTES 0-1
appliquées'
IF (KCONT.EQ.2) WRITE(99,'(/A26)')'CONTRAINTES 1/2
appliquées'
ENDIF

```

```
RETURN
```

```
c-----
ENTRY BEGIN
```

```

IF (KPAR.EQ.1) THEN
KPAR=0
KPARSTOP=1 !set to 1 to stop the run after compof is performed
ENDIF

```

```
c TO OBTAIN THE NONDIM SS SOLUTION TMAX+
REQUIRED IN OPT RUN
```

```

OR THE INITIAL SS TEMPERATURE FIELD REQUIRED IN
EST RUN
IF (KSS.EQ.1) THEN
KDT=1
DT=BIG
LASTT=50
ENDIF

```

```

c reset statements before starting loop for T calculations
TIME=0.0D0 !reset markers
ITERT=0
KSTOP=0
KQAV=0
KBC12=1
KBC34=1
KBC5=1
KBCV=1

```

```

c EST run
IF (KESTOPT.EQ.0) THEN
DO 70 I=1,NSENSOR
KTS(I)=0
KDATA(I)=1
70 CONTINUE

```

```

c set thermal properties to the chromosome gene values in EST run
c use actual parameter values when DB=0.
c or apply a par. variation of 0.1% when DB=DELTAB=0.0001
by default
c (IN EITHER EST OR OPT RUN, THE SENSITIVITY
COEFFICIENTS ARE CALCULATED USING A PARAMETER
VARIATION W/ B=(1+DB)*B IN COMPXI)
CDX=PAR(1)*(1.d0+DB(1))
CDY=PAR(2)*(1.d0+DB(2))
RHOC=PAR(3)*(1.d0+DB(3))
ENDIF

```

```

c reset Ti
DO 75 I=1,L2 !reset Ti
DO 75 J=1,M1
T(I,J)=TI
75 CONTINUE

```

```

DO 80 I=1,L1 !sample J1 face
IF (X(I).GE.1.1D-3) T(I,1)=(TI12-TI34)/1.5D-3*(1.85D-3-X(I))
+TI12
80 CONTINUE

```

```

DO 85 J=1,M1 !L1 face
T(L1,J)=TI5
85 CONTINUE

```

```
RETURN
```

```
c-----
ENTRY OUTPUT
```

```

IF (ITERT.EQ.0) GOTO 91
IF (ABS(TIME-TIMEHEAT).LE.DT/2.D0) KQAV=1

```

```

c temperature(s) corresponding to the sensor(s) position(s)
c Recall: if xsensor and ysensor used ISENSOR and JSENSOR
are determined
in DEFIRD2D if KSENSOR=2
in COMPXI if KESTOPT=1 and KSENSOR=1 in INIT
DO 90 I=1,NSENSOR
TSENSOR(I)=T(ISENSOR(I),JSENSOR(I))
IF (KESTOPT.EQ.0) THEN
IF (ABS(TIME-TIMEARR(1,KDATA(I))).LE.DT/2.D0)
KTS(I)=1 !compute S in compof
ENDIF
90 CONTINUE

```

```

91 IF (TIME.LE.TIMEHEAT) THEN
IF (TIME.GT.TIMEV(KBCV)) KBCV=KBCV+1
IF (KBCV.EQ.1) THEN

```

```
VOLTAGE=VOLT(KBCV)
ELSE
VOLTAGE=VOLT(KBCV)-(VOLT(KBCV)-VOLT(KBCV-1))
/(TIMEV(KBCV)-TIMEV(KBCV-1))*(TIMEV(KBCV)-TIME)
ENDIF
QAV=RHEATER*(VOLTAGE*1.D-3)**2/(2*(2*YSAMPLE)**2)
ENDIF
```

```
IF (TIME.GT.TIME12(KBC12)) KBC12=KBC12+1
IF (KBC12.EQ.1) THEN
TEMP12=T12(KBC12)-(T12(KBC12)-TI12)
/TIME12(KBC12)*(TIME12(KBC12)-TIME)
ELSE
TEMP12=T12(KBC12)-(T12(KBC12)-T12(KBC12-1))
/(TIME12(KBC12)-TIME12(KBC12-1))*(TIME12(KBC12)-
TIME)
ENDIF
```

```
IF (TIME.GT.TIME34(KBC34)) KBC34=KBC34+1
IF (KBC34.EQ.1) THEN
TEMP34=T34(KBC34)-(T34(KBC34)-TI34)
/TIME34(KBC34)*(TIME34(KBC34)-TIME)
ELSE
TEMP34=T34(KBC34)-(T34(KBC34)-T34(KBC34-1))
/(TIME34(KBC34)-TIME34(KBC34-1))*(TIME34(KBC34)-
TIME)
ENDIF
```

```
DO 95 I=1,L1 !sample J1 face
IF (X(I).GE.1.1D-3) T(I,1)=TEMP12+
(TEMP12-TEMP34)/1.5D-3*(1.85D-3-X(I))
95 CONTINUE
```

```
IF (TIME.GT.TIME5(KBC5)) KBC5=KBC5+1
IF (KBC5.EQ.1) THEN
TEMP5=T5(KBC5)-(T5(KBC5)-TI5)
/TIME5(KBC5)*(TIME5(KBC5)-TIME)
ELSE
TEMP5=T5(KBC5)-(T5(KBC5)-T5(KBC5-1))
/(TIME5(KBC5)-TIME5(KBC5-1))*(TIME5(KBC5)-TIME)
ENDIF
```

```
DO 96 J=1,M1 !L1 face
T(L1,J)=TEMP5
96 CONTINUE
```

*C THE FOLLOWING IS COMPUTED FOR A PARTICULAR SET OF THERMAL PROPERTIES ONLY
C ATTENTION, KPARSTOP=1 to compute OF and then turns 0
(see COMPOF) and KXTX=1 to compute CI*

```
IF (KPARSTOP.EQ.0.OR.KXTX.EQ.1) GOTO 170
```

```
QINI1=0.D0
DO J=2,M2
QINI1=QINI1+FLUXII(J,1)*YCV(J) !(J,1) for independent
variable I = T
ENDDO
```

```
IF (KSS.EQ.1) THEN !find TMAX+ @ SS required in
COMPXTXOPT or TI
DO 120 IUNIT=IU1,IU2
IF (ITERT.EQ.0) WRITE(IUNIT,100)
100 FORMAT(2X,'ITERT',4X,'TMAX',4X,'QINI1',4X,
'NTC(1)',/)
WRITE(IUNIT,110)ITERT,TSENSOR(1),QINI1,NTC(1)
110 FORMAT(2X,I4,3X,1PE11.4,3X,1PE11.4,3X,I2)
120 CONTINUE
IF (ITERT.EQ.LASTT) THEN
CALL PRINT
STOP 'TMAX calculated and SS done'
ENDIF
```

```
ELSE
```

c write TSENSOR(NSENSOR) to files

```
IF (KESTOPT.EQ.0.AND.KTS(1).EQ.1)
WRITE(199,'(3F10.3)')
TIME,TSENSOR(1),YARR(1,KDATA(1))
IF (KESTOPT.EQ.1)
WRITE(199,'(2F15.3)')TIME,TSENSOR(1)
```

c set title (@ ITERT=0) and data (@ each ITERT) to print in iunit

```
DO 150 IUNIT=IU1,IU2
IF (ITERT.EQ.0) WRITE(IUNIT,130)
130 FORMAT(2X,'ITERT',6X,'TIME',9X,'TSENSOR(1)',
9X,'QINI1',7X,'NTC(1)',/)
WRITE(IUNIT,140)ITERT,TIME,TSENSOR(1),QINI1,NTC(1)
140 FORMAT(2X,I4,3(3X,1PE11.4),3X,I2)
150 CONTINUE
```

c print and plot the Tdistribution when time~th

```
IF (KQAV.EQ.1.AND.KTHPRINT.EQ.0) THEN
CALL PRINT
CALL PLOT
KTHPRINT=1
ENDIF
ENDIF
```

```
170 RETURN
```

ENTRY PHI

c set properties (conductivities and volumetric capacities) of main elements

c OPT or EST run

```
DO 180 I=2,L2
DO 180 J=2,M2
IF (X(I).LE.XP) THEN
GAMX(I,J)=CDP
GAMY(I,J)=CDP
ALAM(I,J)=RHOCPP
ELSE
IF (X(I).GT.XP.AND.X(I).LE.(XP+THK)) THEN
GAMX(I,J)=CDTHK
GAMY(I,J)=CDTHK
ELSE
GAMX(I,J)=CDX
GAMY(I,J)=CDY
ALAM(I,J)=RHOCPP
ENDIF
ENDIF
180 CONTINUE
```

c set BCs (1 for cst T-BY DEFAULT- and 2 for fluxes)

```
DO 200 J=2,M2
KBCII(J)=2
IF (Y(J).LE.YHEAT.AND.TIME.LE.TIMEHEAT)
FLXCI(J)=QAV
200 CONTINUE
DO 210 I=2,L2
KBCM1(I)=2
IF (X(I).LE.XP) THEN
KBCJ1(I)=2
ENDIF
210 CONTINUE
```

```
RETURN
```

ENTRY CHECKCONT(N,ARR)

*c check that the children generation satisfy the constraints inherent to the model (subroutine MODELETA).
c this procedure can also be used to force the children to stay within the ranges defined*

```
DO 220 I=1,N
DO 220 J=1,NP
IF (ARR(I,J).LT.0.D0) THEN
IF (KCONT.EQ.1) ARR(I,J)=0.D0
```

```
IF (KCONT.EQ.2) ARR(L,J)=0.5D0
NCONTMIN=NCONTMIN+1
ENDIF
IF (ARR(I,J).GT.1.D0) THEN
IF (KCONT.EQ.1) ARR(L,J)=1.D0
IF (KCONT.EQ.2) ARR(L,J)=0.5D0
NCONTMAX=NCONTMAX+1
ENDIF
220 CONTINUE
```

```
RETURN
END
```

```
c*****
c include main program of invariant part
INCLUDE 'gaconduct.for'
```

APPENDIX F

GA2DLOPT.FOR Subroutine

This subroutine was written as the adapt part of the program GACONDUCT given in Appendix B. It was developed for the thermophysical characterization of a carbon/epoxy composite material in the range [30-150°C] (Section 5.2.1). More particularly, it was used to optimize seven experimental design variables (x_s , y_s , L_p , t_{h1} , t_{12} , t_{h2} and t_n) from a two-dimensional transient experiment for the simultaneous estimation of 9 thermophysical parameters (k_{x25} , k_{x150} , k_{y25} , k_{y150} , C_{25} , C_{75} , C_{110} , C_{150} , and R_c), and then perform the simultaneous estimation.

```
SUBROUTINE GAPROBLEM
```

```
c HP77 or PC - SG 1998
```

```
C ATTENTION: THE USER MUST DEFINE VARIABLES  
USED THROUGHOUT GAPROBLEM.FOR (BETWEEN  
ENTRY STATEMENTS) IN THE COMMON/PROB/  
NOTE THAT VARIABLES THAT ARE USED ELSEWHERE  
THAN GAADAPT MUST BE DEFINED IN THE FILE  
GACOMMON_CONDUCT.FOR
```

```
C THE USER SHOULD REMEMBER TO CHECK FOR  
VALIDITY OF CONVERGENCE:  
- REASONABLE ASPECT RATIO DX/DY  
- GRID REFINEMENT DX, DY OK (GOOD COMPROMISE  
WITH COMPUTATION COST)  
- FOR TRANSIENT ANALYSIS: TIME STEP DT OK  
- FOR STEADY STATE ANALYSIS: EBAL=0  
- NTC SMALLER THAN NTIMES (10 BY DEFAULT) AT EACH  
ITERATION
```

```
c*****  
INCLUDE 'gacommon_conduct.for'  
c*****  
CHARACTER*24 FDATE  
COMMON/PROB/KQAV, LASTDATA, Tp, QAV, CDAL,  
RHOC PAL, CDAIR, RHOC PAIR, KSYM, JHEAT, YHEAT,  
th1, time12, th2, CDX(2), CDY(2), RHOC P(4), RC,  
TIMEARR(1,500), TCi(8)  
DIMENSION T(NI, NJ), ARR(NSMAX, NP MAX+1)  
EQUIVALENCE (F(1,1,1), T(1,1))  
SAVE  
c-----
```

```
ENTRY INIT
```

```
c give printing informations  
HEADER='Transient 2D Conduction, [25-150C] / Matra sample1'  
PRINTF='run.pr'  
TITLE(1)='TEMPERATURE'  
KSOLVE(1)=1 ! enable to solve for the T
```

```
c come here to change the default values of the following key  
parameters (KCONT?KSCREEN?KESTOPT?TI?TMAX?  
NPEST? OPTCRIT?KSENSOR?NSENSOR?KSS?KTN?  
TIMEHEAT?MODE?)
```

```
c possible to define TIMEHEAT in BEGIN  
OPTCRIT='D'  
KCONT=1  
KSCREEN=1  
KESTOPT=1  
c KSS=1
```

```
c KTN=1  
TI=25.d0  
TMAX=161.71d0 !TO BE FOUND FROM SS ANALYSIS  
NPEST=9
```

```
c to look at a particular set of thermal properties:
```

```
c-----  
KPAR=1  
KPRINT(1)=1 ! enable to print T; open PRINTF  
KXPRINT=1  
KXADIM=1  
KOUT=2  
c KPLOT(1)=1 ! enable to plot T; open PLOTF
```

```
c general output file:
```

```
c-----  
IF (KESTOPT.EQ.0) THEN  
OPEN(UNIT=99, FILE='Estrun.out')  
WRITE(99,1)  
1 FORMAT(2X, 'MATRA1(T) ESTIMATION'/50(1H*)) !EST title!  
PRINT *, 'MATRA1(T) ESTIMATION'  
IF (KSS.EQ.0.AND.KPAR.EQ.1)  
OPEN(UNIT=199, FILE='TYrun.dat') !TSENSOR(s) &  
YARR(s) file output  
ELSE  
OPEN(UNIT=99, FILE='Optrun.out')  
WRITE(99,2)  
2 FORMAT(2X, '2D MATRA1(T) OPTIMIZATION W/  
DIMENSIONS'/50(1H*)) !OPT title!  
PRINT *, '2D MATRA(T) IDEAL OPTIMIZATION W/  
DIMENSIONS'  
PRINT *, 'TO BE USED W/ ORTHOTROPIC PROPERTIES'  
IF (KSS.EQ.0.AND.KPAR.EQ.1)  
OPEN(UNIT=199, FILE='Trun.dat') !TSENSOR(1) file output  
ENDIF
```

```
IF (KPAR.NE.1) THEN  
OPEN(UNIT=10, FILE='POPPRINT.dat')  
OPEN(UNIT=11, FILE='OFPRINT.dat')  
OPEN(UNIT=12, FILE='MTCPRINT.dat')  
ENDIF  
IF (KSCREEN.EQ.1) THEN  
PRINT *, 'GAMAIN running ...'  
PRINT *, 'ITERG=', ITERG  
ENDIF
```

```
c write initial date and time  
WRITE(99, '(2X, A24)') FDATE()
```

```
RETURN
```

```
c-----
```

ENTRY GRID

c come here to change the default value for KXYGRID

c specify whether the complete or half model is to be studied
KSYM=1

c set up the mesh

NZX=8
NCVX(1)=1
XZONE(1)=0.84d-3
NCVX(2)=2
XZONE(2)=0.12d-3
NCVX(3)=2
XZONE(3)=0.16d-3
NCVX(4)=4
XZONE(4)=2.88d-3
NCVX(5)=1
XZONE(5)=0.2d-3
NCVX(6)=1
XZONE(6)=0.1d-3
NCVX(7)=1
XZONE(7)=0.2d-3
NCVX(8)=3
XZONE(8)=12.d-3

IF (KSYM.EQ.1) THEN
NZY= !USE W/ SYMMETRICAL MODEL

ELSE

NZY=11

ENDIF

NCVY(1)=3

YZONE(1)=12.d-3

NCVY(2)=1

YZONE(2)=0.2d-3

NCVY(3)=1

YZONE(3)=0.1d-3

NCVY(4)=1

YZONE(4)=0.2d-3

NCVY(5)=1

YZONE(5)=0.8d-3

IF (KSYM.EQ.1) THEN

NCVY(6)=31 !USE W/ SYMMETRICAL MODEL

YZONE(6)=31.d-3 ! "

ELSE

NCVY(6)=31 !...AND COMMENT THE FOLLOWING

YZONE(6)=62.d-3

NCVY(7)=1

YZONE(7)=0.8d-3

NCVY(8)=1

YZONE(8)=0.2d-3

NCVY(9)=1

YZONE(9)=0.1d-3

NCVY(10)=1

YZONE(10)=0.2d-3

NCVY(11)=3

YZONE(11)=12.d-3

ENDIF

CALL ZGRID !refine grid for homogeneous orthotropic material

c give info about thermocouple position if the node(s) # (IS,JS) is (are) to be found

RETURN

ENTRY SETVAR

c come here to change the default values of the following key parameters

c (KYSIM?KDT?DELTAB?SIGMA?IDATA0?KPRGRID?)

c KYSIM=1

KDT=1

DELTAB=1.d-6

KPRGRID=1

c print grid if asked

IF (KPRGRID.EQ.1) THEN

OPEN(UNIT=299,FILE='GRIDTEST.DAT')

DO I=1,L2

WRITE(299,'(4(F15.6))')X(I)*1000.,Y(1)*1000.,XU(I+1)*1000.,
1 Y(M1)*1000.

ENDDO

WRITE(299,'(2(F15.6))')X(L1)*1000.,Y(1)*1000.

DO J=1,M2

WRITE(299,'(4(F15.6))')X(1)*1000.,Y(J)*1000.,X(L1)*1000.,
1 YV(J+1)*1000.

ENDDO

WRITE(299,'(2(F15.6))')X(1)*1000.,Y(M1)*1000.

STOP

ENDIF

c set GA variables:

c=====

ISEED1=6812 !random number seeds

ISEED2=581

NS=300 !CHOOSE NS EVEN TO MAKE NS/2

CHILDREN

IF (KESTOPT.EQ.0) THEN

NP=NPEST

ELSE

NP=5

ENDIF

PMJ=2.D0/(1.D0*NS)

PMC=PMJ/2.D0

PC=0.9D0

PR=0.9D0

PT=0.9D0

CRITERION=0.01D0

LASTCRITERG=5 !at least (MING + LASTCRITERG)

MING=5

LASTG=15

SELECT='T' !rank (R) or tournament (T) selection

MUT='JC' !Jump mutation alone (J) or {Jump+Creep}

mutation (JC)

KILLTWIN='N' !kill or not the twins (Y/N)

ELIT='SS' !steady state (SS) or basic (B) or "similar

replacement" (SR) elitism NOT SET UP yet

c set OF variables:

c=====

IF (KESTOPT.EQ.1) THEN !initial ranges of unknown parameters to be optimized

PARMIN(1)=0 !th1 - range chosen so that

PARMAX(1)=150 !th1=int(par(2))*DT

FACTADIM(1)='LIN'

PARMIN(2)=0 !time12 - "

PARMAX(2)=100

FACTADIM(2)='LIN'

PARMIN(3)=0 !th2 - "

PARMAX(3)=150

FACTADIM(3)='LIN'

PARMIN(4)=7 !JSENSOR(1)

PARMAX(4)=40.5 !from 7 to 41(.5) / 40(.5) if KSYM=1

FACTADIM(4)='LIN'

PARMIN(5)=5 !JSENSOR(1)

PARMAX(5)=11.5 !from 5 to 11(.5)

FACTADIM(5)='LIN'

PARMIN(6)=7 !JHEAT

PARMAX(6)=41.5 !from 7 to 41.5

FACTADIM(6)='LIN'

ELSE

!initial ranges of unknown parameters to be estimated

```

PARMIN(1)=0.3
PARMAX(1)=0.7
FACTADIM(1)='LIN'

```

```

PARMIN(2)=0.3
PARMAX(2)=0.9
FACTADIM(2)='LIN'

```

```

PARMIN(3)=1.4
PARMAX(3)=2.5
FACTADIM(3)='LIN'

```

```

PARMIN(4)=1.8
PARMAX(4)=6.0
FACTADIM(4)='LIN'

```

```

PARMIN(5)=1.d-5
PARMAX(5)=1.d-3
FACTADIM(5)='LOG'

```

```

PARMIN(6)=1.3d6
PARMAX(6)=1.8d6
FACTADIM(6)='LIN'

```

```

PARMIN(7)=1.5d6
PARMAX(7)=2.2d6
FACTADIM(7)='LIN'

```

```

PARMIN(8)=1.6d6
PARMAX(8)=2.5d6
FACTADIM(8)='LIN'

```

```

PARMIN(9)=1.8d6
PARMAX(9)=2.6d6
FACTADIM(9)='LIN'
ENDIF

```

c EST run

```

IF (KESTOPT.EQ.0) THEN
DT=0.25D0
TNMAX=480.D0
LASTT=TNMAX/DT
Tp=25.D0
QAV=28.D3
th1=101.D0
time12=41.D0
th2=27.D0
YHEAT=32.D-3
ISENSOR(1)=5
JSENSOR(1)=15
CDAIR=0.031d0
RHOCPAIR=1.d3
CDAL=177.d0 !alu alloy plate thermal property values @ 300K
RHOCPAL=2.42375d6 !(pure alu. @ 300K: 237. & 2.439906d6)

```

```

IF (KYSIM.EQ.0) THEN !use simulated or experimental
data
OPEN(UNIT=1,FILE='Ysimin.dat')
READ(1,*)LASTDATA
DO I=1,LASTDATA
READ(1,*)J,TEMPS,TEXACT,TSIMUL
READ(1,*)J,TIMEARR(1,I),TEXACT,YARR(1,I)
ENDDO
CLOSE(1)

```

```

ELSE !generate simulated data
PAR(1)=0.5D0 !define thermal properties
PAR(2)=0.6D0
PAR(3)=2.0D0
PAR(4)=4.0D0
PAR(5)=1.0D-4
PAR(6)=1.50D6
PAR(7)=1.80D6
PAR(8)=2.00D6
PAR(9)=2.25D6

```

```
STDDV=0.1D0 !normal error standard deviation
```

```

OPEN(UNIT=2,FILE='Ysim.dat') !Tsimulated file output
WRITE(2,15)
15 FORMAT('Simulated T / 2D design / for GAMATRAT EST
/50(1H*)/') !title!
WRITE(2,(1X,A4,9(1X,F15.3)/))'PAR=',PAR(1),PAR(2),PAR(3),
PAR(4),PAR(5),PAR(6),PAR(7),PAR(8),PAR(9)
WRITE(2,(1X,A6,F4.2/))'STDDV=',STDDV

```

```
CALL COMPYSIM(STDDV) !generate simulated T
```

```

CLOSE(2)
STOP 'Ysim.dat generated'
ENDIF

```

```

ELSE
c OPT run
DT=1.D0
TNMAX=700.D0
LASTT=TNMAX/DT
Tp=25.D0
QAV=28.D3
YHEAT=32.d-3
TMAX1D=181.19D0
TMAXP=(TMAX-TI)/(TMAX1D-TI)
CDAIR=0.031d0
RHOCPAIR=1.d3
CDAL=177.d0
RHOCPAL=2.42375d6
ENDIF

```

c write in general output file:

```

c=====
WRITE(99,20)
20 FORMAT(2X/,'GEOMETRICAL DIMENSIONS AND
GRID:/'30('-))
WRITE(99,(A3,F12.5))'XL=',X(L1)
WRITE(99,(A3,F12.5))'YL=',Y(M1)
WRITE(99,(A5,I3,A1,I2))'GRID=',L1,'x',M1
WRITE(99,(A12))'ZGRID called'

```

```

WRITE(99,30)
30 FORMAT(/2X,'GA VARIABLES:/'30('-))
WRITE(99,(A7,I5))'iseed1=',ISEED1
WRITE(99,(A7,I5))'iseed2=',ISEED2
WRITE(99,(A3,I3))'ns=',NS
WRITE(99,(A3,I3))'np=',NP
WRITE(99,(A3,F12.5))'pmj (jump)='PMJ
WRITE(99,(A3,F12.5))'pmc (creep)='PMC
WRITE(99,(A3,F12.5))'pc='PC
WRITE(99,(A3,F12.5))'pr='PR
WRITE(99,(A3,F12.5))'pt='PT
WRITE(99,(A10,F12.5))'criterion=',CRITERION
WRITE(99,(A12,I3))'lastcriterg=',LASTCRITERG
WRITE(99,(A5,I3))'ming=',MING
WRITE(99,(A6,I3))'lastg=',LASTG
IF (SELECT.EQ.'R') WRITE(99,(A14))'rank selection'
IF (SELECT.EQ.'T') WRITE(99,(A20))'tournament selection'
IF (MUT.EQ.'J') WRITE(99,(A13))'jump mutation'
IF (MUT.EQ.'JC') WRITE(99,(A21))'jump + creep mutation'
IF (KILLTWIN.EQ.'Y')WRITE(99,(A8))'killtwin'
IF (ELIT.EQ.'SS') WRITE(99,(A20))'steady state elitism'

```

```

WRITE(99,40)
40 FORMAT(/2X,'OF VARIABLES:/'30('-))
DO I=1,NP
WRITE(99,(2(A7,I2,A3,E14.3,1X),A9,A3))
'parmin(',I,')=',PARMIN(I),
'parmax(',I,')=',PARMAX(I),
'Factadim=',FACTADIM(I)
ENDDO
IF (KESTOPT.EQ.0) THEN
IF (KYSIM.EQ.0) THEN
WRITE(99,50)

```

```

50 FORMAT(/'Arrays read: timearr and Yarr')
/EXPERIMENTAL ARRAYS READ!
WRITE(99,(A9,I4))'lastdata=',LASTDATA
WRITE(99,(A6,I4))'lastt=',LASTT
ELSE
WRITE(99,60)
60 FORMAT(/'Arrays(lastt) simulated: Yarr')      !ARRAYS
SIMULATED!
ENDIF
ELSE
WRITE(99,(/A36))'2D design variables to be optimized:'
WRITE(99,(A26)) 'ys,xs,yheat,th1,time12,th2,tn'
WRITE(99,(/A6,I4))'lastt=',LASTT
WRITE(99,(A5,G10.5))'TMAX=',TMAX
ENDIF

WRITE(99,(A7,E10.1))'DELTAB=',DELTAB

IF (KDT.EQ.1) WRITE(99,(A3,F10.5))'DT=',DT

IF (KSYM.EQ.1) WRITE(99,(A19))'HALF MODEL
STUDIED'

IF (KCONT.EQ.0) THEN
WRITE(99,(/A18))'PAS DE CONTRAINTES'
ELSE
IF (KCONT.EQ.1) WRITE(99,(/A26))'CONTRAINTES 0-1
appliquées'
IF (KCONT.EQ.2) WRITE(99,(/A26))'CONTRAINTES 1/2
appliquées'
ENDIF

RETURN
c-----

ENTRY BEGIN

IF (KPAR.EQ.1) THEN
KPAR=0
KPARSTOP=1  !set to 1 to stop the run after compof is performed
ENDIF

c TO OBTAIN THE NONDIM SS SOLUTION TMAX+
REQUIRED IN OPT RUN OR THE INITIAL SS
TEMPERATURE FIELD REQUIRED IN EST RUN
IF (KSS.EQ.1) THEN
KDT=1
DT=BIG
LASTT=50
ENDIF

c reset statements before starting loop for T calculations
TIME=0.0D0      !reset markers
ITERT=0
KSTOP=0
KQAV=0

c EST run
IF (KESTOPT.EQ.0) THEN
DO 70 I=1,NSENSOR
KTS(I)=0
KDATA(I)=1
70 CONTINUE

c set thermal properties to the chromosome gene values in EST run
use actual parameter values when DB=0.
or apply a par. variation of DELTAB=0.0001 by default
(IN EITHER EST OR OPT RUN, THE SENSITIVITY
COEFFICIENTS ARE CALCULATED USING A PARAMETER
VARIATION W/ B=(1+DB)*B IN COMPXI)
CDX(1)=PAR(1)*(1.d0+DB(1))
CDX(2)=PAR(2)*(1.d0+DB(2))
CDY(1)=PAR(3)*(1.d0+DB(3))
CDY(2)=PAR(4)*(1.d0+DB(4))
RC=PAR(5)*(1.d0+DB(5))
RHOC(1)=PAR(6)*(1.d0+DB(6))

```

```

RHOC(2)=PAR(7)*(1.d0+DB(7))
RHOC(3)=PAR(8)*(1.d0+DB(8))
RHOC(4)=PAR(9)*(1.d0+DB(9))

c OPT run
ELSE
CDX(1)=0.5d0*(1.d0+DB(1))      !@ 25C
CDX(2)=0.6d0*(1.d0+DB(2))      !@ 150C
CDY(1)=2.d0*(1.d0+DB(3))      !@ 25C
CDY(2)=4.d0*(1.d0+DB(4))      !@ 150C
RC=1.d-4*(1.d0+DB(5))          !CST
RHOC(1)=1.50d6*(1.d0+DB(6))    !@ 25C
RHOC(2)=1.80d6*(1.d0+DB(7))    !@ 75C
RHOC(3)=2.00d6*(1.d0+DB(8))    !@ 110C
RHOC(4)=2.25d6*(1.d0+DB(9))    !@ 150C
th1=int(PAR(1))*DT
time12=int(PAR(2))*DT
th2=int(PAR(3))*DT
TIMEHEAT=th1+time12+th2
JSENSOR(1)=int(PAR(4))
ISENSOR(1)=int(PAR(5))
JHEAT=int(PAR(6))
ENDIF

c reset Ti
DO 85 J=1,M1
T(L1,J)=Tp
DO 80 I=1,L1
T(I,J)=Tp
80 CONTINUE
85 CONTINUE

RETURN
c-----

ENTRY OUTPUT

IF (ABS(TIME-th1).LE.DT/2.D0) THEN
KQAV=1
ELSE
IF (ABS(TIME-(th1+time12)).LE.DT/2.D0) KQAV=0
IF (ABS(TIME-(th1+time12+th2)).LE.DT/2.D0) KQAV=2
ENDIF

c temperature(s) corresponding to the sensor(s) position(s)
Recall: if xsensor and ysensor used ISENSOR and JSENSOR are
determined in DEFRD2D if KSENSOR=2 OR in COMPXI if
KESTOPT=1 and KSENSOR=1 in INIT
DO 90 I=1,NSENSOR
TSENSOR(I)=T(ISENSOR(I),JSENSOR(I))
IF (KESTOPT.EQ.0) THEN
IF (KYSIM.EQ.0.AND.ABS(TIME-
TIMEARR(1,KDATA(I))).LE.DT/2.D0)
THEN
KTS(I)=1      !compute S in compof
ELSE
IF (KYSIM.EQ.1) KTS(I)=1
ENDIF
ENDIF
90 CONTINUE

C THE FOLLOWING IS COMPUTED FOR A PARTICULAR
SET OF THERMAL PROPERTIES ONLY
C ATTENTION, KPARSTOP=1 to compute OF and then turns 0
(see COMPOF) and KXTX=1 to compute CI

IF (KPARSTOP.EQ.0.OR.KXTX.EQ.1) GOTO 170

QINI1=0.D0
DO J=2,M2
QINI1=QINI1+FLUXII(J,1)*YCV(J)  !(J,1) for independent
variable I = T
ENDDO

IF (KSS.EQ.1) THEN      !find TMAX+ @ SS required in
COMPXTXOPT or TI

```

```

DO 120 IUNIT=IU1,IU2
IF (ITERT.EQ.0) WRITE(IUNIT,100)
100 FORMAT(2X,'ITERT',4X,'TMAX',4X,'QINI1',4X,
'NTC(1)',/)
WRITE(IUNIT,110)ITERT,TSSENSOR(1),QINI1,NTC(1)
110 FORMAT(2X,I4,3X,1PE11.4,3X,1PE11.4,3X,I2)
120 CONTINUE
IF (ITERT.EQ.LASTT) THEN
CALL PRINT
STOP 'TMAX calculated and SS done'
ENDIF

ELSE
c write TSENSOR(NSENSOR) to files
IF (KESTOPT.EQ.0.AND.KTS(1).EQ.1)
WRITE(199,'(3F10.3)')
TIME,TSSENSOR(1),YARR(1,KDATA(1))
IF (KESTOPT.EQ.1)
WRITE(199,'(2F15.3)')TIME,TSSENSOR(1)

c set title (@ ITERT=0) and data (@ each ITERT) to print in iunit
DO 150 IUNIT=IU1,IU2
IF (ITERT.EQ.0) WRITE(IUNIT,130)
130 FORMAT(2X,'ITERT',6X,'TIME',9X,'TSSENSOR(1)',
9X,'QINI1',7X,'NTC(1)',/)
WRITE(IUNIT,140)ITERT,TIME,TSSENSOR(1),QINI1,NTC(1)
140 FORMAT(2X,I4,3(3X,1PE11.4),3X,I2)
150 CONTINUE

c print and plot the Tdistribution when time~th1
IF (KQAV.EQ.1.AND.KTHPRINT.EQ.0) THEN
CALL PRINT
CALL PLOT
KTHPRINT=1
ENDIF

c print and plot the Tdistribution when time~th2
IF (KQAV.EQ.2.AND.KTHPRINT.EQ.1) THEN
CALL PRINT
KTHPRINT=2
ENDIF
ENDIF

170 RETURN
c-----

```

ENTRY PHI

```

c set properties (conductivities and volumetric capacities) of
main elements
c OPT or EST run
DO 180 I=2,L2
DO 180 J=2,M2
GAMX(I,J)=CDAL
GAMY(I,J)=CDAL
ALAM(I,J)=RHOCPAL
IF (KSYM.EQ.1) THEN
IF (X(I).GE.0.99d-3.AND.X(I).LE.4.2d-3.AND.Y(J).
GE.12.3d-3) GOTO 175
ELSE
IF (X(I).GE.0.99d-3.AND.X(I).LE.4.2d-3.AND.
Y(J).GE.12.3d-3.AND.Y(J).LE.76.3d-3) GOTO 175
ENDIF
GOTO 180
175 GAMX(I,J)=CDX(1)+(CDX(2)-CDX(1))*(T(I,J)-
25.D0)/125.D0
GAMY(I,J)=CDY(1)+(CDY(2)-CDY(1))*(T(I,J)-
25.D0)/125.D0
IF (T(I,J).LT.75.D0) THEN
ALAM(I,J)=RHOC(1)+
(RHOC(2)-RHOC(1))*(T(I,J)-25.D0)/50.D0
ELSE
IF (T(I,J).GE.75D0.AND.T(I,J).LT.110.D0) THEN
ALAM(I,J)=RHOC(2)+
(RHOC(3)-RHOC(2))*(T(I,J)-75.D0)/35.D0
ELSE
ALAM(I,J)=RHOC(3)+

```

```

(RHOC(4)-RHOC(3))*(T(I,J)-110.D0)/40.D0
ENDIF
ENDIF
180 CONTINUE

```

c set air properties

```

DO I=2,4
DO J=7,8
GAMX(I,J)=CDAIR
GAMY(I,J)=CDAIR
ALAM(I,J)=RHOCPAIR
ENDDO
IF (KSYM.EQ.0) THEN
DO J=40,41 !COMMENT W/ SYMMETRICAL MODEL
GAMX(I,J)=CDAIR ! "
GAMY(I,J)=CDAIR ! "
ALAM(I,J)=RHOCPAIR ! "
ENDDO
ENDIF
ENDDO

```

c take RC into account

```

IF (KSYM.EQ.1) THEN
DO J=9,L2 !USE W/ SYMMETRICAL MODEL
GAMX(4,J)=0.1d-3/RC
GAMY(4,J)=0.d0
ENDDO
ELSE
DO J=9,39
GAMX(4,J)=0.1d-3/RC
GAMY(4,J)=0.d0
ENDDO
ENDIF

```

IF (KSYM.EQ.1) THEN

```

DO J=7,L2 !USE W/ SYMMETRICAL MODEL
GAMX(12,J)=0.1d-3/RC
GAMY(12,J)=0.d0
ENDDO
ELSE
DO J=7,41
GAMX(12,J)=0.1d-3/RC
GAMY(12,J)=0.d0
ENDDO
ENDIF

```

DO I=5,11

```

GAMX(I,6)=0.d0
GAMY(I,6)=0.1d-3/RC
IF (KSYM.EQ.0) THEN
GAMX(I,42)=0.d0 !COMMENT W/ SYMMETRICAL
MODEL
GAMY(I,42)=0.1d-3/RC ! "
ENDIF
ENDDO

```

c set BCs (1 for cst T -BY DEFAULT- and 2 for fluxes) - OPT or EST run

```

DO 200 J=2,M2
KBC11(J)=2
IF (KSS.EQ.1) THEN
IF (Y(J).GE.12.3d-3.AND.Y(J).LE.(12.3d-3+YHEAT))
FLXCI1(J)=QAV
ELSE
IF (Y(J).GE.12.3d-3.AND.J.LE.JHEAT.AND.KQAV.EQ.0)
!Use w/ JHEAT
IF (Y(J).GE.12.3d-3.AND.Y(J).LE.(12.3d-3+YHEAT). !Use if
YHEAT set
AND.KQAV.EQ.0) FLXCI1(J)=QAV
ENDIF
200 CONTINUE

```

DO 210 I=2,L2

```

KBCJ1(I)=2
KBCM1(I)=2
210 CONTINUE

```


RETURN

c-----

ENTRY CHECKCONT(N,ARR)

*c check that the children generation satisfy the constraints
inherent to the model (subroutine MODELETA).
c this procedure can also be used to force the children to stay
within the ranges defined*

```
DO 220 I=1,N
DO 220 J=1,NP
IF (ARR(I,J).LT.0.D0) THEN
IF (KCONT.EQ.1) ARR(I,J)=0.D0
IF (KCONT.EQ.2) ARR(I,J)=0.5D0
NCONTMIN=NCONTMIN+1
ENDIF
IF (ARR(I,J).GT.1.D0) THEN
IF (KCONT.EQ.1) ARR(I,J)=1.D0
IF (KCONT.EQ.2) ARR(I,J)=0.5D0
NCONTMAX=NCONTMAX+1
ENDIF
220 CONTINUE
```

RETURN
END

c*****

c include main program of invariant part
INCLUDE 'gaconduct.for'

APPENDIX G

GA2DRTM.FOR Subroutine

This subroutine was written as the adapt part of the program GACONDUCT given in Appendix B. It was developed for the thermophysical characterization of a carbon/epoxy composite material from RTM experimental data in the range [100-130°C] (Section 5.2.2). More particularly, it was used to simultaneously estimate 7 thermophysical parameters (k_x , k_{y100} , k_{y130} , C_{100} , C_{115} , C_{130} , and R_c).

SUBROUTINE GAPROBLEM

c HP77 or PC - SG 1998

C ATTENTION: THE USER MUST DEFINE VARIABLES USED THROUGHOUT GAPROBLEM.FOR (BETWEEN ENTRY STATEMENTS) IN THE COMMON/PROB/ NOTE THAT VARIABLES THAT ARE USED ELSEWHERE THAN GAADAPT MUST BE DEFINED IN THE FILE GACOMMON_CONDUCT.FOR

*C THE USER SHOULD REMEMBER TO CHECK FOR VALIDITY OF CONVERGENCE:
- REASONABLE ASPECT RATIO DX/DY
- GRID REFINEMENT DX, DY OK (GOOD COMPROMISE WITH COMPUTATION COST)
- FOR TRANSIENT ANALYSIS: TIME STEP DT OK
- FOR STEADY STATE ANALYSIS: EBAL=0
- NTC SMALLER THAN NTIMES (10 BY DEFAULT) AT EACH ITERATION*

```
c*****  
INCLUDE 'gacommon_conduct.for'  
c*****  
CHARACTER*24 FDATE  
COMMON/PROB/LASTDATA,h1,h2,hf,Tf,Tp,Tamb,TC5(125),  
CDAL,RHOCPCAL,CDUCU,RHOCPCU,CDTE,RHOCPTC,  
CDRE,RHOCPRECRUE(3),CDX(2),CDY,RHOCPCOMP(3),RC,  
TIMEARR(1,150),TIARR(NI,NJ),TIMEPRINT  
DIMENSION T(NI,NJ),TCO(2,125),ARR(NSMAX,NPMAX+1)  
EQUIVALENCE (F(1,1,1),T(1,1))  
SAVE  
c-----
```

ENTRY INIT

c give printing informations
HEADER='Conduction transitoire 2D resine crue / Damien
Lecointe'
PRINTF='crue1.pr'
TITLE(1)='TEMPERATURE'
KSOLVE(1)=1 *! enable to solve for the T*

c come here to change the default values of the following key parameters (KCONT?KSCREEN?KESTOPT?TI?TMAX? NPEST?OPTCRIT?KSENSOR?NSENSOR?KSS?KTN? TIMEHEAT?MODE?)
KCONT=1
KSCREEN=1
c KSS=1
NPEST=7
NSENSOR=4
KSENSOR=2
!TMAX is defined after Tp

c to look at a particular set of thermal properties:

```
c-----  
KPAR=1  
KPRINT(1)=1 ! enable to print T; open PRINTF  
KXPRINT=1  
KXADIM=0  
KOUT=2  
KPLOT(1)=1 ! enable to plot T; open PLOTF
```

c general output file:

```
c-----  
IF (KESTOPT.EQ.0) THEN  
OPEN(UNIT=99,FILE='Estrun.out')  
WRITE(99,1)  
1 FORMAT(2X,'DAMIEN ESTIMATION'/50(1H*)) !EST title!  
PRINT *,'DAMIEN ESTIMATION'  
IF (KSS.EQ.0.AND.KPAR.EQ.1)  
OPEN(UNIT=199,FILE='TYrun.dat') !TSENSOR(s) &  
YARR(s) file output  
ELSE  
OPEN(UNIT=99,FILE='Optrun.out')  
WRITE(99,2)  
2 FORMAT(2X,'2D1 DAMIEN OPTIMIZATION W/  
DIMENSIONS'/50(1H*)) !OPT title!  
PRINT *,'2D1 DAMIEN IDEAL OPTIMIZATION W/  
DIMENSIONS'  
PRINT *,'TO BE USED W/ ORTHOTROPIC PROPERTIES'  
IF (KSS.EQ.0.AND.KPAR.EQ.1)  
OPEN(UNIT=199,FILE='Trun.dat') !TSENSOR(1) file output  
ENDIF
```

```
IF (KPAR.NE.1) THEN  
OPEN(UNIT=10,FILE='POPPRINT.dat')  
OPEN(UNIT=11,FILE='OFPRINT.dat')  
OPEN(UNIT=12,FILE='MTCPRINT.dat')  
ENDIF  
IF (KSCREEN.EQ.1) THEN  
PRINT *,'GAMAIN running ...'  
PRINT *,'ITERG=',ITERG  
ENDIF
```

c write initial date and time
WRITE(99,'(2X,A24)') FDATE()

RETURN

ENTRY GRID

c come here to change the default value for KXYGRID

c set up the mesh
NZX=16
NCVX(1)=1
XZONE(1)=1.d-3

```

NCVX(2)=5
XZONE(2)=13.75d-3
NCVX(3)=7
XZONE(3)=8.75d-3
NCVX(4)=2
XZONE(4)=2.d-3
NCVX(5)=1
XZONE(5)=0.5d-3
NCVX(6)=4
XZONE(6)=3.d-3
NCVX(7)=3
XZONE(7)=4.d-3
NCVX(8)=3
XZONE(8)=3.d-3
NCVX(9)=1
XZONE(9)=1.34d-3
NCVX(10)=7
XZONE(10)=17.82d-3/13.d0*7.d0
NCVX(11)=7
XZONE(11)=9.331d-3
NCVX(12)=8
XZONE(12)=10.7025d-3
NCVX(13)=7
XZONE(13)=4.007d-3/3.d0*7.d0
NCVX(14)=9
XZONE(14)=10.8916d-3
NCVX(15)=5
XZONE(15)=151.688d-3/11.d0
NCVX(16)=1
XZONE(16)=1.d-3

NZY=8      !only half studied because of symmetry
NCVY(1)=1
YZONE(1)=1.d-3
NCVY(2)=5
YZONE(2)=15.25d-3
NCVY(3)=3
YZONE(3)=5.25d-3
NCVY(4)=3
YZONE(4)=4.1d-3
NCVY(5)=3
YZONE(5)=3.4d-3
NCVY(6)=1
YZONE(6)=1.d-3
NCVY(7)=3
YZONE(7)=1.5d-3
NCVY(8)=8
YZONE(8)=4.5d-3

CALL ZGRID  !refine grid for homogeneous orthotropic
material

c give thermocouple position(s)
XSENSOR(1)=36.67d-3
YSENSOR(1)=36.d-3
XSENSOR(2)=46.25d-3
YSENSOR(2)=36.d-3
XSENSOR(3)=55.60d-3
YSENSOR(3)=36.d-3
XSENSOR(4)=66.30d-3
YSENSOR(4)=36.d-3

RETURN
c-----

ENTRY SETVAR

c come here to change the default values of the following key
parameters (KYSIM?KDT?DELTAB?SIGMA?IDATA0?
KPRGRID?NEXP?JEXPCI?)
KDT=1
DELTAB=1.D-7
JEXPCI=1

c print grid if asked
IF (KPRGRID.EQ.1) THEN

OPEN(UNIT=299,FILE='GRIDTEST.DAT')
DO I=1,L2
WRITE(299,'(4(F15.3))')X(I)*1000.,Y(1),
1 XU(I+1)*1000.,Y(M1)*1000.
ENDDO
WRITE(299,'(2(F15.3))')X(L1)*1000.,Y(1)
DO J=1,M2
WRITE(299,'(4(F15.3))')X(1),Y(J)*1000.,
1 X(L1)*1000.,YV(J+1)*1000.
ENDDO
WRITE(299,'(2(F15.3))')X(1),Y(M1)*1000.
STOP
ENDIF

c set GA variables:
c=====
ISEED1=10496  !random number seeds
ISEED2=04517
NS=50  !CHOOSE NS EVEN TO MAKE NS/2 CHILDREN
IF (KESTOPT.EQ.0) THEN
NP=NPEST
ELSE
NP=4
ENDIF
PMJ=2.D0/(1.D0*NS)
PMC=PMJ/2.D0
PC=0.9D0
PR=0.9D0
PT=0.9D0
CRITERION=0.01D0
LASTCRITERG=3  !at least 3
MING=2        !+ 2 =5 generations
LASTG=10
SELECT='T'    !rank (R) or tournament (T) selection
MUT='JC'      !Jump mutation alone (J) or {Jump+Creep}
mutation (JC)
KILLTWIN='N'  !kill or not the twins (Y/N)
ELIT='SS'     !steady state (SS) or basic (B) or "similar
replacement" (SR) elitism NOT SET UP yet

c set OF variables:
c=====
IF (KESTOPT.EQ.0) THEN  !initial ranges of unknown
parameters to be estimated
PARMIN(1)=3.0D0  !
PARMAX(1)=3.5D0
FACTADIM(1)='LIN'

PARMIN(2)=3.3D0
PARMAX(2)=4.5D0
FACTADIM(2)='LIN'

PARMIN(3)=0.50D0  !
PARMAX(3)=0.66D0
FACTADIM(3)='LIN'

PARMIN(4)=0.8D-3  !
PARMAX(4)=10.D-3
FACTADIM(4)='LIN'

PARMIN(5)=2.00D6  !
PARMAX(5)=2.20D6
FACTADIM(5)='LIN'

PARMIN(6)=2.10D6  !
PARMAX(6)=2.40D6
FACTADIM(6)='LIN'

PARMIN(7)=2.10D6  !
PARMAX(7)=2.50D6
FACTADIM(7)='LIN'
ENDIF

c EST run
IF (KESTOPT.EQ.0) THEN
IF (KYSIM.EQ.0) THEN  !use experimental data

```

```

LASTDATA=125
OPEN(UNIT=1,FILE='crue1.dat')
READ(1,*)TIME,TC01i,TC02i,TC1i,TC2i,TC3i,TC4i,TC5i
DO I=1,LASTDATA
READ(1,*)TIMEARR(1,I),TC0(1,I),TC0(2,I),YARR(1,I),
YARR(2,I),YARR(3,I),YARR(4,I),TC5(I)
ENDDO
CLOSE(1)
DT=0.1D0
LASTT=LASTDATA*4/DT
TIMEPRINT=180.D0
h1=1.D0
h2=2.D0
hf=3000.D0
Tf=82.45D0
Tp=133.7D0
Tmax=Tp
Tamb=15.5D0
CDAL=232.D0
RHOPAL=2600.D0*879.D0
CDCU=401.D0
RHOCPCU=8933.D0*385.D0
CDTE=0.26D0
RHOCPT=2200.D0*1000.D0
CDRECRUE=0.11D0
RHOPRECRUE(1)=1117.D0*1208.16D0
RHOPRECRUE(2)=1117.D0*15.197D0
RHOPRECRUE(3)=1117.D0*(-4.99758D-2)
IF (KSS.NE.1) THEN
OPEN(UNIT=3,FILE='crue1_2810.in')  !initial SS
distribution found from previous SS analysis
DO 10 J=M1,1,-1
READ(3,*)(TIARR(I,J),I=1,L1)
10 CONTINUE
ENDIF
ENDIF
c no OPT run performed in this study
ENDIF

c write in general output file:
=====
WRITE(99,20)
20 FORMAT(2X/, 'SAMPLE DIMENSIONS AND
GRID:/30(-)')
WRITE(99, '(A8,G10.3)')XSAMPLE=',X(L1)
WRITE(99, '(A8,G10.3)')YSAMPLE=',Y(M1)
WRITE(99, '(A5,I3,A1,I2)')GRID=',L1,'x',M1
WRITE(99, '(A12)')ZGRID called'

WRITE(99,30)
30 FORMAT(//2X, 'GA VARIABLES:/30(-)')
WRITE(99, '(A7,I5)')iseed1=',ISEED1
WRITE(99, '(A7,I5)')iseed2=',ISEED2
WRITE(99, '(A3,I3)')ns=',NS
WRITE(99, '(A3,I3)')np=',NP
WRITE(99, '(A3,F12.5)')pmj (jump)=',PMJ
WRITE(99, '(A3,F12.5)')pmc (creep)=',PMC
WRITE(99, '(A3,F12.5)')pc=',PC
WRITE(99, '(A3,F12.5)')pr=',PR
WRITE(99, '(A3,F12.5)')pt=',PT
WRITE(99, '(A10,F12.5)')criterion=',CRITERION
WRITE(99, '(A12,I3)')lastcriterg=',LASTCRITERG
WRITE(99, '(A5,I3)')ming=',MING
WRITE(99, '(A6,I3)')lastg=',LASTG
IF (SELECT.EQ.'R') WRITE(99, '(A14)')rank selection'
IF (SELECT.EQ.'T') WRITE(99, '(A20)')tournament selection'
IF (MUT.EQ.'J') WRITE(99, '(A13)')jump mutation'
IF (MUT.EQ.'JC') WRITE(99, '(A21)')jump + creep mutation'
IF (KILLTWIN.EQ.'Y')WRITE(99, '(A8)')killtwin'
IF (ELIT.EQ.'SS') WRITE(99, '(A20)')steady state elitism'

WRITE(99,40)
40 FORMAT(//2X, 'OF VARIABLES:/30(-)')
DO I=1,NP
WRITE(99, '(2(A7,I2,A3,E14.3,1X),A9,A3)')
1 'parmin(',I,')=',PARMIN(I),

```

```

2 'parmax(',I,')=',PARMAX(I),
3 'Factadim=',FACTADIM(I)
ENDDO
IF (KESTOPT.EQ.0) THEN
IF (KYSIM.EQ.0) THEN
WRITE(99,50)
50 FORMAT('Arrays(lastm) read: timearr and Yarr')
!EXPERIMENTAL ARRAYS READ!
WRITE(99, '(A9,I4)')lastdata=',LASTDATA
WRITE(99, '(A6,I4)')lastt=',LASTT
ELSE
WRITE(99,60)
60 FORMAT('Arrays(lastm) simulated: Yarr') !ARRAYS
SIMULATED!
ENDIF
ENDIF

IF (KDT.EQ.1) WRITE(99, '(A3,F10.5)')DT=',DT

IF (KCONT.EQ.0) THEN
WRITE(99, '(/A18)')PAS DE CONTRAINTES'
ELSE
IF (KCONT.EQ.1) WRITE(99, '(/A26)')CONTRAINTES 0-1
appliquées'
IF (KCONT.EQ.2) WRITE(99, '(/A26)')CONTRAINTES 1/2
appliquées'
ENDIF

RETURN
c-----

ENTRY BEGIN

IF (KPAR.EQ.1) THEN
KPAR=0
KPARSTOP=1  !set to 1 to stop the run after compof is
performed
ENDIF

c TO OBTAIN THE NONDIM SS SOLUTION TMAX+
REQUIRED IN OPT RUN OR THE INITIAL SS TEMPERATURE
FIELD REQUIRED IN EST RUN
IF (KSS.EQ.1) THEN
KDT=1
DT=BIG
LASTT=300
ENDIF

c reset statements before starting loop for T calculations
TIME=0.0D0  !reset markers
ITERT=0
KSTOP=0

c EST run
IF (KESTOPT.EQ.0) THEN
DO 70 I=1,SENSOR
KTS(I)=0
KDATA(I)=1
70 CONTINUE

c set thermal properties to the chromosome gene values in EST run
c use actual parameter values when DB=0. or apply a par.
variation when DB=DELTAB=0.0001 by default
(IN EITHER EST OR OPT RUN, THE SENSITIVITY
COEFFICIENTS ARE CALCULATED USING A PARAMETER
VARIATION W/ B=(1+DB)*B IN COMPMI)
CDX(1)=PAR(1)*(1.d0+DB(1))
CDX(2)=PAR(2)*(1.d0+DB(2))
CDY=PAR(3)*(1.d0+DB(3))
RC=PAR(4)*(1.d0+DB(4))
RHOCPCOMP(1)=PAR(5)*(1.d0+DB(5))
RHOCPCOMP(2)=PAR(6)*(1.d0+DB(6))
RHOCPCOMP(3)=PAR(7)*(1.d0+DB(7))
ENDIF

c reset Ti

```

```

DO 80 I=1,L1
IF (KSS.EQ.1) THEN !to get SS TIARR(I,J)
T(I,1)=Tp
T(I,M1)=0.0224671D0*X(I)*1.D3+127.361D0
DO 85 J=2,M2
T(I,J)=128.3D0 !use same as Damien
85 CONTINUE
ELSE
DO 86 J=1,M1
T(I,J)=TIARR(I,J)
86 CONTINUE
ENDIF
80 CONTINUE

RETURN
c-----

ENTRY OUTPUT

c temperature(s) corresponding to the sensor(s') position(s)
c Recall: ISENSOR and JSENSOR are determined in DEF2D2D
if KESTOPT=0 / in COMPXI if KESTOPT=1
DO 90 I=1, NSENSOR
TSENSOR(I)=T(ISENSOR(I),JSENSOR(I))
IF (KESTOPT.EQ.0) THEN
IF (KYSIM.EQ.0.AND.ABS(TIME-
TIMEARR(1,KDATA(I))).LE.DT/2.D0)
1 THEN
KTS(I)=1 !compute S in compof
ELSE
IF (KYSIM.EQ.1) KTS(I)=1
ENDIF
ENDIF
90 CONTINUE

C THE FOLLOWING IS COMPUTED FOR A PARTICULAR
SET OF THERMAL PROPERTIES ONLY
C ATTENTION, KPARSTOP=1 to compute OF and then turns 0
(see COMPOF) and KXTX=1 to compute CI

IF (KPARSTOP.EQ.0.OR.KXTX.E.1) GOTO 170

RA=(CDCU*YCV(8))/(CDTE*YCV(9))
TCZERO=(RA*T(17,9)+T(17,8))/(RA+1.D0)

IF (KSS.EQ.1) THEN !find TMAX+ @ SS required in
COMP or TI
DO 120 IUNIT=IU1,IU2
IF (ITERT.EQ.0) WRITE(IUNIT,100)
100 FORMAT(2X,'ITERT',4X,'TSENSOR(1-4)',4X,'NTC(1)')
WRITE(IUNIT,110)ITERT,(TSENSOR(I),I=1,NSENSOR),T(57,29),
1 TCZERO,NTC(1) !format to change w/I
110 FORMAT(2X,I4,6(3X,1PE11.4),3X,I2)
120 CONTINUE
IF (ITERT.EQ.LASTT) THEN
CALL PRINT
STOP 'SS done'
ENDIF

ELSE
c write TSENSOR(NSENSOR) to files
IF (KESTOPT.EQ.0.AND.ITERT.EQ.0)
WRITE(199,'(14F10.3)') !format to change
TIME,TSENSOR(1),TC1i,TSENSOR(2),TC2i,TSENSOR(3),
TC3i,TSENSOR(4),TC4i,T(57,29),TC5i,TCZERO,TC01i,TC02i
IF (KESTOPT.EQ.0.AND.KTS(1).EQ.1)
WRITE(199,'(19F10.3)') !format to change w/I
TIME,(TSENSOR(I),YARR(I,KDATA(I)),I=1,NSENSOR),
T(57,29),
TC5(KDATA(1)),TCZERO,TC0(1,KDATA(1)),
TC0(2,KDATA(1)),
(TSENSOR(I)-YARR(I,KDATA(I)),I=1,NSENSOR),
T(57,29)-TC5(KDATA(1))

c set title (@ ITERT=0) and data (@ each ITERT) to print in iunit
DO 150 IUNIT=IU1,IU2

```

```

IF (ITERT.EQ.0) WRITE(IUNIT,130)
130 FORMAT(2X,'ITERT',6X,'TIME',9X,'TSENSOR(1-4+1)',
7X,'NTC(1)')
WRITE(IUNIT,140)ITERT,TIME,(TSENSOR(I),I=1,
NSENSOR),T(57,29),NTC(1) !format to change w/I
140 FORMAT(2X,I4,6(3X,1PE11.4),3X,I2)
150 CONTINUE

```

```

c print and plot the Tdistribution when time~timeprint
IF (TIME.GE.TIMEPRINT.AND.KTHPRINT.EQ.0) THEN
CALL PRINT
CALL PLOT
KTHPRINT=1
ENDIF

```

ENDIF

170 RETURN

c-----

ENTRY PHI

```

c set conductivity and volumetric capacity
DO 180 I=2,L2 !EST or OPT run
DO 180 J=2,M2
GAMX(I,J)=CDTE
GAMY(I,J)=CDTE
ALAM(I,J)=RHOCPTTE
IF (X(I).LE.1.d-3.OR.X(I).GE.101.d-3.OR.Y(J).LE.1.d-3)
THEN
GAMX(I,J)=CDAL
GAMY(I,J)=CDAL
ALAM(I,J)=RHOCPAL
ENDIF
IF (X(I).GE.16.d-3.AND.X(I).LE.36.d-3.AND.Y(J).GE.18.d-3)
THEN
GAMX(I,J)=CDCU
GAMY(I,J)=CDCU
ALAM(I,J)=RHOCPCU
ENDIF
IF (X(I).GE.26.d-3.AND.X(I).LE.86.d-3.AND.Y(J).GE.31.d-3)
THEN
GAMX(I,J)=CDX(1)+(CDX(2)-CDX(1))*(T(I,J)-100.D0)/30.D0
GAMY(I,J)=CDY
IF (T(I,J).LE.115.D0) THEN
ALAM(I,J)=RHOCPCOMP(1)+(RHOCPCOMP(2)-
RHOCPCOMP(1))*(T(I,J)-100.D0)/15.D0
ELSE
IF (T(I,J).GT.115.D0) ALAM(I,J)=RHOCPCOMP(2)+
(RHOCPCOMP(3)-RHOCPCOMP(2))*(T(I,J)-115.D0)/15.D0
ENDIF
ENDIF
IF (X(I).GE.29.d-3.AND.X(I).LE.33.d-3.AND.Y(J).GE.29.d-3.
AND.Y(J).LE.31.d-3) THEN
GAMX(I,J)=CDRECRUE
GAMY(I,J)=CDRECRUE
ALAM(I,J)=RHOCPCOMP(1)+RHOCPCOMP(2)*T(I,J)+
RHOCPCOMP(3)*T(I,J)**2
ENDIF
180 CONTINUE

```

c set the duct (inactive zone containing oil) properties to 0.

```

DO 190 I=11,14
DO 190 J=11,13
GAMX(I,J)=0.D0
GAMY(I,J)=0.D0
ALAM(I,J)=0.D0
190 CONTINUE

```

c set the convective heat flux into the near-boundary control volumes via the source term

```

IF (KSS.NE.1) THEN
DO I=11,14
SC(I,10)=Tf/(YCV(10)*(1.D0/hf+.5D0*YCV(10)/GAMY(I,10)))
SP(I,10)=-1.D0/(YCV(10)*(1.D0/hf+.5D0*YCV(10)/GAMY(I,10)))
SC(I,14)=Tf/(YCV(14)*(1.D0/hf+.5D0*YCV(14)/GAMY(I,14)))

```

```

SP(I,14)=-1.D0/(YCV(14)*
(1.D0/hf+.5D0*YCV(14)/GAMY(I,14)))
ENDDO
DO J=11,13
SC(10,J)=Tf/(XCV(10)*(1.D0/hf+.5D0*XCV(10)/GAMX(10,J)))
SP(10,J)=-1.D0/(XCV(10)*
(1.D0/hf+.5D0*XCV(10)/GAMX(10,J)))
SC(15,J)=Tf/(XCV(15)*(1.D0/hf+.5D0*XCV(15)/GAMX(15,J)))
SP(15,J)=-1.D0/(XCV(15)*
(1.D0/hf+.5D0*XCV(15)/GAMX(15,J)))
ENDDO
ENDIF

c take RC into account
DO J=20,28
GAMX(17,J)=XCV(17)/RC
GAMY(I,J)=0.D0
ALAM(17,J)=RHOCPCU
ENDDO
DO I=18,21
GAMX(I,J)=0.D0
GAMY(I,19)=YCV(19)/RC
ALAM(I,19)=RHOCPCU
ENDDO
DO I=25,27
GAMX(I,J)=0.D0
GAMY(I,19)=YCV(19)/RC
ALAM(I,19)=RHOCPCU
ENDDO

c set BCs (1 for cst T -BY DEFAULT- and 2 for fluxes)
DO 200 J=2,M2
KBCI1(J)=2
FLXCI1(J)=h1*Tamb
FLXPI1(J)=-h1
KBCL1(J)=2
FLXCL1(J)=h2*Tamb
FLXPL1(J)=-h2
200 CONTINUE

IF (KSS.NE.1) THEN
DO 210 I=2,L2
KBCM1(I)=2
210 CONTINUE
ENDIF

RETURN
c-----

ENTRY CHECKCONT(N,ARR)

c check that the children generation satisfy the constraints
inherent to the model (subroutine MODELETA).
c this procedure can also be used to force the children to stay
within the ranges defined

DO 220 I=1,N
DO 220 J=1,NP
IF (ARR(I,J).LT.0.D0) THEN
IF (KCONT.EQ.1) ARR(I,J)=0.D0
IF (KCONT.EQ.2) ARR(I,J)=0.5D0
NCONTMIN=NCONTMIN+1
ENDIF
IF (ARR(I,J).GT.1.D0) THEN
IF (KCONT.EQ.1) ARR(I,J)=1.D0
IF (KCONT.EQ.2) ARR(I,J)=0.5D0
NCONTMAX=NCONTMAX+1
ENDIF
220 CONTINUE

RETURN
END

c*****

c include main program of invariant part

```

APPENDIX H

GAKINETIC.FOR Subroutine and its Dependencies

The GAKINETIC.FOR subroutine was written as the adapt part of the program GAMAIN given in Appendix A. It was used to determine the kinetic parameters of the Kamal and Sourour model for the kinetic characterization of the curing of three different thermosetting compounds analyzed in Chapter 6.

This subroutine calls five other subroutines:

- ALPHARK2.FOR, to compute the degree of cure using the order 2 Runge Kunta method.
- ALPHACN.FOR, to compute the degree of cure using the Crank-Nicholson scheme.
- DALPHAFACTALPHA.FOR, to compute the rate of cure according to strategy S_1 or S_2 (see Section 6.2).
- XDALPHAFACTALPHA.FOR, to compute the sensitivity coefficients of the kinetic parameters using the estimation strategy S_1 .
- TIREFNI.FOR, to determine the parameters of the inhibition time model.

These five subroutines are provided at the end of the GAKINETIC.

SUBROUTINE GAPROBLEM

c HP77 or PC - SG 1998

C ATTENTION: THE USER MUST DEFINE VARIABLES USED THROUGHOUT GAPROBLEM.FOR (BETWEEN ENTRY STATEMENTS) IN THE COMMON/PROB/ VARIABLES THAT ARE USED ELSEWHERE THAN GAPROBLEM MUST BE DEFINED IN THE FILE GACOMMON_MAIN.FOR.

C DEFAULT VALUES FOR USER MARKERS ARE ZERO IN DEFLT (KPAR,KYSIM,KXPRINT,KEST, ...)

```
c*****
INCLUDE 'gacommon_main.for'
c*****
CHARACTER*15 WHICHMETHOD,WHICHTIMODEL
CHARACTER*24 FDATE
COMMON/PROB/KTIMEINH, KRK1, RK1I, KALPHA,
NTCMAX, DELTAB, WHICHMETHOD, WHICHTIMODEL,
TIMEI(NEXPMAX), ALPHAI(NEXPMAX),
DALPHAI(NEXPMAX), TI(NEXPMAX), PASDTI(NEXPMAX),
ALPHA(NEXPMAX), LASTETAMAX, DALPHA(NEXPMAX),
LASTETAMAX, T(NEXPMAX), LASTETAMAX),
DALPHAMAX(NEXPMAX), NDATA(NEXPMAX),
DB(NPMAX), V(NEXPMAX)
DIMENSION ARR(NSMAX, NPMAX+1),
ETA1(LASTETAMAX), ETA2(LASTETAMAX)
```

c-----

ENTRY INIT

c give printing informations

!iunit=output file PRINTF only (dependent variable output file='ETAPRINT.DAT' in DEFLT)

c come here to change the default values of the following key parameters [KSCREEN, KMINMAX, KETA, NPEST, OPTCRIT, KTN, KSS, ETAMAX TIMEHEAT, KCONT, KYSIM, SIGMA, IDATA0, NEXP, JEXPCI?]

```
KSCREEN=1
KETA=1
KCONT=1
```

```
NEXP=6
JEXPCI=6
```

c the following is problem dependent

```
KTIMEINH=0 !1 to find the parameters of the inhibition time model
KRK1=1
RK1I=1.d-300
NTCMAX=20 !to be used w/ the method 'ALPHACN'
```

c choice for solving ALPHA=f(t) : 'ALPHARK2' or 'ALPHACN' c or solve DALPHA=f(ALPHA) : 'DALPHAFACTALPHA' WHICHMETHOD='ALPHARK2'

c choice for which ALPHA to use if DALPHAFACTALPHA is to be compared

```
c KALPHA=1 to first reconstruct ALPHA
c =0 to use experimental ALPHA
cATTENTION, if WHICHMETHOD='ALPHARK2' then
KALPHA=0
KALPHA=0
DELTAB=1.D-6
DO I=1,NPEST ! used to numerically compute the XI
DB(I)=0.D0
ENDDO
```

c choice of inhibition time model: 'TIISOTHERME' or 'TIREFNI'

```
WHICHTIMODEL='TIREFNI'
IF (KTIMEINH.EQ.0) THEN
IF (KRK1.EQ.1) THEN
NPEST=6
ELSE
NPEST=4
ENDIF
ELSE
NPEST=2
ENDIF
```

c to look at a particular set of properties:

```
c=====
KPAR=1
KPRINT=1
KXPRINT=1
```

```

KOUT=2
c general output file:
c=====
OPEN(UNIT=99,FILE='output.out') !general GAoutput file
WRITE(99,20)
20 FORMAT(2X,'kinetic parameter estimation'/50(1H*)//)
!GAoutput file title!
IF (KPAR.NE.1) THEN
OPEN(UNIT=10,FILE='POPPRINT.dat')
OPEN(UNIT=11,FILE='OFPRINT.dat')
OPEN(UNIT=12,FILE='MTCPRINT.dat')
ENDIF
IF (KSCREEN.EQ.1) THEN
PRINT *,'GAMAIN running ...'
PRINT *,'ITERG=',ITERG
ENDIF
WRITE(99,(2X,A24)) FDATE() !initial date and time

RETURN
c-----

ENTRY SETVAR

c set GA variables:
c=====
ISEED1=57
ISEED2=4831
IF (KETA.EQ.2) THEN
NP=NPEST           != Number of parameters optimized
ELSE
NP=NPEST           != Number of parameters estimated
ENDIF
NS=NPEST*100 !CHOOSE NS EVEN TO MAKE NS/2 CHILDREN
SELECT='T'        !modified rank (R) or tournament (T) selection
PT=0.9D0
PC=0.9D0
MUT='JC' !Jump mutation alone (J) or {Jump+Creep}
mutation (JC)
PMJ=10.D0/(NS*1.D0) !1/NS
PMC=PMJ/5.D0 !PMJ/5
ELIT='SS' !steady state (SS) or basic (B) or "similar
replacement" (SR) elitism NOT SET UP yet
PR=0.9D0
KILLTWIN='N' !kill or not the twins (Y/N)
CRITERION=0.01D0
LASTCRITERG=100
MING=100 !at least (MING+LASTCRITERG) generations
LASTG=500 !at most LASTG generations

c set OF variables:
c=====
c set initial ranges + adimensionalization factor of unknown
parameters to be determined
IF (KTIMEINH1.EQ.0) THEN
PARMIN(1)=1.D5
PARMAX(1)=1.D9
FACTADIM(1)='LOG'

PARMIN(2)=30.D3
PARMAX(2)=80.D3
FACTADIM(2)='LIN'

PARMIN(3)=0.8D0
PARMAX(3)=1.2D0
FACTADIM(3)='LIN'

PARMIN(4)=1.5D0
PARMAX(4)=2.0D0
FACTADIM(4)='LIN'

IF (KRK1.EQ.1) THEN
PARMIN(5)=1.D3
PARMAX(5)=1.D60
FACTADIM(5)='LOG'

PARMIN(6)=50.D3

```

```

PARMAX(6)=600.D3
FACTADIM(6)='LOG'
ENDIF

ELSE
PARMIN(1)=40.D0
PARMAX(1)=160.D0
FACTADIM(1)='LIN'

PARMIN(2)=1.D0
PARMAX(2)=100.D0
FACTADIM(2)='LOG'
ENDIF

IF (KETA.EQ.1.OR.KETA.EQ.2) THEN
IF (KTIMEINH1.EQ.1) THEN
OPEN(UNIT=1,FILE='Ctirefni.dat')
DO JEXP=1,NEXP
LASTETA(JEXP)=1
IF (WHICHTIMODEL.EQ.'TIISOTHERME') THEN
READ(1,*)YARR(JEXP,1),TI(JEXP)
ELSE
YARR(JEXP,1)=0.D0
READ(1,*)NDATA(JEXP),PASDT(JEXP),PASDT1(JEXP),V(JEXP)
DO I=1,NDATA(JEXP)+1
READ(1,*)TIMEEXP(JEXP,I),T(JEXP,I)
ENDDO
ENDIF
ENDDO
CLOSE(1)
ELSE
IF (KYSIM.EQ.0) THEN !use experimental data
OPEN(UNIT=1,FILE='Cniref.dat')
DO JEXP=1,NEXP
READ(1,*)LASTETA(JEXP),PASDT1(JEXP),PASDT(JEXP),
DALPHAMAX(JEXP)
READ(1,*)TIMEI(JEXP),ALPHA(JEXP),DALPHAI(JEXP),
TI(JEXP)
DALPHAI(JEXP)=DALPHAI(JEXP)/100.D0
ALPHAI(JEXP)=ALPHAI(JEXP)/100.D0
DO I=1,LASTETA(JEXP)
IF (WHICHMETHOD.EQ.'DALPHAFCTALPHA') THEN
READ(1,*)TIMEEXP(JEXP,I),ALPHA(JEXP,I),
YARR(JEXP,I),T(JEXP,I)
ALPHA(JEXP,I)=ALPHA(JEXP,I)/100.D0
YARR(JEXP,I)=YARR(JEXP,I)/100.D0
ELSE
READ(1,*)TIMEEXP(JEXP,I),YARR(JEXP,I),
DALPHA(JEXP,I),T(JEXP,I)
YARR(JEXP,I)=YARR(JEXP,I)/100.D0
DALPHA(JEXP,I)=DALPHA(JEXP,I)/100.D0
ENDIF
ENDDO
ENDDO
CLOSE(1)
ENDIF
ENDIF

c output:
c=====
WRITE(99,30)
30 FORMAT(/2X,'GA VARIABLES:/'30('-')/
WRITE(99,(A7,I5))'iseed1=',ISEED1
WRITE(99,(A7,I5))'iseed2=',ISEED2
WRITE(99,(A3,I4))'ns=',NS
WRITE(99,(A3,I3))'np=',NP
WRITE(99,(A3,F15.6))'pmj (jump)=',PMJ
WRITE(99,(A3,F15.6))'pmc (creep)=',PMC
WRITE(99,(A3,F15.6))'pc=',PC
WRITE(99,(A3,F15.6))'pr=',PR
WRITE(99,(A3,F15.6))'pt=',PT
WRITE(99,(A10,F15.6))'criterion=',CRITERION
WRITE(99,(A12,I3))'lastcriterg=',LASTCRITERG
WRITE(99,(A5,I3))'ming=',MING
WRITE(99,(A6,I4))'lastg=',LASTG

```



```

IF (SELECT.EQ.'R') WRITE(99,'(A14)')'rank selection'
IF (SELECT.EQ.'T') WRITE(99,'(A20)')'tournament selection'
IF (MUT.EQ.'J') WRITE(99,'(A13)')'jump mutation'
IF (MUT.EQ.'JC') WRITE(99,'(A21)')'jump + creep mutation'
IF (KILLTWIN.EQ.'Y')WRITE(99,'(A8)')'killtwin'
IF (ELIT.EQ.'SS') WRITE(99,'(A20)')'steady state elitism'

WRITE(99,40)
40 FORMAT(/2X,'OF VARIABLES:'30('-')/)
DO I=1,NP
WRITE(99,'(2(A7,I2,A3,E14.3,1X),A9,A3)')
'parmin(',I,')=',PARMIN(I),
'parmax(',I,')=',PARMAX(I),
'Factadim=',factadim(I)
ENDDO
IF (KTIMEINHLEQ.1) THEN
WRITE(99,'(/,A31)')Find the tinhi model parameters'
WRITE(99,'(A12,A14)')WHICHTIMODEL=',WHICHTIMODEL

ELSE
WRITE(99,'(/,A40)')Find the kinetic model parameters using:'
IF (KRK1.EQ.1) THEN
WRITE(99,'(A30)')COMPLETE KAMAL & SOUROUR
MODEL'
ELSE
WRITE(99,'(A40)')SIMPLIFIED KAMAL & SOUROUR
MODEL w/ K1=0'
ENDIF
WRITE(99,'(A12,A14)')WHICHMETHOD=',WHICHMETHOD
ENDIF

WRITE (99,'(/A8,E10.2)')DELTAB=',DELTAB
WRITE (99,'(/A6,I2)')NEXP=',NEXP

IF (KCONT.EQ.0) THEN
WRITE(99,'(/A18)')PAS DE CONTRAINTES'
ELSE
IF (KCONT.EQ.1) WRITE(99,'(/A26)')CONTRAINTES 0/1
appliquées'
IF (KCONT.EQ.2) WRITE(99,'(/A26)')CONTRAINTES 1/2
appliquées'
ENDIF

IF (KYSIM.EQ.1) THEN
WRITE(99,50)
50 FORMAT('/Arrays(lastm) simulated: Yarr'//) !ARRAYS
SIMULATED!
ENDIF

WRITE(99,*)'-----'

RETURN
c-----

ENTRY MODELETA

c run to determine the parameters of the kinetic model
IF (KTIMEINHLEQ.0) THEN

! find ETA using the method defined by WHICHMETHOD
IF (WHICHMETHOD.EQ.'DALPHAFCTALPHA') THEN
IF (KALPHA.EQ.0) THEN
CALL DALPHAFCTALPHA(DB,KRK1,PASDT1,TIMEI,
ALPHA,DALPHA,TI,ALPHA,T)
ELSE
CALL
ALPHARK2(KALPHA,DB,KRK1,RK11,PASDT1,TIMEI,
ALPHA,TI,T,ALPHA)
IF (ETA.GT.1.) RETURN
CALL DALPHAFCTALPHA(DB,KRK1,PASDT1,TIMEI,
ALPHA,DALPHA,TI,ALPHA,T)
IF (ITERETA.NE.0) ETA1(ITERETA)=ETA
ITERETA=ITERETA+1
IF (ITERETA.LE.(LASTETA(JEXP)-1)) GOTO 90

DO J=1,NPEST
DB(J)=DELTAB
ITERETA=0
100 CALL ALPHARK2(KALPHA,DB,KRK1,RK11,PASDT1,
TIMEI,ALPHA,TI,T,ALPHA)
IF (ETA.GT.1.) RETURN

```

```

ALPHA,TI,T,ALPHA)
ELSE
CALL
ALPHACN(NTCMAX,KRK1,RK11,PASDT1,TIMEI,ALPHA,
TI,T)
ENDIF
ENDIF

c run to determine the parameters of the inhibition time model
ELSE
IF (WHICHTIMODEL.EQ.'TIISOTHERME') THEN
CALL TIISOTHERME(TI)
ELSE
CALL TIREFNI(NDATA,PASDT1,T,V)
ENDIF
ENDIF

RETURN
c-----

ENTRY MODELXI

IF (KTIMEINHLEQ.1) STOP 'Particular set of genes analyzed'

IF (KXPRINT.EQ.1) WRITE(IUXI,'(/,A5,I2,/)')JEXP=',JEXP

c find NONDIMENSIONAL XI
IF (WHICHMETHOD.EQ.'ALPHARK2') THEN
ITERETA=0
60 CALL
ALPHARK2(KALPHA,DB,KRK1,RK11,PASDT1,TIMEI,
ALPHA,TI,T,ALPHA)
IF (ITERETA.NE.0) ETA1(ITERETA)=ETA
ITERETA=ITERETA+1
IF (ITERETA.LE.(LASTETA(JEXP)-1)) GOTO 60

DO J=1,NPEST
DB(J)=DELTAB
ITERETA=0
70 CALL ALPHARK2(KALPHA,DB,KRK1,RK11,PASDT1,
TIMEI,ALPHA,TI,T,ALPHA)
IF (ITERETA.NE.0) THEN
ETA2(ITERETA)=ETA
XI(ITERETA,J)=(ETA2(ITERETA)-ETA1(ITERETA))
/(PAR(J)*DELTAB)
ENDIF
ITERETA=ITERETA+1
IF (ITERETA.LE.(LASTETA(JEXP)-1)) GOTO 70
DB(J)=0.D0
ENDDO
ELSE

IF (KALPHA.EQ.0) THEN
ITERETA=1
80 CALL XDALPHAFCTALPHA(KRK1,ALPHA,T)
ITERETA=ITERETA+1
IF (ITERETA.LE.(LASTETA(JEXP)-1)) GOTO 80
ELSE

ITERETA=0
90 CALL
ALPHARK2(KALPHA,DB,KRK1,RK11,PASDT1,TIMEI,
ALPHA,TI,T,ALPHA)
IF (ETA.GT.1.) RETURN
CALL DALPHAFCTALPHA(DB,KRK1,PASDT1,TIMEI,
ALPHA,DALPHA,TI,ALPHA,T)
IF (ITERETA.NE.0) ETA1(ITERETA)=ETA
ITERETA=ITERETA+1
IF (ITERETA.LE.(LASTETA(JEXP)-1)) GOTO 90

DO J=1,NPEST
DB(J)=DELTAB
ITERETA=0
100 CALL ALPHARK2(KALPHA,DB,KRK1,RK11,PASDT1,
TIMEI,ALPHA,TI,T,ALPHA)
IF (ETA.GT.1.) RETURN

```

```

CALL DALPHAFCTALPHA(DB,KRK1,PASDT1,TIMEI,
ALPHA1,DALPHA1,TI,ALPHA,T)
IF (ITERETA.NE.0) THEN
ETA2(ITERETA)=ETA
XI(ITERETA,J)=(ETA2(ITERETA)-ETA1(ITERETA))
/(PAR(J)*DELTA)
ENDIF
ITERETA=ITERETA+1
IF (ITERETA.LE.(LASTETA(JEXP)-1)) GOTO 100
DB(J)=0.D0
ENDDO
ENDIF
ENDIF

```

c if KXPRINT=1, print nondimensional sensitivity coefficients in file

```

IF (KXPRINT.EQ.1) THEN
ITERETA=1
TIME=TIMEI(JEXP)+PASDT1(JEXP)
110 IF (WHICHMETHOD.EQ.'ALPHARK2') THEN
WRITE(IUXI,(F11.4,6(3X,E10.4)))TIME,
(XI(ITERETA,J)*PAR(J),J=1,NPEST)
ELSE
WRITE(IUXI,(F11.4,6(3X,E10.4)))TIME,
(XI(ITERETA,J)*PAR(J)/DALPHAMAX(JEXP),J=1,NPEST)
ENDIF
ITERETA=ITERETA+1
TIME=TIME+PASDT1(JEXP)
IF (ITERETA.LE.(LASTETA(JEXP)-1)) GOTO 110
ENDIF

```

```

DO I=1,NPEST
XI(LASTETA(JEXP),I)=XI(LASTETA(JEXP)-1,I)
ENDDO

```

```

RETURN

```

```

ENTRY CHECKCONT(N,ARR)

```

*c check that the children generation satisfy the constraints inherent to the model (subroutine MODELETA).
c this procedure can also be used to force the children to stay within the ranges defined*

```

DO 120 I=1,N
DO 120 J=1,NP
IF (ARR(I,J).LT.0.D0) THEN
IF (KCONT.EQ.1) ARR(I,J)=0.D0
IF (KCONT.EQ.2) ARR(I,J)=0.5D0
NCONTMIN=NCONTMIN+1
ENDIF
IF (ARR(I,J).GT.1.D0) THEN
IF (KCONT.EQ.1) ARR(I,J)=1.D0
IF (KCONT.EQ.2) ARR(I,J)=0.5D0
NCONTMAX=NCONTMAX+1
ENDIF
120 CONTINUE

```

```

RETURN
END

```

```

c*****

```

c include main program et problem specific subroutines

```

INCLUDE 'gamain.for'
INCLUDE 'dalphafctalpha.for'
INCLUDE 'alphark2.for'
INCLUDE 'alphaCN.for'
INCLUDE 'tirefni.for'
INCLUDE 'xdalphafctalpha.for'

```

```

c*****

```

```

SUBROUTINE ALPHARK2(KALPHA,DB,KRK1,RK1I,
PASDT1,TIMEI,ALPHA1,TI,T,ALPHA)

```

c HP77 or PC -

```

c*****

```

```

INCLUDE 'gacommon_main.for'

```

```

c*****

```

```

DIMENSION PASDT1(NEXPMAX),TI(NEXPMAX),
TIMEI(NEXPMAX),ALPHA1(NEXPMAX),
T(NEXPMAX,LASTETAMAX),DB(NPMAX),
ALPHA(NEXPMAX,LASTETAMAX)
C-----

```

```

RCST=8.31D0

```

```

RK1=0.D0 !takes a value if KRK1=1

```

```

RM=PAR(3)*(1.D0+DB(3))

```

```

RN=PAR(4)*(1.D0+DB(4))

```

```

IF (ITERETA.EQ.0) THEN

```

```

TEMP=TI(JEXP)+273.15D0

```

```

ETA=ALPHA1(JEXP)

```

```

IF (KRK1.EQ.0.AND.ETA.EQ.0.) ETA=RK1I

```

```

ELSE

```

```

IF (KALPHA.EQ.1) THEN !when alphark2 used to reconstruct

```

```

IF (ITERETA.EQ.1) THEN !alpha before computing dalphafctalpha

```

```

ETA=ALPHA1(JEXP)

```

```

IF (KRK1.EQ.0.AND.ETA.EQ.0.) ETA=RK1I

```

```

ELSE

```

```

ETA=ALPHA(JEXP,ITERETA-1)

```

```

ENDIF

```

```

ENDIF

```

```

IF (KRK1.EQ.1)

```

```

RK1=PAR(5)*(1.D0+DB(5))*EXP(-

```

```

PAR(6)*(1.D0+DB(6))/(RCST*TEMP))

```

```

RK2=PAR(1)*(1.D0+DB(1))*EXP(-

```

```

PAR(2)*(1.D0+DB(2))/(RCST*TEMP))

```

c apply penalty

```

IF ((1.D0-ETA).LT.0.D0) THEN

```

!stop the calculation for this chromosome and assign it a BIG S

```

ETA=DSQRT(BIG)

```

```

ITERETA=LASTETA(JEXP)

```

```

JEXP=NEXP

```

```

GOTO 50

```

```

ENDIF

```

```

IF (ITERETA.EQ.1) THEN

```

```

R1=PASDT1(JEXP)*((RK1+RK2*ETA**RM)*(1.D0-

```

```

ETA)**RN)

```

```

ELSE

```

```

R1=PASDT1(JEXP)*((RK1+RK2*ETA**RM)*(1.D0-

```

```

ETA)**RN)

```

```

ENDIF

```

c apply penalty

```

IF ((1.D0-(ETA+R1/2.D0)).LT.0.D0) THEN

```

!stop the calculation for this chromosome and assign it a BIG S

```

ETA=DSQRT(BIG)

```

```

ITERETA=LASTETA(JEXP)

```

```

JEXP=NEXP

```

```

GOTO 50

```

```

ENDIF

```

```

IF (ITERETA.EQ.1) THEN

```

```

R2=PASDT1(JEXP)*((RK1+RK2*(ETA+R1/2.D0)**RM)*

```

```

(1.D0-(ETA+R1/2.D0)**RN)

```

```

ELSE

```

```

R2=PASDT1(JEXP)*((RK1+RK2*(ETA+R1/2.D0)**RM)*

```

```

(1.D0-(ETA+R1/2.D0)**RN)

```

```

ENDIF

```

```

ETA=ETA+R2

```

```

TEMP=T(JEXP,ITERETA)+273.15D0

```

```

ENDIF

```

```

IF (KALPHA.EQ.1) THEN
IF (ITERETA.NE.0) ALPHA(JEXP,ITERETA)=ETA
ELSE

IF (KPAR.EQ.1.AND.KSENS.EQ.0) THEN
IF (ITERETA.EQ.0) THEN
TIME=TIMEI(JEXP)
ELSE
IF (ITERETA.EQ.1) THEN
TIME=TIME+PASDT1(JEXP)
ELSE
TIME=TIME+PASDT(JEXP)
ENDIF
ENDIF
c set title (@ ITERETA=0) and data (@ each ITERETA) to print in iunit
DO 40 IUNIT=IU1,IU2
IF (ITERETA.EQ.0) THEN
WRITE(IUNIT,20)
20 FORMAT(2X,'JEXP',1X,'ITERETA',6X,'TIME',
13X,'ETA',15X,'YARR',16X,'RES',/)
WRITE(IUNIT,30)JEXP,ITERETA,TIME,ETA,
ALPHA(JEXP),ETA-ALPHA(JEXP)
ELSE
WRITE(IUNIT,30)JEXP,ITERETA,TIME,ETA,
YARR(JEXP,ITERETA),ETA-YARR(JEXP,ITERETA)
30 FORMAT(2X,I2,2X,I4,2X,1PE13.6,2X,1PE16.9,
2X,1PE16.9,2X,1PE16.9)
ENDIF
40 CONTINUE
ENDIF
ENDIF

50 RETURN
END

```

```

SUBROUTINE ALPHACN(NTCMAX,KRK1,RK1I,PASDT1,
TIMEI,ALPHAI,TI,T)

```

c HP77 or PC -

```

c*****
INCLUDE 'gacommon_main.for'
c*****
DIMENSION PASDT1(NEXPMAX),TI(NEXPMAX),
TIMEI(NEXPMAX),ALPHAI(NEXPMAX),
T(NEXPMAX,LASTETAMAX)
C-----

```

```

RCST=8.31D0

```

```

IF (ITERETA.EQ.0) THEN
TIME=TIMEI(JEXP)
ETA=ALPHAI(JEXP)
Tkp1=TI(JEXP)
ELSE
IF (ITERETA.EQ.1) THEN
RDT=PASDT1(JEXP)
ELSE
RDT=PASDT(JEXP)
ENDIF
TIME=TIME+RDT
Tk=Tkp1
Tkp1=T(JEXP,ITERETA)
IF (KRK1.EQ.1) THEN
RK1k=PAR(5)*EXP(-PAR(6)/(RCST*(Tk+273.15D0)))
RK1kp1=PAR(5)*EXP(-PAR(6)/(RCST*(Tkp1+273.15D0)))
ELSE
RK1k=RK1I
RK1kp1=RK1I
ENDIF
RK2k=PAR(1)*EXP(-PAR(2)/(RCST*(Tk+273.15D0)))
RK2kp1=PAR(1)*EXP(-PAR(2)/(RCST*(Tkp1+273.15D0)))
RM=PAR(3)
RN=PAR(4)
ALPHAk=ETA
NTC=1

```

```

10 ALPHAkp1=ETA

```

c apply penalty : stop the calculation for a bad chromosome and assign it a BIG S

```

IF ((1.D0-ALPHAkp1).LT.0.D0) THEN
ETA=DSQRT(BIG)
ITERETA=LASTETA(JEXP)
JEXP=NEXP
GOTO 50
ENDIF
ETA=ALPHAk+RDT/2.D0*
(((RK1k+RK2k*ALPHAk**RM)*(1.D0-ALPHAk)**RN)+
((RK1kp1+RK2kp1*ALPHAkp1**RM)*(1.D0-ALPHAkp1)**RN))
IF ((DABS(ETA-ALPHAkp1)/(ETA+10.D0**(-10.))).GT.
CRITERION) THEN
NTC=NTC+1
IF (NTC.GT.NTCMAX) THEN !apply penalty
ETA=DSQRT(BIG/2.D0)
ITERETA=LASTETA(JEXP)
JEXP=NEXP
GOTO 50
ENDIF
GOTO 10
ENDIF
ENDIF

```

```

IF (KPAR.EQ.1) THEN

```

c set title (@ ITERETA=0) and data (@ each ITERETA) to print in iunit

```

DO 40 IUNIT=IU1,IU2
IF (ITERETA.EQ.0) THEN
WRITE(IUNIT,20)
20 FORMAT(2X,'JEXP',1X,'ITERETA',6X,'NTC',6X,
'TIME',13X,'ETA',15X,'YARR',16X,'RES',/)
WRITE(IUNIT,30)JEXP,ITERETA,NTC,TIME,ETA,ALPHAI(
JEXP),

```

```

ETA-ALPHAI(JEXP)
ELSE
WRITE(IUNIT,30)JEXP,ITERETA,NTC,TIME,ETA,
YARR(JEXP,ITERETA),ETA-YARR(JEXP,ITERETA)
30 FORMAT(2X,I2,2X,I4,1X,I2,1X,1PE13.6,1X,1PE16.9,
1X,1PE16.9,1X,1PE16.9)
ENDIF
40 CONTINUE
ENDIF

50 RETURN
END

```

```

SUBROUTINE DALPHAFACTALPHA(DB,KRK1,PASDT1,
TIMEI,ALPHAI,DALPHAI,TI,ALPHA,T)

```

c HP77 or PC -

```

c*****
INCLUDE 'gaccommon_main.for'
c*****
DIMENSION PASDT1(NEXPMAX),TIMEI(NEXPMAX),
TI(NEXPMAX),ALPHAI(NEXPMAX),
DALPHAI(NEXPMAX),DB(NPMAX),
T(NEXPMAX,LASTETAMAX),
ALPHA(NEXPMAX,LASTETAMAX)
C-----

```

```

RCST=8.31D0
RK1=0.D0      !takes a value if KRK1=1
RM=PAR(3)*(1.D0+DB(3))
RN=PAR(4)*(1.D0+DB(4))

```

```

IF (ITERETA.EQ.0) THEN
IF (KRK1.EQ.1) RK1=PAR(5)*(1.D0+DB(5))*
EXP(-PAR(6)*(1.D0+DB(6)))/(RCST*(TI(JEXP)+273.15D0)))
RK2=PAR(1)*(1.D0+DB(1))*
EXP(-PAR(2)*(1.D0+DB(2)))/(RCST*(TI(JEXP)+273.15D0)))
ETA=(RK1+RK2*ALPHAI(JEXP)**RM)
*(1-ALPHAI(JEXP)**RN)
ELSE
IF (KRK1.EQ.1) RK1=PAR(5)*(1.D0+DB(5))*
EXP(-PAR(6)*(1.D0+DB(6)))/(RCST*(T(JEXP,ITERETA)
+273.15D0)))
RK2=PAR(1)*(1.D0+DB(1))*
EXP(-PAR(2)*(1.D0+DB(2)))/(RCST*(T(JEXP,ITERETA)
+273.15D0)))
ETA=(RK1+RK2*ALPHA(JEXP,ITERETA)**RM)
*(1-ALPHA(JEXP,ITERETA)**RN)
ENDIF

```

```

IF (KPAR.EQ.1) THEN
IF (ITERETA.EQ.0) THEN
TIME=TIMEI(JEXP)
ELSE
IF (ITERETA.EQ.1) THEN
TIME=TIME+PASDT1(JEXP)
ELSE
TIME=TIME+PASDT(JEXP)
ENDIF
ENDIF

```

c set title (@ ITERT=0) and data (@ each ITERT) to print in iunit

```

DO 40 IUNIT=IU1,IU2
IF (ITERETA.EQ.0) THEN
WRITE(IUNIT,20)
20 FORMAT(2X,'JEXP',1X,'ITERETA',5X,'TIME',9X,
'ETA',10X,'YARR',12X,'RES',10X,'ALPHA')
WRITE(IUNIT,30)JEXP,ITERETA,TIME,ETA,DALPHAI(JEXP),
ETA-DALPHAI(JEXP),ALPHAI(JEXP)
ELSE
WRITE(IUNIT,30)JEXP,ITERETA,TIME,ETA,YARR(JEXP,I
TERETA),ETA-YARR(JEXP,ITERETA),
ALPHA(JEXP,ITERETA)
30 FORMAT(2X,I2,2X,I4,3X,1PE12.5,3X,1PE13.6,
3X,1PE13.6,3X,1PE12.5,3X,1PE12.5)
ENDIF
40 CONTINUE
ENDIF

```

```

RETURN
END

```

SUBROUTINE XDALPHAFACTALPHA(KRK1,ALPHA,T)

c HP77 or PC -

```
C*****  
INCLUDE 'gacommon_main.for'  
C*****  
DIMENSION T(NEXPMAX, LASTTETAMAX),  
ALPHA(NEXPMAX, LASTTETAMAX)  
C-----
```

RCST=8.31D0

```
A2=PAR(1)  
E2=PAR(2)  
RM=PAR(3)  
RN=PAR(4)  
IF (KRK1.EQ.1) THEN  
A1=PAR(5)  
E1=PAR(6)  
ENDIF
```

```
RALPHA=ALPHA(JEXP, ITERETA)  
TEMP=T(JEXP, ITERETA)+273.15D0  
RK2=A2*EXP(-E2/(RCST*TEMP))
```

```
IF (KRK1.EQ.1) THEN  
RK1=A1*EXP(-E1/(RCST*TEMP))  
XI(ITERETA,5)=EXP(-E1/(RCST*TEMP))*(1.D0-  
RALPHA)**RN /XA1  
XI(ITERETA,6)=-RK1/(RCST*TEMP)  
*(1.D0-RALPHA)**RN /XE1  
ELSE  
RK1=0.D0  
ENDIF
```

```
XI(ITERETA,1)=EXP(-E2/(RCST*TEMP))*RALPHA**RM  
*(1.D0-RALPHA)**RN /XA2  
XI(ITERETA,2)=-RK2/(RCST*TEMP)*RALPHA**RM  
*(1.D0-RALPHA)**RN /XE2  
XI(ITERETA,3)=RK2*RALPHA**RM /Xm  
*(1.D0-RALPHA)**RN*DLOG(RALPHA)  
XI(ITERETA,4)=(RK1+RK2*RALPHA**RM)  
*(1.D0-RALPHA)**RN*DLOG(1.D0-RALPHA) /Xn
```

```
RETURN  
END
```

SUBROUTINE TIREFNI(NDATA,PASDT1,T,V)

c HP77 or PC -

```
C*****  
INCLUDE 'gacommon_main.for'  
C*****  
DIMENSION NDATA(NEXPMAX), PASDT1(NEXPMAX),  
T(NEXPMAX, LASTTETAMAX), V(NEXPMAX),  
ADDSUM(NEXPMAX), SUMINT(NEXPMAX)  
C-----
```

```
IF (ITERETA.EQ.0.OR.ITERETA.GT.LASTTETA(JEXP))  
GOTO 100  
TREF=PAR(1)  
B=PAR(2)  
PASTIME=0.01D0
```

```
IF (JEXP.EQ.1) SUMSUMINT=0.D0  
SUMINT(JEXP)=0.D0  
DO 10 IDATA=1, NDATA(JEXP)  
TEMP=(T(JEXP, IDATA)+T(JEXP, IDATA+1))/2.D0  
FACTB=(TREF+273.15D0)/(TEMP+273.15D0)-1.D0  
IF (IDATA.NE. NDATA(JEXP)) THEN  
ADDSUM(JEXP)=PASDT(JEXP)*EXP(-B*FACTB)  
ELSE  
ADDSUM(JEXP)=PASDT1(JEXP)*EXP(-B*FACTB)  
ENDIF  
SUMINT(JEXP)=SUMINT(JEXP)+ADDSUM(JEXP)  
10 CONTINUE  
SUMSUMINT=SUMSUMINT+SUMINT(JEXP)
```

```
IF (JEXP.NE.NEXP) THEN  
ETA=0.D0  
ELSE
```

```
IF (KPAR.EQ.1) THEN  
OPEN(UNIT=98, FILE='Ctirefni.ind')  
WRITE(98,15)  
15 FORMAT(2X, 'TREF', 4X, 'B', 8X, 'SUMINT(JEXP=1, NEXP)',  
4X, 'SUMSUMINT/NEXP', /)  
WRITE(98,20) TREF, B, (SUMINT(JEXP), JEXP=1, NEXP), SUM  
SUMINT/NEXP  
20 FORMAT(8(1X, 1F11.5), /)  
ENDIF
```

```
DO 60 J=1, NEXP  
IF (KPAR.EQ.1) WRITE(98,30)  
30 FORMAT(2X, 'TIME', 4X, 'SUMI', 4X, 'TIMEREF',  
4X, 'TEMP', /)
```

```
TEMP=T(J,1)  
TIME=0.D0  
SUMI=0.D0  
40 IF (TIME.EQ.0.D0) THEN  
TEMP=TEMP+V(J)*PASTIME/2.D0  
ELSE  
TEMP=TEMP+V(J)*PASTIME  
ENDIF  
TIME=TIME+PASTIME  
FACTB=(TREF+273.15D0)/(TEMP+273.15D0)-1.D0  
ADDS= PASTIME*EXP(-B*FACTB)  
SUMI=SUMI+ADDS  
IF (SUMI.GT.SUMSUMINT/NEXP) THEN  
ETA=ETA+ABS(TIME-TIMEEXP(J, NDATA(J)+1))  
IF (KPAR.EQ.1) THEN  
WRITE(98, '(A4, F10.3)') 'RES=' ,  
ABS(TIME-TIMEEXP(J, NDATA(J)+1))  
PAUSE  
ENDIF  
GOTO 60  
ENDIF
```

```
IF (KPAR.EQ.1) THEN  
WRITE(98,50) TIME, SUMI, SUMSUMINT/NEXP,  
(TEMP+V(J)*PASTIME/2.D0)  
WRITE(*,50) TIME, SUMI, SUMSUMINT/NEXP,
```

```
(TEMP+V(J)*PASTIME/2.D0)  
50 FORMAT(4(3X,1F11.4))  
ENDIF
```

```
GOTO 40  
60 CONTINUE
```

```
IF (KPAR.EQ.1) CLOSE(98)  
ENDIF
```

```
100 RETURN  
END
```

Vita

Sandrine Garcia was born on July 13, 1971 in Béziers, France. During her childhood she lived in different places in France. In 1985 she moved to Bordeaux, and graduated from the *lycée privé de l'Assomption* in 1989. She attended the *Université des Sciences de Bordeaux I* and received the *Diplôme d'Etudes Universitaire Général (DEUG A)* in June, 1991. That fall, she started the chemical engineering program at the *Université de Technologie de Compiègne (UTC)*.

In August 1993, Sandrine enrolled in an exchange program between UTC and the Virginia Polytechnic Institute and State University (Virginia Tech), in Blacksburg, Virginia, USA, and began her graduate studies under the direction of Dr. Elaine P. Scott. She received the *Diplôme d'Ingénieur* in Chemical Engineering from UTC in September, 1994, and completed the requirements for the Master of Science degree in Mechanical Engineering from Virginia Tech in December, 1994.

Immediately following, Sandrine continued her graduate studies in a dual US-French Ph.D. program between Virginia Tech and the *Laboratoire de Thermocinétique de l'ISITEM*, University of Nantes, France, under the co-direction of Dr. Elaine P. Scott and Prof. Yvon Jarny. During her doctoral studies, she had the opportunity to participate to a teaching exchange program between Virginia Tech and the *Universidad Politecnica de Puerto Rico (UPPR)* in San Juan, Puerto Rico. She taught Mechanical Engineering courses at the UPPR from August 1996 to June 1997. Back at Virginia Tech, she volunteered for an instructor position during Summer I and taught Thermodynamics II. With the completion of this dissertation, she has fulfilled the requirements for the Doctor of Philosophy degree in Mechanical Engineering and the *Doctorat en Sciences Pour l'Ingénieur, Spécialité Transferts Thermiques, Energétique et Génie des Procédés*, on the 04th day of June, 1999.

Sandrine Garcia